

# **Outdoor noise control by natural/sustainable materials in urban areas**

**Hong-Seok Yang**

**September 2013**



**The  
University  
Of  
Sheffield.**

**Thesis for the degree of Doctor of Philosophy**

**School of Architecture  
The University of Sheffield**

## **ABSTRACT**

This study explores the effects of natural and sustainable materials including vegetation, green roof systems and green walls on outdoor noise control in urban areas. The concept of this study starts with a hypothesis that well-planned use of the natural materials on building and urban surfaces can achieve useful reductions in noise levels and reverberation in urban spaces. Firstly, this study examines random-incidence absorption and scattering coefficients of vegetation through a series of measurements in a reverberation chamber in order to characterise the effects of various designable factors such as soil depths, soil water content and vegetation densities. This data is used later in acoustic computer simulations. To quantify the scattering effect of trees and to allow including it in numerical predictions, a series of measurements are carried out for individual trees in an open field. Green roof systems are placed on a low profiled structure to examine sound transmission through the vegetated low barrier. To suggest noise abatement schemes in relatively small urban spaces, the acoustic effects of landscape designs using vegetation in a courtyard are studied through a case study. As a preliminary study on the noise reduction effect of vegetation in relatively large urban spaces, field measurements are carried out at outdoor spaces in high-rise apartment complexes. Based on the measurement results, the noise reduction effect of vegetation in apartment complexes is also predicted. The overall results for each research topic can be summarised as follows: It is shown that low-growing vegetation can be an effective measure for absorbing/scattering sound energy, especially at high frequencies. Results of field measurements show that tree reverberation exerts an influence only on frequencies above 1 kHz. At 4 kHz, RT (reverberation time) can be as long as 0.28 sec. Measurements made near the same deciduous tree with and without leaves indicate that

leaves increase reverberation at 4 kHz by 0.08 sec. The results on sound transmission over the low barrier with green roof systems suggest that SPL attenuation increases with the increasing green roof areas. The extra SPL (sound pressure level) attenuation caused by green roof systems could be up to 9.5 dB at certain frequencies. With well-planned application of landscape designs in a courtyard, speech levels and RT at 500 Hz are decreased by 9.3 dBA and 81 %, respectively. In outdoor spaces of apartment complexes, RT is generally rather long, over 4 sec at 500 Hz, influenced by many factors such as openness, source-receiver distance and building height. In terms of SPL distribution, the measured SPL is up to 8 dB higher compared to the semi-free field situation. It is also found that vegetation at the apartment complex can be effective in reducing RT by 0.95 sec (46 % decrease).

## **ACKNOWLEDGEMENT**

First of all, I would like to acknowledge and greatly thank my PhD supervisor, Professor Jian Kang. His continuous support, encouragement and academic advice have led me to complete the Ph.D.

I am deeply indebted to Dr. Chris Cheal and Dr. Yuliya Smyrnova, for helping me set up and carry out a series of experiments. I would also like to thank Dr. Min-Sung Choi for the use of green roof systems for experiments. I am grateful to Dr. Timothy Van Renterghem and Professor Dick Botteldooren, for insightful reviews and comments to publish a journal paper. I also gratefully acknowledge the review and comments of Professor David Oldham and Professor Steve Fotios who are the examiners of Viva Voce.

I sincerely appreciate my former supervisors, Professor Myung-Jun Kim and Professor Yong-Shik Kim for continuous encouragement to study acoustics. I am also thankful to the member of Acoustics Group in the University of Sheffield and University of Seoul for their invaluable help and advices. I thank Sheffield Korean Church for support and prayers.

I would like to express my deepest gratitude to my parents who raised me with endless love and supported me in all my pursuits.

# CONTENTS

<b>ABSTRACT</b> .....	<b>i</b>
<b>ACKNOWLEDGEMENT</b> .....	<b>iii</b>
<b>CONTENTS</b> .....	<b>iv</b>
<b>LIST OF ABBREVIATIONS</b> .....	<b>ix</b>
<b>LIST OF FIGURES</b> .....	<b>xi</b>
<b>LIST OF TABLES</b> .....	<b>xvii</b>
<b>1 Introduction</b> .....	<b>1</b>
1.1 Research background .....	1
1.2 Aims and objectives .....	2
1.3 Thesis structure.....	3
<b>2 Literature Review</b> .....	<b>7</b>
2.1 Sound propagation in an urban environment .....	7
2.1.1 Site measurements .....	8
2.1.2 Physical scale modelling .....	9
2.1.3 Numerical modelling.....	9
2.2 Noise reduction mechanisms by vegetation .....	10
2.2.1 Absorption .....	11
2.2.2 Scattering and reflection.....	15
2.2.3 Ground effect.....	17
2.3 Noise reduction by tree belts .....	18
2.3.1 Measurement results .....	18
2.3.2 Prediction schemes .....	21
2.4 Vegetation in urban situations .....	22
2.4.1 Measurement and prediction results.....	22
2.5 Summary (Justification for the research work) .....	27
2.5.1 Acoustic properties of vegetation (Chapter 3).....	27
2.5.2 Sound propagation through a single tree (Chapter 4).....	28
2.5.3 Acoustic effect of green roof systems (Chapter 5).....	29
2.5.4 Effect of landscape designs in courtyards on noise reduction (Chapter 6) .....	29
2.5.5 Acoustic characteristics in outdoor spaces of residential areas (Chapter 7&8) .....	30

<b>PART I. ACOUSTIC PROPERTIES OF VEGETATION AND TREES .....</b>	<b>31</b>
<b>3 Random-incidence Absorption and Scattering Coefficients of Vegetation .....</b>	<b>32</b>
3.1 Introduction .....	32
3.2 Methodology .....	35
3.2.1 Measurement method .....	35
3.2.2 Calculation method for the absorption and scattering coefficients .....	37
3.2.3 Measurement of absorption coefficient for soil without vegetation.....	38
3.2.4 Measurement of absorption coefficient for soil with vegetation.....	40
3.2.5 Leaves and stems.....	43
3.2.6 Green wall .....	45
3.3 Measurement results.....	47
3.3.1 Soil without vegetation.....	47
3.3.2 Soil with vegetation.....	49
3.3.3 Absorption by leaves and stems .....	50
3.3.4 Scattering of leaves and stems.....	52
3.3.5 Green wall .....	54
3.4 Summary .....	55
<b>4 Quantifying Scattered Sound Energy from a Single Tree by means of Reverberation Time.....</b>	<b>57</b>
4.1 Introduction .....	57
4.2 Principle of quantifying scattered sound energy from a single tree by means of reverberation time.....	59
4.3 Measurement method .....	60
4.3.1 Experimental conditions.....	60
4.3.2 Measurement setup.....	64
4.4 Validation for measurement and data analysis methods.....	65
4.4.1 Data analysis method.....	65
4.4.2 Impulse response to noise ratio .....	65
4.4.3 Determination of RT .....	66
4.4.4 Repeatability of the measurement method .....	69
4.4.5 Ground conditions and receiver heights.....	69
4.5 Measurement Results .....	72
4.5.1 Effects of tree size with and without foliage .....	72
4.5.2 Source-receiver angle .....	75
4.5.3 Source-receiver distance.....	77
4.6 Summary .....	78

<b>PART II. GREEN ROOF SYSTEMS ON A LOW BARRIER .....</b>	<b>81</b>
<b>5 Noise Reduction by Green Roof Systems at Street Level .....</b>	<b>82</b>
5.1 Introduction .....	82
5.2 Methodology .....	84
5.2.1 Physical properties of the green roof system.....	84
5.2.2 Absorption coefficient of the substrates .....	87
5.2.3 Experimental setup .....	89
5.2.4 Examination of the geometrical effect using FEM.....	91
5.2.5 Experimental parameters .....	94
5.3 Results .....	98
5.3.1 SPL attenuation by empty trays.....	98
5.3.2 Green roof area .....	99
5.3.3 Depth and type of the substrates.....	103
5.3.4 Position of the green roof system .....	104
5.3.5 Vegetation .....	105
5.4 Summary .....	107
<b>PART III. VEGETATION IN URBAN SITUATIONS .....</b>	<b>109</b>
<b>6 A Case Study on Controlling Sound Fields by Landscape Designs in a     Courtyard.....</b>	<b>110</b>
6.1 Introduction .....	110
6.2 Methodology .....	113
6.2.1 Description of the study site.....	113
6.2.2 Measurement and analysis methods .....	116
6.3 Measurement results.....	118
6.4 Computer simulations.....	120
6.4.1 Computer model calibration.....	120
6.4.2 Landscape design schemes using vegetation.....	122
6.4.3 Simulation results in the courtyard.....	124
6.4.4 Simulation result at different floor levels in the accommodation building .....	130
6.5 Summary .....	133
<b>7 A Preliminary Study on Acoustic Characteristics of Outdoor Spaces in an     Apartment Complex.....</b>	<b>136</b>
7.1 Introduction .....	136
7.2 Methods .....	139
7.3 Results .....	144

7.3.1	Impulse Responses and Decay Curves at S1 .....	144
7.3.2	Acoustic Characteristics of the Long Outdoor Spaces (S1, S2, S3).....	146
7.3.3	Acoustic Parameters of the Outdoor Square (S4).....	151
7.3.4	Acoustic Parameters with Different Receiver Heights (S2).....	153
7.4	Summary .....	154
<b>8</b>	<b>A Parametric Study on Outdoor Reverberation in Apartment Complexes.....</b>	<b>157</b>
8.1	Introduction .....	157
8.2	Methodology .....	159
8.2.1	Studied sites.....	159
8.2.2	Measurement method .....	162
8.3	Measurement results.....	163
8.3.1	Overall characteristics and distribution of RT .....	163
8.3.2	RT for the linear-shaped building layout.....	166
8.3.3	RT for the parallel-shaped building layout.....	167
8.3.4	RT for the L-shaped building layout.....	169
8.3.5	RT for the U-shaped building layout .....	170
8.3.6	RT for the □-shaped building layout.....	171
8.4	Empirical method to estimate RT .....	173
8.5	Vegetation in the outdoor spaces .....	180
8.6	Summary .....	182
<b>9</b>	<b>Conclusions and Future Work .....</b>	<b>184</b>
9.1	Contributions of the thesis.....	184
9.1.1	Examination on the acoustic properties of vegetation.....	184
9.1.2	Quantification of scattered sound energy from a tree.....	186
9.1.3	Examination of potential use of green roof systems on a low barrier ...	186
9.1.4	Verification on noise reduction effects of vegetation in a courtyard.....	187
9.1.5	Investigation of sound propagation in high-rise apartment complexes.	188
9.1.6	Evaluation of parameters on reverberation in apartment complexes ....	189
9.2	Future work .....	190
9.2.1	Prediction of random-incidence absorption and scattering coefficients	190
9.2.2	Numerical modelling of scattering of sound by trees.....	191
9.2.3	Noise reduction by vegetated low barriers in real urban situations.....	191
9.2.4	Practical landscape designs in a courtyard .....	191
9.2.5	Application of vegetation in outdoor spaces of apartment complexes..	192
9.2.6	Acoustic parameters for evaluating acoustic comfort in urban situations .....	193



<b>REFERENCES</b> .....	<b>194</b>
<b>PUBLICATIONS</b> .....	<b>208</b>

## LIST OF ABBREVIATIONS

ANSI	American national standards institute
ASE	Apparent Source Width
BEM	Boundary element method
dB	Decibel (unweighted)
dBA	Decibel (A-weighted)
EDT	Early decay time
LEV	Listener envelopment
FDTD	Finite difference time domain
FEM	Finite element method
Hz	Hertz
IACC	Inter-aural cross correlation
IEC	International Electrotechnical Commission
ISO	International Standards Organization
kHz	kilohertz
PE	Parabolic equation
RASTI	Rapid speech transmission index
RT	Reverberation time

SPL	Sound pressure level
STI	Speech transmission index
WHO	World Health Organization

## LIST OF FIGURES

Fig. 1.1 Diagram showing overall structure of this study .....	6
Fig. 2.1 Extensive green roof on top of a building at the University of Sheffield .....	24
Fig. 2.2 Modular of the green wall containing substrate (left) and an example of the application (right). <i>Copyright of the figures: Canevaflor, <a href="http://www.canevaflor.com">http://www.canevaflor.com</a></i> .....	25
Fig. 3.1 Schematic diagram of the experimental arrangement.....	37
Fig. 3.2 Photo of the measurement setup for the baseplate with water.....	37
Fig. 3.3 Topsoil of 50 mm depth.....	40
Fig. 3.4 200 mm topsoil with eight plant species: (a) 40 % vegetation coverage (106 plants); (b) 100 % vegetation coverage (264 plants).....	42
Fig. 3.5 Measurement conditions of random-incidence scattering coefficient: (a) Buxus with 100 % vegetation coverage using 110 plants; (b) Holly with 100 % vegetation coverage using 123 plants; (c) Ivy prunings of 200 mm depth.....	44
Fig. 3.6 Green wall without vegetation, mounted on a flat wall of reverberation chamber.....	46
Fig. 3.7 Absorption coefficient of topsoil with different soil depths .....	48
Fig. 3.8 Absorption coefficient of 200 mm topsoil with different soil moisture content (%).....	48
Fig. 3.9 Absorption coefficient of topsoil with different levels of vegetation coverage.....	49
Fig. 3.10 Absorption coefficient of vegetation with different levels of vegetation coverage/density: (a) Buxus; (b) Holly; (c) Ivy .....	51
Fig. 3.11 Scattering coefficient of the baseplate containing water with 200 mm depth .....	52
Fig. 3.12 Scattering coefficient of vegetation with different levels of vegetation coverage/density: (a) Buxus; (b) Holly; (c) Ivy .....	53
Fig. 3.13 Absorption coefficient of the green wall with different levels of substrate moisture content, shown in terms of water added.....	55
Fig. 4.1 Diagram for sound paths through a single tree from a point source to a receiver .....	60
Fig. 4.2 Impulse responses measured in open field in the absence and presence of a single tree.....	60
Fig. 4.3 Conditions for five trees with foliage on Day 3.....	63

Fig. 4.4 Measurement conditions, where $d_r$ is the trunk-receiver distance, $d_s$ is trunk-source distance, $h_r$ is the receiver height, and $h_s$ is the source height.....	64
Fig. 4.5 Comparison of decay curves in the absence and presence of a single tree (Tree 3) .....	67
Fig. 4.6 RT with the three decay ranges corresponding to T10, T20 and T30: (a) Open field; (b) Tree 3 with foliage .....	68
Fig. 4.7 Decay curves with the four different ground conditions at the receiver and source heights of 0.2 m for Tree 2. Each figure shows the decay curves in octave band frequencies from 500 Hz to 4 kHz .....	71
Fig. 4.8 Effect of the different ground conditions on RT20 for Tree 2 with different receiver heights from 0.2 m to 4.0 m (source height 0.2 m).....	72
Fig. 4.9 Decay curves for the five trees with foliage. Each figure shows the decay curves in octave band frequencies from 500 Hz to 4 kHz.....	73
Fig. 4.10 Effect of the surface area of tree crown with and without foliage on RT20. Each figure shows RT20 in octave band frequencies from 500 Hz to 4 kHz .....	75
Fig. 4.11 Decay curves for Tree 2 without foliage with different source-receiver angles. Each figure shows the decay curves in octave band frequencies from 125 Hz to 4 kHz.....	76
Fig. 4.12 RT20 with different source-receiver distances from 15 m to 40 m, with $d_s=10$ m and $d_r=5, 10, 20, 30$ m for each tree. Each figure shows the decay curves in octave band frequencies from 500 Hz to 4 kHz .....	78
Fig. 5.1 Components of the tray.....	85
Fig. 5.2 Zinco (top) and limestone-based substrates (bottom) used in the experiment.....	85
Fig. 5.3 Pruned fresh leaves (top) and polyester cotton (bottom) used in the experiment.....	87
Fig. 5.4 Random-incidence absorption coefficient of studied substrates in dry condition .....	88
Fig. 5.5 Normal-incidence absorption coefficient of the studied substrates in dry condition.....	89
Fig. 5.6 Schematic diagrams of the cross section (top) and ground plan (bottom) for the experimental condition.....	90
Fig. 5.7 Cross-section of the modelling condition with a panel of 300 mm high .....	92
Fig. 5.8 Comparison between measured and predicted extra SPL attenuation by the panel with a 300mm height .....	92
Fig. 5.9 Predicted SPL attenuation due to the geometrical effect for a height of 130 mm according to the number of rows at two receivers with a height of 1600 mm (top) and 1000 mm	

(bottom) .....	93
Fig. 5.10 Predicted SPL attenuation due to the geometrical effect for a height of 80 mm according to the number of rows at two receivers with a height of 1600 mm (top) and 1000 mm (bottom) .....	94
Fig. 5.11 Measurement of SPL for empty trays with 5 rows .....	96
Fig. 5.12 Empty trays with plastic panels surrounding the periphery parts .....	96
Fig. 5.13 Experimental condition with different areas of the green roof system .....	96
Fig. 5.14 Experimental conditions to demonstrate the acoustic effect of vegetation with pruned fresh leaves (top) and polyester cotton (bottom) .....	97
Fig. 5.15 Measured extra SPL attenuation by the empty tray at the receiver height with 1600 mm .....	98
Fig. 5.16 Measured extra SPL attenuation by plastic panel with 80 mm and 130 mm height at the receiver height with 1600 mm.....	99
Fig. 5.17 Measured SPL attenuation with increasing area of the green roof system at two receivers with a height of 1600 mm (top) and 1000 mm (bottom) .....	100
Fig. 5.18 Difference in measured SPL between the empty tray (result in Figure 5.15) and green roof system (result in Figure 5.17) at two receivers with a height of 1600 mm (top) and 1000 mm (bottom) .....	101
Fig. 5.19 Comparison of relative SPL for the geometrical effect (predicted result in Figure 5.9, dotted line) and the geometrical+absorption effects (measured result in Figure 5.18, solid line) at the receiver height of 1600 mm. The difference in SPL between dotted and solid lines indicates the absorption effect by the substrate.....	102
Fig. 5.20 Measured SPL attenuation with different types and depths of substrates at the receiver height of 1600 mm .....	104
Fig. 5.21 Measured SPL attenuation with different types and depths of substrates at the receiver height of 1000 mm .....	105
Fig. 5.22 Measured SPL attenuation with different position of the green roof system for 1 row .....	106
Fig. 5.23 Measured SPL attenuation considering possible effects of vegetation types.....	107
Fig. 6.1 Site conditions before (left) and after (right) the refurbishment using vegetation, wood decking and street furniture .....	113

Fig. 6.2 Cross section (top) and ground plan (bottom) for the accommodation building ( <i>Unit: m</i> ) .....	114
Fig. 6.3 Cross-section of the wood decking ( <i>Unit: mm</i> ).....	115
Fig. 6.4 Ground plan of the measurement conditions: (a) Source point located at 1m from the façade; (b) Source point located in the centre.....	117
Fig. 6.5 SPL measured before and after the refurbishment according to receiver distances from the source point at 1 m from the façade.....	118
Fig. 6.6 RT20 averaged over all receiver points measured at the two different source points according to the refurbishment: (a) Source point at 1 m from the wall, (b) Source point in the centre of the courtyard.....	119
Fig. 6.7 Computer model for the courtyard before the refurbishment.....	121
Fig. 6.8 Comparison between measured and predicted data in the landscaping condition before the refurbishment: (a) Squared impulse response at the receiver point, <i>RI5</i> ; (b) RT20 averaged over 15 receiver points.....	123
Fig. 6.9 Predicted extra SPL attenuation in octave bands at three receiver points by the vegetation on the façade: (a) Ivy; (b) Green wall.....	125
Fig. 6.10 Predicted RT20 averaged over 15 receiver points according to the landscape design with and without the Ivy and green wall on the façade.....	126
Fig. 6.11 Predicted extra SPL attenuation in octave bands at three receiver points by the vegetation on the ground: (a) Grass; (b) Bedding plants.....	127
Fig. 6.12 Predicted RT20 averaged over 15 receiver points according to the landscape design with and without the grass and bedding plants on the ground.....	128
Fig. 6.13 Predicted extra SPL attenuation in octave bands at three receiver points by the combined use of the green wall and bedding plants on the façade and ground.....	129
Fig. 6.14 Predicted RT20 averaged over 15 receiver points according to the landscape design with and without the combined use of the green wall and bedding plants on the façade and ground.....	130
Fig. 6.15 Predicted extra SPL attenuation at the 1 <sup>st</sup> , 4 <sup>th</sup> and 7 <sup>th</sup> floors in the accommodation building by the three landscape designs of the inner courtyard: (a) Green wall on the façade; (b) Bedding plants on the ground; (c) Combined use of a) and b).....	131
Fig. 6.16 Predicted RT20 averaged over 3 receiver points at the 1 <sup>st</sup> , 4 <sup>th</sup> and 7 <sup>th</sup> floors in the accommodation building according to the three landscape designs using vegetation on the	

façade (green wall), ground (bedding plants), and façade (green wall)+ground (bedding plants)	132
.....	
Fig. 7.1 The studied apartment complex.....	139
Fig. 7.2 Three zones of outdoor spaces and the position of each source (S1, S2, S3, S4).....	141
Fig. 7.3 Receiver points for each source position including source-receiver distances.....	142
Fig. 7.4 Site conditions for each source position .....	143
Fig. 7.5 Impulse responses at two source-receiver distances: (a) 10 m; (b) 40 m .....	145
Fig. 7.6 Decay curves at 500 Hz according to source-receiver distance from 1 m to 120 m....	145
Fig. 7.7 RT20 measured at 3 source positions (S1, S2, S3) according to source-receiver distance, with regression curves (S1: — —, S2: — , S3: ----) and correlation coefficients $R^2$ : (a) 125 Hz; (b) 250 Hz; (c) 500 Hz; (d) 1000 Hz; (e) 2000 Hz; (f) 4000 Hz .....	147
Fig. 7.8 RT20 and EDT measured at S1, with regression curves (EDT: — —, RT20: — ) and correlation coefficients $R^2$ : (a) 500 Hz; (b) 1000 Hz .....	148
Fig. 7.9 RASTI according to source-receiver distance at S1, S2 and S3 with regression curves (S1: — —, S2: — , S3: ----) and correlation coefficients $R^2$ .....	150
Fig. 7.10 Sound attenuation according to source-receiver distance at S1, S2 and S3.....	151
Fig. 7.11 RT20 and EDT according to source-receiver distance measured at S4: (a) RT20; (b) EDT.....	152
Fig. 7.12 RASTI according to source-receiver distance at S4 with a regression curve and correlation coefficient $R^2$ .....	152
Fig. 7.13 RT20 and EDT at different floor levels: (a) RT20; (b) EDT .....	153
Fig. 7.14 RASTI at different receiver heights with S2, and a log regression and correlation coefficient $R^2$ .....	154
Fig. 8.1 Bird's-eye views for each apartment complex: (a) Site 1; (b) Site 2; (c) Site 3; (d) Site 4; (e) Site 5; (f) Site 6 .....	159
Fig. 8.2 Photographs for each apartment complex: (a) Site 1; (b) Site 2; (c) Site 3; (d) Site 4; (e) Site 5; (f) Site 6.....	160
Fig. 8.3 Ground plan and measurement zones for each apartment complex: (a) Site 1; (b) Site 2; (c) Site 3; (4) Site 4; (5) Site 5; (6) Site 6.....	161
Fig. 8.4 Illustration for the experimental condition .....	163



Fig. 8.5 Maximum, average and minimum RT20 with frequency at the 15 outdoor spaces: (a) 125 Hz; (b) 250 Hz; (c) 500 Hz; (d) 1000 Hz; (e) 2000 Hz; (f) 4000 Hz .....	164
Fig. 8.6 Overall averaged RT20 for maximum, average and minimum values measured at the 15 outdoor spaces.....	165
Fig. 8.7 Overall RT20 at 500 Hz with different source-receiver distances measured at the 15 measurement zones .....	165
Fig. 8.8 RT20 for the linear building layout: (a) RT20 at 500 Hz with different source-receiver distances; (b) RT20 with frequency at the source-receiver distance with 20 m.....	167
Fig. 8.9 RT20 for the parallel building layout: (a) RT20 at 500 Hz with different source-receiver distances; (b) RT20 with frequency at the source-receiver distance with 20 m.....	168
Fig. 8.10 RT20 for the L-shaped building layout: (a) RT20 at 500 Hz with different source-receiver distances; (b) RT20 with frequency at the source-receiver distance with 20 m.....	169
Fig. 8.11 RT20 for the U-shaped building layout: (a) RT20 at 500 Hz with different source-receiver distances; (b) RT20 with frequency at the source-receiver distance with 20 m.....	171
Fig. 8.12 RT20 for the □-shaped building layout: (a) RT20 at 500 Hz with different source-receiver distances; (b) RT20 with frequency at the source-receiver distance with 20 m.....	172
Fig. 8.13 Example of the calculation method for effective ray and openness at Z1-1 .....	175
Fig. 8.14 Relationship of RT20 with openness and averaged ray length .....	176
Fig. 8.15 Relationship of RT20 with the weighted ray length and area .....	177
Fig. 8.16 Computer model for the apartment complex studied in Chapter 7 .....	180
Fig. 8.17 Points of source and receivers .....	180
Fig. 8.18 Measured (without green wall) and predicted (with and without green wall) results at 125 Hz to 4 kHz in octave bands .....	181

## LIST OF TABLES

Table 2.1 Attenuation $A_f$ of an octave band of noise due to propagation a distance $d_f$ through dense foliage .....	22
Table 3.1 Characteristics of 264 plants of eight species providing soil vegetation coverage .....	41
Table 3.2 Physical properties of Buxus, Holly and Ivy.....	45
Table 4.1 Dimensional properties of the trees.....	62
Table 4.2 Meteorological conditions for each measurement day .....	62
Table 5.1 Product data of the sedum carpet and roof garden substrate used for Zinco substrate	85
Table 5.2 Physical properties of the Zinco substrate and limestone-based substrates .....	86
Table 5.3 Parameters considered in the experiment.....	97
Table 6.1 Absorption coefficient of the vegetation used for the computer simulation .....	123
Table 6.2 Landscape design schemes using vegetation.....	124
Table 7.1 Source-receiver distance .....	143
Table 8.1 Site and measurement conditions for each apartment complex .....	160
Table 8.2 Details for site and measurement conditions for each measurement zone .....	162
Table 8.3 Openness, averaged ray length and building height for each measurement zone .....	175
Table 8.4 Empirical formula and correlation coefficient for each parameter .....	178
Table 8.5 Empirical formula for RT20 in outdoor spaces of apartment complexes.....	179

# 1 Introduction

## 1.1 Research background

Detrimental effects of noise pollution in urban areas have become a major environmental problem in recent years. Urban noise sources appear in various forms; construction work, human endeavours, industrial activity and traffic, etc. Road traffic has been reported as the dominant noise source affecting a number of people. In the European Union, about 44 % of the population is exposed to road traffic noise levels over 55 dBA in the daytime and 20 % of the population is exposed to levels exceeding 65 dBA (Berglund *et al.*, 1999). A growing body of evidence confirms that urban noise pollution produces direct and cumulative adverse health effects such as cardiovascular disease, cognitive impairment, sleep disturbance, tinnitus and annoyance (Fritschi *et al.*, 2011). Therefore, reducing road traffic noise is an important part of improving residential, social, working, and learning environments with corresponding economic and wellbeing impacts.

Currently, typical measures for noise abatement in urban areas focus on traffic speed limits, reductions in noise exposure on the building façades through noise barriers and tunnels, improvements of window and façade insulation, and applications of low-noise road surface, etc. However, sustainable approaches to outdoor noise control have rarely been paid attention.

In urbanised cities, allocation for green spaces is a key element in addressing sustainable development but, due to the scarcity of land, urban developers are currently searching for other possible areas to plant vegetation. For this reason the greening of

building façades and the rooftops is gaining in popularity. The widespread use of vegetation on external building surfaces provides many ecological and environmental advantages. For example, the vegetated surfaces can reduce storm water runoff and the rate at which it enters surface water systems. They can increase urban bio-diversity, mitigate the urban heat island and reduce air pollution (Alexandri *et al.*, 2008; Fioretti *et al.*, 2010; Getter *et al.*, 2006; Gregoire *et al.*, 2011; Mentens *et al.*, 2006; Takebayashi *et al.*, 2007). The measures using vegetation instead of acoustically reflective surfaces (i.e., bricks, concrete, asphalts and glass) could also moderate noise pollution. Greening external building surfaces to tackle noise issues can therefore be considered as a highly sustainable goal.

## **1.2 Aims and objectives**

This study aims to investigate the effects of natural/sustainable materials on outdoor noise control in urban spaces. The main objectives can be stated briefly as follows:

- 1) Review previous works on noise reduction by vegetation (Chapter 2)
- 2) Examine the acoustic properties of low-growing vegetation (Chapter 3)
- 3) Characterise the sound scattering by a single tree (Chapter 4)
- 4) Investigate potential use of green roof systems on a low barrier (Chapter 5)
- 5) Suggest noise abatement schemes using vegetation in courtyards (Chapter 6)
- 6) Examine measurement methodology for sound propagation in an apartment complex (Chapter 7)
- 7) Examine factors affecting outdoor reverberation, and vegetation effect in various apartment complexes (Chapter 8)

### 1.3 Thesis structure

The methods to achieve the objectives for each chapter are described as follows:

Chapter 2, '*Literature Review*', presents a literature review on sound propagation in an urban environment, as well as noise reduction mechanisms by an individual or combined use of vegetation/trees/green roofs in open fields and urban situations. Firstly, sound propagation in an urban environment is covered by reviewing publications on site measurements, physical scale modelling and numerical modelling. Followed by the interaction of vegetation/trees with sound waves, including absorption, scattering (or diffusion), reflection, ground effect, and noise reduction by tree belts. Lastly publications on the effects of vegetation in urban situations on noise control are reviewed.

Chapter 3, '*Random-incidence Absorption and Scattering Coefficients of Vegetation*', describes experimental results on the characteristics of sound absorption and scattering by low-growing vegetation. This study presents the quantified data for the acoustic properties of vegetation, which can also be used in acoustic computer simulations. A series of measurements has been carried out in a reverberation chamber to examine the absorption and scattering coefficients of vegetation, by considering various factors such as: soil depth, soil moisture content and the level of vegetation coverage.

Chapter 4, '*Quantifying Scattered Sound Energy from a Single Tree by means of Reverberation Time*', is about the investigation of sound scattering by a single tree in open field. This effect is quantified by means of decay curves, closely linked to the

calculation of RT, according to the ground condition, receiver heights, tree crown shape and size, amount and condition of foliage, and source-receiver angle and distance.

Chapter 5, '*Noise Reduction using Green Roof Systems at Street Levels*', systematically explores the effects of various designable parameters of green roof systems, on a low-profiled structure on noise reduction through sound transmission. A series of measurements have been carried out in a semi-anechoic chamber using green roof systems. Numerical simulations (Finite element method) have also been carried out. Studied parameters include the structure, area, depth, type and position of the green roof system, and the type of vegetation.

Chapter 6, '*A Case Study on Controlling Sound Fields by Landscape Designs in a Courtyard*', focuses on how applicable landscape designs can contribute to noise control in a relatively small urban space, a courtyard. Through a case study, differences between courtyard sound fields were examined by in-situ measurements before and after applying a practical landscape design using vegetation, wood decking and street furniture. In addition, computer simulations were carried out to explore the acoustic effects of applicable landscape designs using vegetation, including: climbing Ivy, green wall, grass and bedding plants.

Chapter 7, '*A Preliminary Study on Acoustic Characteristics of Outdoor Spaces in an Apartment Complex*', investigates the accuracy of the measurement method using a starting pistol to examine the acoustic characteristics of outdoor spaces surrounded by multi-storey apartment buildings. In-situ measurements, in three outdoor spaces were carried out, to evaluate the acoustic parameters, including RT, EDT, RASTI and SPL distribution.

Chapter 8, '*A Parametric Study on Reverberation Time in Outdoor Spaces of Apartment Complexes*', studies the influential factors for RT in outdoor spaces surrounded by buildings with complicated topographical conditions. A series of measurements were carried out for 15 outdoor spaces in 6 apartment complexes with different building layouts. The 15 outdoor spaces were categorised into 5 types as: linear, parallel, L, U and □ (courtyard type) building layouts. An empirical method considering the openness, averaged ray length and building high was also suggested, to predict RT approximately in the outdoor spaces. Initial results showing the vegetation effect are also presented.

Chapter 9, '*Conclusions and Future Work*', concludes the thesis, summarising the new findings from the original research. Limitations and future work of this thesis are also addressed.

In summary, this thesis consists of three key parts of original research work; 1) Part I: Acoustic properties of vegetation/tree, 2) Part II: Green roof systems on a low barrier, and 3) Part III: Vegetation in urban situations. The overall structure of this study is described in Figure 1.1.

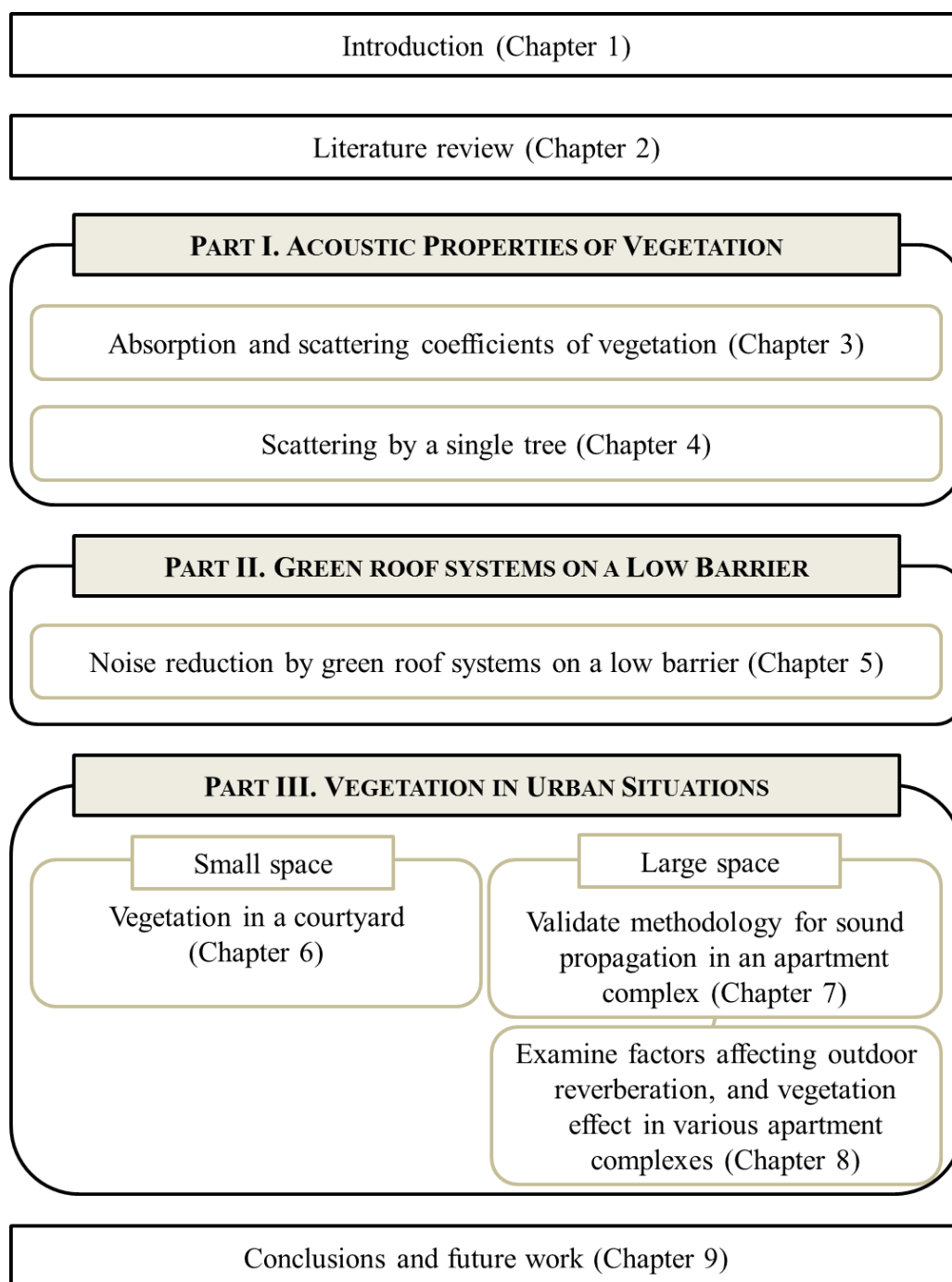


Fig. 1.1 Diagram showing overall structure of this study



## **2 Literature Review**

This chapter aims to review previous studies on outdoor sound propagation, and the individual or combined effect of vegetation/trees on noise reduction in open fields as well as urban situations. Section 2.1 reviews previous publications on sound propagation in urban environments where multipath propagation is observed. Section 2.2 reviews mechanisms for noise reduction by vegetation to reveal individual and physical aspects of the interaction between vegetation and sound waves, including absorption, scattering, reflection and ground effect. Section 2.3 covers previous studies on sound propagation through tree belts to understand the combining effects of individual trees, mainly against road traffic noise. In Section 2.4, previous works on noise control by using the natural materials such as vegetation in urban situations are addressed.

### **2.1 Sound propagation in an urban environment**

Reducing background noise levels is important to create a comfortable acoustic environment in an urban area (Berglund *et al.*, 2006; Yang *et al.*, 2005). However, outdoor background noise level is increased due to complicated physical phenomena including multiple reflections, diffraction and diffusion by building façades during sound propagation between a source and receiver. As a result, the quantification of a surrounding's influence in increasing noise levels has been an important topic. In a case where multipath propagation is observed, arrival patterns and amplitude of the reflections can be seen through an impulse response in the time domain (Albert *et al.*,

2010). The impulse response also gives useful information on decay of transient sound levels, which is closely linked to reverberation. The amount of reverberation is quantified by RT; and is defined as the time taken for the energy in an initially-steady reverberant sound field to attenuate by 60 dB, given the slope of the level function. Generally, a long reverberation time means relatively strong influence of multiple reflections on loudness in comparison with a direct sound. Furthermore, it could have an adverse effect on the perceived spatial impression and speech transmission index in urban spaces.

Due to the reasons outlined above, numerous studies have been carried out to investigate sound propagation in urban spaces through measurements and numerical modelling. This section reviews these previous studies.

### **2.1.1 Site measurements**

In the past few decades, several site measurements of sound propagation in urban spaces have been conducted since the first work performed in 1940s to determine an optimal location of air raid sirens (Ball, 1942; Jones, 1946; Volkmann *et al.*, 1942). In terms of the sound propagation in streets, Wiener *et al.* (1965) conducted the first measurements on both noise level and reverberation as well as speech intelligibility. In 1970s, Aylor *et al.* (1973) measured reverberation in a city street to investigate the absorption coefficients of ivy grown on building façades. Sound field in built-up areas was also measured by the researchers (Steenackers *et al.*, 1976; Yeow, 1976, 1977). Ko and Tang (1978) attempted to predict reverberation in built-up areas using an empirical method based on the bounded volume, which shows the proportional relationship between the

reverberation and the volume bounded by the buildings. Picaut *et al.*(2005) also carried out a systematic measurement in a street canyon by considering source-receiver distance, source height and back scattering effect, etc. The recent measurement result (Mijic *et al.*, 2012) shows that reverberation in urban spaces can be as long as 7, or more sec due to multiple reflections. The results from the previous works can be summarised as follows; noise levels and reverberation in urban areas are increased by multiple reflections which are influenced by many factors such as boundary conditions, topological conditions, source-receiver distances, street width, building height, and gaps between buildings, etc.

### **2.1.2 Physical scale modelling**

Experiments using scale modelling have also been carried out to investigate sound propagation in urban spaces. In comparison with computer simulation, a notable advantage of scale modelling is that some complex acoustic phenomena such as diffraction and diffusion by buildings can be examined more accurately. Scale modelling can also investigate the factors affecting sound propagation in urban spaces under a more controlled environment compared with full-scale measurements. Due to the reasons above, several laboratory measurements using scale modelling has been conducted to investigate the role of multiple reflections, diffusion, absorption and diffraction by building facades on sound propagation in urban areas (Delany *et al.*, 1972; Horoshenkov *et al.*, 1999; Ismail *et al.*, 2005; Iu *et al.*, 2002; Kang, 1996b; Kerber *et al.*, 1981; Lyon, 1974; Mulholland, 1979; Picaut *et al.*, 2001).

### **2.1.3 Numerical modelling**

Many investigations have attempted to develop theoretical and numerical models of sound propagation in urban areas using an image source model or a diffuse reflection model; as well as, wave-based models including: acoustic finite element method (FEM), boundary element method (BEM), finite difference time domain method (FDTD) and parabolic equation (PE) method. The development of theoretical models for sound propagation in urban areas was conducted in the 1970s by several researchers (Lee *et al.*, 1975; Lyon, 1974; Schlatter, 1971; Steenackers *et al.*, 1976). However, these early studies ignored the possibilities of ground interference and a diffusion effect between two parallel walls. Kang (2000, 2002b, 2005) investigated acoustic parameters such as: RT, EDT and sound attenuation in urban streets and squares through the comparison of geometrical and diffuse boundary conditions using image source and radiosity methods. The results showed that the RT and sound attenuation in a single street canyon depends on boundary conditions, and in particular, the importance of façade diffusion in urban spaces was demonstrated. Kang (2001, 2002a, 2002d, 2007) also investigated the effect of architectural and urban design on the sound field, including boundary absorption, boundary pattern and building arrangement. Using a scale model measurement, Ismail and Oldham (2005) suggested that the scattering coefficient of building façades with irregular surfaces is relatively low with a range between 0.1 and 0.15 for the configurations tested. Through a simplified model, Onaga and Rindel (2007) estimated the sum of absorption and scattering coefficients of facades in urban streets were within the range of 0.1 to 0.25.

## **2.2 Noise reduction mechanisms by vegetation**

In the last few decades, studies on sound propagation through vegetation/trees have been a popular research topic, since the pioneering work by Eyring (1946). Since then, there have been a number of studies to demonstrate the effect of vegetation on noise reduction. Various numerical and experimental methods have also been used to investigate and characterise the influential factors affecting sound propagation through forests and vegetation. In summary, previous works suggest that absorption, scattering, reflection and ground effect by vegetation play an important role in sound propagation through vegetation. An additional effect is, while atmospheric refraction leads to higher sound levels over grassland, the levels in forests are comparatively unaffected. (Swearingen *et al.*, 2007; Tunick, 2003).

The way vegetation affects sound propagation can generally be split into three different frequency ranges (Cox, 2009). At low frequencies, ground effect, which is the result of interference between direct and ground-reflected sound is dominant. The scattering effect from trunks, branches and leaves is small due to their relatively small size in comparison with the wavelength. In addition to this, absorption from the leaves themselves is negligible at these low frequencies. At mid frequencies, around 1 kHz, the trunks and large branches begin to scatter the sound energy. At high frequencies, typically above 1 kHz, scattering is still important, and in addition, the foliage attenuates the sound by viscous friction. Publications related to each mechanism have been reviewed in detail in the following sections.

### **2.2.1 Absorption**

Sound energy impinging on soil and leaves is absorbed by thermo-viscous effects at the

surface. Furthermore, an individual leaf contributes to the sound attenuation by its compliant mechanical vibrations at certain resonant frequencies, thus dissipating the sound energy into heat (Martens *et al.*, 1981).

Previous studies examined the vibration velocity of leaves using a laser vibrometer system and accelerometer in anechoic chambers. Martens and Michelsen (1981) measured the vibration of leaves for four plant species: *Ligustrum*, *Betula*, *Corylus* and *Quercus*. Similar measurements utilising a light-weight accelerometer were carried out by Tang *et al.* (1986) on the leaves of six plant species: *Acalyphia*, *Ficus*, *Lonicera*, *Cratoxylon*, *Lonicera* and *Erythrina*. Embleton (1963) also used accelerometers to study oscillations of branches.

Embleton (1963) measured oscillations of branches of deciduous trees at 300 Hz for lower (big) branches. Near the top of a tree, smaller branches appear and resonance frequencies were measured up to 1100 Hz. These frequencies were inversely proportional to the branch length.

Martens (1981) suggested that leaves behave as linear systems when driven by sound and noise at SPL up to 100 dB. The experimental results indicated that the re-emission of sound from a leaf is very small for two reasons. Firstly, the vibration velocity of the leaves is smaller than the vibration velocity of the air particles. This means that only a part of the sound energy reaching the leaf will cause the leaf to vibrate. The other part of the sound energy is reflected and diffracted around the leaf. Secondly, the complex vibration mode of a leaf causes the different areas of the leaf to be out of phase, cancelling the pressure variation generated by these areas. As a result, the sound energy

causing vibrations in a leaf is effectively absorbed by the leaf tissue and converted into heat.

Tang (1986) showed the vibrational modes of leaves clustered into two groups by simplifying the frequency-absorption curves to two superimposing Gaussian curves. The first group of modes is associated with the length of the leaves, and the second group of modes is linked to the width of the leaves. Correspondingly, these modes generate the longitudinal and transverse vibrations of the leaf with two-dimensional surface. The lower frequency Gaussian curve is related to the longitudinal vibration mode while the upper frequency curve is induced by the transverse mode. It seems that the transverse mode is more pronounced, leading to a higher degree of absorption. Given the dimensions of the leaves of typical trees, sound waves lower than 1 kHz do not excite such vibrations so that for frequencies below 1 kHz there is little sound absorption.

Few studies have also measured the effects of vibrations and thermo-viscous absorption of leaves, trunks and branches in reverberant situations. Burns (1979) discusses effects of thermo-viscous absorption and resonances of branches and needles in parts of pine trees. The branch velocity was smaller than the air particle velocity. Fundamental needle resonances were measured at very low frequencies, from 4 Hz (8 cm needles) to 49 Hz (2.3 cm needles).

Aylor (1973) examined the effect of Ivy covered on the facades in a street canyon on reverberation. The experimental result showed that the effect of the ivy on reverberation in the street was negligible except around 4 kHz. For a sound frequency of 4 kHz, an

effective absorption coefficient was calculated as 0.5. It was expected, however, that this effect could also be attributed to increased scattering by the ivy.

Yamada (1996) measured absorption coefficients of four kinds of trees in a reverberation chamber; two conifers and two broad leaves, were used in the measurements. It has been shown that the absorption coefficient values of the broadleaf are comparatively greater than those of the conifers. Results showed that acoustic attenuation is independent of the leaf surface area and mainly derived from the leaves and not the trunk. It was also shown that the absorption coefficient increases proportional to the square of the frequency. The maximum absorption coefficient of the trees was approximately 0.2 at 10 kHz.

Wong *et al.* (2010) examined the absorption coefficient of vertical greenery systems with 10 m<sup>2</sup> area of vegetation in a reverberation chamber. The vertical greenery system consisted of plants called *Nephrolepis exaltata* in pots and wooden frames. With different greenery coverage (41 %, 71 % and 100 %), the pots were placed within wooden frames. Results showed that the absorption coefficient is increased with increasing greenery coverage at all frequencies (100 Hz to 5 kHz). At low frequencies, the differences in sound absorption coefficients between different greenery coverage are small, while after 1 kHz, the differences in sound absorption coefficients were found to be fairly constant.

Random-incidence absorption coefficients of some common outdoor materials were also measured in a reverberation chamber by Kaye (1940). This study investigated the absorption coefficients of gravel, turf, sand, ashes, railway-track ballast and snow with



10 feet × 10 feet specimen size. The results showed that the absorption coefficients are increased with increasing frequency. The absorption coefficient values were found to be relatively high.

Reethof (1977) measured normal incident absorption coefficients of tree bark using an impedance tube. Six species of the tree bark were tested: *Quercus rubra*, *Carya*, *Fagus*, eastern white pine, eastern hemlock and *Quercus subra*. It was seen that the absorption coefficients were generally less than 0.1 at frequencies between 400 Hz and 1.6 kHz. For most species, the absorption coefficients are frequency independent.

### **2.2.2 Scattering and reflection**

Sound is reflected and scattered by all parts of vegetation/trees such as leaves, twigs, branches and trunks. The amount of scattering increases with increasing frequency, and becomes an important factor in acoustic propagation when the wavelength approaches the size of the scattering/reflecting obstacles.

In an anechoic chamber, Martens (1980) measured sound transmission through four model forest situation. Three models consisted of three different plant species, and the fourth model forest consisted of a mixture of tropical plant species. In this experiment, sound attenuation mainly by scattering effect was measured even though even in the presence of a small degree of absorption effect. SPL in absence of vegetation were compared to the situations with vegetation. The main conclusion of this work was that plant canopies can act as sound amplifier in the mid frequencies. Starting from 2 kHz, a rapid increase in the sound attenuation was observed by 10 dB at 4 kHz, depending on

the mixture of species.

Martens *et al.* (1985) studied the sound reflection of a plant leaf by comparing an aluminium disc. Furthermore, the plant leaf reflection was measured as a function of leaf mass. The result indicated that the reflection of the leaf and the aluminium disc are linearly dependent on frequency. The reflection of a plant leaf was dependent on leaf mass. It was concluded that leaf dimension and leaf mass are important parameters for sound reflection of a plant leaf.

Price *et al.* (1988) predicted the sound attenuation by the scattering effect of trunks and foliage in woodland; this work used an empirically modified multiple scattering approach by reducing the number density of trees by 60% to obtain a better fit to data. Trunks and foliage were represented by perfectly reflecting large and partly absorbing small vertical cylinders, respectively. This worked reasonably well in predicting the shape of the attenuation spectrum. But it is necessary to adjust several parameters to predict the levels accurately. For example, the density, surface impedance, and radius of the small scatterers representing the acoustical effect of the foliage were adjusted to fit the measured attenuation data. It was found that foliage has an important effect above 1 kHz and the foliage attenuation increased approximately in a linear fashion with frequency.

Lyon *et al.* (1977) carried out field studies and laboratory scale-model experiments to investigate the effect of trees on scattered sound energy. Field studies were undertaken measuring sound propagation through a line of maple trees in leaf and leafless condition. The measurement results showed that observed spectra with and without

leaves begin to diverge above 2.5 kHz, corresponding to a wavelength of the leaf size. It was also found that at the position below the canopy, leaves scatter some additional high-frequency sound to the microphone, resulting in reduced or even negative attenuation. Scale-model experiments were conducted to study interaction between sound scattering by trees and shadowing by barriers. It was shown that planting a single row of trees on top of a barrier can have a negative effect in the barrier's effectiveness.

Experientially, the well-audible reverberation in a forest demonstrates the scattering effect of the trees and branches. There have been few attempts to measure reverberation within forests and to relate such measurements to theoretical predictions. Huisman *et al.* (1991) dealt with scattering by tree trunks using a stochastic particle bounce model, and found acceptable agreement between measurement and theory even though the theoretical model was inadequate at mid frequencies and higher receiver positions.

Padgham (2004) measured the reverberation decay and frequency attenuation within two forests. The results showed that source-receiver distance is the most influential factor affecting rate of reverberation decay. Generally, the RT was increased with the decrease of source-receiver distances. Between 1 and 3 kHz, reverberation varied relatively little with source-receiver distances in comparison with other frequencies. Increasing the source height generally reduces reverberation, while increasing the receiver height generally reduces attenuation.

### **2.2.3 Ground effect**

Sound propagation above ground is influenced by the acoustical properties of the

ground surface. The porous ground surface absorbs sound energy, and changes the phase and amplitude. Thus, there is interference between direct and ground reflected sound, known as the ground effect, which is dependent on the acoustic properties of the ground, the position of the source and receiver (Cox, 2009).

The ground effect results in constructive and destructive interference causing increase and decrease of SPL, respectively. For acoustically rigid surface (i.e., concrete and asphalt), the amplitude of sound is increased or decreased due to the strong interference effect. For porous surfaces (i.e., soil, sand, grass and snow), the ground effect can influence at relatively low frequencies. However, at high frequencies, sound can be absorbed through porous ground so the surface reflection is changed in phase and amplitude (Attenborough, 1988).

In a forest, the ground effect could be more important at low frequencies due to decomposing vegetation on the floor. Thus, the ground effect in a forest gives an excess attenuation maximum at low frequencies. This phenomenon often causes an insignificant effect of tree belts alongside traffic road on noise reduction as a constructive interference is appeared at around 1 kHz for traffic noise (Attenborough *et al.*, 2007).

## **2.3 Noise reduction by tree belts**

### **2.3.1 Measurement results**

It is generally stated that trees have no practical part to play in noise control (Kragh, 1981; Tang *et al.*, 1988). Kragh (1981) concluded that tree belts near the roads with a

width between 3 and 25 m result in only little attenuation for traffic noise. Tang and Ong (1988) also reported that trees in an urban canyon do not significantly influence traffic noise at ground level. However, it has been demonstrated that tree belts can cause sound reduction compared with open grassland, provided a wide tree belt is used, say greater than 30 m (Reethof, 1973).

Aylor (1972) made a series of measurements to look at sound propagation over dense reeds (*Phragmites*), above a water surface. Ground attenuation can therefore be easily calculated. It was concluded that vegetation should be dense and broadleaf would attenuate noise effectively.

Huisman *et al.* (1991) showed how the sound from a typical traffic noise spectrum is attenuated by the presence of a 100 m tree belt of pine trees and open pasture, in comparison with the free field level. The pine forest attenuated the overall A-weighted sound level by 10 dB more than the pasture.

Pal *et al.* (2000) measured the extra attenuation in eight tree belts near two coalfields, and found that the average density and height of the plants has only a limited effect on the noise reduction. Larger plant heights could even be negative, probably due to increased downward scattering towards receivers. Vertical and horizontal light penetration was found to be major parameters. The excess attenuation by the tree belts with a depth of 50 m was 3.3-6.0 and 3.6-5.7 dBA in the two coalfields, respectively.

Fang *et al.* (2003) measured the noise reduction effect of 35 evergreen tree belts using a speaker generating traffic noise spectrum at 1.2 m high. Factors affecting the noise

reduction included visibility, width, height and length of the tree belts. Multiple regression analysis on the measured data showed that the visibility and width of the tree belts were the major parameter determining the extra attenuation, while height and length of the tree belts were the less significant factors affecting the noise reduction. The overall results showed that with low visibility and high density of tree belts, extra 9 dBA attenuation can be achieved or more at 20 m source-receiver distance. However, this result seems to be overestimated due to the use of a point source at 1.2 m high which is not a true reflection of traffic noise, which would normally be represented by a line source.

The measurement result from the work by Tyagi (2006) showed that tree belts with a depth of 15 m can provide an extra attenuation at 3.15 kHz in one-third octave bands more than 24 dB. At low frequencies between 315 Hz and 400 Hz, the extra attenuation was observed by 16 dB.

Van Renterghem *et al.* (2012) applied the 3D-finite difference time-domain method to predict sound propagation through an infinitely long and 15 m deep vegetation belt along a traffic road. The results showed that the presence of a forest floor alone, compared to sound propagation over grassland, reduces traffic noise level by around 3 dBA. With increasing tree stem diameter, traffic noise was decreased. It was found that spacing parallel to the road was important in determining road traffic noise shielding. With reference to grassland, shrubs gave an average road traffic noise insertion loss of 4.7 dBA. It was also estimated that downward scattering from tree canopy has negative effect from -0.8 to -0.4 dBA.

It has been shown that strategic tree and shrub arrangements are important for the effective noise reduction. In linear and random arrangements of trees, the noise reduction by scattering of trunks and branches could be relatively small in comparison with well-planned arrangements like sonic crystals (Umnova *et al.*, 2006). Sonic crystals could be formed from trees, since trees can be arranged in periodic arrays. At mid-frequencies around 1 kHz, a part of trees including trunks and branches begin to scatter the sound out of the path between source and receiver. Due to the constructive interference by the ground effect, however, it has been seen that there is little difference in the attenuation between the grassland and forest. Therefore, it has been suggested that, by arranging the trees in particular arrangements to form sonic crystals, it could lead to the reduction in transmitted sound at these crucial mid-frequencies (Martínez-Sala *et al.*, 2006).

### **2.3.2 Prediction schemes**

In prediction schemes for outdoor sound propagation such as ISO 9613-2, Nord 2000 and Harmonoise, the excess attenuation by a forest is estimated using empirical and semi-empirical methods.

ISO 9613-2 (ISO, 1996) gives the attenuation values in Table 2.1 for sound propagation through dense foliage. For distances less than 20 m, the values given are absolute dB. For distances between 20 and 200 m, the values given are dB/m and for distances greater than 200 m, the value for 200 m is used. However, measured attenuation rates are greater than predicted one according to ISO 9613-2 (Attenborough *et al.*, 2007).

Nord 2000 (Kragh *et al.*, 2002) allows for prediction of sound propagation through forests by considering two main effects. This model takes account of the reduced coherence between direct and reflected sound at mid frequencies and the attenuation effect at high frequencies. Tarrero *et al.* (2008) showed that predicted reduction of the ground effect dip due to loss of coherence is in reasonable agreement with the experimental results. At high frequencies, however, the agreement was poor in most cases.

Table 2.1 Attenuation  $A_f$  of an octave band of noise due to propagation a distance  $d_f$  through dense foliage

	Octave band centre frequency (Hz)							
	63	125	250	500	1000	2000	4000	8000
$A_f$ (dB) for $10\text{m} \leq d_f \leq 20\text{m}$	0	0	1	1	1	1	2	3
$A_f$ (dB/m) for $20\text{m} \leq d_f \leq 200\text{m}$	0.02	0.03	0.04	0.05	0.06	0.08	0.09	0.12

## 2.4 Vegetation in urban situations

### 2.4.1 Measurement and prediction results

Use of green spaces instead of impervious surfaces is becoming important to improve sustainability of cities. Greening urban spaces with vegetation such as green roofs and walls provides numerous ecological and economic benefits, including stormwater management, energy conservation, mitigation of the urban heat island effect, and increased longevity of roofing membranes, as well as providing a more aesthetically pleasing environment in which to work and live (Getter *et al.*, 2006). Recently, there have also been attempts to investigate the acoustical benefits of greening buildings and



urban spaces (Connelly, 2011; Tang *et al.*, 1988; Van Renterghem *et al.*, 2008a, 2009, 2011; Van Renterghem *et al.*, 2013; Wong *et al.*, 2010).

The presence of acoustically hard materials in urban areas (asphalts, bricks, concrete, windows, etc.) leads to the increase of noise levels and reverberation due to multiple reflections between buildings (Aylor *et al.*, 1973; Kang, 2000, 2005; Ko *et al.*, 1978; Lyon, 1974; Mijic *et al.*, 2012; Picaut *et al.*, 1999; Steenackers *et al.*, 1976; Wiener *et al.*, 1965; Yeow, 1976, 1977). The results from the previous works can be summarised that reverberation in urban spaces can be as long as over 7 sec with reverberation gain of 2-7 dB (Mijic *et al.*, 2012) due to multiple reflections which are influenced by many factors such as boundary conditions, topological conditions, source-receiver distances, street width, building height, and gaps between buildings, etc. These results imply the possibilities of vegetated roofs, walls and ground to urban streets, squares and roadside courtyards for noise abatement.

In urban contexts, natural and sustainable materials including trees, shrubs, bushes, grass and seasonal flowers represent the common vegetation growing on the ground. Recently, the concept of greening in cities has been extended to roof and vertical gardens on buildings by means of green roofs and walls.

Green roofs are vegetated layers sitting on top of the conventional waterproofed roof surfaces of a building. The type of green roofs can be categorized as intensive or extensive, depending mainly on the depth of the growing medium. Extensive green roofs (see Figure 2.1) are composed of lightweight layers of free-draining material that support low-growing, hardy, drought-tolerant vegetation. The depth of the growing

media is less than 15 cm. Intensive green roofs consist of large perennial herbaceous plants and, occasionally, shrubs and small trees. The depth of growing media on an intensive green roof is usually over 20 cm (Dunnett *et al.*, 2004).

A green wall is defined as a structure which is placed on building façades with vegetation. Green walls include green facades consisting of climbing leafy plants growing on a wall. Another type of green wall (see Figure 2.2) is the ‘living wall’ consisting of modular steel containers, geotextiles, irrigation systems, a growing medium and vegetation. Greening buildings with green roofs and walls can provide improved visual appearance especially in urban settings. They can also provide a habitat for wildlife including birds and beneficial insects. In comparison of roofs and walls consisting of concrete and glass, acoustic properties of green roofs and walls are rather absorptive and diffusive. Through sound absorption on the greening surface, green roofs and walls also have the potential to reduce urban noise pollution.



Fig. 2.1 Extensive green roof on top of a building at the University of Sheffield



Fig. 2.2 Modular of the green wall containing substrate (left) and an example of the application (right). Copyright of the figures: Canevaflor, <http://www.canevaflor.com>

Vegetation could be more effective in urban areas such as street canyons and squares where a strong amplification of the emitted sound from road traffic noise is observed due to multiple reflections. The increased sound levels could be reduced by replacing geometrically reflecting surfaces with absorptive and diffusive vegetation. In urban courtyards, the amount of sound energy propagating over rooftops from noisy sides to quiet sides is mainly determined by the height, width and shape of buildings (Hornikx *et al.*, 2007, 2009; Kang, 1996c; Van Renterghem *et al.*, 2006). In this case, green roof systems on top of buildings can act as absorbers especially for diffracted sound waves between parallel streets and for that, parametric studies have been carried out (Van Renterghem *et al.*, 2008a, 2009, 2010, 2011), showing that green roof systems are effective on noise mitigation, and therefore creating quiet sides. Moreover, it has been shown that green roofs can be used to effectively increase the sound insulation of light-weight roof structures (Kang *et al.*, 2009).

Van Renterghem and Botteldooren (2008a) predicted sound propagation over intensive and extensive green roofs on a building between street canyons by using the finite-difference time domain method. The result showed that the presence of a green roof results in an important decrease in SPL at the non-exposed side of a building. The effect of a green roof, relative to a rigid one, increases with increasing octave band centre frequency, and amounts to 10 dB decrease at 1000 Hz. The width-height ratio of the street canyon has only a limited influence. A good overall efficiency is observed near the maximum layer thickness of extensive green roofs, which is between 15 and 20 cm. With a substrate layer thickness exceeding 20 cm, positive effects are not influenced anymore by substrate thickness.

For the different building configurations, the effect of green roofs in reducing total A-weighted road traffic noise level was predicted according to the traffic speed (Van Renterghem *et al.*, 2009). It was found that a green roof in a terrace-like configuration reduced road traffic noise level by approximately 5 dB, just above the terrace level. In a street canyon configuration, the acoustical façade load in the non-exposed canyon is largely influenced by both the roof slope and the presence of a green roof. With increasing traffic speed, the green roof effect increases for light vehicles rather than heavy vehicles.

In-situ measurements of sound propagating over flat, extensive green roofs showed that green roofs may lead to a useful sound reduction at locations where only diffracted sound waves arrive (Van Renterghem *et al.*, 2011). Among the single diffraction cases, green roofs reduced sound levels by 10 dB, over a wide frequency range. For the double

diffraction cases, positive effects in reducing noise levels were found up to 10 dB.

## **2.5 Summary (Justification for the research work)**

### **2.5.1 Acoustic properties of vegetation (Chapter 3)**

Previous studies reviewed above examined absorption and scattering properties of vegetation, usually by means of free field and impedance tube methods. In acoustic computer simulations, based on ray tracing and radiosity, however, random-incidence absorption coefficient could be more appropriate acoustic properties for predicting diffuse sound fields accurately, rather than normal-incidence absorption coefficient (Cox, 2009). Unfortunately, up to now only limited measurements have been carried out using vertical greenery systems (Wong *et al.*, 2010), gravel, turf, sand, snow (Kaye *et al.*, 1940) and bedding plants (Smyrnova *et al.*, 2010) in a reverberation chamber. Moreover, it is still essential to characterise the absorption coefficient of each of the components such as soil and leaf systematically.

Random-incidence scattering coefficient, the ratio between non-specularly reflected sound energy and total reflected energy from boundaries, has been well recognised as an essential factor for improving the accuracy of sound field predictions (Zeng *et al.*, 2006). Previous studies on sound propagation in urban spaces such as street canyons (Kang, 2000) and urban squares (Kang, 2005), also suggest that scattering properties of boundaries, such as building façades play an important role in determining the acoustic parameters such as RT. Therefore, the random-incidence scattering coefficient of vegetation becomes more important as it is increasingly grown on building façades and

the neighbouring ground. Unfortunately, no previous data for the scattering coefficient of vegetation have been found.

Therefore, Chapter 3 examines random-incidence absorption and scattering coefficients of vegetation through a series of measurements in a reverberation chamber in order to characterise the effects of various designable factors such as soil depths, soil water content and vegetation densities.

The use of green walls has become popular as a tool for sustainable urban developments. However, few studies have attempted to measure acoustic properties of green walls. In Chapter 3, therefore, a series of measurements in a reverberation chamber has been conducted to examine the absorption coefficient of a green wall without vegetation by considering different moisture contents.

### **2.5.2 Sound propagation through a single tree (Chapter 4)**

Although previous works reviewed above have been carried out in forests (groups of trees), it is important to examine sound scattering by a single tree. This is useful to validate theoretical models for predicting sound propagation through forests. In reverberant urban spaces such as street canyons and courtyards, it is also expected that trees might influence acoustic characteristics including RT and sound level distribution. Information on the reverberation effect from a single tree would be useful for a better understanding of acoustic effects of trees in urban environments.

In Chapter 4, therefore, a series of measurements are carried out to investigate the effect of a single tree in open field on sound scattering and reverberation, and to examine what

parameters are relevant.

### **2.5.3 Acoustic effect of green roof systems (Chapter 5)**

As reviewed above, natural and sustainable materials can be a useful tool to moderate noise pollution in urban areas. Previous studies showed that green roof systems can reduce noise levels for diffracted sound waves between parallel streets. At street level, various kinds of green roof systems can also be used, for example, on the top of underground car parking spaces. In particular, semi-extensive green roof systems can be installed in many places instead of grass land at street level due to various reasons such as better visual effects and maintenance. There is a potential that green roof systems on low barriers can be developed to an innovative and sustainable low barrier using natural materials for reducing traffic noise. However, studies on the use of green roof systems at street level have not been reported yet. In Chapter 5, therefore, a series of measurements in a semi-anechoic chamber has been carried out to explore systematically the effects of various designable parameters of green roof systems on a low barrier at street level on noise reduction.

### **2.5.4 Effect of landscape designs in courtyards on noise reduction (Chapter 6)**

Some previous studies estimated the effects of green roof systems on rooftops in reducing traffic noise through case studies, which is helpful to create quiet side. On the other hand, when background noise from external spaces is reduced, sounds from within an outdoor space in residential buildings (i.e., courtyard) such as from social activities and conversation could become more important as sources of noise annoyance. Therefore, it is useful to study methods employing landscape designs to reduce sound

energy propagation within small and large outdoor spaces in residential buildings. To estimate the effect of vegetation in controlling sound field in relatively small outdoor spaces, Chapter 6 investigates the acoustic effect of landscape designs using vegetation through a case study in a courtyard located in an accommodation building.

### **2.5.5 Acoustic characteristics in outdoor spaces of residential areas (Chapter 7&8)**

As reviewed above, previous studies focused mainly on sound propagation in urban street and squares. As with street canyons and urban squares, reducing noise levels and reverberation in outdoor spaces of residential areas could be more important. The reasoning behind this is that residents require environments with a high level of acoustic comfort due to their long-term and frequent use. In many countries, a percentage of the population lives in multi-storey apartment buildings due to the scarcity of available land space. In Korea, in particular, it is estimated that over 50 % of dwellings are multi-storey apartment buildings. Therefore, it is still necessary to carry out further research on acoustic characteristics of outdoor spaces in apartment complexes. In Chapter 7 and 8, a series of field measurements have been conducted to characterise the factors affecting sound fields in outdoor spaces of apartment complexes.

In Chapter 7 and Chapter 8, the acoustic characteristics of relatively large outdoor spaces in apartment complexes have been measured, with particular interests in SPL attenuation and reverberation. On a basis of the measurement results, noise reduction effects of vegetation placed in outdoor spaces of apartment complexes have been predicted by using acoustic computer simulations in Chapter 8.



**PART I.**

**ACOUSTIC PROPERTIES OF VEGETATION AND TREES**

### **3 Random-incidence Absorption and Scattering Coefficients of Vegetation**

The aim of this chapter is to examine random-incidence absorption and scattering coefficients of vegetation through a series of measurements in a reverberation chamber in order to characterise the effects of various designable factors such as soil depths, soil water content and vegetation densities. It begins with a description of the research background in Section 3.1. In Section 3.2, measurement and calculation methods for those coefficients are explained. In Section 3.3, measurement results are described as: 1) absorption coefficient of soil with and without vegetation, 2) absorption and scattering coefficients of leaves and stems, and 3) absorption coefficients of the green wall. In Section 3.4, key findings of this research work are addressed.

#### **3.1 Introduction**

The greening of buildings and surrounding spaces is important for sustainable urban design (Jim, 2004). A previous study suggested that environmental impact can be reduced with a better selection of acoustic materials/components (Yu *et al.*, 2009), and as acoustically sustainable materials, vegetation can be placed on building façades, roofs, or at ground level, which all might influence the sound fields (Van Renterghem *et al.*, 2008a; Wong *et al.*, 2010). It was shown that vertical greenery systems are effective in reducing sound levels as well as absorbing sound energy (Wong *et al.*, 2010). Also, green roof systems on rooftops can reduce noise levels by over 10 dB over a wide frequency range (Van Renterghem *et al.*, 2008a). At street level, green roof systems can be used as vegetative low barriers (see Chapter 5 of this thesis). In terms of subjective

evaluation, this in turn can also contribute to reducing noise annoyance and improving soundscape (Veisten *et al.*, 2012). It is therefore important to examine systematically how vegetation can absorb and scatter sound.

Previous studies suggest that vegetation can absorb and scatter sound through ground effect, thermo-viscous absorption at the soil and at the surface of leaves, scattering by stems and leaves, and damping by vibrating vegetation elements (Attenborough, 1988; Martens *et al.*, 1981; Martens *et al.*, 1985; Price *et al.*, 1988; Tang *et al.*, 1986). Price *et al.* (1988) found that scattering by foliage can contribute to noise attenuation especially above 1 kHz. Martens *et al.* (1985) studied acoustic reflection characteristics of deciduous plant leaves, showing the importance of leaf dimension and leaf mass for sound reflection. Measurements for leaf vibration induced by sound showed that absorption from leaves is important at high frequencies above 1 kHz, whereas below 1 kHz there is little sound absorption from leaves (Martens *et al.*, 1981; Tang *et al.*, 1986). Ground effect is the result of interference between the direct sound and reflection from the ground. In a forest, particularly, this results in a more pronounced noise reduction at low frequencies due to a porous layer consisting of decomposing vegetation on the ground (Attenborough, 1988).

To characterise each mechanism, sound absorbing and scattering properties of vegetation were examined, usually using the free field and impedance tube methods. Although free field data can be converted to random-incidence coefficients approximately using theoretical models (Makita *et al.*, 1988), they are based on an idealised situation and thus, it is still necessary to carry out direct measurements in a diffuse sound field where sound is likely to be incident from all directions onto

boundaries. In acoustic computer simulations, based on ray tracing and radiosity, for example, random-incidence absorption coefficient is one of the important acoustic properties needed for predicting sound fields accurately (Cox, 2009). Unfortunately, up to now only limited measurements have been carried out using vertical greenery systems (Wong *et al.*, 2010), gravel, turf, sand, snow (Kaye *et al.*, 1940) and bedding plants (Smyrnova *et al.*, 2010) in a reverberation chamber. Moreover, it is still essential to characterise the absorption coefficient of each of the components such as soil and leaf systematically.

In room acoustics, random-incidence scattering coefficient, the ratio between non-specularly reflected sound energy and total reflected energy from boundaries, has been well recognised as a factor for improving the accuracy of sound field predictions (Zeng *et al.*, 2006). Previous studies on sound propagation in urban spaces such as street canyons (Kang, 2000) and urban squares (Kang, 2005) also suggest that scattering properties of boundaries such as building façades play an important role in determining the acoustic parameters such as RT. In internal spaces with acoustic defects such as echoes and long reverberation, selecting suitable scattering properties of boundaries is also important to improve speech intelligibility (Kang, 1996a, 2002c). Therefore, the random-incidence scattering coefficient of vegetation becomes more important as it is increasingly grown on building façades and the neighbouring ground. Unfortunately, no previous data for the scattering coefficient of vegetation have been found.

The aim of this chapter is therefore to examine random-incidence absorption and scattering coefficients of vegetation through a series of measurements in a reverberation chamber in order to characterise the effects of various designable factors such as soil

depths, soil water content and vegetation densities. Such data are also useful for acoustic computer simulations. The absorption coefficient of soil without vegetation was measured with different levels of soil depth and moisture content. The combined effect of soil and low-growing vegetation on the absorption coefficient was also investigated with different vegetation densities. Then the absorption and scattering coefficients of the aboveground vegetation components only (i.e., without the effect of soil and roots), such as stems and leaves, were measured using three different plant species, considering different levels of vegetation coverage. Finally, the absorption coefficient of a green wall without vegetation was measured, considering different moisture contents.

## **3.2 Methodology**

### **3.2.1 Measurement method**

Random-incidence absorption coefficient was measured and calculated according to ISO 354 (ISO, 2003) in a reverberation chamber of 216 m<sup>3</sup>. A 01dB acquisition system was used, connected to a 01dB DO12 omni-directional speaker with a M700 power amplifier and two ½” microphones (G.R.A.S type MCE 201) with 01dB-Stell Pre 12H preamplifiers. An MLS (maximum length sequence) signal was generated for the measurement. RTs in one-third octave bands were averaged over 12 source-receiver positions (three source and four receiver positions) and three repeated tests for each source-receiver position. The RT was calculated with the decay curve between 5 dB and 25 dB from the initial level, using the DIRAC analysis program from B&K (2010) which has a noise compensation function to reduce the effect of background noise on RT calculation. The signal to noise ratio was greater than 46 dB across frequencies in an

unweighted value.

Measurements for random-incidence scattering coefficient were carried out based on ISO 17497-1 (ISO, 2004). The principle of the measurement method is to extract the specular energy by synchronised (phase-locked) averaging of the impulse responses obtained for different sample orientations. By synchronised averaging of the pressure impulse responses, the specular components add up in phase, whereas the scattered sound interferes destructively. To obtain impulse responses for different sample orientations, the scattering coefficient is measured using a circular rotatable turntable. The turntable used in this chapter has a 3 m diameter baseplate of area  $7.07 \text{ m}^2$  over an air gap of 220 mm to mount a drive motor. Made from 18 mm thick plywood, the baseplate is mounted on a central bearing and is supported by twelve wheels. A perimeter wall of height 200 mm constructed from 12 mm thick MDF board is attached to the baseplate and the inside has a waterproof liner made from 1 mm thick EPDM rubber. To determine the impulse response from which the RT can be calculated using the Schroeder methods, an MLS signal was again used. The angular step for the measurement of the scattering coefficient was determined as  $5^\circ$ , corresponding to 72 measurements during one continuous rotation of the turntable. One complete rotation of the turntable took approximately 12 minutes, a short enough time to suggest that any effect of variations in temperature and relative humidity on the measurement of scattering coefficient would be small. In this experiment, eight measurements consisting of two source and four microphone positions were conducted with the same equipment used for the measurement of random-incidence absorption coefficient. Figure 3.1 shows the schematic diagram of the experimental condition. In Figure 3.2, a photo of the measurement setup for the baseplate with water is shown.

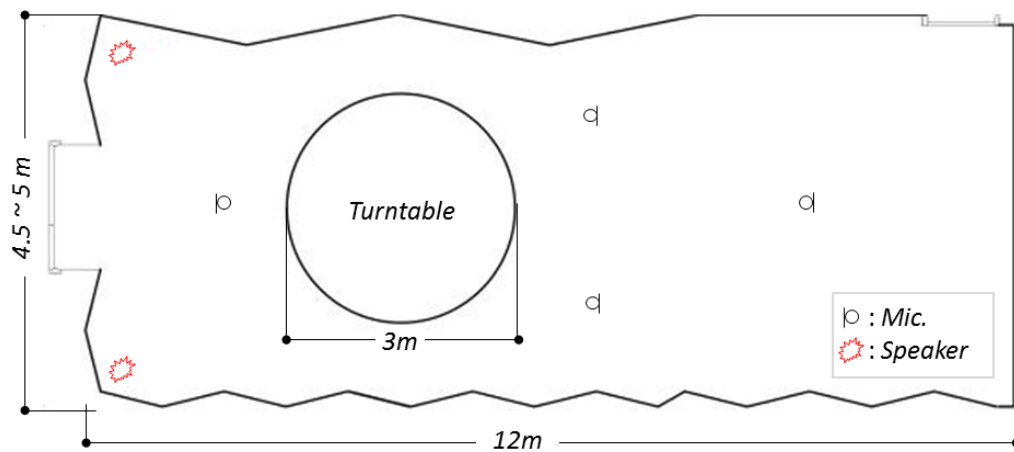


Fig. 3.1 Schematic diagram of the experimental arrangement



Fig. 3.2 Photo of the measurement setup for the baseplate with water

### 3.2.2 Calculation method for the absorption and scattering coefficients

Impulse responses were measured without and with the test sample on the non-rotating turntable, giving reverberation times  $T_1$  and  $T_2$ , respectively. The random-incidence absorption coefficient is then determined by the difference between  $T_1$  and  $T_2$  (ISO, 2003).

The result of the measurement with the continuously rotating turntable without the test

sample is reverberation time  $T_3$  and the result for the rotating turntable with the test sample is reverberation time  $T_4$ .

The scattering coefficient,  $s$ , can be derived using the random-incidence absorption coefficient,  $\alpha_s$ , and the specular absorption coefficient,  $\alpha_{spec}$  (ISO, 2004):

$$\alpha_s = 55.3 \frac{V}{S} \left( \frac{1}{c_2 T_2} - \frac{1}{c_1 T_1} \right) \quad \text{Eq. 3.1}$$

$$\alpha_{spec} = 55.3 \frac{V}{S} \left( \frac{1}{c_4 T_4} - \frac{1}{c_3 T_3} \right) \quad \text{Eq. 3.2}$$

where,  $\alpha_s$ : Random-incidence absorption coefficient

$\alpha_{spec}$ : Random-incidence specular absorption coefficient

V: Volume of the reverberation room ( $m^3$ )

S: Surface area of test sample ( $m^2$ )

c: Speed of sound (m/s)

T: Reverberation time (s)

The scattering coefficient can then be calculated using the following formula:

$$s = 1 - \frac{1 - \alpha_{spec}}{1 - \alpha_s} = \frac{\alpha_{spec} - \alpha_s}{1 - \alpha_s} \quad \text{Eq. 3.3}$$

While the scattering coefficient should be between 0 and 1, actual measurements could deliver a scattering coefficient greater than 1 due to the edge effect. The calculation method of the scattering coefficient for the test sample compensates the one of the baseplate alone based on Eq. 3.2. This enables the scattering coefficient of the test sample to be less than that of the baseplate.

### 3.2.3 Measurement of absorption coefficient for soil without vegetation

Topsoil is the naturally occurring uppermost layer of soil (above subsoil and underlying



rock) that is relatively high in organic matter and nutrients (Tucker *et al.*, 1995). When there is vegetation, the topsoil contains most of the plant roots. Topsoil used for measuring the absorption coefficient was placed on a polythene sheet on the floor of the reverberation chamber and within a rectangular perimeter frame constructed from MDF board. External dimensions of the frame were 3.8 m (L)  $\times$  2.7 m (W)  $\times$  200 mm (H) and its walls were 36 mm thick, giving the soil a surface area of 10 m<sup>2</sup>. There were no air gaps between the soil sample and the floor or perimeter frame. At the maximum soil depth of 200 mm the frame supported two cubic-metres of topsoil weighing approximately 3000 kg. The porosity and density of the topsoil tested were 0.39 and 1255 kg/m<sup>3</sup>, respectively (Benkreira *et al.*, 2011).

Soil depths of 50 mm, 100 mm, 150 mm and 200 mm were tested. Some compaction of soil (reducing porosity) was expected due to its own weight on lower layers but no additional pressure was applied. Accordingly, it is expected that this could result in a relatively high absorption coefficient even with a thin layer of the topsoil, due to the low compactness.

With a 200 mm soil depth, soil moisture content was increased from the initial in-bag level with a saturation of 12.5 %, by adding measured volumes of water manually by watering can. To help in the even distribution of water a grid of ten equal rectangles was marked on the soil surface with string and the watering can was fitted with a rose to create a spray. Also, thirty minutes were allowed each time for the water to soak down into the soil before starting the measurements. Sound absorption was measured for the sample with no watering and for seven increases in moisture content: 0.003, 0.007, 0.01, 0.013, 0.017, 0.02, 0.033 litres of water in total added per 1 kg of soil. Corresponding

volumetric soil moisture levels, measured with a Delta-T HH2 meter and SM200 probe just before each set of acoustical measurements, were  $12.5\pm0.5$ ,  $17.0\pm0.6$ ,  $20.4\pm1.9$ ,  $23.8\pm2.6$ ,  $25.4\pm2.9$ ,  $26.3\pm1.9$ ,  $28.9\pm2.0$  and  $34.1\pm2.4$  %, respectively. These were measured in the top layer of soil. The total amount of moisture added to the soil ( $10 \text{ litres/m}^2$ ) was equivalent to 10 mm of rainfall. Figure 3.3 shows the experimental condition of topsoil with a 50 mm depth.



Fig. 3.3 Topsoil of 50 mm depth

### **3.2.4 Measurement of absorption coefficient for soil with vegetation**

Random-incidence absorption coefficient for different levels of soil vegetation coverage were measured using specimens of eight plant species normally used in urban planting and landscaping schemes. Table 3.1 shows the plants' dimensional characteristics and the proportion of each species. The maximum level of vegetation coverage (100 %) used 264 plants. All plants were individually potted (pot diameter 130-180 mm) and sunk into 200 mm of soil so that the rim of the pot was approximately 15 mm below the soil surface. The moisture content of topsoil was 12.5 %, at the initial in-bag level. To

remove a plant its pot was lifted out and the cavity filled-in with more topsoil to restore the general surface. Approximate values for total leaf area were calculated from digital images of individual leaves and the number of leaves on a plant from each species. The final column in Table 3.1 shows relative contributions of different plant species to the total leaf area which was estimated at 17.5 m<sup>2</sup> for the maximum vegetation coverage level tested.

Table 3.1 Characteristics of 264 plants of eight species providing soil vegetation coverage

Plant	Leaf area per plant (m <sup>2</sup> )	Plant max. height (mm)	Plant max. diameter (mm)	Number of plants used for 100% of max. coverage	Percentage of all plants in sample (%)	Percentage of total leaf area in sample (%)
<i>Origanum Vulgare Aureum</i>	0.038	90	220	3	1	1
<i>Ceratostigma Plumbagincides</i>	0.173	240	280	18	7	18
<i>Spiraea Japonica</i>	0.076	230	230	84	32	36
<i>Hebe Great Orme</i>	0.070	200	200	72	27	29
<i>Azalea</i>	0.125	150	260	6	2	4
<i>Hylotelephium telephium</i>	0.014	120	140	32	12	3
<i>Cistus Dansereaui</i>	0.082	300	320	11	4	5
<i>Helianthemum</i>	0.020	100	220	38	14	4



Fig. 3.4 200 mm topsoil with eight plant species: (a) 40 % vegetation coverage (106 plants); (b) 100 % vegetation coverage (264 plants)

To examine its effect on sound absorption vegetation coverage was gradually reduced by removing plants in a way that maintained the original proportions of different species while keeping the distribution of plants reasonably even across the soil surface. Sound absorption was measured for six levels of vegetation coverage: 264 plants (100 % of maximum coverage); 211 plants (80 % coverage); 158 plants (60 % coverage); 106

plants (40 % coverage); 53 plants (20 % coverage); and no plants (0 % coverage). Figure 3.4(a) shows the experimental condition of 200 mm topsoil with 40 % of maximum vegetation coverage.

### 3.2.5 Leaves and stems

Buxus (*Buxus Sempervirens*), Holly (*Ilex aquifolium*) and Ivy (*Hedera helix*), which are commonly used for green landscaping in Europe, were selected to measure random-incidence absorption and scattering coefficients of aboveground components of plants such as leaves and stems. These species have different sizes of leaf for examining the effect of leaf size on absorption and scattering.

With the test sample consisting of living plants in pots (Buxus and Holly) and the requirement to measure only the aboveground plant structure it was necessary to fill the void space between pots with an acoustically hard and flat material to reduce the absorption and scattering coefficients of the baseplate. Thus, the plant pots holding the root ball and soil were excluded from the measurements by submerging them in water, leaving only the plant stems and leaves above the water surface. They were positioned with an even distribution across the baseplate/water surface.

To examine its effect on random-incidence absorption and scattering coefficients of Buxus and Holly, the density of vegetation coverage was gradually reduced by removing plants and replenishing the water. Six steps of vegetation coverage for Buxus were considered as 100 % of maximum coverage (110 plants), 80 % (88 plants), 60 % (66 plants), 40 % (44 plants), 20 % (22 plants), and 0 % (no plants). For Holly, the density of vegetation coverage was changed in a similar way with 100 % (123 plants), 80 % (98 plants), 60 % (74 plants), 40 % (49 plants), 20 % (25 plants) and 0 % (no

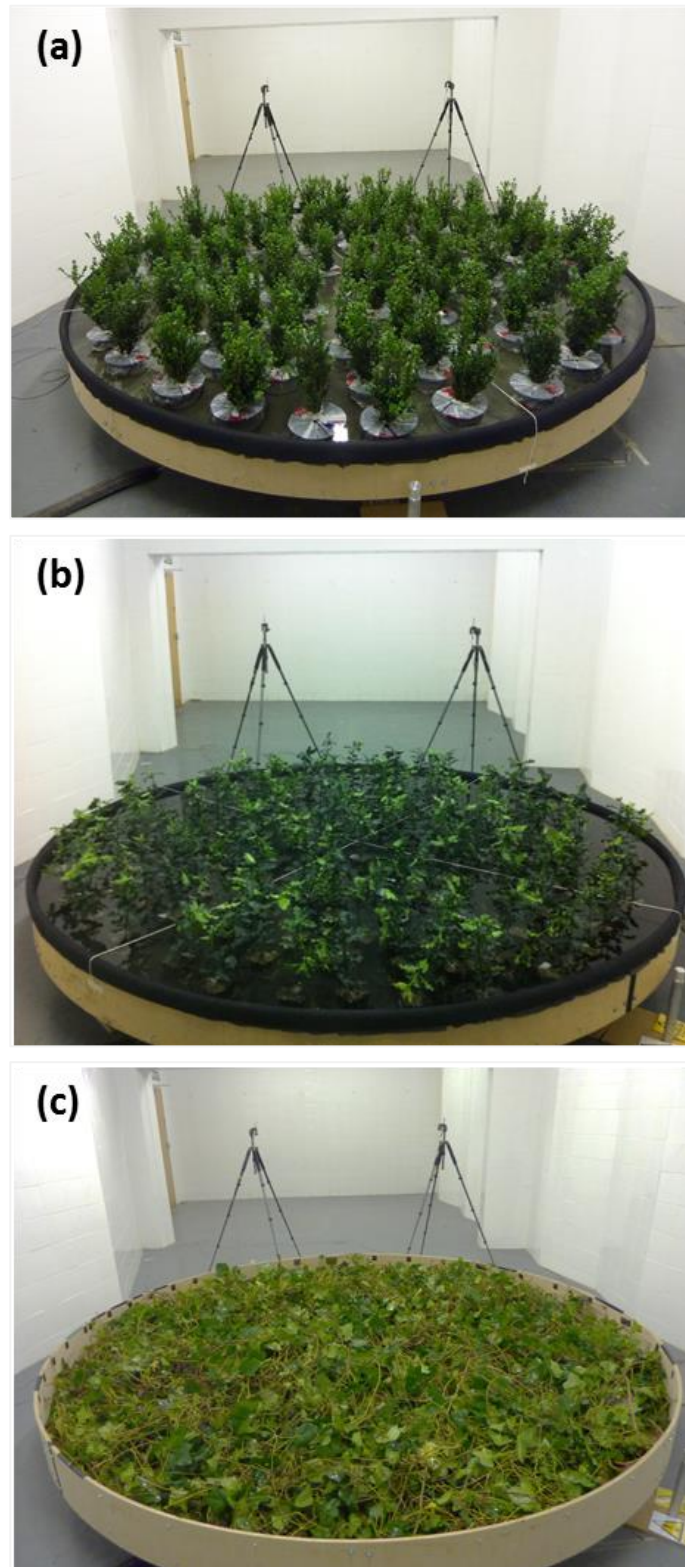


Fig. 3.5 Measurement conditions of random-incidence scattering coefficient: (a) Buxus with 100 % vegetation coverage using 110 plants; (b) Holly with 100 % vegetation coverage using 123 plants; (c) Ivy prunings of 200 mm depth

Table 3.2 Physical properties of Buxus, Holly and Ivy

Plant	Area per leaf (cm <sup>2</sup> )	Leaf area per plant (m <sup>2</sup> )	Plant max. height (mm)	Plant max. diameter (mm)	Height of pot (mm)	Diameter of pot (mm)
Buxus	0.98	0.048	300	230	150	190
Holly	14.1	0.027	200	210	100	90
Ivy (prunings)	38.5	-	-	-	-	-

plants). In the case of Ivy, three different levels of vegetation density were considered using 100 % (200 mm depth), 50 % (100 mm depth) and 25 % (50 mm depth) layers of fresh prunings, all evenly distributed on the baseplate. The 200 mm of Ivy was assumed as a maximum depth growing on building façades and grounds. In Figure 3.5, measurement setups for the scattering coefficient of Buxus, Holly and Ivy with the maximum vegetation coverage and density are shown. Table 3.2 describes the plant properties used for this experiment.

### 3.2.6 Green wall

Figure 3.6 shows a green wall made of a substrate from Canevaflor (<http://www.canevaflor.com/>), as located in the reverberation chamber for measurements. The size of the green wall was 10 m<sup>2</sup> (2 m high by 5 m long). The wall has a depth of 200 mm and contains approximately 750 kg of substrate (in-bag condition with no water added). It comprises a modular system of five identical galvanized steel frames designed to clad a building. These frames rested on the floor of the reverberation chamber and were fixed to a section of flat wall. Geotextile linings within the steel mesh hold the substrate – coconut fibres with some perlite and a water-retaining polymer. The porosity of the substrate is 0.76, which is much higher than that of topsoil, 0.39. The substrate has a density of 250 kg/m<sup>3</sup>, which is much lighter than

that of topsoil,  $1255 \text{ kg/m}^3$  (Benkreira *et al.*, 2011).

Irrigation came through five horizontal drip pipes embedded in the substrate and running the full width of the wall. Connection to the mains water supply was via a flow meter which enabled accurate control of the increases in substrate moisture content. Two factors allowed greater time for water to be absorbed more evenly throughout the substrate: flow rate from the supply was regulated at 170 litres per hour (<3 litres/min.) and, following each increase in moisture content, measurements commenced after a 30 minute delay.

Substrate moisture content was increased from its initial in-bag level with a saturation of 37.8 % in volumetric moisture level by adding 1, 5, 15, 30, 60 litres of water in total per square metre of wall which is equivalent to 0.01, 0.07, 0.2, 0.4 and 0.8 litres of water added per 1 kg of substrate. Eventually, with 600 litres of water added, there was some pooling at the base of the wall which was enclosed by an impermeable membrane suggesting the substrate was saturated. The procedure of measurements of RT was the same as with the topsoil measurement.



Fig. 3.6 Green wall without vegetation, mounted on a flat wall of reverberation chamber



### **3.3 Measurement results**

#### **3.3.1 Soil without vegetation**

Figure 3.7 shows random-incidence absorption coefficients for topsoil of four different depths of 50 mm, 100 mm, 150 mm and 200 mm. The result suggests that even the thin soil layer with a depth of 50 mm provides a absorption coefficient at mid and high frequencies with an absorption coefficient over 0.9 at around 1 kHz. Also there were only slight changes in the absorption coefficient of about 0.1 with increased soil depth. In comparison with 50 mm depth, a slight increase in the absorption coefficient is found with increased soil depth at low and mid frequency ranges. On the other hand, a slight decrease in the absorption coefficient can be seen at high frequencies over 2 kHz due to the increase in soil compaction with increasing soil depths. Overall, the results indicate that increasing soil depth does not significantly increase the absorption coefficient in the case of topsoil with a depth over 50 mm. The main reason for this result is that topsoil is of low permeability with a relatively low porosity and small pores, making the acoustic penetration depth very small. Therefore, increasing the layer depth beyond 50 mm has insignificant influence on the measured absorption coefficient. It is expected that the effect of soil depth on the absorption coefficient depends more on the soil conditions such as porosity and flow resistivity.

In Figure 3.8, a decrease in the absorption coefficient of about 0.2-0.6 at different frequencies was observed with the increase in soil moisture content. It can be seen that the absorption coefficient is rapidly decreased after the initial application of water to the soil surface, especially at mid and high frequencies, since this reduces the porosity and effective pore size of topsoil. A comparatively large increase in moisture content when

the total water added went from 6 litres/m<sup>2</sup> to 10 litres/m<sup>2</sup>, namely 12.5 % to 34.1 % in terms of moisture content, produced a small decrease in sound absorption, indicating a nearly saturated surface layer. Such results are comparable to the previous work (Horoshenkov *et al.*, 2006) showing the effect of moisture on the acoustic admittance of porous sands and sandy soils.

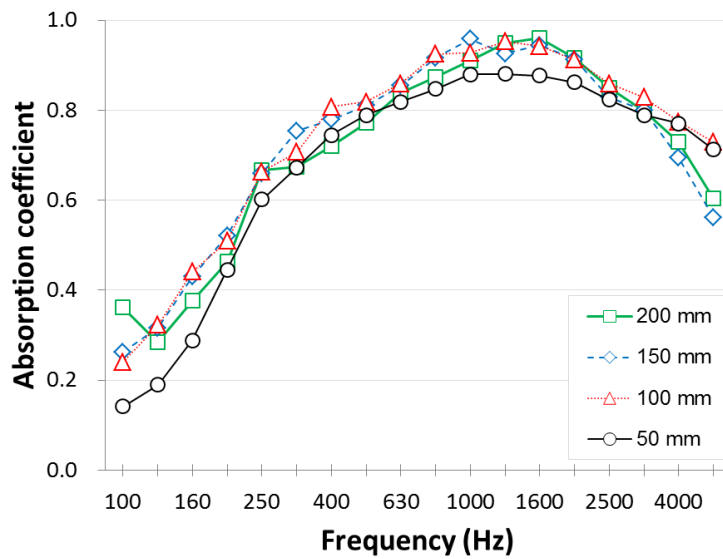


Fig. 3.7 Absorption coefficient of topsoil with different soil depths

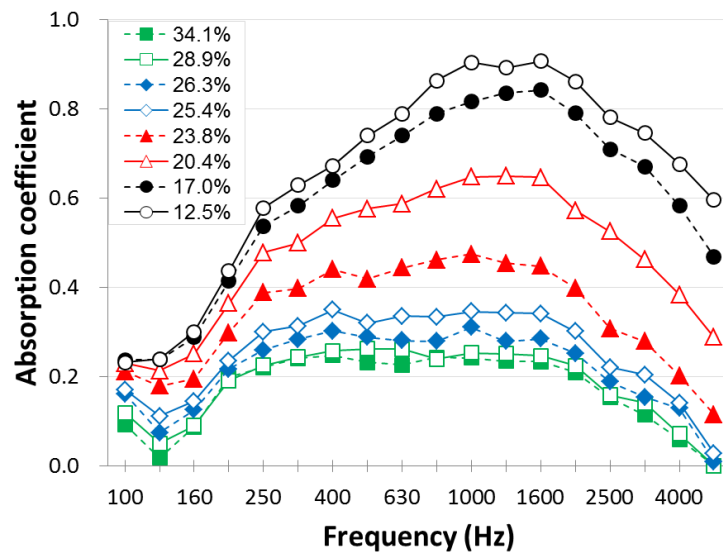


Fig. 3.8 Absorption coefficient of 200 mm topsoil with different soil moisture content (%)

### 3.3.2 Soil with vegetation

Figure 3.9 shows the absorption coefficient of topsoil with six different levels of vegetation coverage. The result indicates that with increasing vegetation coverage, the absorption coefficient increased by about 0.2 at low and mid frequencies. This is likely because viscous friction losses and the inertia effect of vegetation affect sound absorption at low and mid frequencies. This result is similar to that of a parallel study (Benkreira *et al.*, 2011), which shows that vegetation with relatively large leaves (i.e., Primrose) can increase normal-incidence absorption coefficient at low frequencies when it is planted in soil. Generally speaking, the increase of absorption at low and mid frequencies can be regarded as a result of the increased thickness and density of the porous materials on top of the topsoil. However, when it comes to frequencies around 2 kHz the changes in vegetation coverage appear to have no effect on sound absorption. Over 2 kHz, the absorption coefficient was slightly decreased by about 0.1 with the increase in vegetation coverage. This is perhaps due to the increased reflection with increased leaf surface areas, and the effect of soil absorption becomes relatively less.

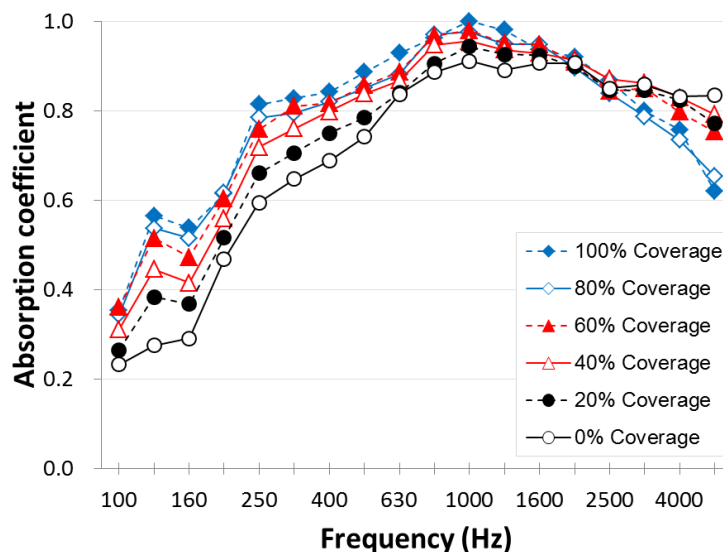


Fig. 3.9 Absorption coefficient of topsoil with different levels of vegetation coverage

Overall, these results imply that there is a possibility to choose suitable leaf types, sizes, and densities to reduce noise levels by considering the spectrum of sound sources.

### **3.3.3 Absorption by leaves and stems**

Figure 3.10 shows the absorption coefficient of aboveground components such as stems and leaves for three different types of vegetation including Buxus, Holly and Ivy. Different levels of vegetation density of coverage were considered for each type of vegetation. As shown in Figure 3.10(a) and 3.10(b), the maximum absorption coefficient for Buxus and Holly are about 0.2 at 5 kHz with 100 % vegetation coverage. With increasing vegetation coverage, generally speaking, the absorption coefficient is gradually increased for both species. It can also be seen that Buxus and Holly have a slightly higher absorption coefficients at high frequencies than that at low frequencies. The result in Figure 3.10(c) shows that the absorption coefficient of Ivy increases with increasing vegetation density of coverage, especially at above 1.6 kHz. The maximum absorption coefficient is 0.49 at 5 kHz with the maximum coverage (200 mm depth). Ivy with a depth of 50 mm, which can be regarded as a more realistic depth growing on building façades, has a maximum absorption coefficient of 0.39 at 4 kHz. In comparison with Buxus and Holly, the maximum absorption coefficient for Ivy is considerably higher, possibly due to the larger size and amount of leaves. Similar to Buxus and Holly, with Ivy, with increasing frequency, the absorption also becomes higher. The overall results suggest that the absorption coefficient of vegetation is increased with increasing vegetation coverage and leaf sizes, especially at high frequencies.

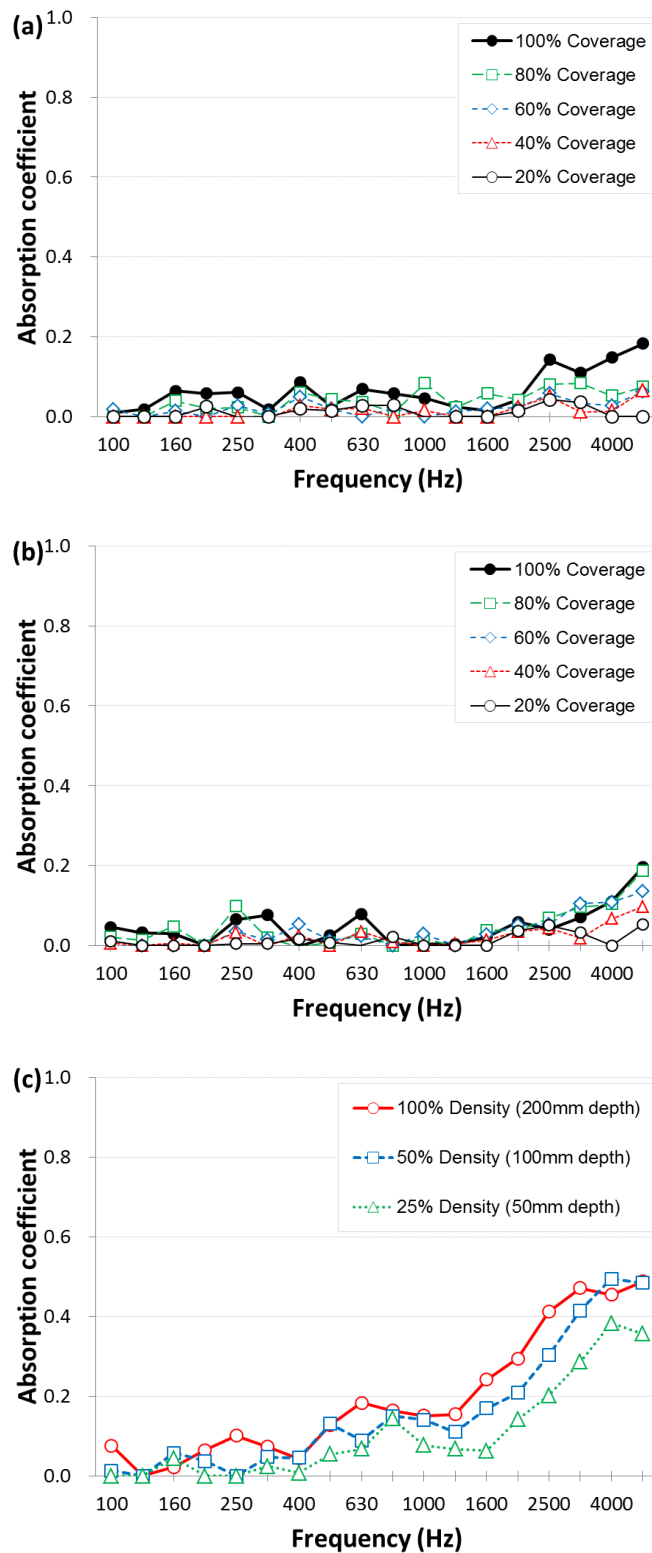


Fig. 3.10 Absorption coefficient of vegetation with different levels of vegetation coverage/density: (a) Buxus; (b) Holly; (c) Ivy

### 3.3.4 Scattering of leaves and stems

The scattering coefficient of the baseplate itself is an important factor determining the measurement accuracy for the scattering coefficient of the test sample. In ISO 17497-1 (ISO, 2004), the maximum scattering coefficient of the baseplate alone is specified with frequency-dependent values in one-third octave bands from 100 Hz to 5 kHz, in order to ensure the quality of the experimental arrangement. Figure 3.11 shows the scattering coefficient of the baseplate containing water of depth 200 mm. It can be seen that the scattering coefficient of the baseplate is generally below the ISO maximum values.

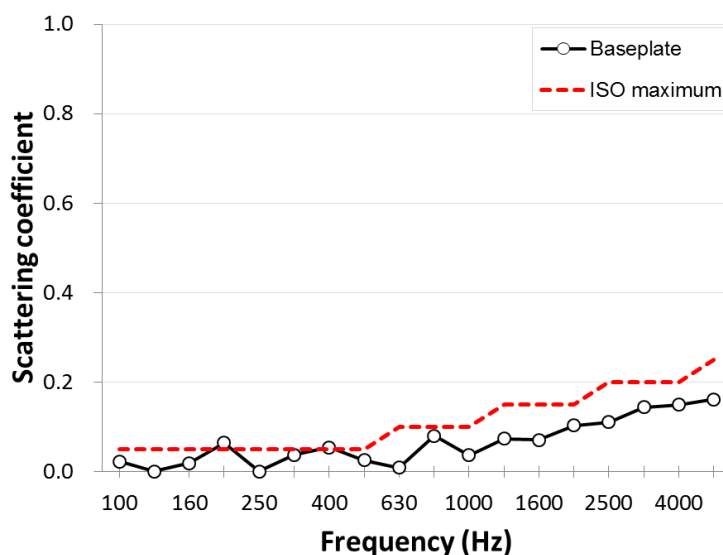


Fig. 3.11 Scattering coefficient of the baseplate containing water with 200 mm depth

In Figure 3.12, the scattering coefficient of leaves and stems for Buxus, Holly and Ivy is shown. It can be seen that in general, the scattering coefficient increases with increasing vegetation coverage for all three plant species. The scattering coefficient is also higher at high frequencies, perhaps due to the size of leaves and stems. The maximum scattering coefficient of Buxus is 0.26 at 5 kHz, and for Holly, the maximum scattering coefficient is 0.33 at 5 kHz. The result for Ivy shows that the vegetation density

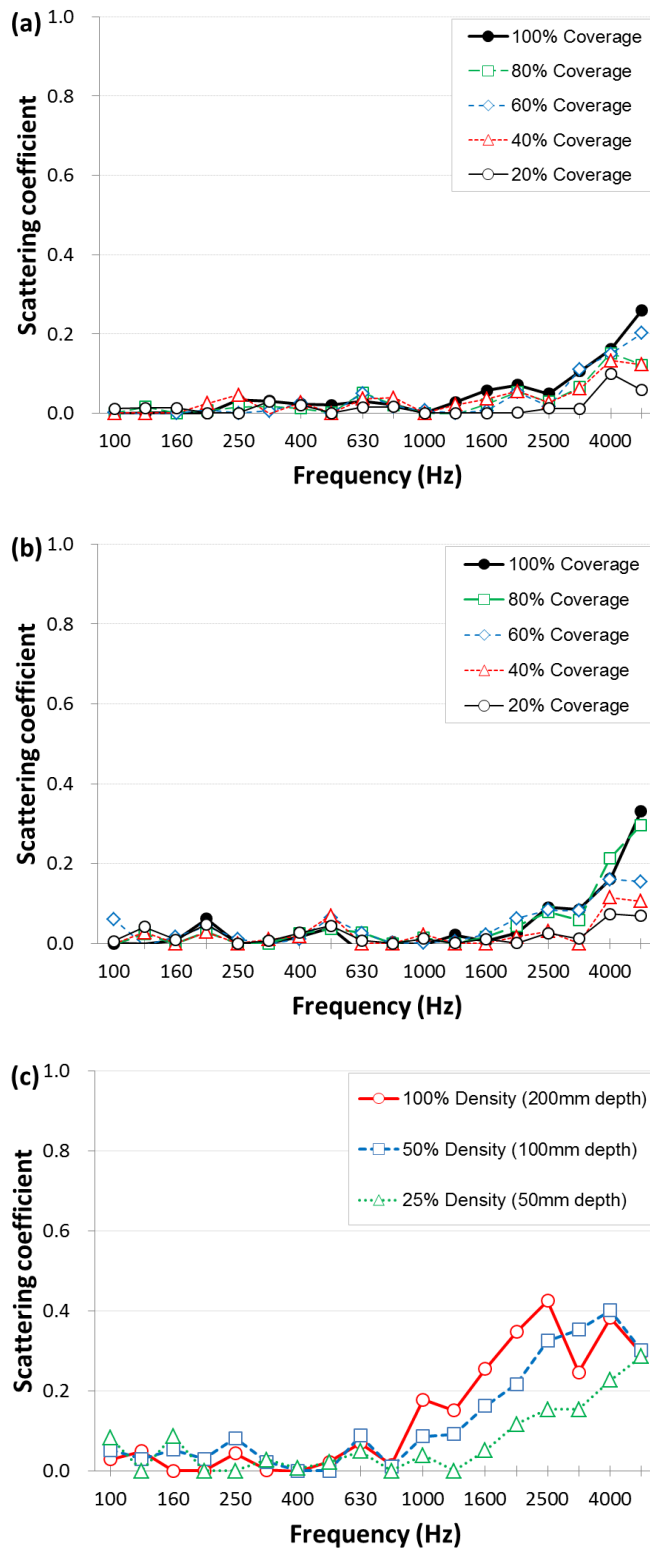


Fig. 3.12 Scattering coefficient of vegetation with different levels of vegetation coverage/density: (a) Buxus; (b) Holly; (c) Ivy

of coverage plays an important role in increasing the scattering coefficient, especially above 1 kHz. The maximum scattering coefficient is 0.43 at 2.5 kHz for 100 % density (200 mm depth). In comparison with Buxus and Holly, Ivy can scatter sound energy at relatively lower frequencies, say from 1 kHz, due to its relatively larger size and density of leaves.

### 3.3.5 Green wall

Figure 3.13 shows the absorption coefficient of the unplanted green wall, considering different amounts of water added to the substrate. It can be seen that the absorption coefficient gradually decreases with increasing substrate moisture content, especially at low frequency, and the total decrease is about 0.2. However, the variation in the absorption coefficient for the green wall is considerably less in comparison with that for topsoil. This result is comparable with the previous study using an impedance tube (Benkreira *et al.*, 2011). The main reason is that the substrate of the green wall, which consists of very porous and lightweight materials including a water-retaining polymer, can absorb more water in comparison with topsoil while keeping a considerable level of porosity. The two measurement results at the water level of 60 litres per square metre, which were carried out on consecutive days with a 16 hour interval, show that there is an insignificant variation in the absorption coefficient. It is noted that at lower frequencies than 100 Hz, the absorption coefficient goes down to zero abruptly.

A previous study based on impedance tube measurement suggested that the green wall with vegetation can give a higher absorption coefficient compared to that without vegetation (Horoshenkov *et al.*, 2011).



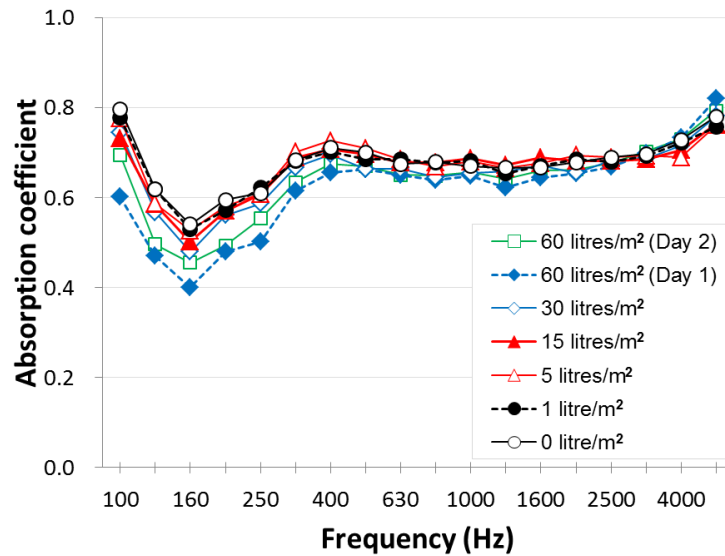


Fig. 3.13 Absorption coefficient of the green wall with different levels of substrate moisture content, shown in terms of water added.

### 3.4 Summary

In this chapter, a series of measurements were carried out in a reverberation chamber to examine random-incidence absorption coefficients and scattering coefficients of vegetation, by considering various factors such as soil depth, soil moisture content, the level of vegetation coverage and leaf size.

Measurements for different depths (50, 100, 150, 200 mm) of soil without vegetation have shown that even a relatively thin soil layer with a depth of 50 mm provides an absorption coefficient of about 0.9 at around 1 kHz and there are only slight changes of the absorption coefficient of about 0.1 with increased soil depth. A decrease in absorption coefficient, by about 0.2-0.6 at different frequencies, has been observed with the increase of soil moisture content. A rapid decrease in absorption has been shown after adding a small amount of water on a relatively dry soil surface, especially at mid and high frequencies. On the other hand, there is an insignificant change in sound

absorption when the soil is nearly saturated. Different from topsoil, the result for the green wall shows that it can absorb sound effectively at mid and high frequencies with the absorption coefficient over 0.6 even if the substrate is nearly saturated.

The experiment results for soil with different levels of vegetation coverage have suggested that with increasing vegetation coverage, the absorption coefficient increases by about 0.2 at low and mid frequencies, whereas over about 2 kHz the absorption coefficient could be slightly decreased by about 0.1.

It has been shown that the aboveground vegetation components such as leaves and stems can absorb sound, especially at high frequencies. Generally speaking, the absorption coefficient is increased with increasing vegetation coverage and density. The maximum absorption coefficients of Buxus, Holly and Ivy are 0.18, 0.20 and 0.49 at 5 kHz, respectively. The aboveground components can also scatter sound energy at high frequencies. With increasing vegetation coverage and density, the scattering coefficient increases gradually. The scattering coefficients of Buxus and Holly can reach 0.26 and 0.33 at 5 kHz with 100% vegetation coverage, where the maximum scattering coefficient of Ivy is 0.43 at 2.5 kHz.

## **4 Quantifying Scattered Sound Energy from a Single Tree by means of Reverberation Time**

The aim of this chapter is to investigate the effect of a single tree in open field on sound scattering by means of RT, and to examine which parameters are relevant. Therefore, a series of field measurements involving five single trees of different species and crown sizes were carried out. It starts, in Section 4.1, with a review of previous studies allowing the research background to be defined. In Section 4.2, it explains the principle of quantifying scattered sound energy from a single tree by means of reverberation time. Measurement methods and reliability are examined in Section 4.3 and Section 4.4, respectively. In Section 4.5, measurement results are described as: 1) tree sizes with and without foliage, 2) source-receiver angles, and 3) source-receiver distances. Lastly, Section 4.6 summarises key findings of this chapter.

### **4.1 Introduction**

In the last few decades since the pioneering work by Eyring (1946), studies on the acoustic effect of trees have been focused on sound propagation through forests and tree belts. A number of studies have demonstrated the effect of forests and tree belts on noise reduction (Embleton, 1963; Fang *et al.*, 2003; Fricke, 1984; Kragh, 1981; Tyagi *et al.*, 2006; Van Renterghem *et al.*, 2012). Various numerical and experimental methods have also been investigated to characterise the influential factors affecting sound propagation through forests. Previous work suggests that ground effect, sound scattering, and sound absorption by tree elements (trunks, branches, stems, leaves, etc.) play a role in sound propagation through forests (Aylor, 1972; Burns, 1979; Fan *et al.*, 2010; Heimann,

2003; Martínez-Sala *et al.*, 2006; Martens, 1980; Martens *et al.*, 1981; Price *et al.*, 1988; Swearingen *et al.*, 2007; Van Renterghem *et al.*, 2002, 2008b; Watanabe *et al.*, 1996; Wunderli *et al.*, 2009; Wunderli, 2012). Ground effect is the result of interference between direct sound and sound reflected from the ground. It depends on the acoustic properties of the ground, as well as the positions of the source and receiver. At frequencies above 1 kHz, trees contribute to sound attenuation increasingly with frequency due to sound scattering by trunks and branches, as well as foliage scattering and absorption by viscous friction and damped vibrations. There have also been a few attempts to show that forests induce a reverberant sound field, indicating the importance of sound scattering by tree elements (Huisman *et al.*, 1991; Padgham, 2004; Richards *et al.*, 1980).

While there have been numerous studies involving groups of trees, it is also worth examining sound scattering by a single tree. Firstly, this helps validate theoretical models for predicting sound propagation through forests. Secondly, in reverberant urban spaces such as street canyons and courtyards, trees are expected to influence sound field characteristics including RT and sound level distribution. Compared to open field, the effect of trees could even be enhanced since there are multiple passages through the trees due to multiple reflections between building façades (Kang, 2000, 2002b; Van Renterghem *et al.*, 2006). Thus, information on sound scattering from a single tree would be useful for better understanding acoustic effects of trees in these urban environments.

Previously, Ding *et al.* (2010) attempted to examine sound scattering from a single tree by performing time-domain analysis as well as comparing early and late scattered sound

energy. Although these analysis methods are useful to explain the characteristics of a single tree on sound scattering, it is still needed to suggest a suitable acoustic indicator to directly compare the amount of sound energy scattered from various types of a single tree with different conditions, and to validate numerical modelling of sound propagation through a single tree. It is expected that the scattered sound energy is appeared at the late part of an impulse response. Therefore, it is assumed that the method for RT calculation can be applied to examine the effect of a single tree on sound scattering, as stronger scattered sound energy produces longer RT.

The aim of this chapter is therefore to investigate the effect of a single tree in open field on sound scattering by means of RT, and to examine which parameters are relevant. The effect of a single tree on sound scattering is expected to depend on many factors such as the tree canopy size and species, the amount and seasonal condition of foliage, source-receiver angle and distance, ground condition, and source and receiver heights. Consequently, a series of field measurements involving five single trees of different species and crown sizes were carried out.

## **4.2 Principle of quantifying scattered sound energy from a single tree by means of reverberation time**

As shown in Figure 4.1, sound propagating near a single tree can arrive at a receiver by a number of paths, including direct sound, ground reflected, purely scattered, and scattered in combination with ground reflection. This shows complex mechanisms of sound scattering produced by a single tree.

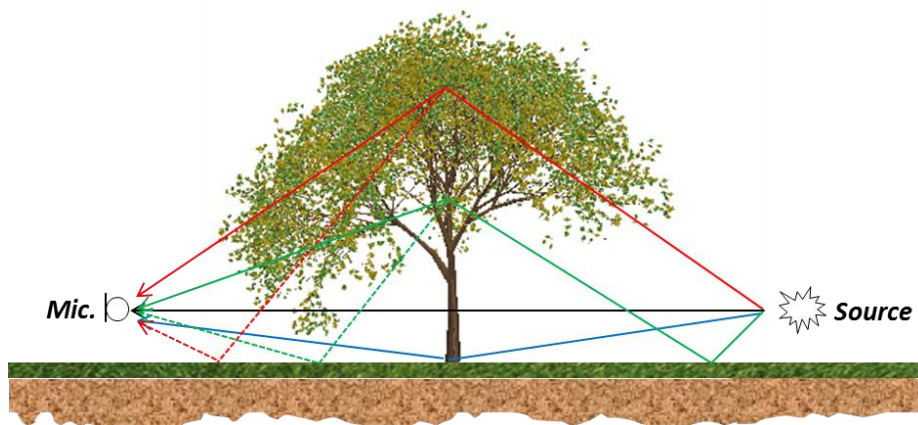


Fig. 4.1 Diagram for sound paths through a single tree from a point source to a receiver

Figure 4.2 shows two impulse responses measured in open field in the presence and absence of a single tree (Tree 5 in Figure 4.3). The measurement was carried out at a source-receiver distance of 60 m for a point source (starting pistol) at 1.5 m height and a receiver at 1.5 m height. The result with the tree has considerably stronger sound energy in the late part of the impulse response in comparison with the result without the tree. Correspondingly, this would bring an increase in RT.

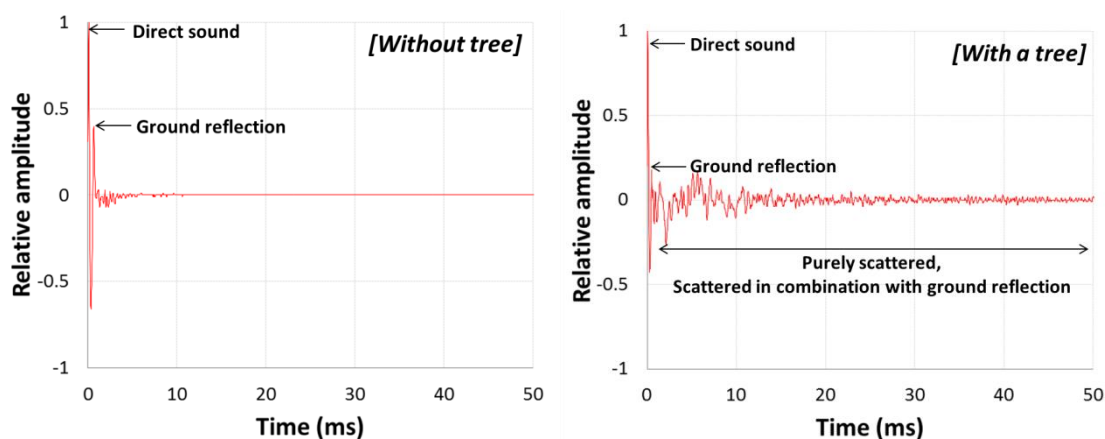


Fig. 4.2 Impulse responses measured in open field in the absence and presence of a single tree

### 4.3 Measurement method

#### 4.3.1 Experimental conditions

Measurements were carried out six times in the Park at Chatsworth House near Sheffield, United Kingdom, between September 2010 and March 2012. Five individual trees of different species and sizes were selected to examine the importance of sound scattering (see Figure 4.3). To suppress late reflections, the selected trees stood alone on flat grassland with sufficiently large distances (over 70 m) to other trees and obstacles. The sound scattered by a targeted tree decays 35 dB from the initial amplitude within 150 ms, or 51 m assuming a sound speed of 340 m/s. Therefore, a maximum source-receiver distance of 60 m was determined to provide a sufficient time interval between scattered sound from a tree and late reflections from other obstacles.

Table 4.1 describes properties of the five individual trees named from Tree 1 to Tree 5 on the basis of increasing size. The areas of imaginary surfaces enclosing the tree crowns, with their complex shapes, were calculated using Google's SketchUp programme with a function to adjust scale on the basis of a reference object (i.e., a human figure in this study). Table 4.2 provides meteorological conditions during the measurements. Humidity and temperature were measured 1.5 m above the ground with a CEM DT-615 meter just before and after each set of acoustical measurements. Wind speed 2.5 m above the ground was recorded with a Testo 405-V1 meter at the same times. Temperatures and relative humidity levels were quite similar during the measurements, except on Days 2 and 6. This inconsistency might have caused different atmospheric absorption especially at high frequencies due to the rather long travelling path in a tree crown. However, the atmospheric attenuation coefficient  $\alpha$  (dB/m) at 4 kHz for each measurement day, calculated based on ISO 9613-1 (ISO, 1993), indicates that the difference in temperature and humidity has a negligible contribution to the variation in scattered sound for the considered distances. The wind speed was less than

## Chapter 4. Quantifying Scattered Sound Energy from a Single Tree by means of Reverberation Time

---

4 m/s, implying low background noise by wind and the rustling of leaves. This has been confirmed by checking INR (impulse-to-noise ratio). In Figure 4.3, the condition for each tree with foliage is shown.

Table 4.1 Dimensional properties of the trees

	Tree 1	Tree 2	Tree 3	Tree 4	Tree 5
Species	Oak ( <i>Q. robur</i> )	Oak ( <i>Q. petraea</i> )	Cherry ( <i>P. avium</i> )	Maple ( <i>A. pseudoplatanus</i> )	Lime ( <i>T. × europaea</i> )
Tree height (m)	7.7	9.2	11.5	14.9	20.6
Tree diameter (m)	6.9	12.3	15.7	19.5	21.5
Crown surface area (m <sup>2</sup> )	30	43	88	161	218
Leaf size (cm)	12.0(L) × 7.5(W)	12.0(L) × 7.5(W)	15.0(L) × 6.0(W)	12.0(L) × 15.0(W)	10.0(L) × 10.0(W)
Trunk diameter (m)	0.14	0.40	0.42	0.51	0.56
Distance from ground to bottom of crown (m)	1.9	1.8	1.9	2.0	2.0

Table 4.2 Meteorological conditions for each measurement day

	Day 1	Day 2	Day 3	Day 4	Day 5	Day 6
Date	21 <sup>st</sup> Sep. 2010	20 <sup>th</sup> Apr. 2011	14 <sup>th</sup> Oct. 2011	26 <sup>th</sup> Oct. 2011	13 <sup>th</sup> Mar. 2012	14 <sup>th</sup> Mar. 2012
Temperature (°C)	20.3	28.2	16.3	15.0	15.6	9.9
Relative humidity (%)	62.0	34.1	65.8	65.1	56.7	74.3
Wind speed (m/s)	<1.0	<1.4	<3.0	<2.3	<2.5	<4.0
Atmospheric attenuation coefficient $\alpha$ at 4000 Hz (dB/m)	0.025	0.031	0.027	0.028	0.031	0.031



Chapter 4. Quantifying Scattered Sound Energy from a Single Tree by means of  
Reverberation Time

---

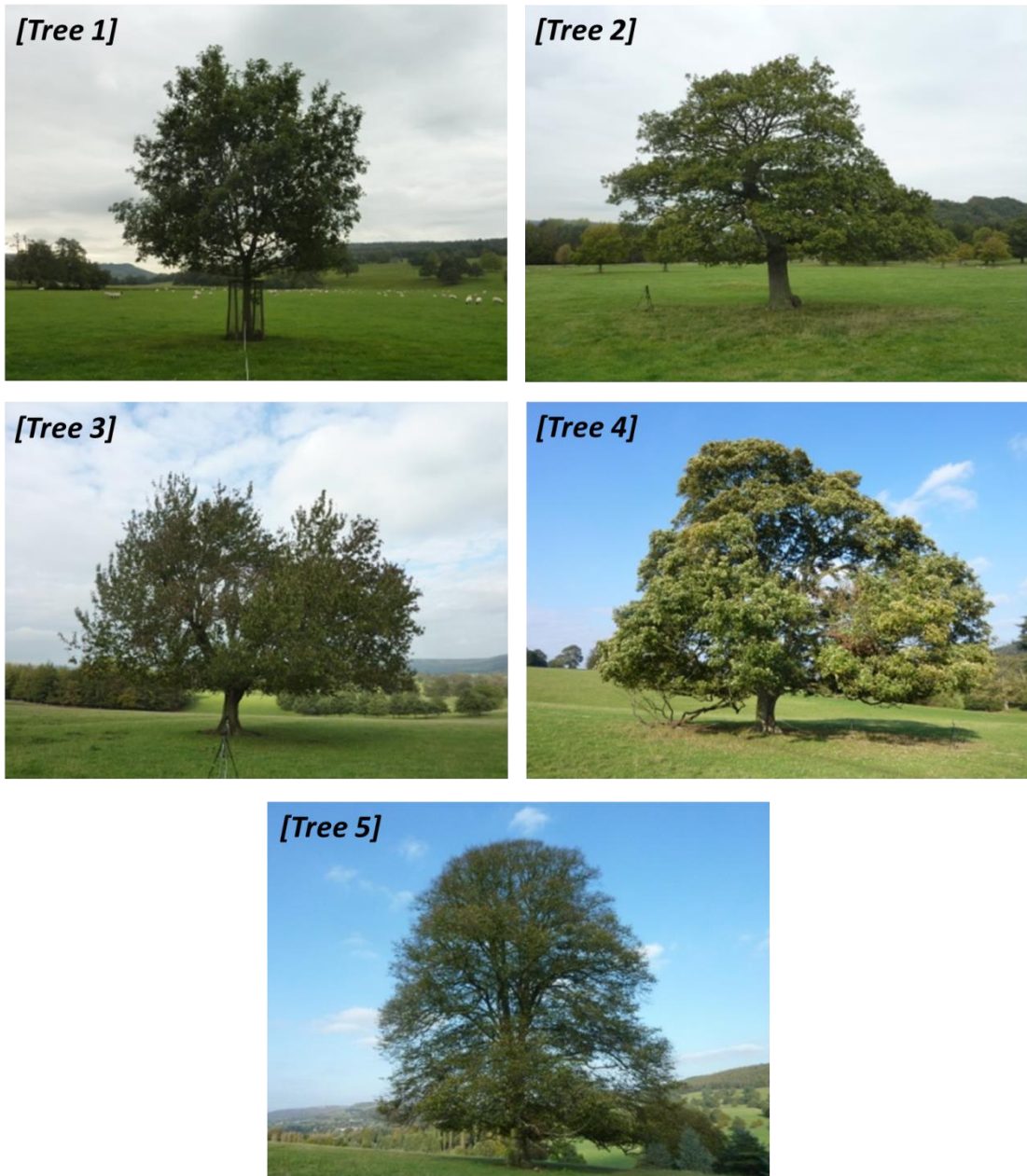


Fig. 4.3 Conditions for five trees with foliage on Day 3

### 4.3.2 Measurement setup

A similar measurement methodology was used as reported before in the work by Ding *et al.* (2010). Shots from a starting pistol were used as acoustic excitation. Five consecutive shots were released and the results averaged out, yielding a sufficient reproducibility for this type of sound source (Van Renterghem *et al.*, 2011). The recording systems comprised 1/2" microphones (BSWA MP 231 and G.R.A.S. MCE 201) and preamplifiers (BSWA MA231T and 01dB-Stell Pre 12H) connected respectively to a 4-channel Edirol R-44 recorder and a 2-channel 01dB Symphonie unit. Sampling frequency and bit depth for both systems were 48 kHz and 24-bit.

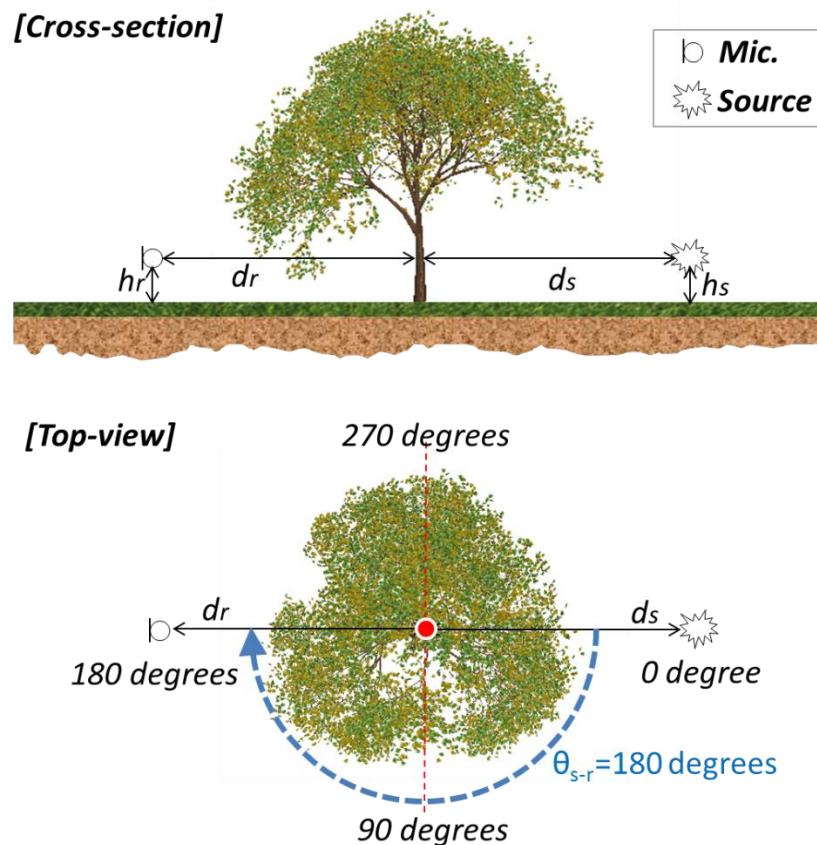


Fig. 4.4 Measurement conditions, where  $d_r$  is the trunk-receiver distance,  $d_s$  is trunk-source distance,  $h_r$  is the receiver height, and  $h_s$  is the source height

Figure 4.4 shows the cross-section and top-view of the measurement condition, where the source and receiver distance from a tree trunk is represented as  $d_s$  and  $d_r$ , respectively, while  $h_s$  and  $h_r$  are the heights of the sound source and receiver. The source-receiver angle is defined with  $\theta_{s-r}$ , indicating the difference in angle between  $d_s$  and  $d_r$ . Therefore,  $\theta_{s-r}=180^\circ$  means a straight sound propagation path connecting source, trunk and receiver.

## **4.4 Validation for measurement and data analysis methods**

### **4.4.1 Data analysis method**

In this chapter, RT based on the impulse responses recorded from the field measurement was analysed using the Dirac programme from B&K (B&K, 2010). RT is derived from the decay curve between 5 dB and 15, 25, 35 dB below the initial level. From the corresponding slope, T10, T20 and T30 are calculated as the times to reach -60 dB relative to the initial level. EDT (early decay time), derived from the decay curve between 0 dB and 10 dB below the initial level, is an inadequate descriptor to evaluate the scattered sound from trees as there is relatively weak energy in comparison with a direct sound. DIRAC has the time reversed filtering function to enable accurate measurement of very short RT which is needed for this study.

### **4.4.2 Impulse response to noise ratio**

The INR (impulse response to noise ratio) is an important parameter, providing information about the quality of the measurement for RT. It is defined as the ratio of the maximum impulse response level and background noise level, reflecting the decay range. According to ISO 3382 (ISO, 2008), the INR should be at least 35 dB and 45 dB

for accurate measurement of T20 and T30, respectively.

At the source-receiver distance of 60 m ( $d_r=30$  m,  $d_s=30$  m,  $\theta_{s-r}=180^\circ$ ), the INR measured for Tree 2 on Day 3 was  $22.2\pm 2.2$  dB at 63 Hz,  $36.8\pm 2.8$  dB at 125 Hz,  $45.0\pm 2.7$  dB at 250 Hz,  $48.8\pm 2.5$  dB at 500 Hz,  $48.4\pm 2.9$  dB at 1000 Hz,  $56.6\pm 1.5$  dB at 2000 Hz and  $54.0\pm 2.5$  dB at 4000 Hz. The standard deviation indicates the variation in the INR for five consecutive pistol shots. The maximum standard deviation of 2.9 dB at 1000 Hz suggests that the measurement method using starting pistol shots is reliable. The result suggests that the INR is sufficiently high to calculate T10 and T20 for source-receiver distances within 60 m, which is the maximum source-receiver distance considered in this study. However, it can be seen that the INR at some frequencies including 63 Hz, 125 Hz and 250 Hz is insufficient to calculate T30. Therefore, it is appropriate to use T10 or T20 in terms of data reliability although the INR at 63 Hz is still insufficient for calculating T20.

#### 4.4.3 Determination of RT

In Figure 4.5, decay curves in octave band frequencies from 125 Hz to 4 kHz are shown for sound propagating in the presence and absence of Tree 3 with foliage. In this measurement, the source and receiver were positioned at  $d_s=10$  m,  $d_r=10$  m,  $h_r=0.2$  m,  $h_s=0.2$  m and  $\theta_{s-r}=180^\circ$ . The measurement without the tree was carried out at the same conditions, except with a slightly different source-receiver distance of  $d_s=13$  m and  $d_r=13$  m which has a negligible contribution to the variation in RT. The result for open field without the tree indicates that RT at low frequency is rather long, mainly because of the filters applied during the post-processing of the time responses. This cannot be avoided, and thus some ghost RT that has no

physical meaning will always be measured at very low frequencies. However, the filter effect induces negligible ghost RT for T10 and T20 less than 0.02 sec. On the other hand, decay curves in the presence of Tree 3 show that above 1 kHz, trees clearly introduce reverberation. It is also noticeable that weak scattering sound at 500 Hz is produced after -25 dB below the initial level, which can cause variation in RT with different decay ranges, especially for T30.

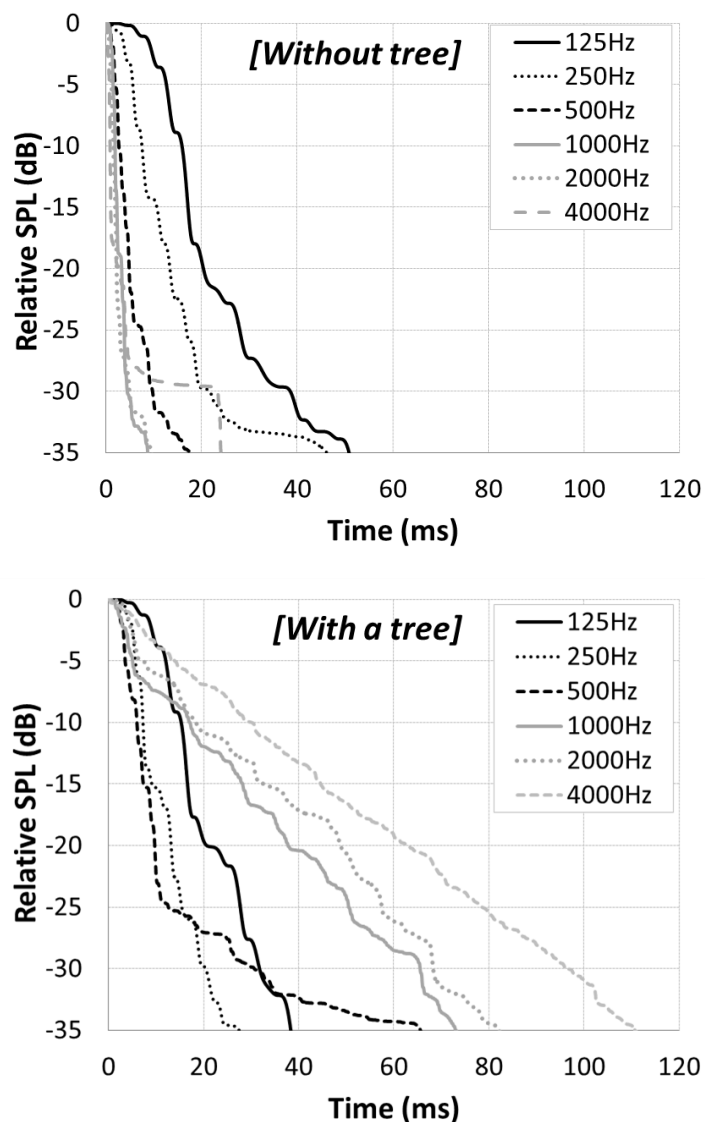


Fig. 4.5 Comparison of decay curves in the absence and presence of a single tree (Tree 3)

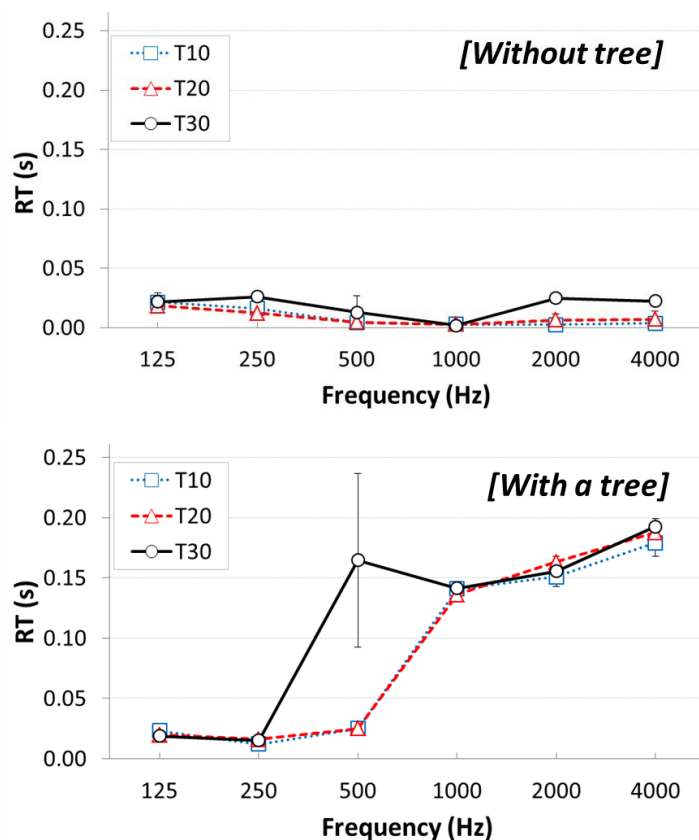


Fig. 4.6 RT with the three decay ranges corresponding to T10, T20 and T30: (a) Open field; (b) Tree 3 with foliage

Figure 4.6 shows RT with the three different decay ranges for the decay curves in Figure 4.5. The standard deviation in Figure 4.6 indicates the variation in RT for five consecutive pistol shots. The result for the presence of Tree 3 shows that RT generally increases with increasing frequency. This corresponds with prior knowledge that sound energy is more effectively scattered by vegetation and trees at high frequencies than at low frequencies, yet RT remains less than 0.2 sec. It is noticeable that T30 at 500 Hz is considerably different from T10 and T20 due to weak scattering of the direct sound but relatively important sound levels arriving after 10 ms. RT measured in open field suggests that the DIRAC programme is accurate for calculating impulse responses with very short RT although T30 is

slightly longer compared to T10 and T20. It is also noted that RT at low frequencies is not caused by the tree because the results with and without the single tree are similar. In this study, therefore, the decay range for T20 is used to investigate the sound scattering effect of a single tree.

#### **4.4.4 Repeatability of the measurement method**

Repeatability of the measurement method was examined on Day 3 and Day 4, with a 12 day interval. The temperature and humidity on both days were rather similar, as can be seen in Table II. The measurement was carried out for Tree 2 with foliage at the source-receiver distance of 20 m ( $d_r=10$  m,  $d_s=10$  m). The measurement condition for source and receiver was  $h_r=0.2$  m,  $h_s=0.2$  m and  $\theta_{s-r}=180^\circ$ . It was estimated that the maximum difference in RT20 between the two days is 0.03 sec at 500 Hz, which indicates the repeatability of the measurement and analysis methods.

To examine uniformity of sound scattering, RT20 for the six straight lines ( $\theta_{s-r}=180^\circ$ ) with  $60^\circ$  interval, meaning one rotation in reference to the tree trunk, was measured for Tree 2 with foliage. The source-receiver distance and height were the same as described above. The maximum difference in RT20 between the results measured at the six different straight lines positions was 0.02 sec. Thus, Tree 2 can be considered as a uniform scatterer in the horizontal plane. It is expected that other trees could also scatter sound uniformly as the canopies are approximately symmetric.

#### **4.4.5 Ground conditions and receiver heights**

Differences in ground conditions can affect RT20 due to the variation in the amplitude of reflected sound. Although field measurements were carried out at the same source

and receiver configurations, the ground condition for each tree could be different due to many factors such as root structure, soil composition, moisture content, and seasonal influences. Therefore, it is necessary to investigate the effect of ground condition on sound scattering. For this, the decay curve for grassland (assumed as soft ground) is compared with that for three different ground conditions using 2 mm thick hard plastic panels covering the source-receiver line from the tree trunk. The four different ground conditions were: (1) bare grassland all around the tree, (2) 11 m long by 2 m wide hard cover on the receiver  $R$  side, (3) 11 m long by 2 m wide hard cover on the source  $S$  side, (4) these hard covers on the  $S$  and  $R$  sides simultaneously. The measurement was conducted for Tree 2 on Day 6 with  $d_r=10$  m,  $d_s=10$  m and  $\theta_{s-r}=180^\circ$ . The effect of receiver height on the decay curve was also examined at  $h_r=0.2, 1.5, 3.0$  and  $4.0$  m with the same source height of  $h_s=0.2$  m. In Figure 4.7, decay curves with the different ground conditions at the receiver height of 0.2 m for Tree 2 are shown from 500 Hz to 4 kHz.

The result in Figure 4.7 indicates that the different ground conditions play an important role in the characteristics of the decay curves, especially at 500 Hz and 1 kHz. At 500 Hz, in comparison with soft grassland, the amplitude near 10 ms with the hard ground on the receiver side is rather high. At 1000 Hz, relatively strong sound energy for soft ground near the receiver can be found at rather late parts of decay curves in comparison with hard ground. At higher frequencies, on the other hand, the variation in the characteristics of the decay curves with different ground conditions is insignificant. This is consistent with the fact that ground effects, averaged over full-octave bands, are not present anymore (ISO, 1996) at these frequency bands. Hard ground on the source side seems to have less influence. This lack of reciprocity remains unexplained.



## Chapter 4. Quantifying Scattered Sound Energy from a Single Tree by means of Reverberation Time

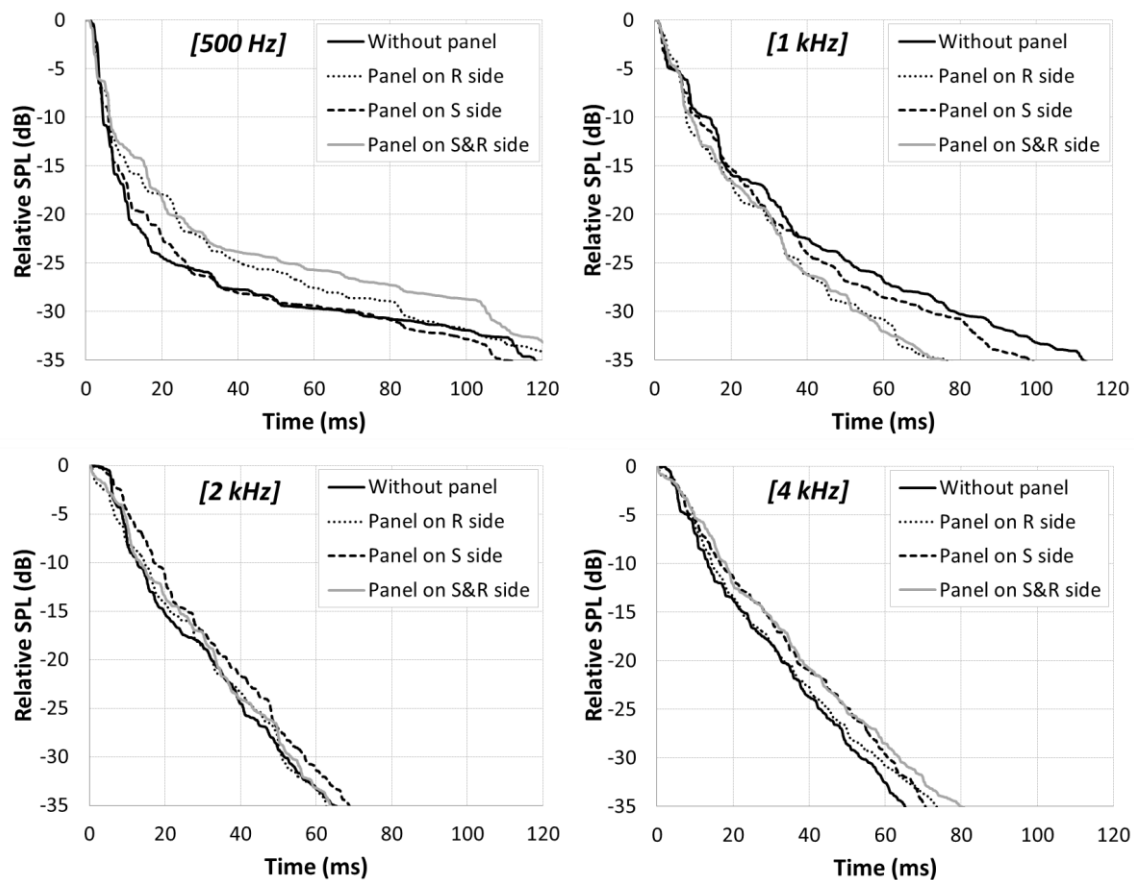


Fig. 4.7 Decay curves with the four different ground conditions at the receiver and source heights of 0.2 m for Tree 2. Each figure shows the decay curves in octave band frequencies from 500 Hz to 4 kHz

Figure 4.8 shows the effect of the ground conditions and receiver heights on RT20 for Tree 2. The standard deviation again indicates the difference in RT20 for five consecutive pistol shots. The result in Figure 4.8 shows that the different ground conditions produce variations in RT20 at all receiver heights, especially at 500 Hz and 1 kHz for the considered source-receiver geometry, while there is an insignificant difference in RT20 at lower and higher frequencies. The results also show that receiver heights can affect the variation in RT20 at certain frequencies.

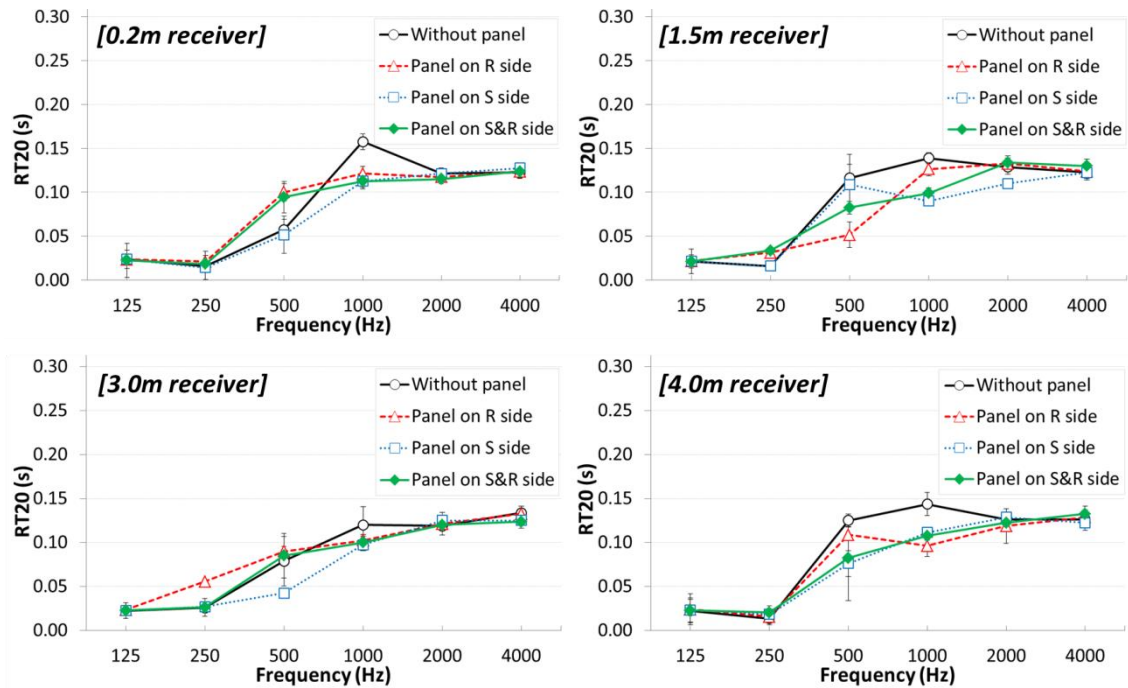


Fig. 4.8 Effect of the different ground conditions on RT20 for Tree 2 with different receiver heights from 0.2 m to 4.0 m (source height 0.2 m)

## 4.5 Measurement Results

### 4.5.1 Effects of tree size with and without foliage

The trees considered in this study have five different heights between 7.7 m and 20.6 m. The diameters of the five tree crowns are between 6.9 m and 21.5 m. To examine the effect of tree crown size on scattered sound energy, measurements were carried out with a source-receiver distance of 20 m ( $d_r=10$  m,  $d_s=10$  m) and  $\theta_{s-r}=180^\circ$  for the five trees with and without foliage. The height of both source and receiver was 0.2 m. The measurements for the five trees with and without foliage were carried out on Day 3 and Day 5, respectively. For the five trees with foliage, Figure 4.9 shows the decay curves in octave band frequencies from 500 Hz to 4 kHz. Decay curves at low frequencies are not shown here because there is insignificant sound scattering by the trees.

The result in Figure 4.9 indicates that the RT20 proportionally increases with increasing size of the trees because a larger tree produces relatively stronger sound scattering and longer sound paths through the crown. Above 500 Hz, it can be seen that the characteristics of decay curves depend on the tree size. For relatively small trees like Tree 1, Tree 2 and Tree 3, the scattered sound energy at 500 Hz is weak relative to direct sound. The results at high frequencies show that the slope of decay curves is rather linear with a slow decrease of sound energy. The decay time at 4 kHz for Tree 4 is approximately 120 ms at -25 dB below the initial level, indicating long travelling paths in the tree crown.

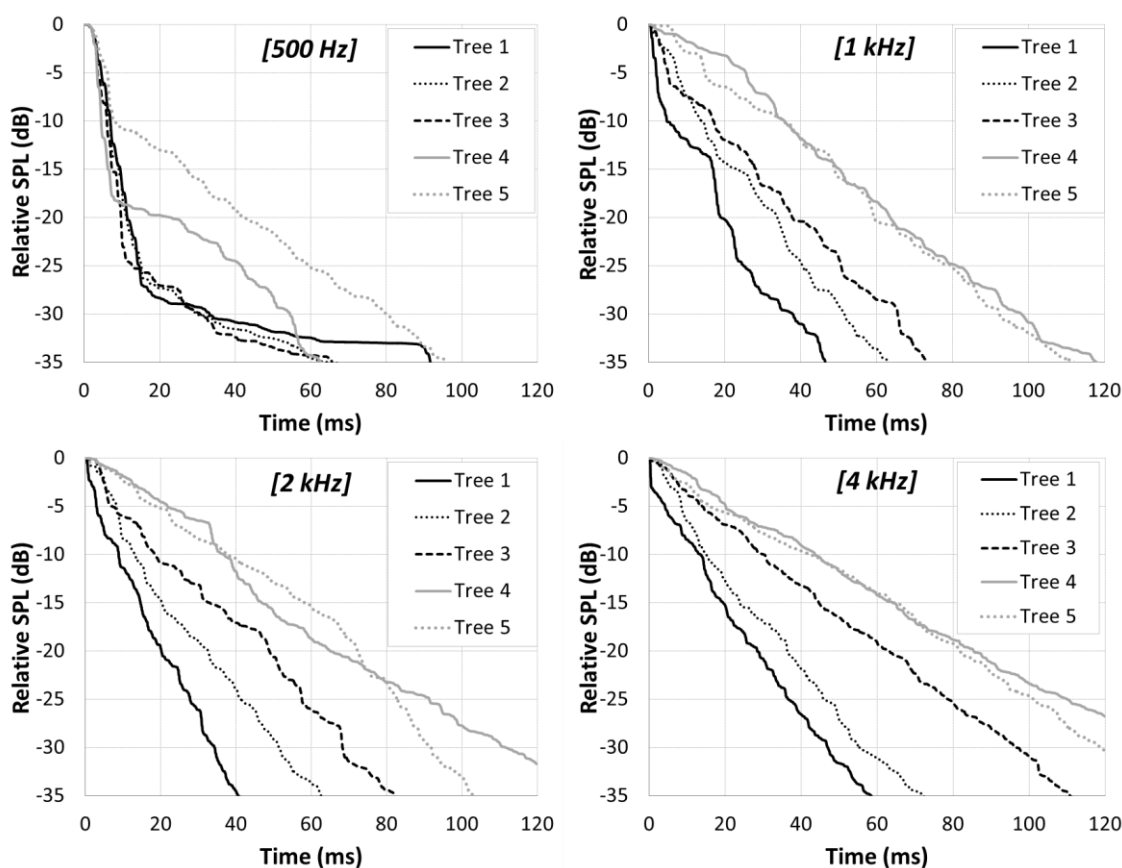


Fig. 4.9 Decay curves for the five trees with foliage. Each figure shows the decay curves in octave band frequencies from 500 Hz to 4 kHz

Figure 4.10 shows RT20 according to the surface area of the trees with and without foliage in octave band frequencies from 500 Hz to 4 kHz. Above 500 Hz, RT20 is gradually increased with the increasing surface area of the trees. The maximum RT20 is 0.26 sec at 4 kHz for Tree 4 with foliage. It is noted that the RT20 at 4 kHz is decreased above around 200 m<sup>2</sup>. This was because a large number of leaves on Tree 5 were fallen on Day 3 due to the season, as shown in Figure 4.3. However, the result from another measurement, obtained on Day 1, indicates that RT20 at 4000 Hz can reach 0.28 sec when Tree 5 is in full leaf. It can also be seen that single trees without foliage can contribute to the increase in RT20 with increasing tree crown size. Compared to the trees with foliage, RT20 for the relatively small trees (Tree 1, Tree 2 and Tree 3) without foliage is higher at 500 Hz and 1 kHz due to different ground conditions between Day 3 and Day 5. Since the sound source is low ( $h_s = 0.2\text{m}$ ), interference patterns only appear for relatively high frequencies, i.e., above 500 Hz. Thus, this leads to some important uncertainties in the analysis of the effect of trees without and with foliage due to different ground conditions.

The leaves on the five single trees studied here have widths and lengths below 15 cm. This size corresponds to the wavelength of sound at 2250 Hz, and thus it is expected that foliage has an influence mainly on sound scattering at or above this frequency. At 4 kHz, it is shown that RT20 for trees with foliage is higher than those without foliage. In particular, RT20 by Tree 4 is increased by 0.08 sec in the presence of foliage, confirming that foliage scattering occurs at high frequencies. As for Tree 5, RT20 at 4 kHz can be increased by 0.08 sec when in full leaf. Overall, the results indicate that leaves increase RT20 at high frequencies. The size and thickness of leaves as well as LAI (Leaf Area Index) and LAD (Leaf Area Density) could also play a role, but this was

not studied here.

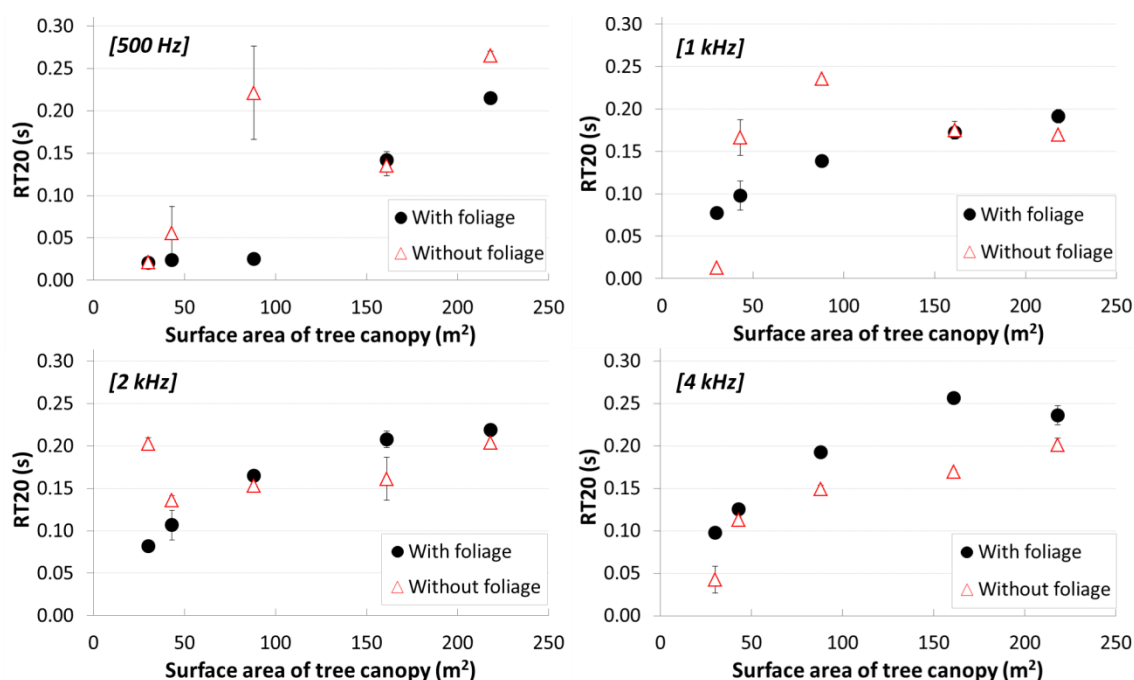


Fig. 4.10 Effect of the surface area of tree crown with and without foliage on RT20. Each figure shows RT20 in octave band frequencies from 500 Hz to 4 kHz

#### 4.5.2 Source-receiver angle

The characteristics of decay curves are influenced by source-receiver angle ( $\theta_{s-r}$ ) (see Figure 4.4). In this experiment, the effect of source-receiver angle on the decay curve is examined using Tree 2 without foliage on Day 2. The measurement condition was  $d_s=13$  m,  $d_r=13$  m,  $h_s=1.5$  m and  $h_r=1.5$  m. The source-receiver angles were 0, 90, 135 and 180°. The source-receiver angle of 0° was used to estimate the back scattered sound energy (or reflection), which was measured with  $d_s=40$  m and  $d_r=10$  m arranged in a line without the tree between the source and receiver.

In Figure 4.11, the decay curves for Tree 2 without foliage with different source-receiver angles are shown at different frequencies. The result shows that decay curves

Chapter 4. Quantifying Scattered Sound Energy from a Single Tree by means of  
Reverberation Time

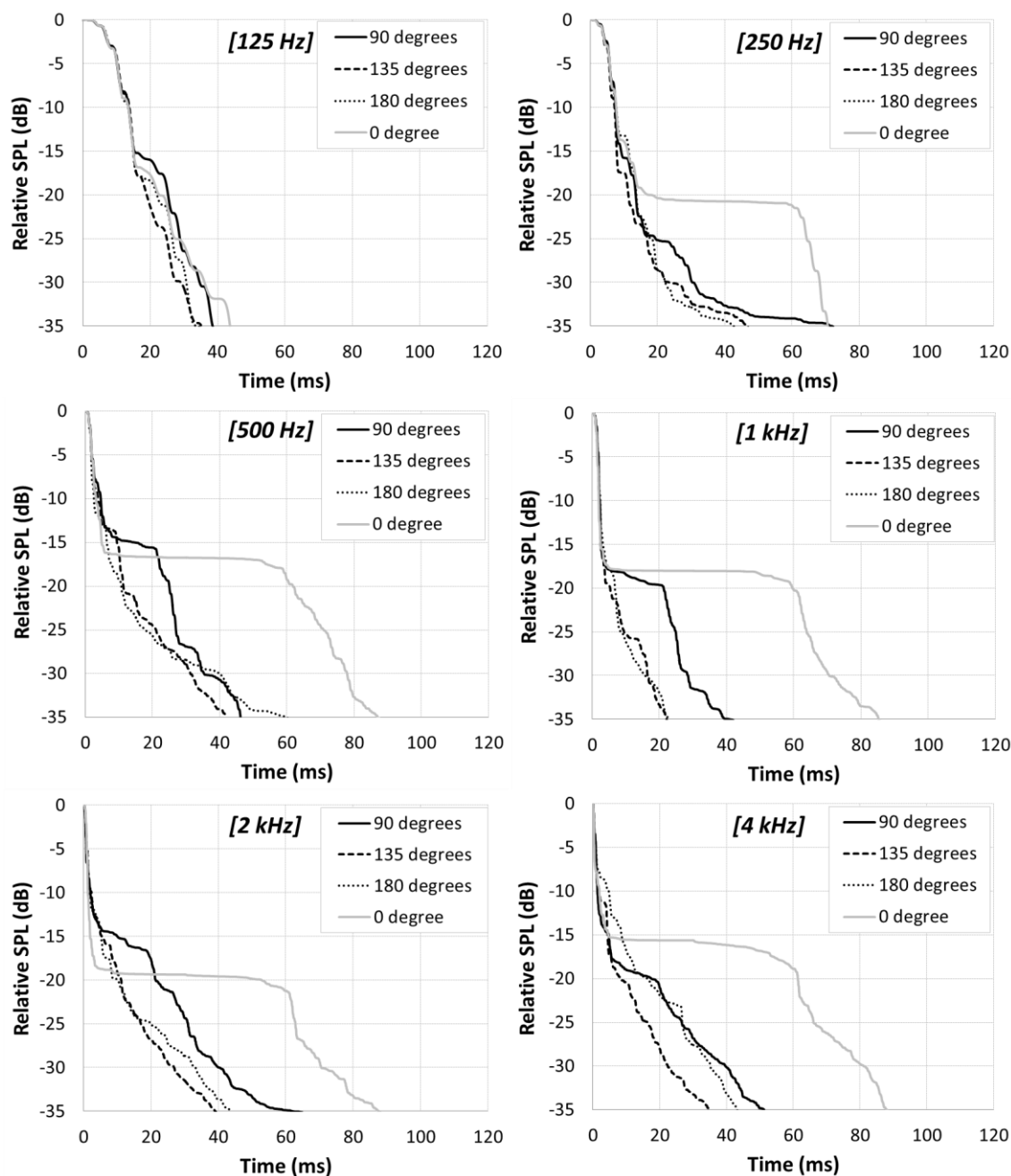


Fig. 4.11 Decay curves for Tree 2 without foliage with different source-receiver angles. Each figure shows the decay curves in octave band frequencies from 125 Hz to 4 kHz

for the source-receiver angle of  $135^\circ$  ( $45^\circ$  in reference to  $180^\circ$ ) is similar to that for  $180^\circ$ . This is because the time interval between direct and scattered sound is very short for both source-receiver angles due to the relatively close receiver distance from the edge of the tree crown. For the source-receiver angle of  $90^\circ$ , there is a plateau between

direct and scattered sound with the time interval of approximately 15 ms (5.1 m for a speed of sound of 340 m/s). This is caused by the difference in distance for the direct sound path (18.4 m) with scattered sound paths (21.5m ~ 26.0 m) from the edge of the crown and the trunk. The decay curve for the source-receiver angle of  $0^\circ$  (back scattering) suggests that the tree can reflect sound energy backwards effectively. It can be seen that there is a pronounced plateau with the time interval of approximately 50 ms (17.0 m) between direct and reflected sound, which indicates strong reflection from the vicinity of the tree trunk. The relative SPL vs. time in Figure 4.11 suggests that Tree 2 without foliage can reflect sound at frequencies above 250 Hz. In summary, the source-receiver angle can affect characteristics of the decay curve, especially for  $0^\circ$  and  $90^\circ$ . Calculation of RT20 is omitted here due to the long-time interval between direct and reflected sound.

### 4.5.3 Source-receiver distance

Measurements for the five individual trees with foliage on Day 3 were conducted to investigate the effect of source-receiver distance on RT20. Values for  $d_s$  (source-trunk distance) were 10 m, and for  $d_r$  (receiver-trunk distance) 5, 10, 20 and 30 m. Therefore, the angle subtended by the tree crown at the receiver points ranges between  $18^\circ$ - $62^\circ$  for Tree 1,  $20^\circ$ - $66^\circ$  for Tree 2,  $24^\circ$ - $70^\circ$  for Tree 3,  $29^\circ$ - $74^\circ$  for Tree 4, and  $37^\circ$ - $78^\circ$  for Tree 5. The source, tree and receiver were arranged in a straight line with  $\theta_{s-r}=180^\circ$ . Therefore, the range of source-receiver distances was between 15 m and 40 m. The height of the source and receiver was 0.2 m. Figure 4.12 presents RT20 measured with  $d_s=10$  m for different frequencies as a function of  $d_r=5, 10, 20, 30$  m. At 125 Hz and 250 Hz, RT20 is under 0.03 sec and independent of source-receiver distance. It can be

seen that the source-receiver distance plays an insignificant role on RT20 above 500 Hz, except in the case of Tree 5. The variation in RT20 for Tree 5 might be due to the relatively thick trunk and low leaf density, and measurement locations slightly deviating from the straight line between source and receiver. Therefore, it can be concluded that the different source-receiver distances studied here have an insignificant effect on the variation in RT20.

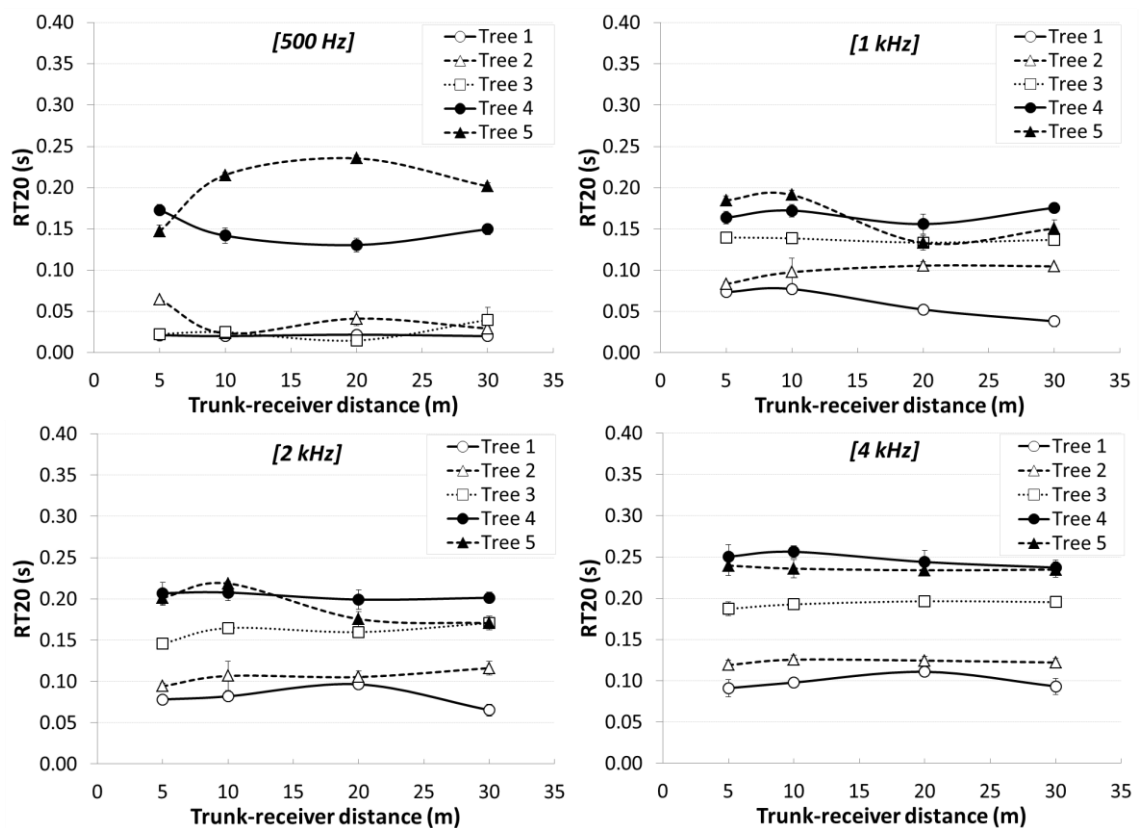


Fig. 4.12 RT20 with different source-receiver distances from 15 m to 40 m, with  $d_s=10$  m and  $d_r=5, 10, 20, 30$  m for each tree. Each figure shows the decay curves in octave band frequencies from 500 Hz to 4 kHz

## 4.6 Summary

This chapter has shown that sound scattering is an important aspect of the interaction



between sound waves and trees. This effect is quantified by means of decay curves, closely linked to the RT, as influenced by the ground condition, receiver heights, tree crown shape and size, the amount and condition of foliage, and source-receiver angle and distance. Repeatability for the measurement using a starting pistol has also been confirmed.

The results quantify the amount of scattered sound energy from a single tree at different frequencies. At very low frequencies, below 250 Hz, no difference in RT20 has been found compared to the same measurement setup and post-processing in absence of a tree (open field). At higher frequencies, the amount of scattered sound energy is generally increased with increasing frequency. It has been found that tree crown size is the most important factor in relation to scattering of sound energy. With increasing surface area of the crown (area of an enclosing surface), RT20 is increased up to 0.28 sec at 4 kHz. A tree without foliage also produces a similar amount of scattered sound energy as a tree with foliage. Presence of leaves increases RT20 starting from 2 kHz, by 0.08 sec at 4 kHz. The characteristics of decay curves are influenced by source-receiver angle, especially for 0 and 90 °. Back scattering (or reflection) from a tree has also been observed at frequencies above 250 Hz. It has been observed that distance between source and receiver (within 40 m) under the same angle has insignificant effect on the variation in RT20. Ground condition can contribute to the variation in decay and RT20 at certain frequencies depending on the tree size and source-receiver geometry. However, for the source-receiver geometry of this study the effect is important especially at low and mid frequencies where sound scattering is of relatively limited importance.

Although many field measurements have been carried out in this study, further work is still needed to characterise the effect of other factors such as leaf size, leaf shape and thickness, but also the distribution of biomass over the crown, quantified by LAD (Leaf Area Density). Numerical modelling of scattering of sound energy by trees (as initiated by Van Renterghem *et al.* (2012) and Hornikx *et al.* (2011), as well as scale modelling could further clarify the physical phenomena involved and allow evaluation of potential applications. A previous study (Haron *et al.*, 2009) showed only a slight effect (less than 1.5 dB) on sound reduction by the presence of trees in street canyons. On the other hand, trees in street canyons could be important in RT distribution since a slight increase in the scattering coefficient of building façades reduces street canyon reverberation, as shown in previous studies (Kang, 2002a, 2002b, 2007; Onaga *et al.*, 2007). Thus, it is necessary to suggest effective planting patterns of trees in urban situations to reduce noise levels. Optimisation of planting schemes was shown to be essential, e.g. in the context of tree belts (Van Renterghem *et al.*, 2012), to achieve useful noise reduction.

**PART II.**

**GREEN ROOF SYSTEMS ON A LOW BARRIER**

## **5 Noise Reduction by Green Roof Systems at Street Level**

The aim of this chapter is to explore the effects of various designable parameters of green roof systems at street level on noise reduction. Green roof systems were placed on a low barrier in a semi-anechoic chamber for measurements. Studied parameters include the structure, area, depth, type and position of the green roof system, and the type of vegetation. Section 5.1 discusses the background to the research by reviewing acoustic benefits of green roof systems. In Section 5.2, acoustic properties of green roof systems as well as measurement methods are described. Section 5.3 deals with results for the effects on noise reduction of area, depth, type and position of the green roof systems. Results also include the effect of different vegetation types on noise reduction. Section 5.4 concludes key findings of this chapter.

### **5.1 Introduction**

Along with the strong movement towards sustainable urban environments, green roof systems have become widely used in urban spaces since they have numerous ecological and environmental advantages. For example, green roof systems can reduce storm water runoff, increase urban bio-diversity, and mitigate the urban heat island and air pollution (Alexandri *et al.*, 2008; Fioretti *et al.*, 2010; Getter *et al.*, 2006; Gregoire *et al.*, 2011; Mentens *et al.*, 2006; Takebayashi *et al.*, 2007).

In terms of acoustic benefits, green roof systems have been regarded as an effective structure to reduce noise pollution in urban spaces arising from road, rail and air traffic (Dunnett *et al.*, 2004). Such sustainable materials using natural means can also

contribute to the reduction of environmental impact as well as the improvement of soundscapes (Kang *et al.*, 2010; Yu *et al.*, 2009). In street canyons and courtyards, the amount of sound energy propagating over rooftops from noisy sides to quiet sides is mainly determined by the height, width and shape of buildings (Hornikx *et al.*, 2007, 2009; Kang, 1996c; Van Renterghem *et al.*, 2006). In this case, green roof systems on the top of buildings can act as absorbers especially for diffracted sound waves between parallel streets and for that, parametric studies have been carried out (Van Renterghem *et al.*, 2008a, 2009, 2010, 2011), showing that green roof systems are effective on noise mitigation, and therefore creating quiet sides. Moreover, it has been shown that green roofs can be used to effectively increase the sound insulation of light-weight roof structures (Kang *et al.*, 2009).

At street level, various kinds of green roof systems can also be used, for example, on the top of underground car parking spaces. In particular, semi-extensive green roof systems, which support low-growing, tough, and drought-resistant vegetation (Dunnett *et al.*, 2004), can be installed in many places instead of grass land at street level due to various reasons such as better visual effects and maintenance. There is a potential that green roof systems on low-profiled structures can be developed to an innovative and sustainable low barrier using natural materials for reducing traffic noise (Baulac *et al.*, 2005; Baulac *et al.*, 2008). However, studies on the use of green roof systems at street level have not been reported yet.

The aim of this chapter is therefore to explore systematically the effects of various designable parameters of green roof systems at street level on noise reduction. A series of measurements have been carried out in a semi-anechoic chamber using green roof

systems which consist of the Zinco (brand name of green roof substrate) and limestone-based substrates. They are placed on a box with a height of 1200 mm. Numerical simulations have also been carried out for selected cases. Studied parameters include the structure, area, depth, type and position of the green roof system, and the type of vegetation.

## **5.2 Methodology**

### **5.2.1 Physical properties of the green roof system**

The green roof systems in this experiment were comprised of 600 mm × 400 mm × 280 mm (outer dimension) plastic trays. Figure 5.1 shows the components of the tray: a 30 mm drainage layer on the bottom and plastic panels as walls; a geotextile membrane filter layer to prevent obstruction of the drainage layer by small particles of growing media; and growing media of Zinco or limestone-based substrates. In Figure 5.2 Zinco and limestone-based substrates used in this experiment are shown. The Zinco substrate was a mixture of Zinco sedum carpet substrate and Zinco roof garden substrate, with a ratio of 1:1. Table 5.1 describes detailed product data for these components. The limestone-based substrate consists of 60 % limestone (< 3.35 mm particle size), 20 % loam and 20 % organic matter. The physical properties of Zinco and limestone-based substrates are given in Table 5.2.

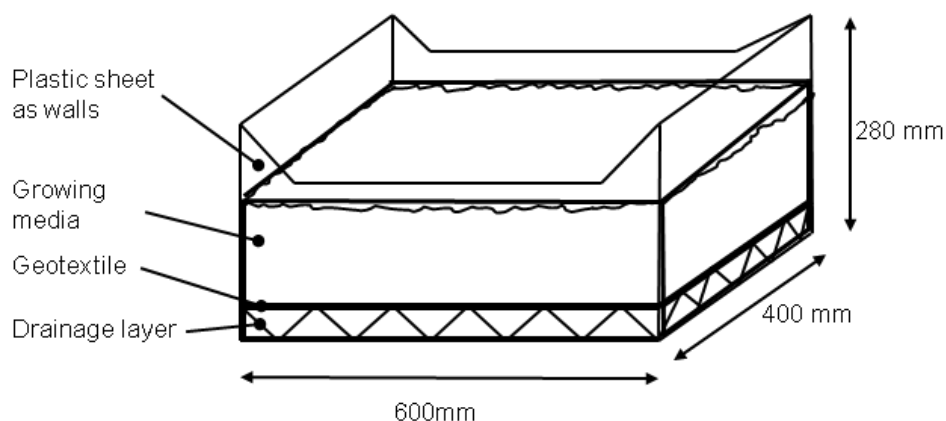


Fig. 5.1 Components of the tray

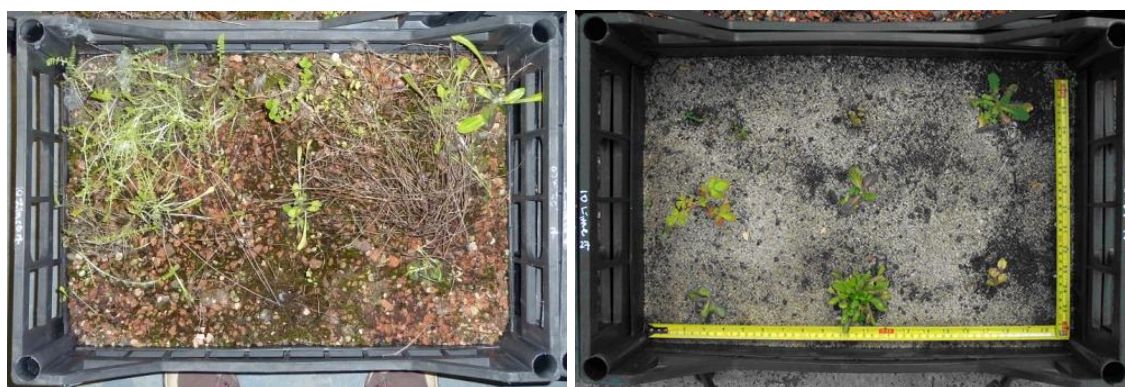


Fig. 5.2 Zinco (left) and limestone-based substrates (right) used in the experiment

Table 5.1 Product data of the sedum carpet and roof garden substrate used for Zinco substrate

	Sedum carpet substrate	Roof garden substrate
Granules of < 0.063 mmØ	≤ 7 %	≤ 20 %
Granules of < 4 mmØ	≥ 25 %	-
Organic content	≤ 4 %	-
Porosity	63 %	64 %
Dry weight	980 kg/m <sup>3</sup>	930 kg/m <sup>3</sup>
Saturated weight	1240 kg/m <sup>3</sup>	1400 kg/m <sup>3</sup>
Maximum water capacity	25 %	46 %
Air content at saturation	38 %	18 %
Water permeability	≥0.1 cm/s	≥0.034 cm/s

\* Source: Alumasc product data sheet

Table 5.2 Physical properties of the Zinco substrate and limestone-based substrates

	Loose bulk density (g/cm <sup>3</sup> )	Bulk density at saturation (g/cm <sup>3</sup> )	Increase in bulk density (%)	Air filled porosity (%)	Water holding capacity (%)
Zinco	1.02	1.26	23.5	33.5	26.6
Limestone-based	1.43	1.80	26.2	12.0	29.8

In the experiment, 3 different substrate conditions were used: Zinco substrate with depths of 50 mm and 100 mm, and limestone-based substrate with a depth of 100 mm. For Zinco substrate, 20 trays for each depth condition were used. The mean weight for each tray of Zinco substrate with depths of 50 mm and 100 mm was recorded as 11.3 kg and 24.0 kg, respectively. For the limestone-based substrate, 18 trays with a mean weight of 29.1 kg per tray were used. In the spring of 2007, each tray was planted with 9 native forbs individuals originating from calcareous grassland habitat. However, few plants with 0~10 % vegetation coverage for each tray remained due to unfavourable planting season. Therefore, the substrate dominates the effect of SPL attenuation.

To examine the acoustic effect of vegetation growing on green roof systems, pruned fresh leaves (*Buxus sempervirens*) and 100 % polyester cotton were applied respectively, as shown in Figure 5.3. Here the polyester cotton, with a mean weight of 159.5 g per tray, was used to simulate an extreme condition in terms of sound absorption by vegetation. The pruned *Buxus sempervirens*, for simulating dense leaf conditions on green roof systems (although it is noted that the loose leaves and twigs could lead to some vibration-related effects such as free vibration), have leaf sizes ranging from 8 mm to 30 mm long and 5 mm to 13 mm wide, and mean weight of 606.8



g per tray. For both of pruned fresh leaves and polyester cotton, the filling depth in the trays was 120 mm approximately, representing a relatively thick layer of vegetation planted in a common green roof system.



Fig. 5.3 Pruned fresh leaves (top) and polyester cotton (bottom) used in the experiment

### **5.2.2 Absorption coefficient of the substrates**

The random-incidence absorption coefficient for the 3 different substrates in dry conditions was measured using an area of 4.8 m<sup>2</sup> in a reverberation chamber. As shown in Figure 5.4, the limestone-based substrate has a relatively low absorption above 200 Hz compared to the Zinco substrate when the depth is the same, possibly due to the differences in density and porosity between the two materials. By comparing Zinco substrate with depths of 50 mm and 100 mm, it can be seen that there are considerable

differences below 400 Hz. With a greater depth the low frequency absorption is increased, as expected. It is noted that absorption coefficient over 1 is observed due to the strong edge effect, and this is further enhanced due to the smaller sample size of 4.8 m<sup>2</sup> compared with standard 10 m<sup>2</sup> (Cox, 2009; Makita *et al.*, 1988). As peak performance of them in sound absorption is found around 1 kHz, the green roof systems are subjectively beneficial to noise control against road traffic which shows the peak level around 1 kHz in A-weighted value.

Measurements for normal-incidence absorption coefficient under dry condition were carried out using an impedance tube. Figure 5.5 shows the results for the three types of substrate. Again, it can be seen that the Zinco substrate has relatively high normal-incidence absorption coefficients compared to the limestone-based substrate, although the difference is greater than that in random-incidence absorption coefficient. The depth of Zinco substrate strongly affects the absorption coefficient below 400 Hz, which is also similar to the results for random-incidence absorption coefficient.

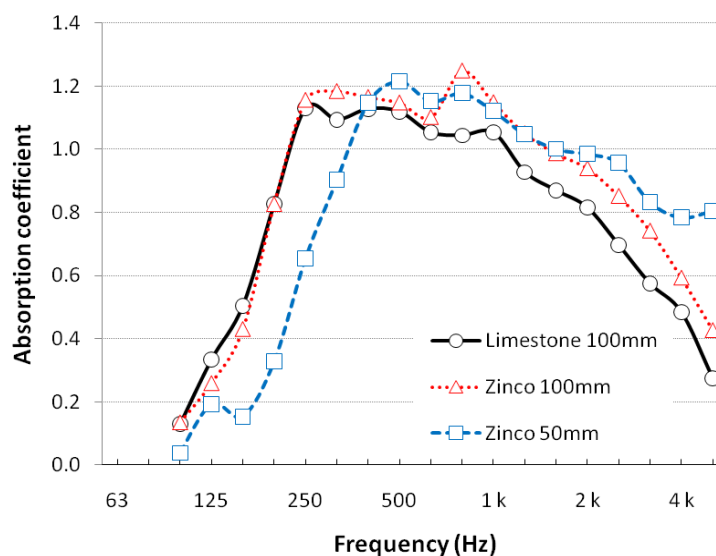


Fig. 5.4 Random-incidence absorption coefficient of studied substrates in dry condition

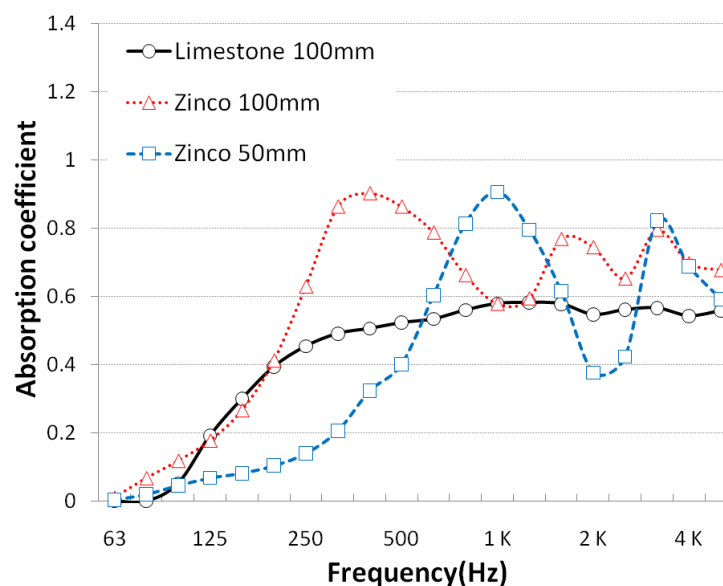


Fig. 5.5 Normal-incidence absorption coefficient of the studied substrates in dry condition

### 5.2.3 Experimental setup

The experiment was carried out in a semi-anechoic chamber which had a size of 3500 mm (W) × 3500 mm (L) × 2400 mm (H). To simulate a low profiled structure at street level, a box of 1600 mm (W) × 3000 mm (L) × 1200 mm (H) was located on the centre of the floor. The green roof trays were positioned on top of the box with a maximum of 5 rows by 4 columns. Figure 5.6 shows the schematic diagrams of the experimental condition. The box was made with MDF (medium-density fibreboard) boards to stop sound transmission through the box. For the front and rear walls, additional extended MDF boards were installed to prevent the sound transmission through side paths of the box.

The 01dB two-channel Symponie system was used for data acquisition. The two 1/2 inch microphones were positioned at a 200 mm distance from the rear wall, and the height of the receivers was 1600 mm and 1000 mm, which can be regarded as an average person's standing and sitting heights on street, respectively. An omni-directional

loudspeaker, which was connected to an amplifier to generate white-noise, was located on the floor with vibration isolation materials and it was at 100 mm from the box, to examine the effect of green roof systems on diffracted sound waves.

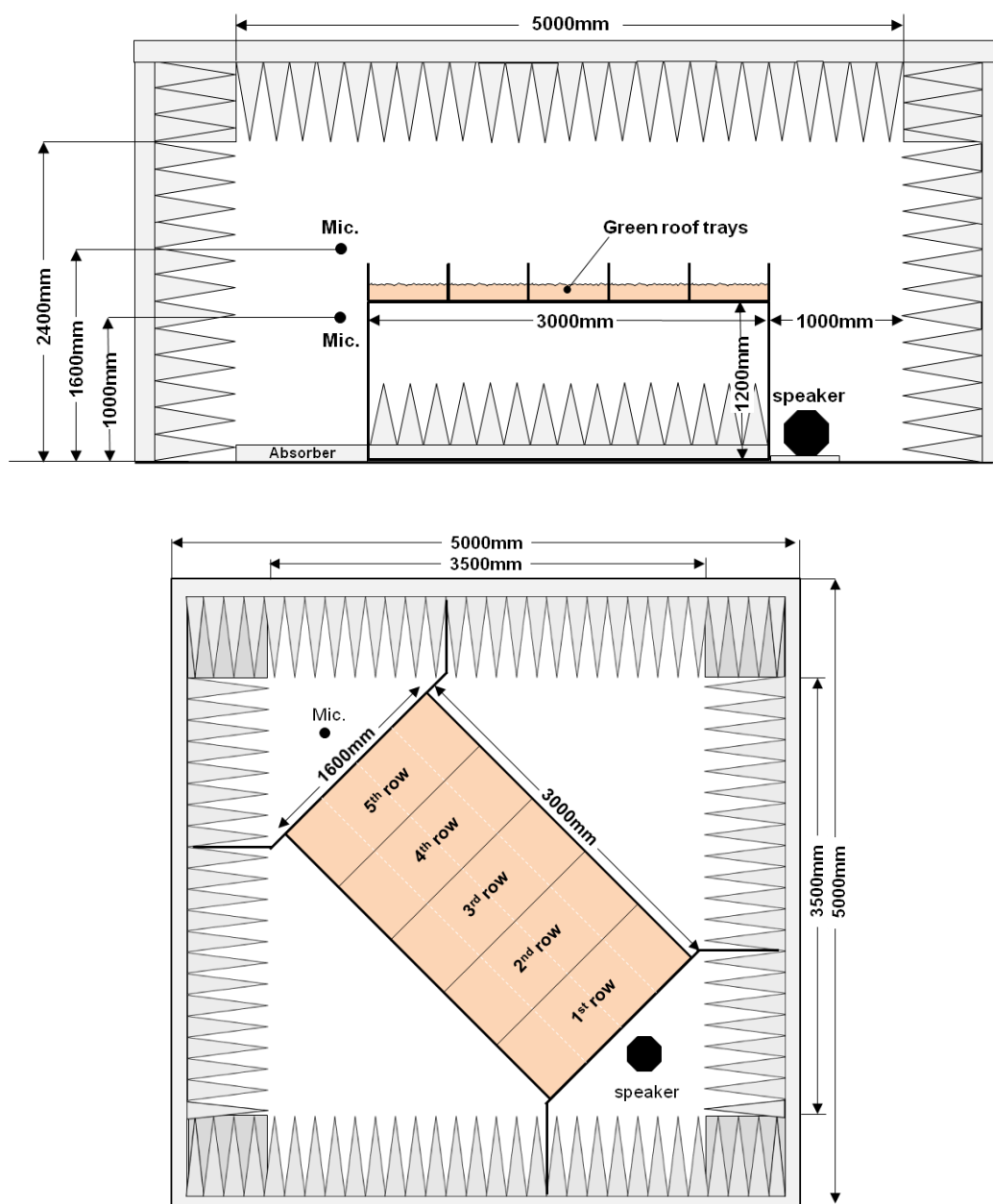


Fig. 5.6 Schematic diagrams of the cross section (top) and ground plan (bottom) for the experimental condition

#### **5.2.4 Examination of the geometrical effect using FEM**

Due to the installation of the green roof systems on the box, there are variations in configuration, namely, with two different additional heights of 130 mm (100 mm substrate + 30 mm drainage layer) and 80 mm (50 mm substrate + 30 mm drainage layer).

The configuration also varies according to the number of rows of the green roof system. Therefore, extra attenuation can be produced by the change of configuration, referred to as geometrical effect below.

To quantify the geometrical effect in idealised situations, difference in SPL by the change of configuration was predicted with FEM (finite element method) using COMSOL. The numerical models were constructed by considering the experimental condition in Figure 5.6. Due to the limitation in computing power, the calculation was performed up to 500 Hz. To simulate free-field, PML (perfectly matched layer) was used as the external sub-domain with a hemispherical shape. A point source was located at a distance of 200 mm and height of 200 mm from the box and floor, respectively.

The accuracy of prediction using FEM for the geometrical effect was examined by the comparison between measured and predicted SPL with the installation of a panel of 300 mm high, 1200 mm long and 20 mm wide on the top edge of the box, as shown in Figure 5.7. In Figure 5.8, the measured and predicted extra SPL attenuation, relative to the box without the panel, are shown. It can be seen that the agreement is very good, with an accuracy of about 1.6dB.

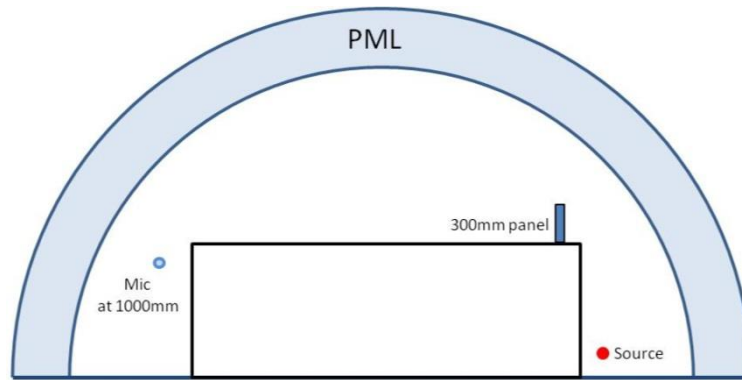


Fig. 5.7 Cross-section of the modelling condition with a panel of 300 mm high

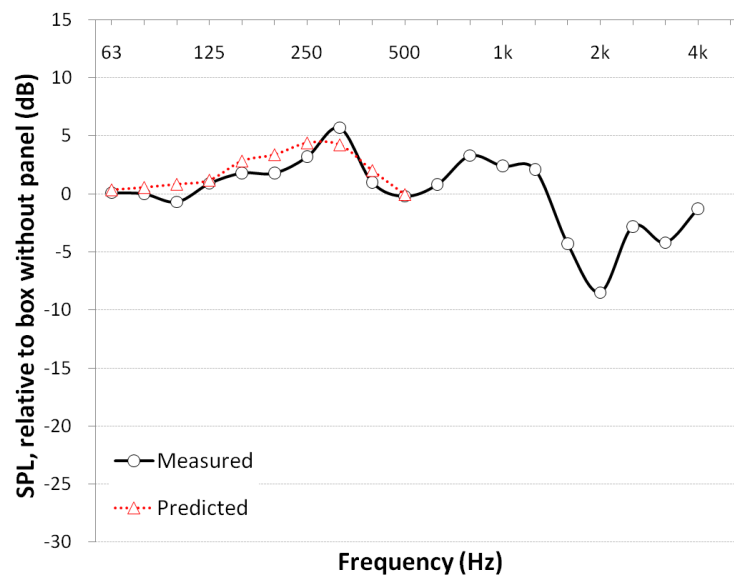


Fig. 5.8 Comparison between measured and predicted extra SPL attenuation by the panel with a 300mm height

One of the main interests is how absorption of substrate affect noise reduction when sound propagates over the green roof systems. This could be approximately obtained by subtracting the predicted geometrical effect from the measured SPL attenuation. To provide baselines, in Figure 5.9 and Figure 5.10, the FEM predicted extra SPL attenuation by the geometrical effect is shown with different number of rows, considering two green roof heights, 130 mm and 80 mm. The boundary condition of the configuration is assumed as acoustically hard.

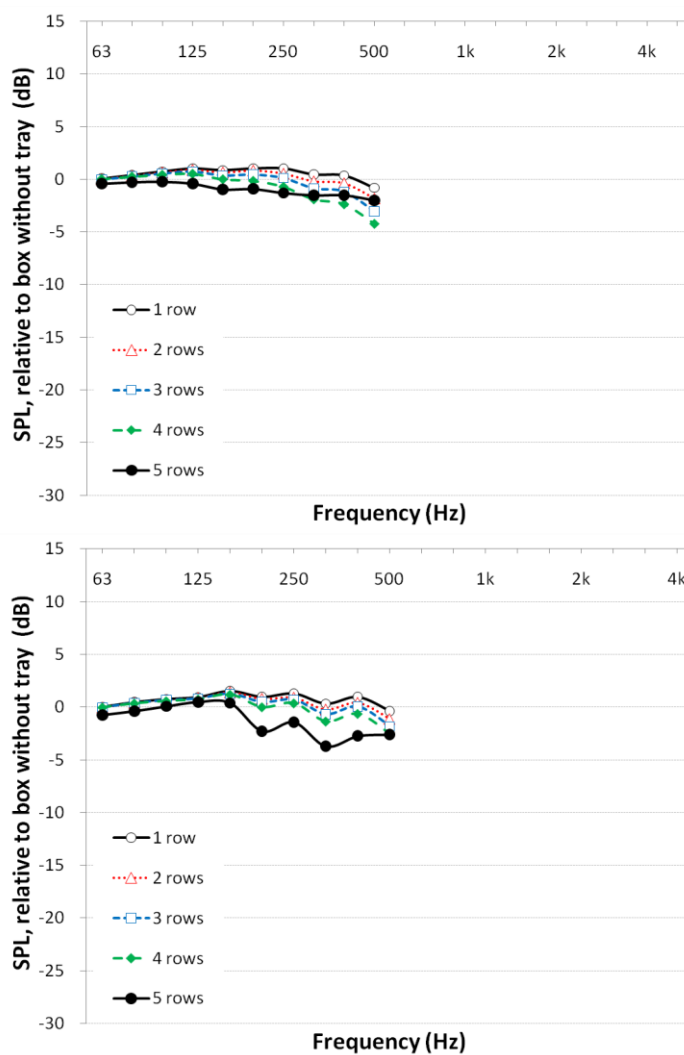


Fig. 5.9 Predicted SPL attenuation due to the geometrical effect for a height of 130 mm according to the number of rows at two receivers with a height of 1600 mm (top) and 1000 mm (bottom)

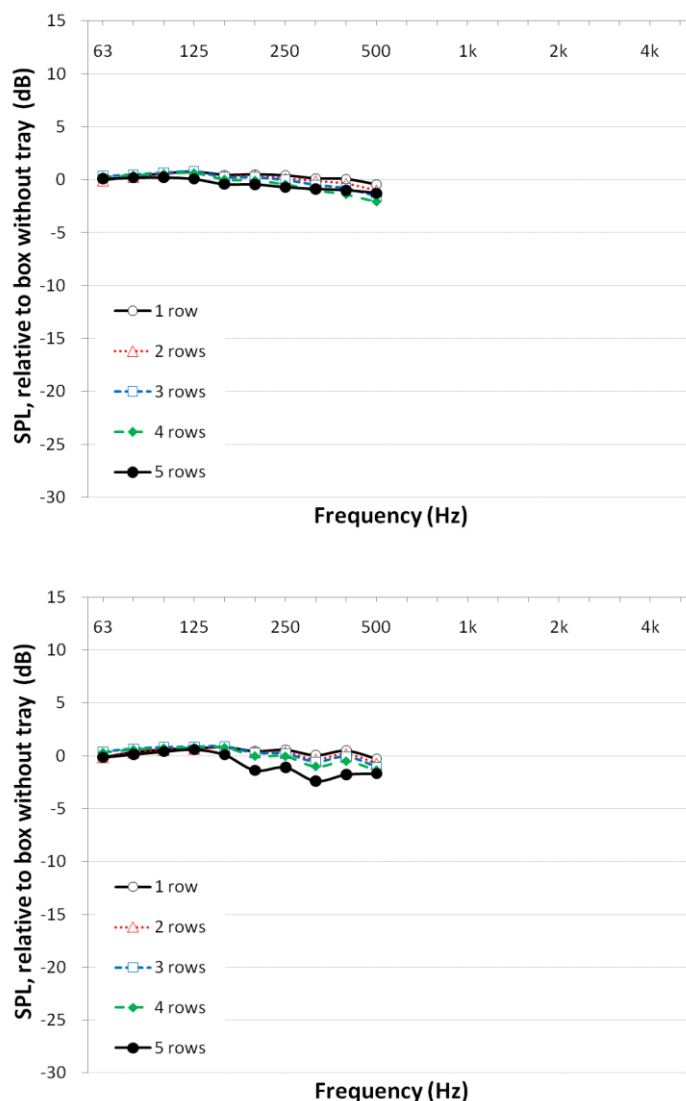


Fig. 5.10 Predicted SPL attenuation due to the geometrical effect for a height of 80 mm according to the number of rows at two receivers with a height of 1600 mm (top) and 1000 mm (bottom)

### 5.2.5 Experimental parameters

Overall, five main experimental parameters have been considered, as shown in Table 5.3 and described below:

(1) Structure of the empty trays. SPL attenuation due to the physical shape of the empty trays should be measured in order to obtain the effect of substrates. In this chapter,



experiments were carried out with empty trays from 1 to 5 rows, as shown in Figure 5.11. To examine the geometrical effect, measurements of SPL attenuation due to different heights of plastic panels surrounding the periphery of the trays were carried out, where two heights of plastic panels, 80mm and 130mm were installed at 1<sup>st</sup> row using 4 trays, as shown in Figure 5.12.

(2) Green roof area (number of rows). The number of rows of the trays used in the experiment was from 1 to 5, which means that the number of trays was from 4 to 20, as shown in Figure 5.13.

(3) Depth and type of substrates. Experiments were conducted using 3 different substrate conditions, as mentioned above, to examine the effects of substrate depth (Zinco substrate with depths of 50 mm and 100 mm), as well as substrate type (comparing Zinco and limestone-based substrates with a depth of 100 mm).

(4) Position of the green roof system. This was investigated using 1 row of the trays with pruned fresh leaves, at three positions, namely the front (1<sup>st</sup> row), centre (3<sup>rd</sup> row) and end part (5<sup>th</sup> row) of the box.

(5) Types of vegetation. Pruned fresh leaves and polyester cotton were used to examine the acoustic effect of vegetation on the growing media. The experiments were carried out using 1 row only at 1<sup>st</sup> row, as shown in Figure 5.14.



Fig. 5.11 Measurement of SPL for empty trays with 5 rows

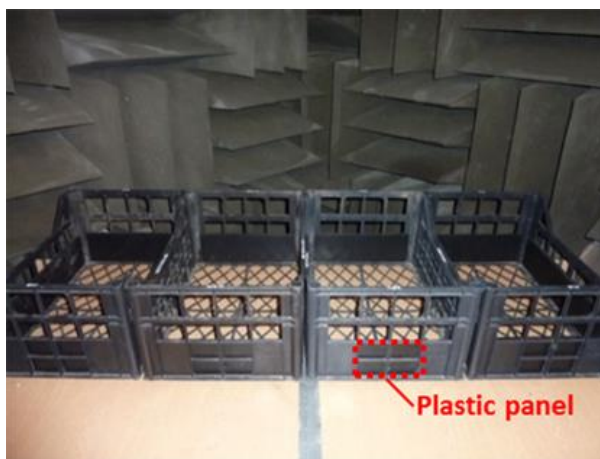


Fig. 5.12 Empty trays with plastic panels surrounding the periphery parts



Fig. 5.13 Experimental condition with different areas of the green roof system



Fig. 5.14 Experimental conditions to demonstrate the acoustic effect of vegetation with pruned fresh leaves (top) and polyester cotton (bottom)

Table 5.3 Parameters considered in the experiment

Parameters	Purpose
Structure of the empty trays	Verification for SPL attenuation due to the shielding effect of the empty trays
Green roof area (number of rows)	Investigation on the effect of green roof area on SPL attenuation according to the number of rows
Depth and type of substrates	Experiments using 3 different substrate conditions to verify the effect of depth and type of substrates on SPL attenuation
Position of the green roof system	Measurement for the effect of the position of the green roof system equipped on the low-profiled structure
Types of vegetation	Measurement of the acoustic effect of vegetation on the growing media

## 5.3 Results

### 5.3.1 SPL attenuation by empty trays

In Figure 5.15, the extra SPL attenuation by the empty trays with 1 row to 5 rows is shown at a receiver height of 1600 mm. It can be seen that the empty trays have a strong effect on SPL attenuation, up to about 10 dB at above 1 kHz. Moreover, it can be observed that generally speaking, the effect of the empty trays on the SPL attenuation is gradually increased with the increasing number of rows. On the other hand, some negative effects on SPL attenuation are observed at lower frequencies.

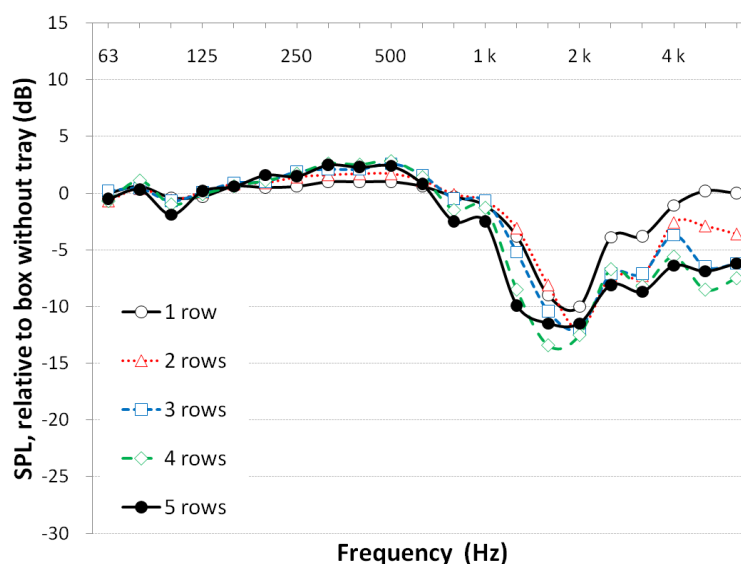


Fig. 5.15 Measured extra SPL attenuation by the empty tray at the receiver height with 1600 mm

The experiment to verify the geometrical effect which causes extra SPL attenuation was performed using 80 mm and 130 mm plastic panels surrounding the periphery parts of the trays as illustrated in Figure 5.12. Figure 5.16 shows the measurement results, relative to the empty trays without the plastic panels. It can be seen that the plastic panels with both heights play an important role in SPL attenuation above 1 kHz. In

comparison with the 80 mm plastic panels, the effects of the 130 mm plastic panels shift to relatively lower frequencies, as expected.

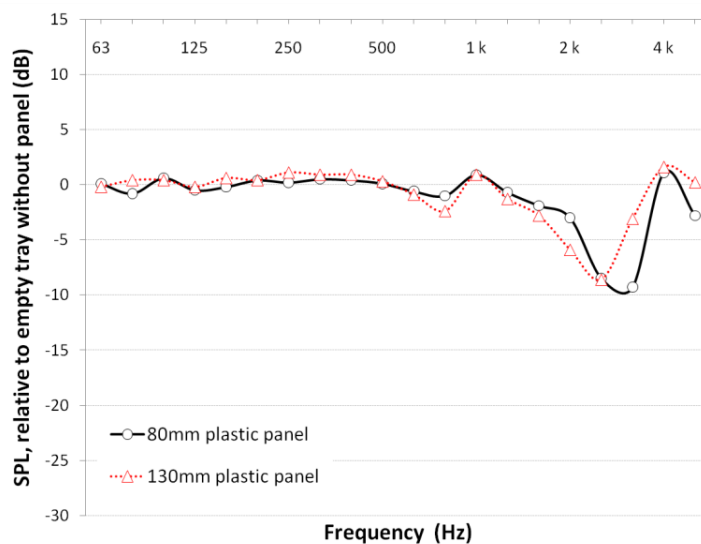


Fig. 5.16 Measured extra SPL attenuation by plastic panel with 80 mm and 130 mm height at the receiver height with 1600 mm

### 5.3.2 Green roof area

Figure 5.17 shows the measured SPL attenuation according to the area of the green roof system, relative to the box without empty trays, where the effects are due to the absorption by the substrate, shielding effect by the empty trays, and the geometrical effect by the increased height of the green roof structures. It reveals that the green roof system on the low profiled structure can reduce SPL, even by more than 20 dB approximately at high frequency for diffracted sound. With the results at various frequencies, the effect of a given source type can be derived. The effect on SPL attenuation against a typical road traffic spectrum with 70 km/h (Nota *et al.*, 2005) is considered here to represent a relatively worse condition, and it is gradually increased with the increasing green roof area from 4.8 dBA to 9.7 dBA at the receiver height of

1600 mm, and from 3.8 dBA to 7.7 dBA at the receiver height of 1000 mm. However, it is noted that some negative effects are still observed at lower frequencies, at both receiver heights.

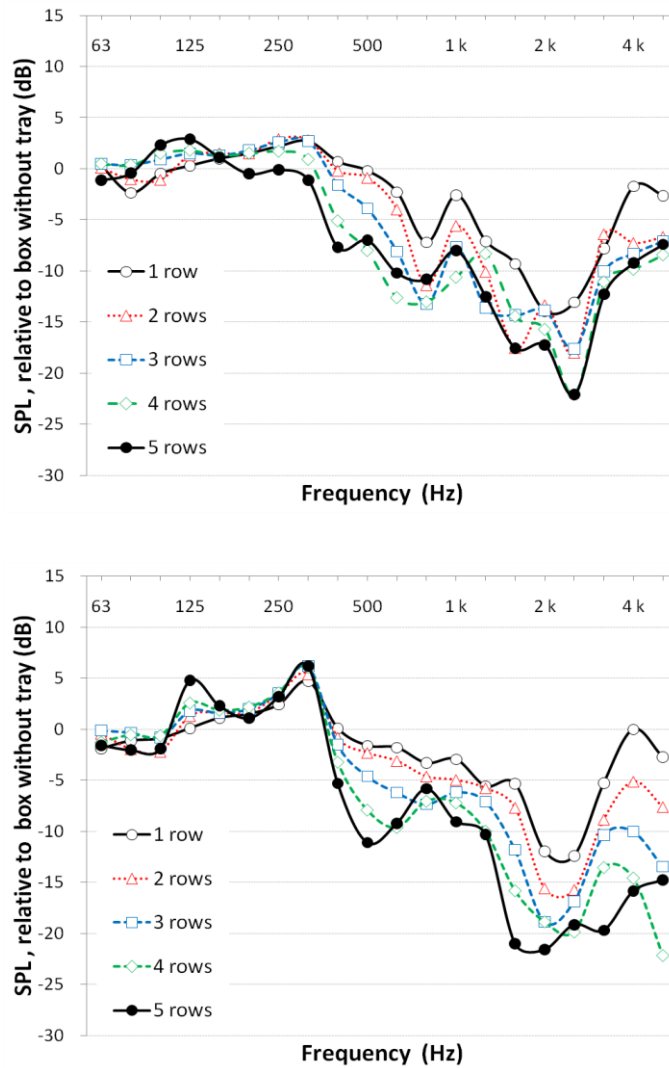


Fig. 5.17 Measured SPL attenuation with increasing area of the green roof system at two receivers with a height of 1600 mm (top) and 1000 mm (bottom)

To compare the SPL attenuation between filled and empty trays, Figure 5.18 shows the difference in SPL between Figure 5.17 and Figure 5.15. In other words, the result in Figure 5.18 is due to the geometrical and absorption effects of the green roof system. It can be seen that the extra SPL attenuation occurs over 250 Hz, whereas at lower

frequencies the green roof system has an insignificant impact on SPL attenuation and some limited low-frequency amplification seems to be consistent with increasing number of rows (also seen in Figure 5.19). As expected, considerable variations in the extra SPL attenuation are observed at difference frequencies, but generally speaking, the SPL attenuation increases with the increased rows, and for typical road spectrum with 70 km/h the increase is from 0.8 dBA to 4.0 dBA at the receiver height of 1600 mm, and -0.2dBA to 6.0dBA at the receiver height of 1000 mm.

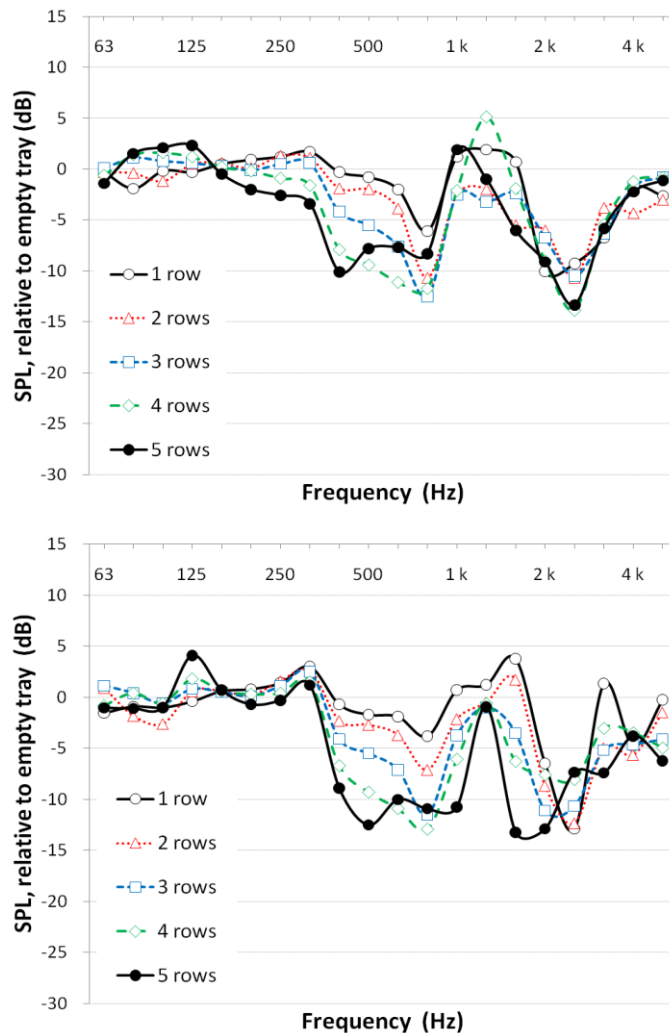


Fig. 5.18 Difference in measured SPL between the empty tray (result in Figure 5.15) and green roof system (result in Figure 5.17) at two receivers with a height of 1600 mm (top) and 1000 mm (bottom)

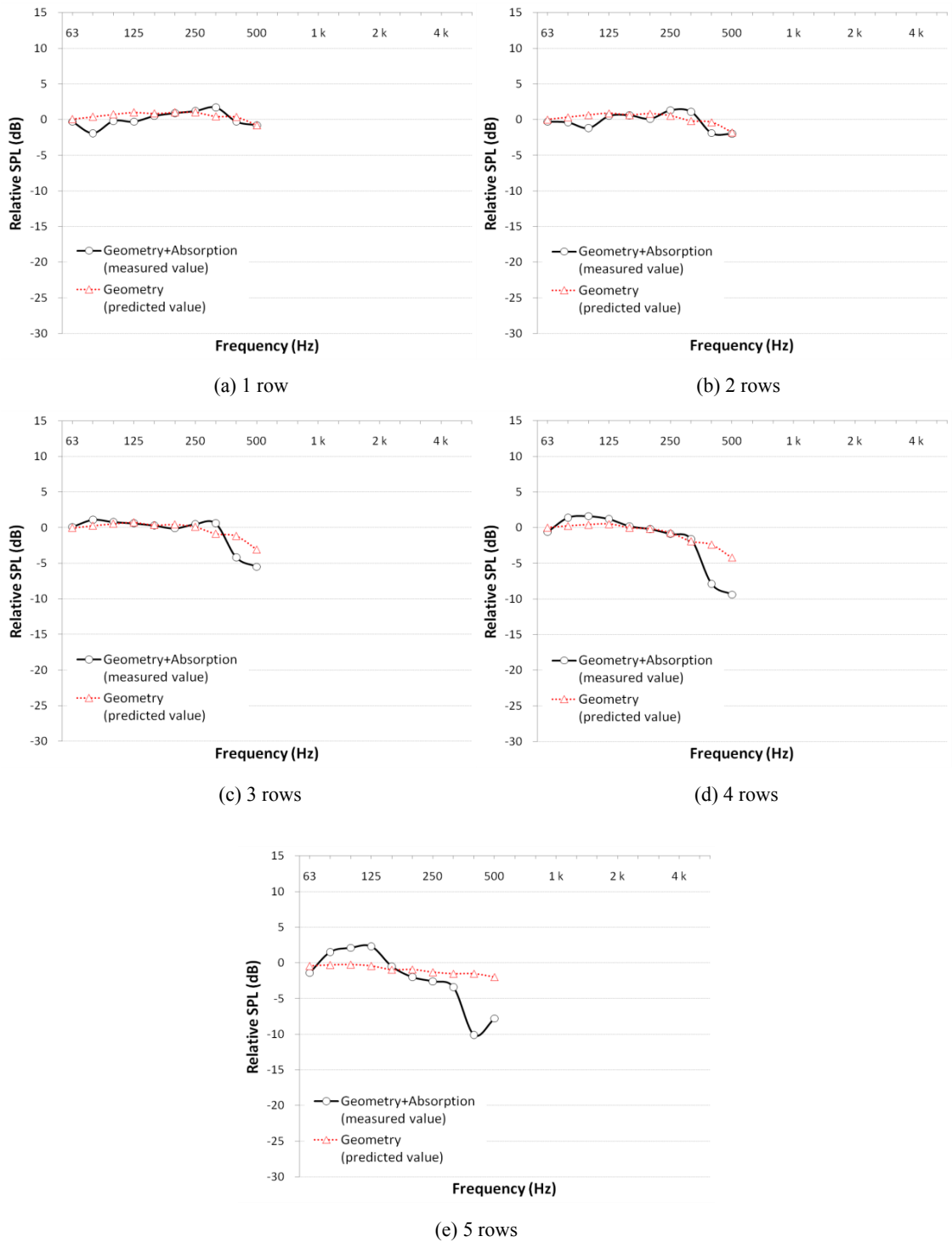


Fig. 5.19 Comparison of relative SPL for the geometrical effect (predicted result in Figure 5.9, dotted line) and the geometrical+absorption effects (measured result in Figure 5.18, solid line) at the receiver height of 1600 mm. The difference in SPL between dotted and solid lines indicates the absorption effect by the substrate



To examine the effects of substrate absorption, in Figure 5.19 the simulated value using FEM for the geometrical effect only as shown in Figure 5.9 and the measured values as shown in Figure 5.18 are compared at the receiver height of 1600 mm. It can be seen that with the increase in the number of rows from 1 to 5 the SPL attenuation caused by absorption is increased, and this occurs mainly from 315 Hz, up to about 8.6 dB. At the receiver height of 1000 mm, the tendency of SPL attenuation is similar, with a maximum SPL attenuation of 9.5 dB.

### **5.3.3 Depth and type of the substrates**

The effects of the depth and type of the substrates are shown in Figure 5.20 and Figure 5.21, considering the receiver height of 1600 mm and 1000 mm, respectively. The figures show the SPL attenuation by the substrates relative to the condition of empty trays, considering different rows of green roof systems. For Zinco substrate with a depth of 100 mm, it is slightly more effective in reducing noise, especially at the frequency range below about 500 Hz, compared to Zinco substrate with a depth of 50 mm, but generally speaking, the differences between the two substrate depths are not significant and systematic. This corresponds to the fact that Zinco substrate with a depth of 50 mm has relatively low absorption coefficients and geometrical effect at low frequencies. With Zinco and limestone-based substrates with the same depth of 100 mm, the SPL attenuation is similar although at relatively low frequencies, say below 500 Hz, the limestone-based substrate, which has a higher density and smaller particles than Zinco substrate, is relatively effective on SPL attenuation compared to Zinco substrate.

Overall, it seems that the effects of the depth and type of substrates are relatively small compared to the effects of other experimental parameters.

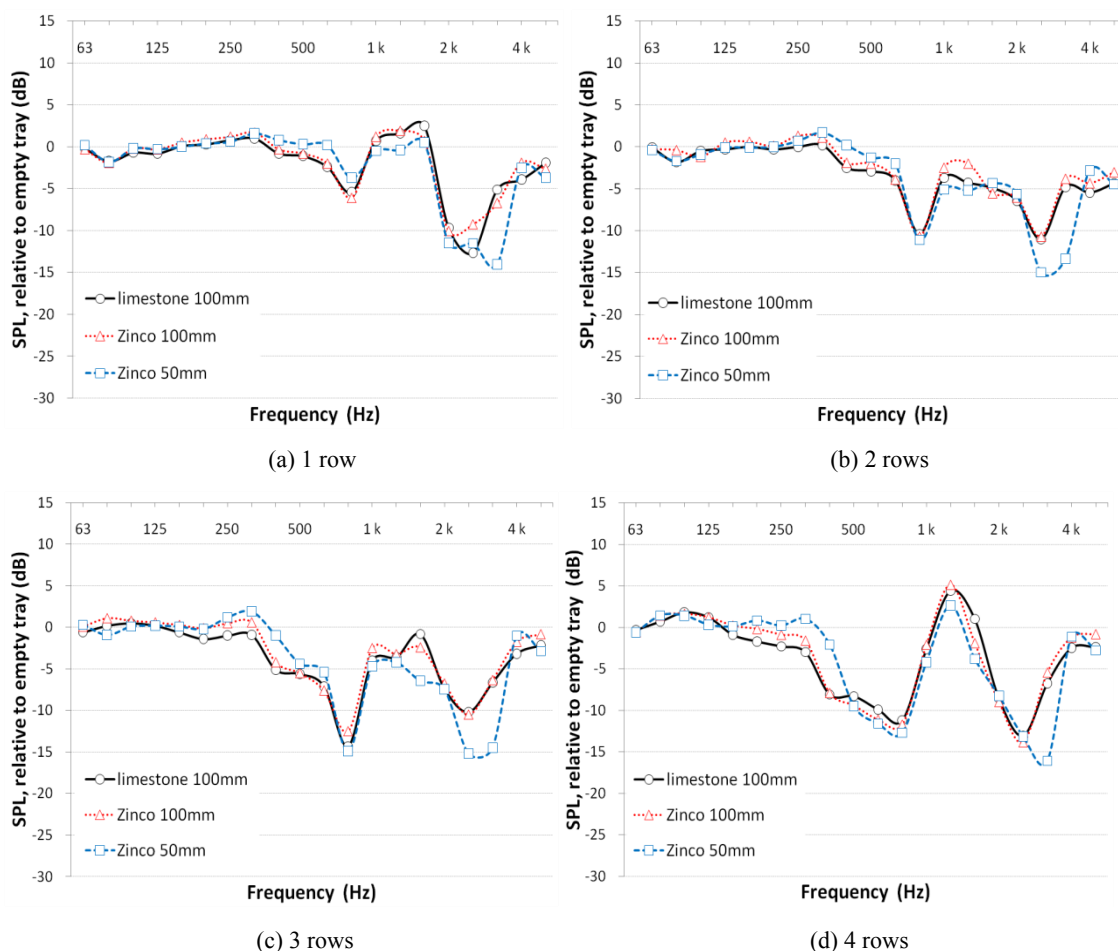


Fig. 5.20 Measured SPL attenuation with different types and depths of substrates at the receiver height of 1600 mm

### 5.3.4 Position of the green roof system

Figure 5.22 shows the experimental results on the effect of the position of 1 row of the trays, where pruned leaves were used on the green roof system. It can be seen that the SPL attenuation has different patterns according to the position of the trays of 1 row, depending on frequency ranges. At the receiver height of 1600 mm, the sound attenuation for traffic noise is 4.9 dBA, 6.2 dBA and 3.1 dBA for the front, centre and end line, respectively. Therefore, it is useful to consider the optimum location according to the spectra of sound sources. Moreover, the effect of the position of the green roof system is rather sensitive at the receiver height of 1600 mm which is perhaps due to

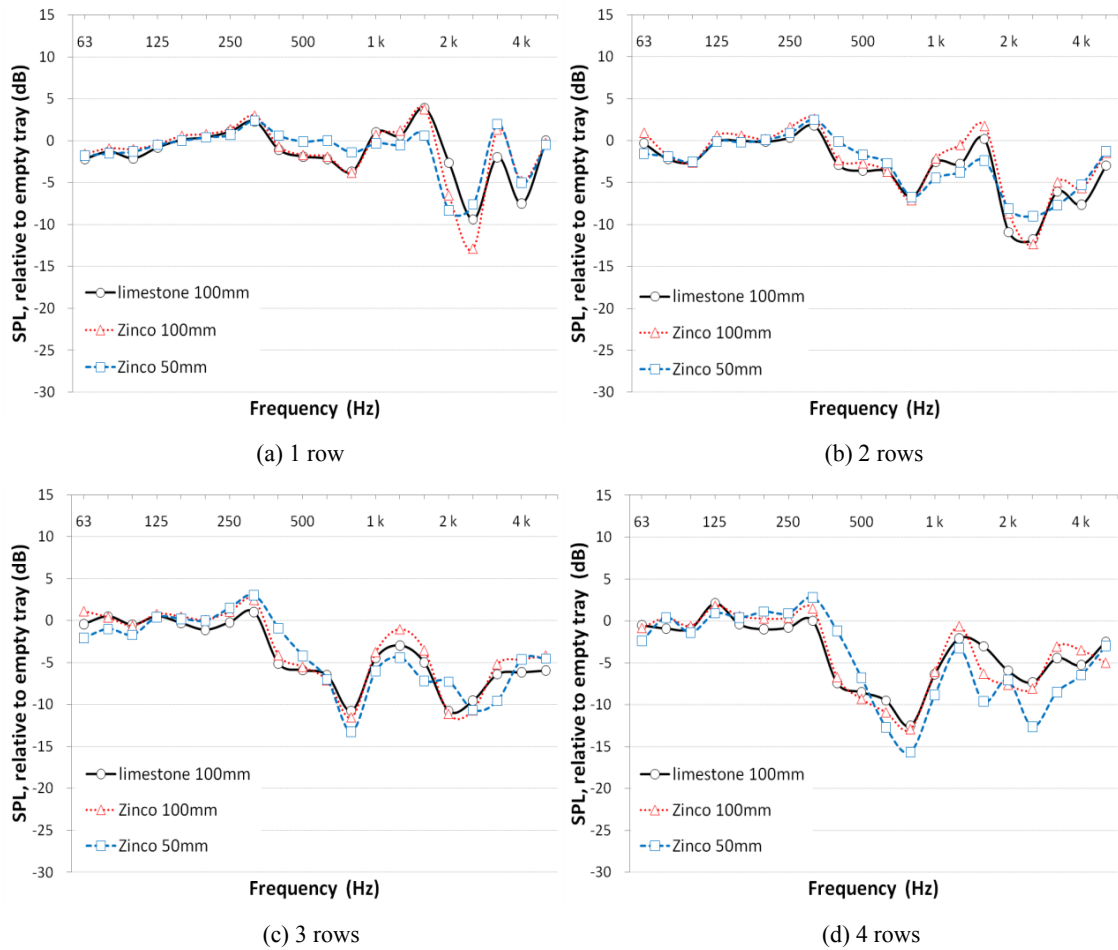
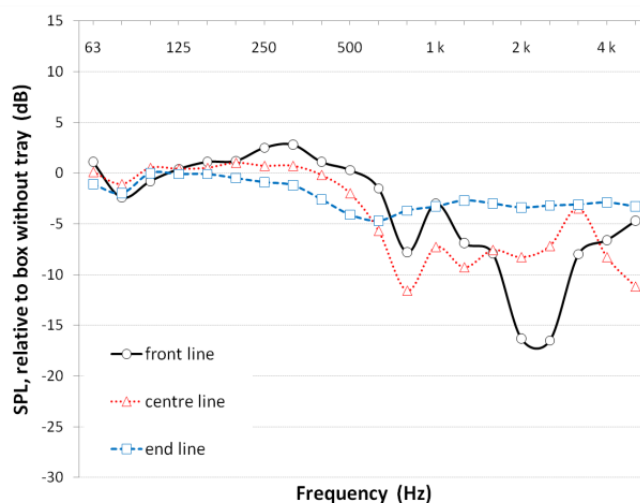


Fig. 5.21 Measured SPL attenuation with different types and depths of substrates at the receiver height of 1000 mm

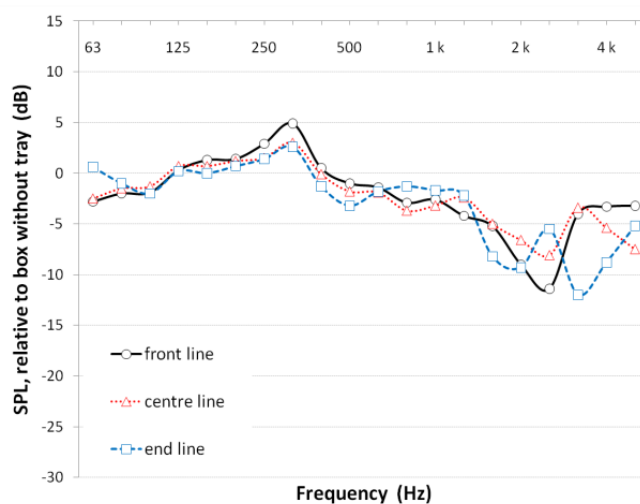
interference shifts relative to the reference case, whereas the variation of SPL attenuation at the receiver height of 1000 mm is relatively insignificant since the receiver is at acoustical shadow zone.

### 5.3.5 Vegetation

The measured extra SPL attenuation with pruned fresh leaves and polyester cotton on 1 row of the green roof system at the front line is shown in Figure 5.23, considering the two receiver heights. It can be seen that the pruned fresh leaves only have a slight effect on noise attenuation above about 3.15 kHz, perhaps due to the leaf scattering,



(a) Receiver at 1600 mm



(b) Receiver at 1000 mm

Fig. 5.22 Measured SPL attenuation with different position of the green roof system for 1 row unclamped leaf vibration and boundary layer absorption. The experimental result with the cotton suggests that there are still possibilities to reduce noise level further, by about 3-4 dBA for traffic noise due to high absorption if the vegetation layer is better designed.

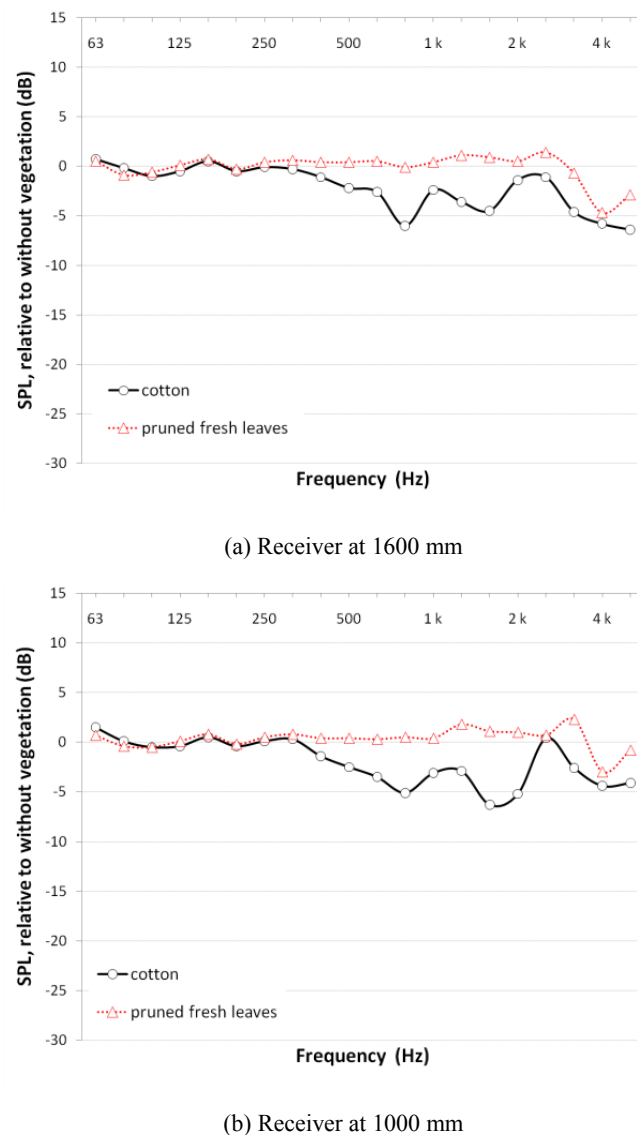


Fig. 5.23 Measured SPL attenuation considering possible effects of vegetation types

## 5.4 Summary

In this chapter, measurements have been carried out to examine the acoustic effects of green roof systems on a low-profiled structure at street level, and numerical simulation has also been carried out for selected cases. The results on the effect of green roof area suggest that SPL attenuation generally gradually increases with the increasing number of rows of the green roof trays although there are variations due to the geometrical

effect. The extra SPL attenuation caused by substrates, compared to the geometrical effect only (i.e., with panels surrounding the periphery of the trays, of the same height as the substrate), could be up to 9.5dB at certain frequencies. Within the ranges of the parameters considered, the effects of the depth and type of substrates are smaller compared to that of the overall configurations of the system. In terms of the acoustic effects of the position of the green roof system, the measurement results suggest that they affect the pattern of SPL attenuation at different frequency ranges. The experimental results with the pruned leaves show positive effects of vegetation on noise mitigation above 4 kHz and there is still a scope for further improvements by about 4dBA if the vegetation layer is better designed. It is therefore useful, in the future work, to study more systematically the effects of vegetation condition, as well as the effects of other factors such as water contents of substrates.

Based on the results for the experiment and prediction, general design methods of green roof systems on a low barrier can be recommended as follows:

- 1) Increase the area of green roof systems for effective noise control;
- 2) Locate green roof systems on a low barrier by considering frequency spectrum of noise sources;
- 3) Use dense/absorbent vegetation growing on the green roof substrate;
- 4) Install ground diffusers (i.e., rib-like structures such as green roof trays) to increase ground diffusion.

**PART III.**

**VEGETATION IN URBAN SITUATIONS**

## **6 A Case Study on Controlling Sound Fields by Landscape Designs in a Courtyard**

The aim of this paper is therefore to investigate the acoustic effect of applicable landscape designs in courtyards, with a particular attention on the acoustic effects of vegetation, through a case study. Firstly, the research background is defined after reviewing relevant publications in Section 6.1. In Section 6.2, site and experimental conditions are explained. Section 6.3 describes the measurement results showing how a practical landscape design reduces noise levels and reverberation. Acoustic effects of different landscape schemes using vegetation are predicted using acoustic computer simulation in Section 6.4. Section 6.5 summarises key findings of this chapter.

### **6.1 Introduction**

A growing body of evidence confirms that urban noise pollution produces direct and cumulative adverse health effects such as cardiovascular disease, cognitive impairment, sleep disturbance, tinnitus and annoyance (Fritschi *et al.*, 2011). These health effects, in turn, can lead to social handicap, reduced productivity, decreased performance in learning, absenteeism in the workplace and school, increased drug use and accidents (Berglund *et al.*, 1999). Noise could also have economic impacts such as loss of property and landscape values (Carles *et al.*, 1999; Jim *et al.*, 2006; Luttik, 2000; Navrud, 2002; Wardman *et al.*, 2004; Wilhelmsson, 2000).

In urban residential areas, road traffic noise is a main source affecting sleep disturbance and annoyance. Therefore, courtyards have been widely used to prevent direct exposure of building façades to road traffic noise (Ettouney *et al.*, 1973; Öhrström *et al.*, 2006;



Oldham *et al.*, 1979). Numerous studies have attempted to predict the sound energy propagating over rooftops from a trafficked road to a courtyard using numerical and experimental methods (Hornikx *et al.*, 2007, 2009; Van Renterghem *et al.*, 2010). The results suggest that courtyards play a role in reducing background noise levels from road traffic. On the other hand, when background noise from external spaces is reduced, sounds from within a courtyard such as from social activities and conversation could become more important as sources of noise annoyance. Therefore, it is useful to study methods employing landscape designs to reduce sound energy propagation within a courtyard.

The sound field in a courtyard is influenced by many designable factors such as the shape and volume of the space, building layout and the materials forming the building façade, etc. These affect the characteristics of sound fields described by acoustic parameters such as RT and SPL distribution. However, most courtyards have been designed without any acoustic consideration, which often leads to acoustic defects such as strong flutter echoes, long RT and increased sound levels due to geometrically reflecting façades with acoustically hard surfaces (Kang, 2000, 2002b). These acoustic defects result in increased noise annoyance for occupants, especially in summer when the courtyard is used more, and windows are open for natural ventilation. Therefore, it is important to absorb and diffuse sound energy propagating in a courtyard. It is also important in the design of a suitable sound field for a comfortable courtyard soundscape to consider pleasant sounds such as fountains and bird song (Kang, 2007).

The typical method to control sound fields is to use acoustic absorbers and diffusers on the wall, ground and ceiling of a space. In enclosed spaces such as concert halls,

absorbers and diffusers can be installed relatively easily since they are not contaminated by rain and dust, a reason why it is more difficult to mount commercial devices in open courtyards. Therefore, it is useful to identify outdoor acoustic materials for controlling the sound field by landscape designs.

Currently, vegetation grown on green roofs and walls has become popular in urban spaces due to numerous environmental benefits (Getter *et al.*, 2006; Ksiazek *et al.*, 2012; Mentens *et al.*, 2006; Veisten *et al.*, 2012). Previous studies have also reported that vegetation can contribute to the mitigation of noise pollution, which suggests its potential use in controlling the sound fields of courtyards by landscape designs (Oldham *et al.*, 2011; Van Renterghem *et al.*, 2008a, 2009, 2011; Van Renterghem *et al.*, 2013; Wong *et al.*, 2010; Yang *et al.*, 2012). With regard to soundscape concepts, greening inner courtyards with vegetation can also moderate noise annoyance by improving the aesthetic/natural appearance (Gidlöf-Gunnarsson *et al.*, 2007, 2010; Langdon, 1976).

In general, vegetation consists of two main components: plant structures (leaf, stem and root) and the growing media (soil or substrate). Previous studies have shown that the plant structures can absorb and diffuse sound energy, especially at high frequencies (Martens *et al.*, 1981; Watanabe *et al.*, 1996; Yang *et al.*, 2013). It has also been found that soil has similar properties to those of a porous material for absorbing sound energy (Kaye *et al.*, 1940; Yang *et al.*, 2013)).

The aim of this chapter is therefore to investigate the acoustic effect of landscape designs using vegetation. This is done through a case study in a courtyard located in an accommodation building of the University of Seoul, where a quiet sound environment is required. The acoustic effect of landscape designs using vegetation has been examined

using two methods: (1) In-situ measurements before and after applying a practical landscape design; (2) Computer simulation for applicable landscape designs using vegetation in the courtyard. The acoustic parameters considered here are the extra SPL attenuation and RT20. Based on the extra SPL attenuation in octave bands, a difference in speech levels before and after applying landscape designs is also calculated.

## 6.2 Methodology

### 6.2.1 Description of the study site

The courtyard investigated in this chapter is located at the accommodation building in the University of Seoul, Seoul, South Korea. The courtyard has a rectangular shape with dimensions of 32.4 m (L)  $\times$  8.2 m (W). The site is surrounded by building façades with different heights, 7.1 m (3 façades) and 24.4 m (1 façade), as shown in Figure 6.1. Figure 6.2 illustrates the cross section and ground plan for the accommodation building.



Fig. 6.1 Site conditions before (left) and after (right) the refurbishment using vegetation, wood decking and street furniture

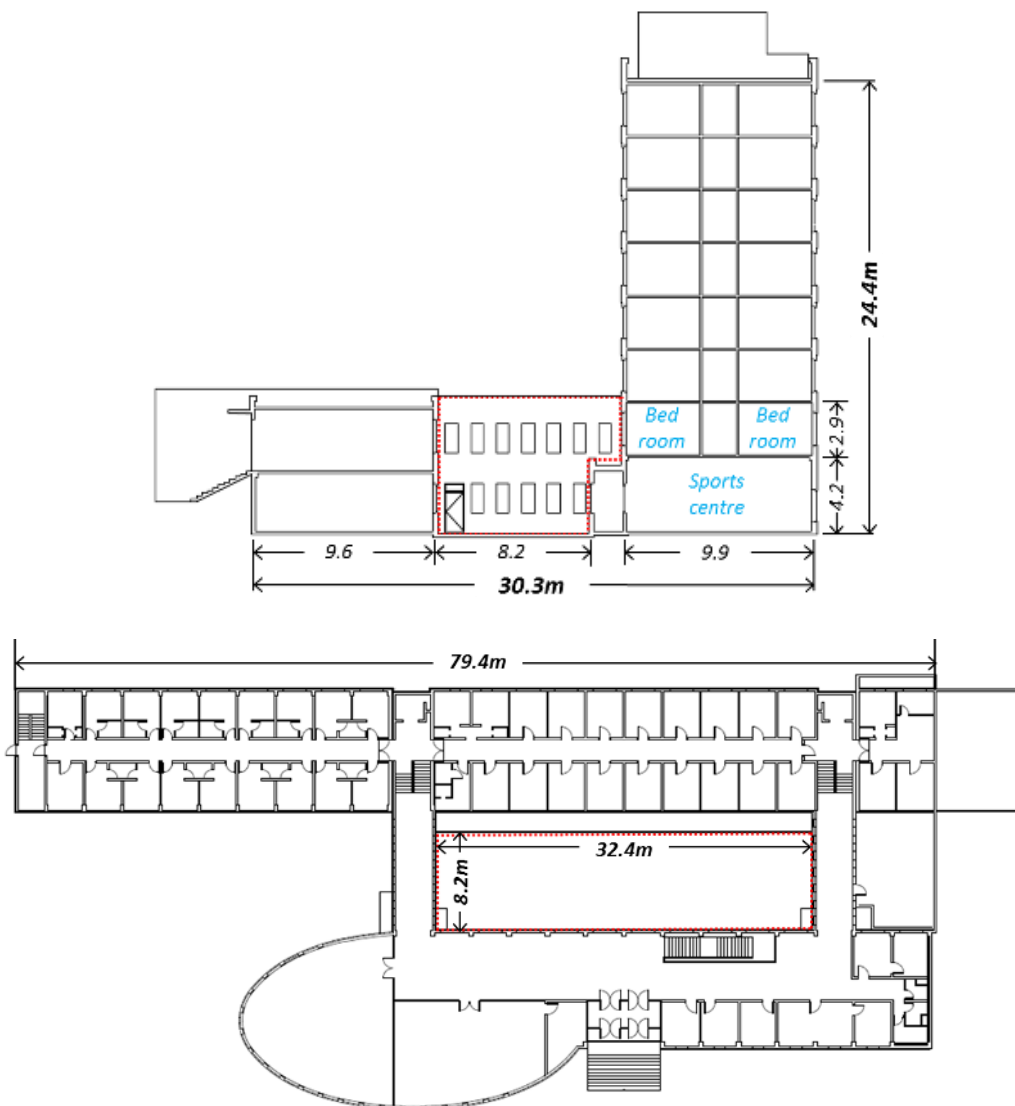


Fig. 6.2 Cross section (top) and ground plan (bottom) for the accommodation building (*Unit: m*)

As Figure 6.1 shows, there was a refurbishment of the inner courtyard using vegetation, wood decking and street furniture in January 2011. Before the refurbishment, the building façade and ground of the courtyard had geometrically reflecting surfaces with acoustically hard materials such as marble and glass. Therefore, it was expected that there would be acoustic defects such as strong flutter echoes, long RT and increased sound level due to multiple reflections, which can cause increased noise annoyance for occupants in the courtyard. Sound levels in front of the windows at different floor levels

play an important role in determining the life quality of the occupants. In particular, students in bedrooms from the 1<sup>st</sup> to 7<sup>th</sup> floor facing towards the courtyard have expressed strong complaints about noise from the courtyard. Noise annoyance is mainly due to excessive sound levels for conversation, the sound energy of which is increased by multiple reflections between geometrically reflecting facades. Therefore, architectural treatments using appropriate acoustic materials to reduce sound levels in front of the accommodation building are also required.

To improve the students' living environment, the university office has decided to refurbish the whole ground and a part of the building façades using low-growing vegetation, small trees, wood decking and street furniture, as shown in Figure 6.1. The wood decking consists of several layers including 3 mm waterproof membrane, 1 mm root barrier, 50 mm drainage layer, 200 g/m<sup>2</sup> nonwoven fabric, 60 mm air cavity and 15 mm wood frame. The fabric layer is a type of porous material, which can absorb sound energy through the slits with 5 mm between wood frames. Figure 6.3 shows the drawing for the cross-section of the wood decking.

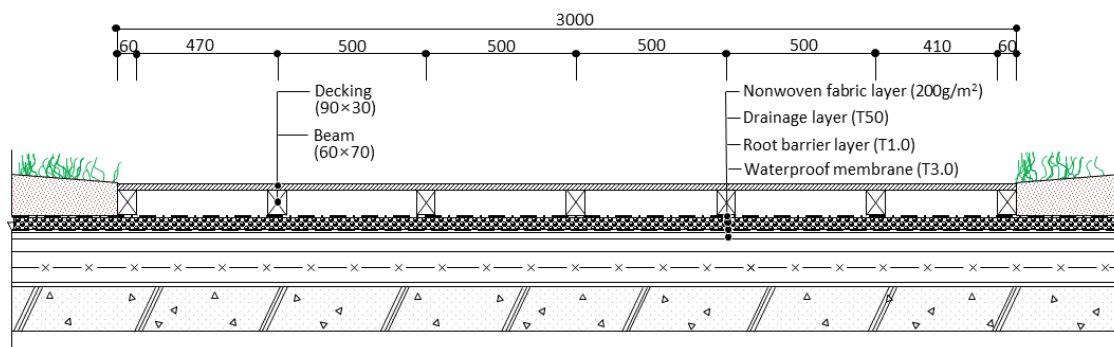


Fig. 6.3 Cross-section of the wood decking (Unit: mm)

In the courtyard after the refurbishment, there are several species of low-growing vegetation including *Miscanthus sinensis*, *Aquilegia buergeriana*, *Carex ligulata*,

*Phalaris arundinacea*, etc. The low-growing vegetation is planted in the growing media with a depth of 100 mm consisting of Sedum mat with lightweight expanded aggregate used as mulch. The diameter of the lightweight expanded aggregate is 5 mm to 15 mm. A few small trees including *Comus kousa* and *Styrax japonica* are also planted in the growing media with a depth of 500 mm. Approximately, 70 % of the whole ground area is covered by the wood decking. The remaining 30 % is comprised of the vegetation. Street furniture such as tables, benches and lighting is also there.

Although designed apparently without any acoustic consideration, the courtyard presents a good experimental condition to investigate how a practical landscape design affects the characteristics of sound fields in such reverberant courtyards. Therefore, in-situ measurements were carried out before the refurbishment (in November 2010) and after the refurbishment (in March 2011) to examine the effect of the landscape design on acoustic parameters such as sound levels and RT. Differences in temperature and relative humidity between the two measurements dates (firstly 8.9 °C and 58 %, then - 0.1 °C and 54.5 %) are generally insignificant.

### **6.2.2 Measurement and analysis methods**

To determine an impulse response from which RT can be calculated using the Schroeder methods, an MLS (maximum length sequence) signal was used. The impulse response at each receiver point was recorded using the 2-channel 01dB Symphonie system with 1/2" microphones (G.R.A.S. Type 40AF) and preamplifiers (01dB-Stell Pre 12H).  $L_{eq}$  for 10 seconds with different source-receiver distances was also examined using a RION NA-28 portable sound level meter to examine sound attenuation. The sound source for the measurement of sound attenuation was white noise generated from an

omni-directional loudspeaker (FP120, CESVA) connected to an amplifier (AP600, CESVA). The measurements for the impulse response and  $L_{eq}$  were repeated three times to confirm the repeatability.

Figure 6.4 shows the ground plan of the measurement conditions. For the sound source 1 m from the building façade (Figure 6.4a) there were 15 receivers along the centreline of the courtyard. With the sound source in the centre (Figure 6.4b), 7 receivers lay along the centreline between the source and one end of the courtyard. The sound source and receivers all had a height of 1.5 m, and neighbouring receivers were 2 m apart.

RT for the impulse response recorded from the in-situ measurement was analysed using the Dirac programme from B&K, which has a noise compensation function to reduce the effect of background noise on RT calculation. RT is derived from the decay curve

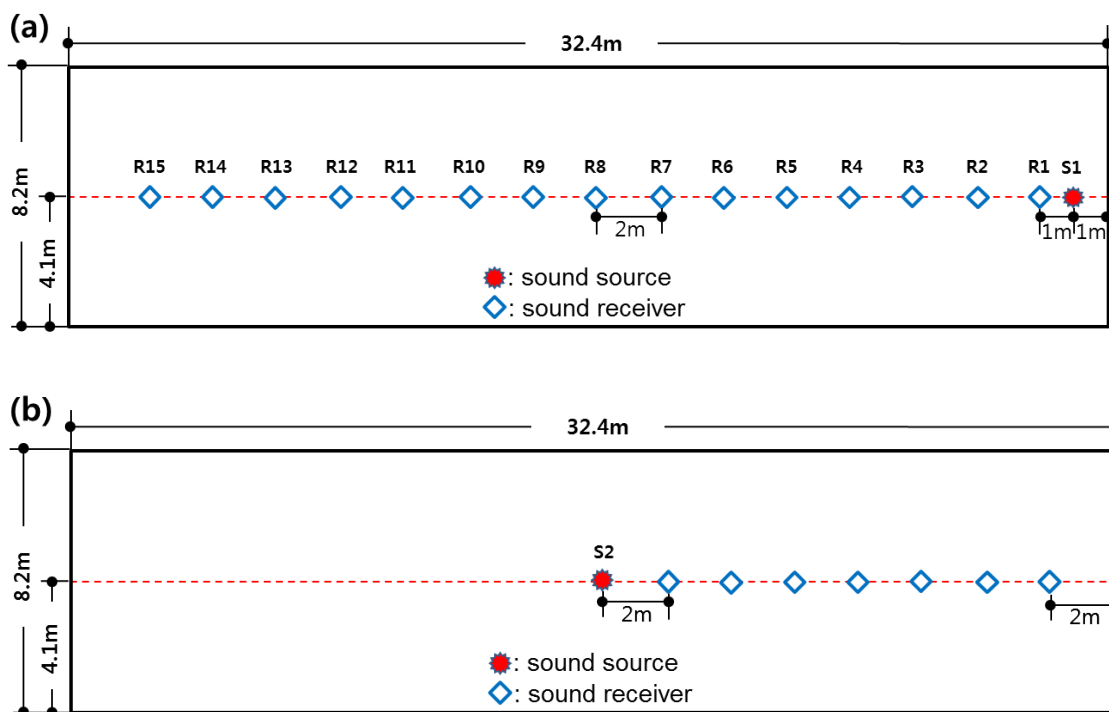


Fig. 6.4 Ground plan of the measurement conditions: (a) Source point located at 1m from the façade; (b) Source point located in the centre

section between 5 dB and 25 dB below the initial level, which is represented as RT20. The signal-to-noise ratio of the steady-state sound source (white noise) was greater than 18 dB across frequencies in an unweighted value.

### 6.3 Measurement results

As mentioned above, sound levels and RT20 were measured in the two conditions, before and after the refurbishment in the courtyard, to estimate the effect of the practical landscape design on variations in the acoustic characteristics.

Figure 6.5 shows a difference in sound levels before and after the refurbishment, according to source-receiver distances illustrated in Figure 6.4(a). The relative SPL in Figure 6.5 is with reference to SPL at 1 m from the sound source. In the near field from the source, it can be seen that a difference in SPL between the two landscape designs is insignificant, which indicates a strong influence of a direct sound. Conversely, a

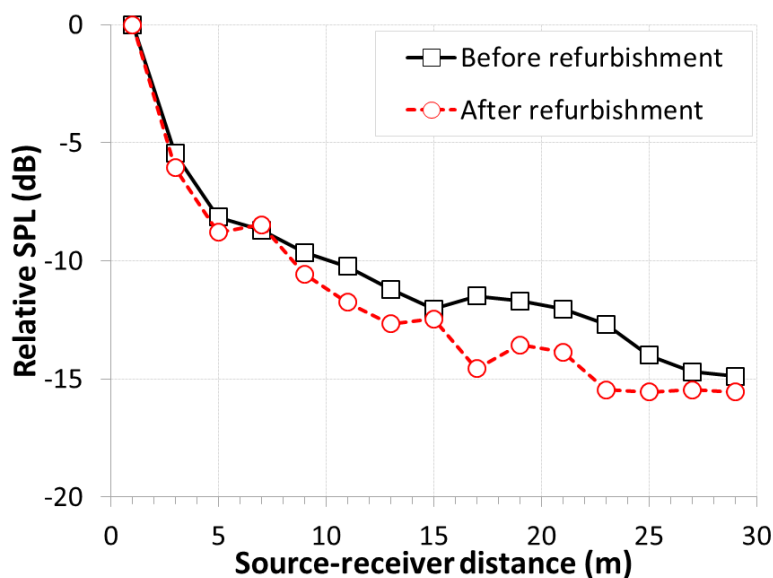


Fig. 6.5 SPL measured before and after the refurbishment according to receiver distances from the source point at 1 m from the façade



increase of source-receiver distances. The maximum difference in sound levels before and after the refurbishment is 3.1 dB in an unweighted overall value. The SPL attenuation is due to the increased absorption, scattering and diffraction effect of the ground after the refurbishment (Kang, 2007). This result implies that the refurbishment using vegetation, wood decking and street furniture can slightly moderate noise annoyance of the occupants in the courtyard.

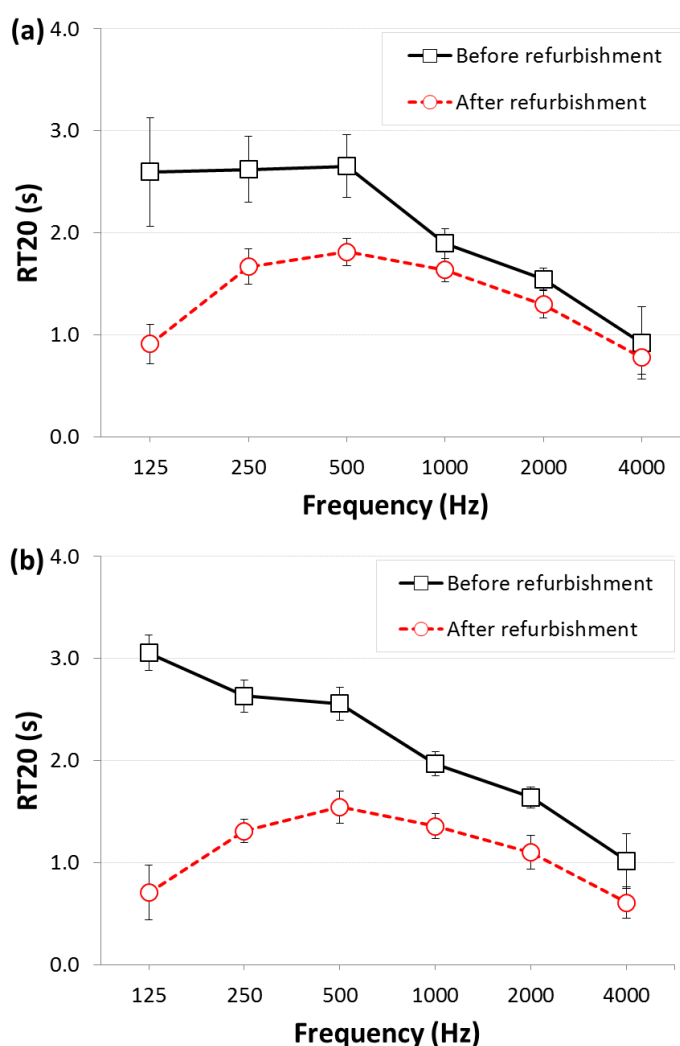


Fig. 6.6 RT20 averaged over all receiver points measured at the two different source points according to the refurbishment: (a) Source point at 1 m from the wall, (b) Source point in the centre of the courtyard

In Figure 6.6, results for RT20 averaged over all receiver points measured at both source points are shown from 125 to 4000 Hz in octave bands. The standard deviation means a difference in RT20 at each receiver point, which also indicates the RT distribution in the courtyard. The result on RT20 before the refurbishment shows that RT20 is relatively long over 2.5 sec at 500 Hz for both source points due to the large number of late reflections. After the refurbishment, RT20 becomes less than 1.5 sec at 500 Hz (47 % decrease). It is noticeable that RT20 is decreased especially at low frequencies by 2.3 sec at 125 Hz (77 %), due to the combined effect of absorption, scattering and diffraction by the wood decking, vegetation, low-profiled garden and street furniture.

## **6.4 Computer simulations**

In-situ measurement results showed that the practical landscape design can reduce sound levels and RT20 in the courtyard. Therefore, it is useful to carry out a systematic study on how landscape designs using acoustically sustainable materials can be applied more effectively to improve sound environments in the courtyard through computer simulations. In this section, prediction using a computer simulation programme has been done to examine the acoustic effect of vegetation in the courtyard and at different floor levels of the accommodation building. Acoustic parameters predicted here are the extra SPL attenuation and RT20. Based on the extra SPL attenuation, the variation in speech levels by vegetation is calculated because conversation in the courtyard is one of the main sources of noise.

### **6.4.1 Computer model calibration**

In this chapter, the computer simulation programme ODEON v.11.23 is used for predicting the acoustic effect of vegetation in the courtyard. This programme employs a

hybrid algorithm combining the image source method and ray tracing for predicting sound fields. It considers both specular and diffuse reflections, as well as diffraction. The absorption coefficient of the model surfaces before the refurbishment, mainly consisting of glass and marble, was selected within the ranges given in the programme. The scattering coefficient of the ground and façade was determined as 0.01 at 707 Hz as they have geometrically reflecting surfaces. In ODEON, the scattering coefficient for each octave band is calculated on a basis of the value at 707 Hz using interpolation or extrapolation. A source generated 300,000 rays. The impulse response time was set to 5000 ms. Figure 7 illustrates the computer model for the courtyard before the refurbishment.

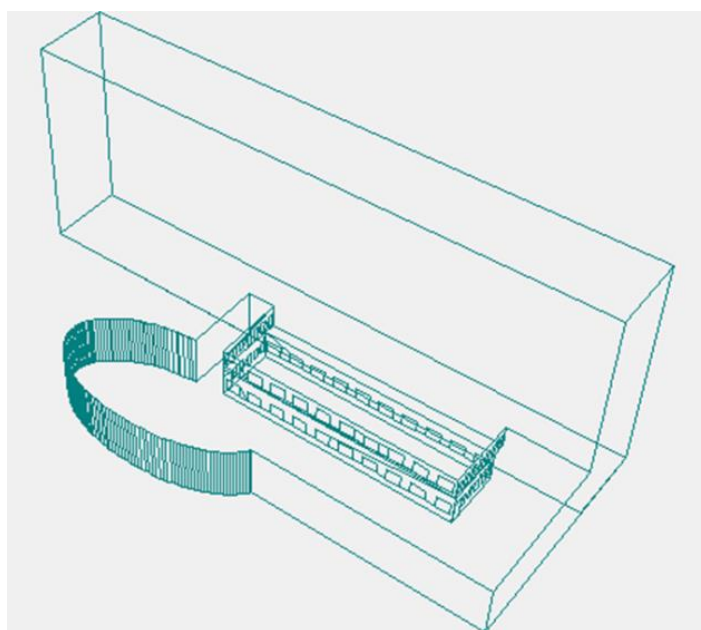


Fig. 6.7 Computer model for the courtyard before the refurbishment

To calibrate the computer model, the squared impulse response measured at *R15* in Figure 6.4(a) is compared to the predicted one, as shown in Figure 6.8(a). The result shows that the characteristics of measured and predicted impulse responses are comparable to each other. In Figure 6.8(b), RT20 averaged over the 15 receiver points in

Figure 6.4(a) is also compared between the measured and predicted one. The standard deviation indicates a difference in RT20 at each receiver point. The calibration goal was set to a difference of less than 5 % across frequencies in the averaged RT20 between the existing courtyard and computer model because the just noticeable difference (JND) is typically given as 5 % for RT (Bork, 2000).

#### **6.4.2 Landscape design schemes using vegetation**

It is important to use reliable absorption and scattering coefficient values of vegetation for accurate prediction of how it affects the characteristics of sound fields in the courtyard. Since the courtyard has a relatively reverberant sound field, it is desirable to use random-incidence absorption and scattering coefficients of vegetation. Those coefficients are collected from the published data for four types of vegetation including grass (Kaye *et al.*, 1940), bedding plants, green wall (Cheal *et al.*, 2011) and Ivy (Data in Chapter 3) which can typically be used in such courtyards. Grass consisted of rough turf on 25 cm of compressed gravel. The bedding plants comprised eight plant species in 20 cm of topsoil. The (horizontal) depth of the green wall was 20 cm consisting of porous substrate without vegetation. Ivy had a depth of 10 cm and consisted only of leaves. Grass and bedding plants are assumed as the type of vegetation for the ground treatment. Ivy and green wall are selected for the façade treatment. Table 6.1 presents the absorption coefficient of the vegetation used for the prediction. Based on the data in Chapter 3, the scattering coefficients of Ivy and bedding plants were determined as 0.06 and 0.02 at 707 Hz, respectively. The scattering coefficient of the grass and green wall was assumed as 0.01 at 707 Hz, which is the same as the surface without vegetation.

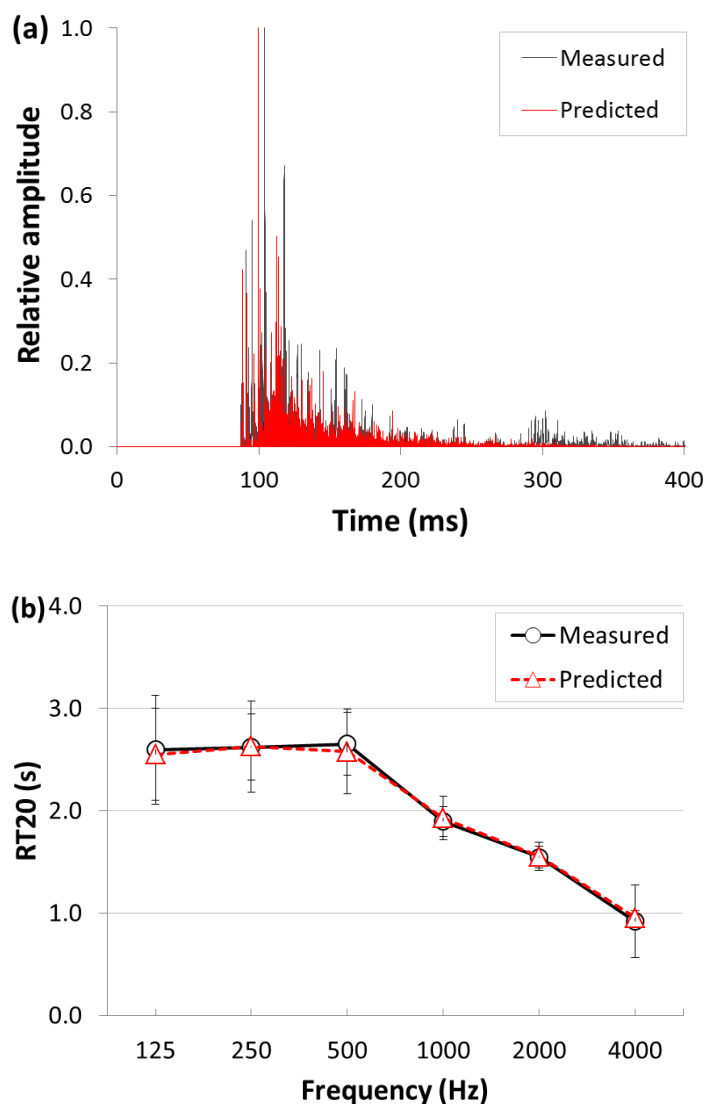





Fig. 6.8 Comparison between measured and predicted data in the landscaping condition before the refurbishment: (a) Squared impulse response at the receiver point, *RI5*; (b) *RT20* averaged over 15 receiver points

Table 6.1 Absorption coefficient of the vegetation used for the computer simulation

Landscape design	Vegetation	Frequency (Hz)					
		125	250	500	1000	2000	4000
Ground treatment	Grass	0.15	0.25	0.40	0.55	0.60	0.60
	Bedding plants	0.56	0.81	0.89	0.98	0.92	0.76
Façade treatment	Green wall	0.62	0.61	0.70	0.67	0.68	0.73
	Ivy	0.00	0.00	0.13	0.14	0.21	0.49

In this chapter, the acoustic effect of vegetation in the courtyard and at different levels of the accommodation building has been investigated by employing 100 % of vegetation coverage on the façade with 7.1 m high (except for windows and doors) and ground. Thus, the areas of the vegetation on the façade and ground are 361 m<sup>2</sup> and 266 m<sup>2</sup>, respectively. Three applicable landscape design schemes are considered as vegetation on the façade only (Case I), ground only (Case II), and on both the façade and ground (Case III). Table 6.2 describes the three landscape design schemes.

Table 6.2 Landscape design schemes using vegetation

	Case I	Case II	Case III
Location of vegetation	Façade	Ground	Both façade and ground
Cross section of the landscape design in the courtyard (green bold line: with vegetation, black dashed line: without vegetation)			
Area of vegetation	361 m <sup>2</sup>	266 m <sup>2</sup>	627 m <sup>2</sup>

### 6.4.3 Simulation results in the courtyard

#### 6.4.3.1 Vegetation on the façade (Case I)

In Figure 6.9, the extra SPL attenuation by the Ivy and green wall on the façade is shown in octave bands at three receiver points, *R1*, *R8* and *R15* in Figure 6.4(a). The distances of *R1*, *R8* and *R15* from the source are 1 m, 15 m and 29 m respectively, corresponding to the first, centre and end points. The height of the source and receiver was 1.5 m. The extra SPL attenuation is a relative value showing a difference in SPL with and without the vegetation.

In Figure 6.9(a), it can be seen that the extra SPL attenuation by the Ivy is increased

with the increase of source-receiver distances at mid and high frequencies by 5.2 dB at 4000 Hz. At low frequencies, on the other hand, some negative effects are observed due to the relatively high scattering coefficient of the Ivy in comparison with that of the façade without vegetation, whereas the absorption coefficients at low frequencies are similar to each other. Based on the speech spectrum for a male speaking normally (IEC, 2003), the Ivy can reduce the speech level by 1.3 dBA at *R15*. This result indicates that

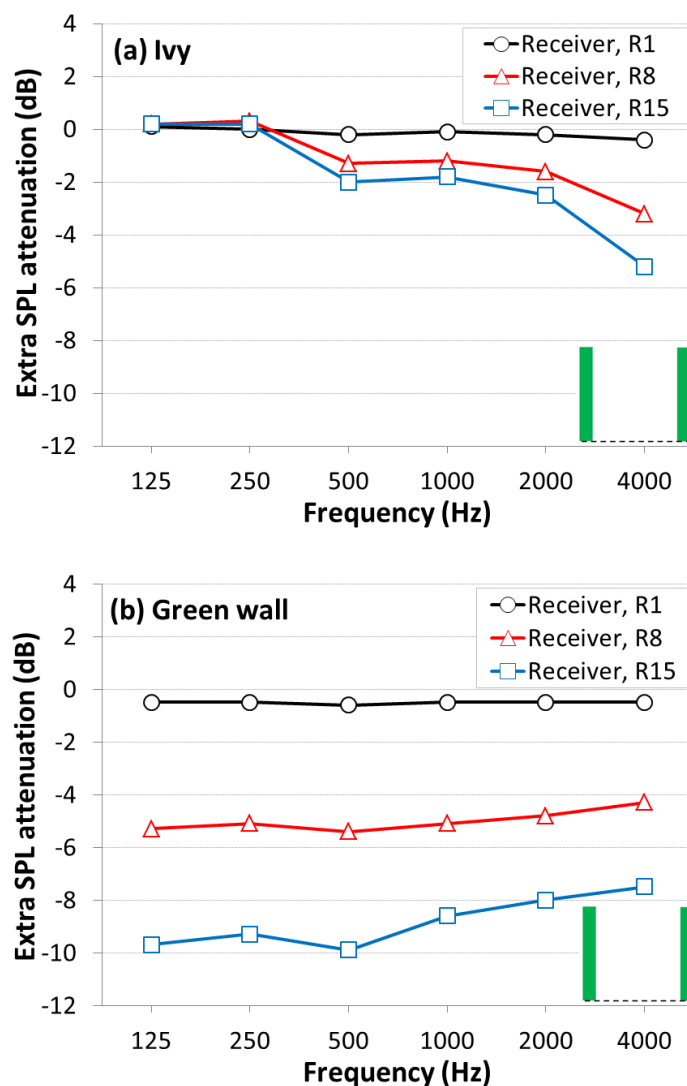


Fig. 6.9 Predicted extra SPL attenuation in octave bands at three receiver points by the vegetation on the façade: (a) Ivy; (b) Green wall

the vegetation with only leaves has a limited effect in moderating noise annoyance for speech in such courtyards. As for the green wall in Figure 7(b), the extra SPL attenuation is also increased with the increase of source-receiver distances at all frequencies. The green wall can reduce sound levels at *R15* by 9.9 dB at 500 Hz and speech level by 9.3 dBA. Therefore, it can be said that the green wall can play an important role in reducing the speech level in the courtyard.

The result for variation in RT20 caused by the vegetation is shown in Figure 6.10. RT20 is a value averaged over 15 receiver points in Figure 6.4(a), and thus the standard deviation indicates differences in RT20 between the points. The result shows that the Ivy and green wall can reduce RT20 at 500 Hz by 52% (1.3 sec) and 81 % (2.1 sec), respectively. This result indicates that the vegetation on the façade is effective at controlling RT in such reverberant courtyards.

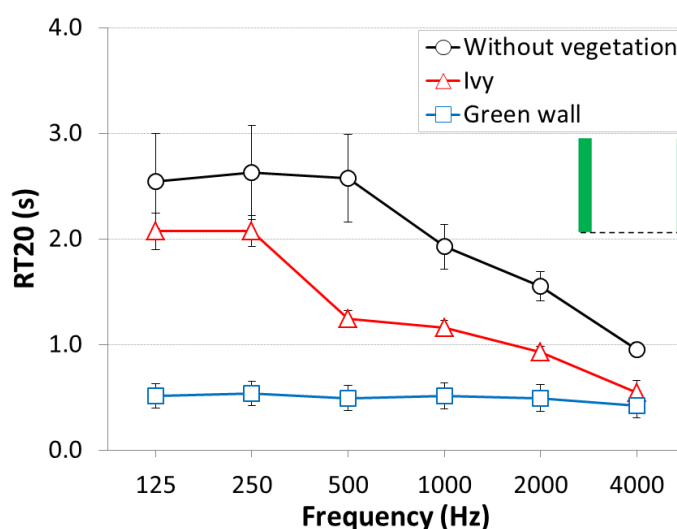


Fig. 6.10 Predicted RT20 averaged over 15 receiver points according to the landscape design with and without the Ivy and green wall on the façade



6.4.3.2 Vegetation on the ground (Case II)

The extra SPL attenuation by the grass and bedding plants on the ground is predicted at three receiver points, *R1*, *R8* and *R15*. As shown in Figure 6.11, the extra SPL attenuation by the vegetation is increased with increasing receiver distance from a source. It can be seen that the grass and bedding plants can reduce sound levels at *R15* by 1.0 dB and 2.5 dB at 1000 Hz, respectively. It is calculated that the speech level at

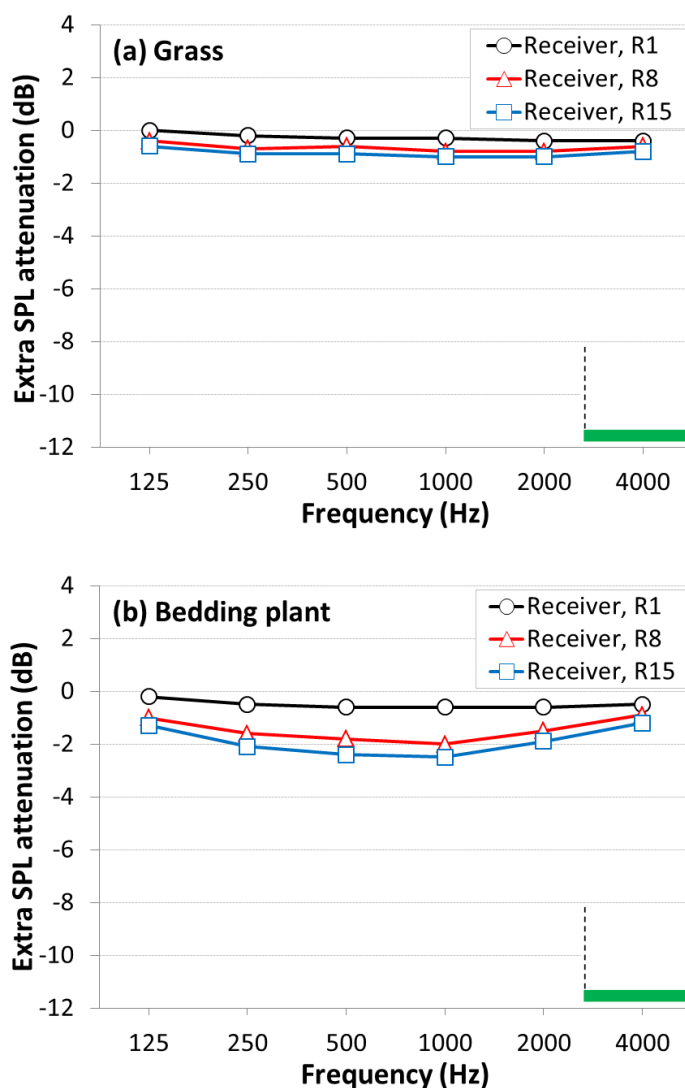


Fig. 6.11 Predicted extra SPL attenuation in octave bands at three receiver points by the vegetation on the ground: (a) Grass; (b) Bedding plants

*R15* can be decreased by the grass and bedding plants by up to 0.9 dBA and 2.2 dBA, respectively. This implies that landscape designs using highly absorptive vegetation on the ground play an insignificant role in moderating noise annoyance caused by speech in the courtyard. This is mainly because most ground-reflected sound waves propagate towards the ‘open ceiling’, with the help of non-diffusively reflecting façades. With diffusely reflecting façades and a covered ceiling, it is expected that the ground with absorptive vegetation can play a more important role in reducing sound levels (Kang, 2007).

In Figure 6.12, RT20 averaged over the 15 receiver points is predicted according to the landscape design with and without the grass and bedding plants on the ground. The standard deviation indicates differences in RT20 between receiver points. The result shows that the bedding plants increase RT20 by 12 % (0.3 sec) at 500 Hz even though the ground is covered with the highly absorptive vegetation. This is perhaps because the early part of decay has a steeper curve due to the absorption by the vegetation on the

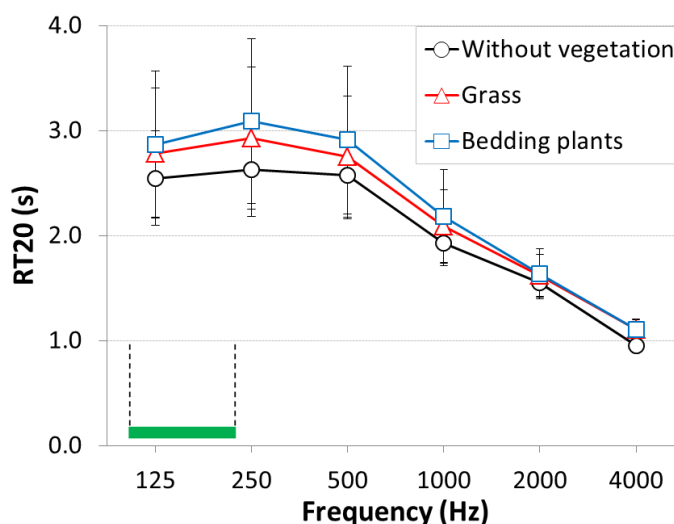


Fig. 6.12 Predicted RT20 averaged over 15 receiver points according to the landscape design with and without the grass and bedding plants on the ground

ground. The large standard deviation at low and mid frequencies also indicates that RT20 distribution is uneven in the courtyard with the absorptive vegetation on the ground. Correspondingly, the difference in RT20 with and without vegetation increases with the increase of source-receiver distance.

#### 6.4.3.3 Combined use of vegetation on the façade and ground (Case III)

The result in Figure 6.13 shows the predicted extra SPL attenuation at the three receiver points by the combined use of the green wall and bedding plants on the façade and ground. As they have high absorption coefficient values, the green wall and bedding plants are selected to examine the maximum effect of vegetation on the extra SPL attenuation. With increasing receiver distance from a source, it can be seen that the extra SPL attenuation is also increased. At the receiver point, *R15*, the maximum decrease in SPL is 11.4 dB at 500 Hz. As for the speech level, it is reduced by 10.7 dBA at *R15*. Therefore, it can be said that the bedding plants on the ground do not contribute

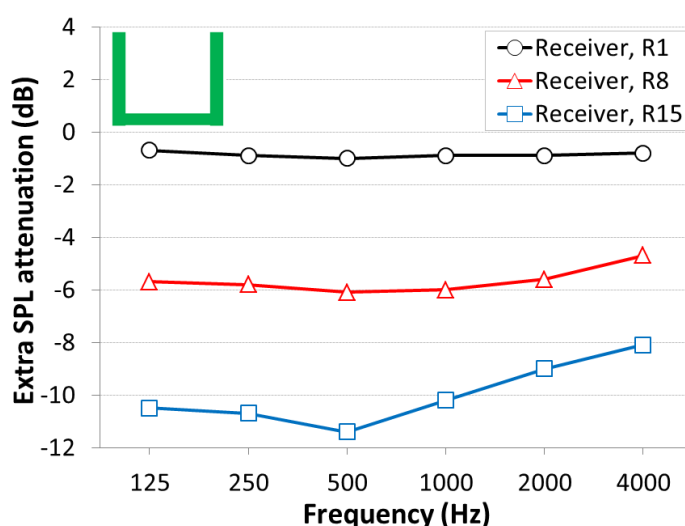


Fig. 6.13 Predicted extra SPL attenuation in octave bands at three receiver points by the combined use of the green wall and bedding plants on the façade and ground

importantly to the extra SPL attenuation when used with the green wall on the façade which itself can reduce the speech level by 9.3 dBA.

The result in Figure 6.14 shows that the combined use of the green wall and bedding plants can reduce RT20 at 500 Hz by 82 % (2.2 sec) in comparison with the same space without the vegetation. The decrease in RT20 by the combined use of the vegetation is similar to that achieved by the green wall alone, which indicates that the bedding plants on the ground have an insignificant effect on reducing RT20.

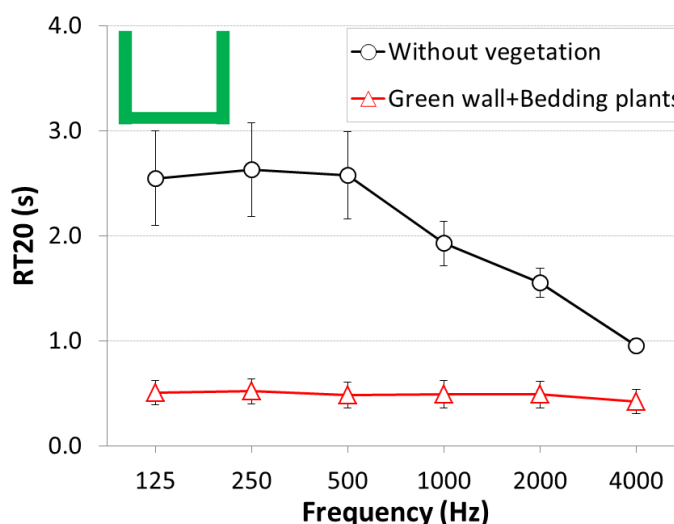


Fig. 6.14 Predicted RT20 averaged over 15 receiver points according to the landscape design with and without the combined use of the green wall and bedding plants on the façade and ground

#### 6.4.4 Simulation result at different floor levels in the accommodation building

Figure 6.15 shows the extra SPL attenuation by vegetation in front of the bedrooms facing towards the courtyard at the 1<sup>st</sup>, 4<sup>th</sup> and 7<sup>th</sup> floors (see building cross-section in Figure 6.2). The three landscape designs considered are green wall on the façade, bedding plants on the ground, and combined use of the green wall and bedding plants

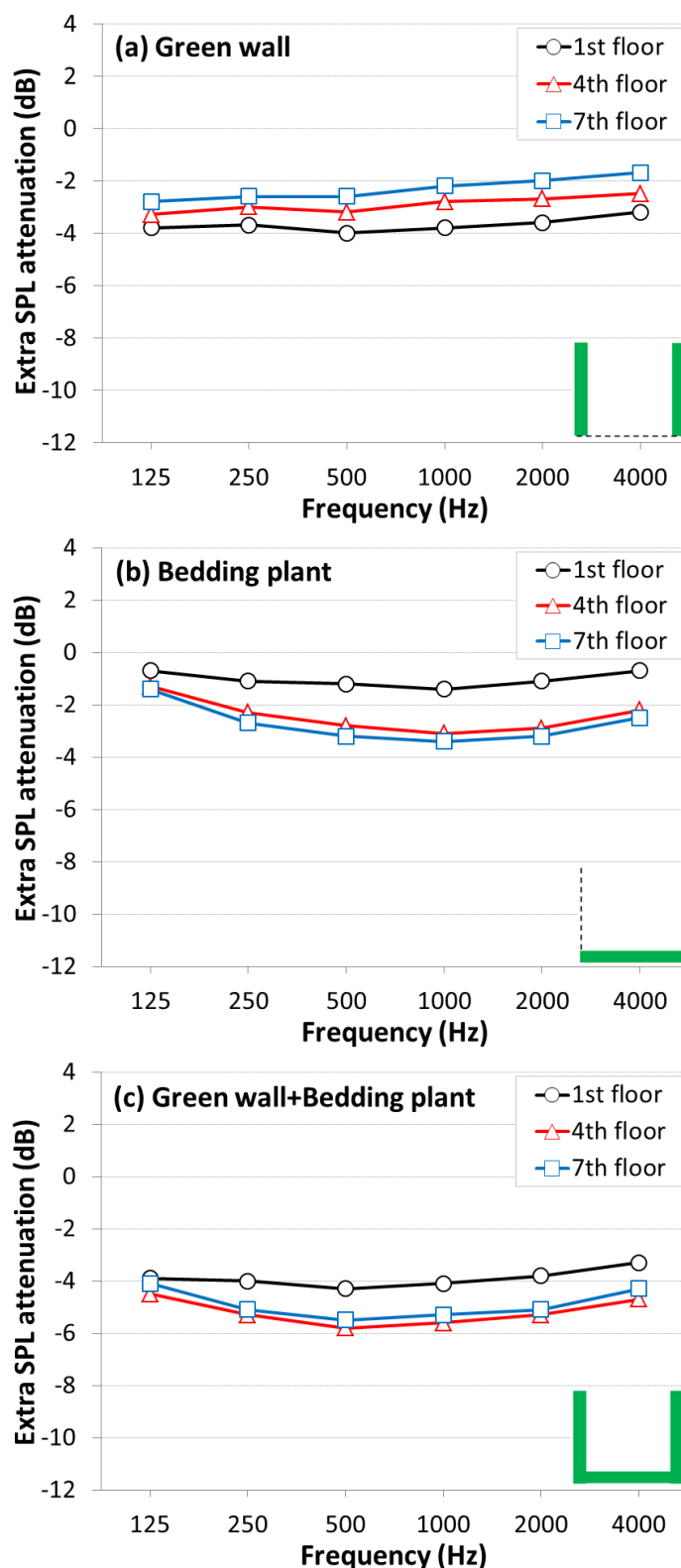


Fig. 6.15 Predicted extra SPL attenuation at the 1<sup>st</sup>, 4<sup>th</sup> and 7<sup>th</sup> floors in the accommodation building by the three landscape designs of the inner courtyard: (a) Green wall on the façade; (b) Bedding plants on the ground; (c) Combined use of a) and b)

on both the façade and ground. The receiver points are positioned at 0.2 m from the windows of bedrooms at the 1<sup>st</sup>, 4<sup>th</sup> and 7<sup>th</sup> floors in the shortest vertical line from the source located in the centre of the courtyard as shown in Figure 6.4(b). In Figure 6.15(a), it can be seen that the green wall on the façade can reduce sound levels at all floors. At the 1<sup>st</sup> floor, especially, it reduces sound levels by 4.0 dB at 500 Hz by absorbing multiple reflections between the parallel façades. As for the speech level, 3.8 dBA is removed by the green wall. In Figure 6.15(b), the bedding plants on the ground also reduce sound levels at all floors. At the 7<sup>th</sup> floor, particularly, sound level is decreased by 3.4 dB at 1000 Hz. As for the speech level, 3.0 dBA is removed at the 7<sup>th</sup> floor by the bedding plants. It seems that at high floor levels, the sound energy from the multiple reflections between the parallel façades is relatively weak in comparison with that from ground reflections. With the combined use of the green wall and bedding plants, as shown in Figure 6.15(c), the maximum extra SPL attenuation is 5.8 dB at 500

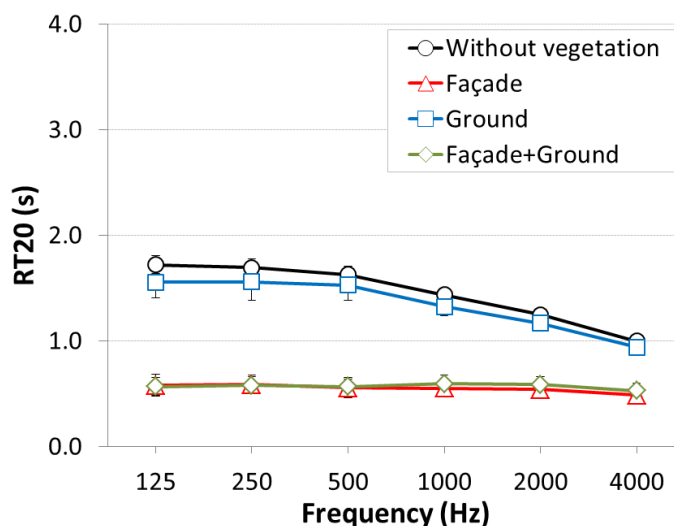


Fig. 6.16 Predicted RT20 averaged over 3 receiver points at the 1<sup>st</sup>, 4<sup>th</sup> and 7<sup>th</sup> floors in the accommodation building according to the three landscape designs using vegetation on the façade (green wall), ground (bedding plants), and façade (green wall)+ground (bedding plants)

Hz which can be seen at the 4<sup>th</sup> floor. It can also reduce the speech level by 5.5 dBA.

Figure 6.16 shows RT20 averaged over three receiver points at the 1<sup>st</sup>, 4<sup>th</sup> and 7<sup>th</sup> floors according to the three landscape designs. The small standard deviation indicates similar RT20s at the 1<sup>st</sup>, 4<sup>th</sup> and 7<sup>th</sup> floors. It can be seen that the vegetation on the façade plays an important role in reducing RT20 at 500 Hz by 66 % (1.1 sec). On the other hand, the vegetation on the ground has a limited effect in reducing RT20.

## 6.5 Summary

In this chapter, in-situ measurements and computer simulations were carried out to investigate how applicable landscape designs can contribute to the variation in sound levels and RT in a courtyard and at different floor levels in an adjacent accommodation building.

In-situ measurements were conducted before and after applying the practical landscape design on the ground using low-growing vegetation, trees, wood decking and street furniture. The results showed subsequent sound levels had reduced by 3.1 dB in an unweighted overall value. RT20 at 500 Hz was decreased by 47 % (1.5 sec). Also, the practical landscape design is relatively effective in reducing RT20 at low frequencies in comparison with high frequencies due to the increased absorption, scattering and diffraction effects of the ground.

Computer simulations showed that the extra SPL attenuation by the vegetation on the façade was increased for larger source-receiver distances in the courtyard. The leafy Ivy decreased sound levels at high frequencies, by 5.2 dB at 4000 Hz. As for the speech spectrum, 1.2 dBA was removed by the Ivy, indicating a limited effect of leaves on the

façade in moderating noise annoyance for speech in such reverberant courtyards. With the Ivy, RT20 at 500 Hz was also decreased by 52 % (1.3 sec). The green wall on the façade decreased sound levels by 9.9 dB at 500 Hz and 9.3 dBA for the speech spectrum. It also reduced RT20 at 500 Hz by 81 % (2.1 sec). Therefore, it can be said that vegetation with porous growing media such as the green wall can be effective in moderating noise annoyance in such reverberant spaces. With the grass and bedding plants on the ground, the speech level was decreased by 0.9 dBA and 2.2 dBA, respectively, with the increase of RT20 by 12 % (0.3 sec) even though they have relatively high absorption coefficient values. With the combined use of vegetation on the ground and façade, it was vegetation on the façade that played the more important role in reducing sound levels and RT20. Therefore it is recommended that landscape designers use absorptive vegetation on facades rather than the ground to control sound fields in courtyards.

Vegetation on the façade is predicted to reduce sound levels more effectively at lower floors than at higher floors, showing the importance of multiple reflections in increasing sound levels nearer the ground. The predicted result showed that the green wall on the façade decreased the speech level by 3.8 dBA at the 1<sup>st</sup> floor. On the other hand, vegetation on the ground was more effective in reducing sound levels at the higher floors than at the lower floors. With bedding plants on the ground, the speech level at the 7<sup>th</sup> floor was decreased by 3.0 dBA. With combined use of the green wall and bedding plants on the façade and ground, the speech level was decreased by 5.5 dBA at the 4<sup>th</sup> floor. The green wall on the façade reduced RT20 by 66 % (1.1 sec), while bedding plants on the ground had a limited effect on reducing RT20.



The overall results indicate that sound environments in reverberant courtyards as well as in rooms in adjacent buildings can be improved by strategic landscape designs using sustainable materials such as vegetation.

Based on the results for the experiment and prediction, general design methods of landscape design in courtyards can be recommended as follows:

- 1) Use sustainable acoustic materials on façades instead of ground for effective noise control in courtyards with non-diffuse surfaces;
- 2) Install vegetation consisting of porous growing media (soil or substrate) as leaves are effective in absorbing/scattering sound energy at high frequencies;
- 3) Place vegetation both on ground and façade if the purpose of landscape designs is to reduce noise levels in rooms at high floors of adjacent buildings;
- 4) Locate garden furniture such as tables and benches to increase ground diffusion as well as diffraction effect.

## **7 A Preliminary Study on Acoustic Characteristics of Outdoor Spaces in an Apartment Complex**

The aim of this chapter is to carry out a preliminary study on sound propagation within outdoor spaces of high-rise apartment buildings, after examining reproducibility and signal to noise ratio for the measurement methodology which will be applied to later large-scale work in Chapter 8. In Section 7.1, the importance of comfortable outdoor sound environments in apartment complexes is defined through reviews of previous studies. Methodology is validated in Section 7.2. Section 7.3 describes the results for the characteristics of sound fields examined at three outdoor spaces. In Section 7.4, key findings of this chapter are addressed.

### **7.1 Introduction**

In many countries, a significant percentage of the population lives in multi-storey apartment buildings due to the scarcity of available land space. In Korea, in particular, it is estimated that over 50 % of dwellings are multi-storey apartment buildings. Therefore, there have been continuous efforts to improve the sound environment in multi-storey apartment buildings, especially in terms of the noise level in the interior spaces.

In recent years, outdoor spaces in typical apartment complexes are also receiving great attention, partly because the available space has been enlarged through increased underground car parking according to sustainable-built and eco-friendly design principles. This leads residents to occupy outdoor spaces more for leisure, rest, or conversation (Baik, 2003), where the acoustic characteristics play an important role in

improving the overall environmental quality (Yang *et al.*, 2005; Yu *et al.*, 2009; Yu *et al.*, 2010).

Outdoor spaces in apartment complexes are generally surrounded by multi-storey buildings with different sizes and dispositions. Therefore, the presence of buildings induces many complicating acoustic effects such as multiple reflections, diffraction, and diffusion, which depend on the size, irregularity and material property of building façades and ground surfaces, etc.

Variation of the sound field due to buildings affects decay of transient sound levels which is related to RT, as well as the steady-state noise levels such as from road traffic noise. In the past few decades, several site measurements of sound propagation in urban spaces have been conducted to evaluate the effect of buildings on the RT and noise levels, especially for road traffic noise (Aylor *et al.*, 1973; Ko *et al.*, 1978; Picaut *et al.*, 2005; Steenackers *et al.*, 1976; Wiener *et al.*, 1965; Yeow, 1976, 1977). To overcome the limitation of full scale measurements, scale models have also been used to validate sound propagation in urban spaces (Delany *et al.*, 1972; Horoshenkov *et al.*, 1999; Kang, 1996b; Kerber *et al.*, 1981; Mulholland, 1979). In summary, the results from site and scale model measurements suggest that buildings in urban spaces contribute to increases in noise levels due to multiple reflections which are influenced by various factors such as street width and acoustic characteristics of building façades and ground surfaces, including absorption, diffusion and diffraction.

Many investigations have been carried out on theoretical and numerical models of sound propagation in urban spaces using an image source model or diffuse reflection model (Davies, 1978; Kang, 2000, 2002b, 2005; Picaut *et al.*, 1999). Kang (2000,

2002b, 2005) investigated acoustic parameters such as RT, EDT and sound attenuation in urban streets and squares through the comparison of geometrical and diffuse boundary conditions using the image source and radiosity methods. The results showed that the RT and sound attenuation in a single street canyon depend on boundary conditions, and in particular, the importance of façade diffusion in urban spaces has been demonstrated. With geometrical boundaries, the RT at 500 Hz is about 4 sec at 60 m from a point source and it increases with increasing source-receiver distance; and the EDT at 500 Hz is about 1.5 sec at 60 m from a point source and also increases with increasing source-receiver distance. With diffusely reflecting boundaries, the RT is considerably shorter in comparison with that of geometrically reflecting boundaries, and EDT is longer than RT beyond a certain source-receiver distance. Kang also investigated the effect of architectural and urban design on the sound field, including boundary absorption, boundary pattern and building arrangement (Kang, 2001, 2002a, 2002d, 2007). Consequently, the results from both measurement and prediction allow the assessment of acoustic treatments to reduce noise levels and RT in urban spaces.

Outdoor spaces in apartment complexes have various types and sizes. Although there are many common features with urban streets, squares and built-up areas, further research on the acoustic characteristics of outdoor spaces in apartment complexes is still required due to the differences in building disposition, material, and façade configuration, etc. In this chapter, therefore, in-situ measurements for three types of outdoor space in an apartment complex were carried out to evaluate the acoustic parameters, including RT, EDT, rapid speech transmission index (RASTI), and SPL attenuation with distance. Along with measurements at street level, acoustic parameters at the different floor levels in an apartment building were also evaluated.

## 7.2 Methods

In-situ measurements were conducted to investigate the acoustic characteristics of outdoor spaces in an apartment complex which is located in Seoul metropolitan city, South Korea. The apartment complex, as shown in Figure 7.1, consists of 15 apartment buildings which have 9 - 15 floors for each building. The buildings are arranged along a major traffic road and two side pedestrian roads which have a width of approximately 13 m in total. The building façades are comprised of concrete walls and windows which can be regarded as geometrically reflecting boundaries.



Fig. 7.1 The studied apartment complex

In order to characterise sound fields in urban spaces, it is essential to measure simultaneously the sound attenuation and the sound decay at different locations. This can be performed by measuring the impulse response at many receiver points in an urban space for various points of sound source. Then, SPL in steady-state and the RT can be extracted from the impulse response. RT has been demonstrated to be a useful index to examine geometrical parameters such as street width, average height, and façade roughness (Lyon, 1974). Thomas *et al.* (2013) estimated that information on reverberation in urban streets is useful to predict the increased SPL by multiple

reflections. It has also been experimentally proven that with a given SPL, noise annoyance is greater with a longer reverberation time in a space (Kang, 1988). EDT, which is highly correlated with speech intelligibility, is also a useful index to characterise the early part of the sound energy decay (Bradley, 1986). STI could be a good indicator to determine the location of PA systems. Due to the reasons above, in this work, acoustic parameters including sound attenuation, RT, EDT and STI are measured. These acoustic parameters are also useful to validate numerical modelling for sound propagation in urban spaces.

Sound attenuation with distance was measured using portable sound level meters (RION, NA-28) with a receiver height of 1.5 m. The sound source for the measurement was white noise generated from an omni-directional loudspeaker with a height of 1.5 m. The background noise level for measurements was 60 dB in unweighted overall level, which is 38 dB lower in comparison with the steady-state signal level measured at 1 m from the source. The signal-to-noise ratio at 120 m from the source was about 4 dB. RT was examined using a starter pistol as the sound source which, compared to the omni-directional speaker, can emit higher sound levels against background noise. The impulse responses for the starter pistol were recorded using the 2 channel Symphonie system (01dB). Five gun shots were generated for each measurement to consider the repeatability. All microphones were calibrated before the measurements. The measurements were conducted with an average temperature of 11.1 °C, relative humidity of 56.5 %, and wind speed less than 3.3 m/s.

Four source points, named S1, S2, S3 and S4 below, were used to evaluate the acoustic characteristics including RT and sound attenuation of the outdoor spaces. The number

and location of the sources were determined by considering the type of outdoor spaces and site conditions. S1 was positioned at an outdoor space with a long length and narrow width which is a comparable space to street canyons. S2 was set up at an opposite side of S1 in the same outdoor space to investigate the effect of source position. S3, located in an outdoor space with a single-side of building façades along a street, was selected to compare the results measured at S1 and S2 which were in the outdoor space with building façades on both sides. S4 was set up to measure acoustic parameters in an outdoor space surrounded by apartment buildings, which can be regarded as an urban square with complex building dispositions. With the source at S2, impulse responses at six different floor levels were recorded to analyse acoustic parameters according to receiver heights. Overall, the outdoor spaces investigated in this chapter can be categorised into 3 zones as shown in Figure 7.2.

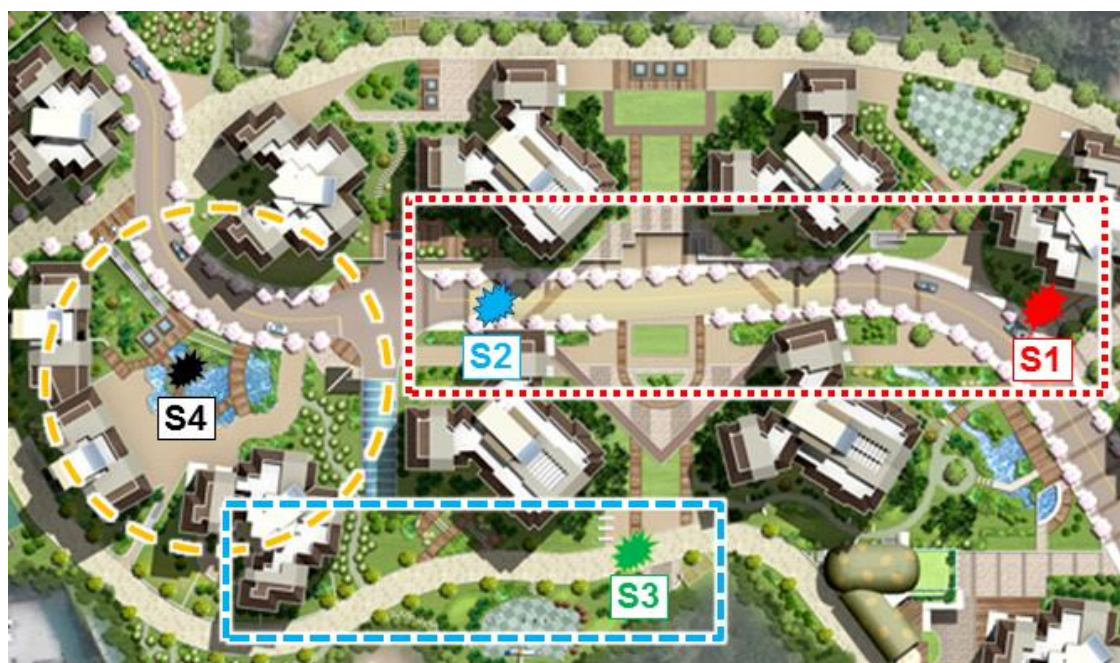


Fig. 7.2 Three zones of outdoor spaces and the position of each source (S1, S2, S3, S4)

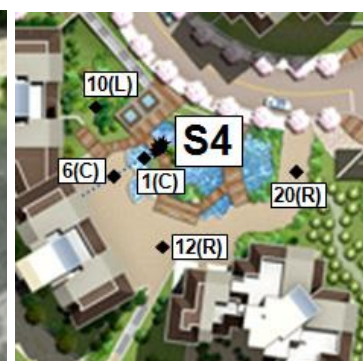
Receivers for S1 and S2 were located along a line-of-sight between S1 and S2 based on log scale source-receiver distance within 120 m to evaluate the effect of distance on RT and sound attenuation. Receivers for S3 were set up based on log scale source-receiver distance up to 80m. In the outdoor space where S4 was located, receiver points were determined to measure the effect of distance and position on acoustic parameters. In Figure 7.3, receiver points at each zone are illustrated. The number below and above the symbol indicates source-receiver distance in metres. Table 7.1 shows the source-receiver distance and the height for each source. Site conditions at each source position are also shown in Figure 7.4.



(a) Receiver points for S1 and S2 (S1: circle, S2: triangle)



(b) Receiver points for S3



(c) Receiver points for S4

Fig. 7.3 Receiver points for each source position including source-receiver distances



## Chapter 7. A Preliminary Study on Acoustic Characteristics of Outdoor Spaces in an Apartment Complex

Table 7.1 Source-receiver distance

Source	Symbol in Fig. 7.3	Source-receiver distance (m)
S1	Circle	1, 5, 10, 20, 40, 80, 120
S2	Triangle	Horizontal: 1, 5, 10, 20, 40, 80, 100, 120
		Vertical: 2 <sup>nd</sup> , 4 <sup>th</sup> , 6 <sup>th</sup> , 8 <sup>th</sup> , 10 <sup>th</sup> , 12 <sup>th</sup> floor
S3	Square	1, 5, 10, 20, 40, 80
S4	Diamond	1(C), 6(C), 10(L), 12(R), 20(R)

\*C: Centre, L: Left, R: Right



Fig. 7.4 Site conditions for each source position

Acoustic parameters including the RT, EDT and RASTI were calculated using the DIRAC analysis program which has a noise compensation function to reduce the effect of background noise on RT calculation. The calculation method of RT was based on T20 in one-octave bands from 125 Hz to 4000 Hz, considering that this was an outdoor field measurement with relatively high background noise level. During the acoustic measurement, all obstacles on streets including vehicles and construction materials were removed. The fountain sound, as shown in Figure 7.4(d) was stopped to reduce background noise.

### **7.3 Results**

#### **7.3.1 Impulse Responses and Decay Curves at S1**

To validate the effect of apartment buildings on multiple reflections, Figure 7.5 shows the pressure squared impulse responses measured at receiver distances of 10 m and 40 m from S1. Because of strong reflections from building façades, it can be seen that there are several peaks with strong sound energy arriving after the direct sound with visible time delay, which could cause acoustic defects including echoes. Between the peaks due to strong reflections, sound energy with relatively low amplitude can be observed, which is due to reflected and diffused sound energy from other boundaries and obstacles such as trees. It is noted that the strong reflections can play an important role in increasing RT and noise levels for transient and steady-state sound sources, which are related to spatial impression and noise annoyance. Therefore, it can be said that it is important to control the reflected impulses with strong sound energy using suitable acoustic material and configuration design of building façades.

In Figure 7.6, decay curves at 500 Hz are shown, which were measured at source-

receiver distances of 1 m to 120 m from S1. The range of the Y-axis is 0 dB to -25 dB for RT20 calculation. It is noted that the decay curves are decreased in a linear shape, indicating that the value of RT30 is similar to that of RT20. The decay curves are analysed using WINMLS 2004 software using Schroeder integration and automatic truncation of impulse responses based on automatic detection of noise floor margin of 5 dB. The result from decay curves indicates that the RT at 500 Hz is relatively long, and gradually increases with increasing source-receiver distance.

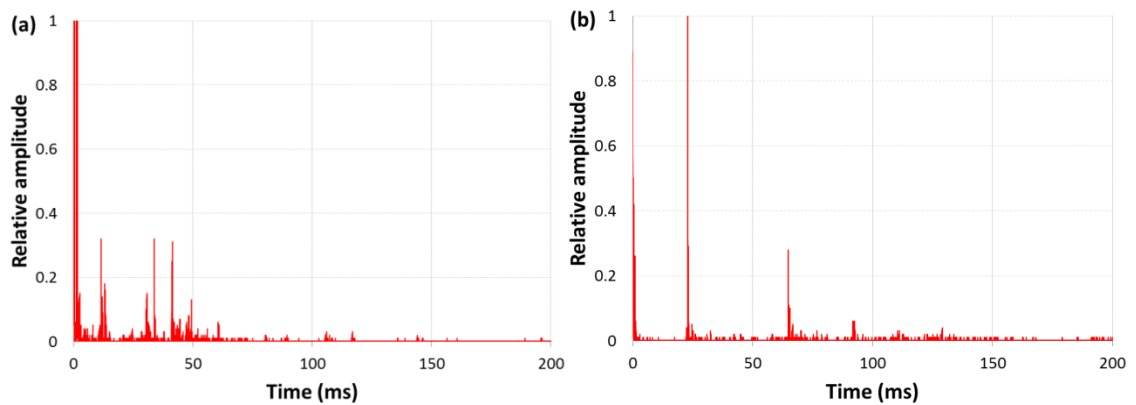


Fig. 7.5 Impulse responses at two source-receiver distances: (a) 10 m; (b) 40 m

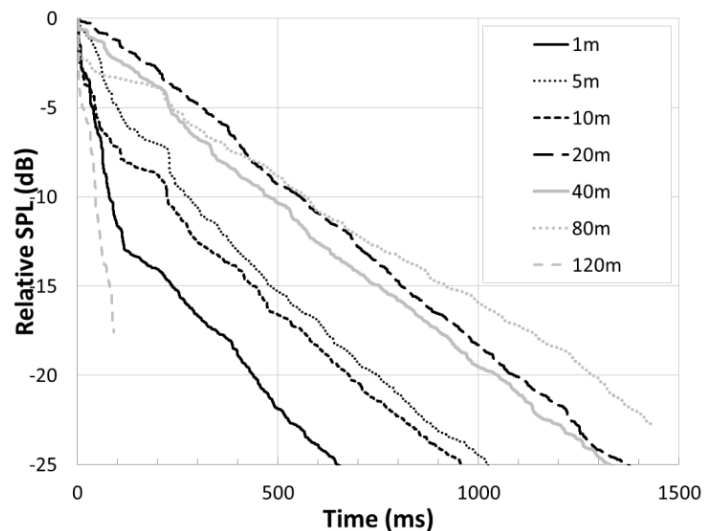


Fig. 7.6 Decay curves at 500 Hz according to source-receiver distance from 1 m to 120 m

### 7.3.2 Acoustic Characteristics of the Long Outdoor Spaces (S1, S2, S3)

As mentioned above, S1, S2 and S3 were positioned in the relatively long outdoor spaces. S1 and S2 were at a long outdoor space surrounded by building façades along both sides of a street so that it was expected that the sound field was relatively reverberant in comparison with the outdoor space where S3 is located. Therefore, it is useful to compare acoustic parameters measured at S1, S2 and S3 to evaluate the effect of source position and building façade conditions. In Figure 7.7, the RT20 measured at S1, S2 and S3 at octave bands from 125 to 4000 Hz is shown according to source-receiver distance, with regression curves and correlation coefficients. The calculation method of the regression curve is determined by considering the correlation coefficient which has the highest value. In case of the polynomial regression curve, 2<sup>nd</sup> order equation is selected.

The result in Figure 7.7 shows that the maximum value in RT20 is over 4 sec at 500 Hz and 1000 Hz, and the RT20 increases with increasing source-receiver distance above 500 Hz. On the other hand, it can be seen that the RT20 is relatively short, less than 2 sec at 125 Hz, which might indicate the effect of diffraction due to the gap between buildings. At 125 Hz, it can be seen that the RT20 is very short, down to about 0 sec at far source-receiver distances over 80 m. This is perhaps because the reflective sound energy at 125 Hz is relatively weak in comparison with that of first-arrived sound due to diffraction. As the measurements were carried out in winter, most of windows were closed, which implies an insignificant effect of absorption by façades on reducing RT20, although windows have a relatively high absorption at low frequencies. The comparison of the RT20s measured at S1 and S2 indicates that the tendency of regression curves is

Chapter 7. A Preliminary Study on Acoustic Characteristics of Outdoor Spaces in an Apartment Complex

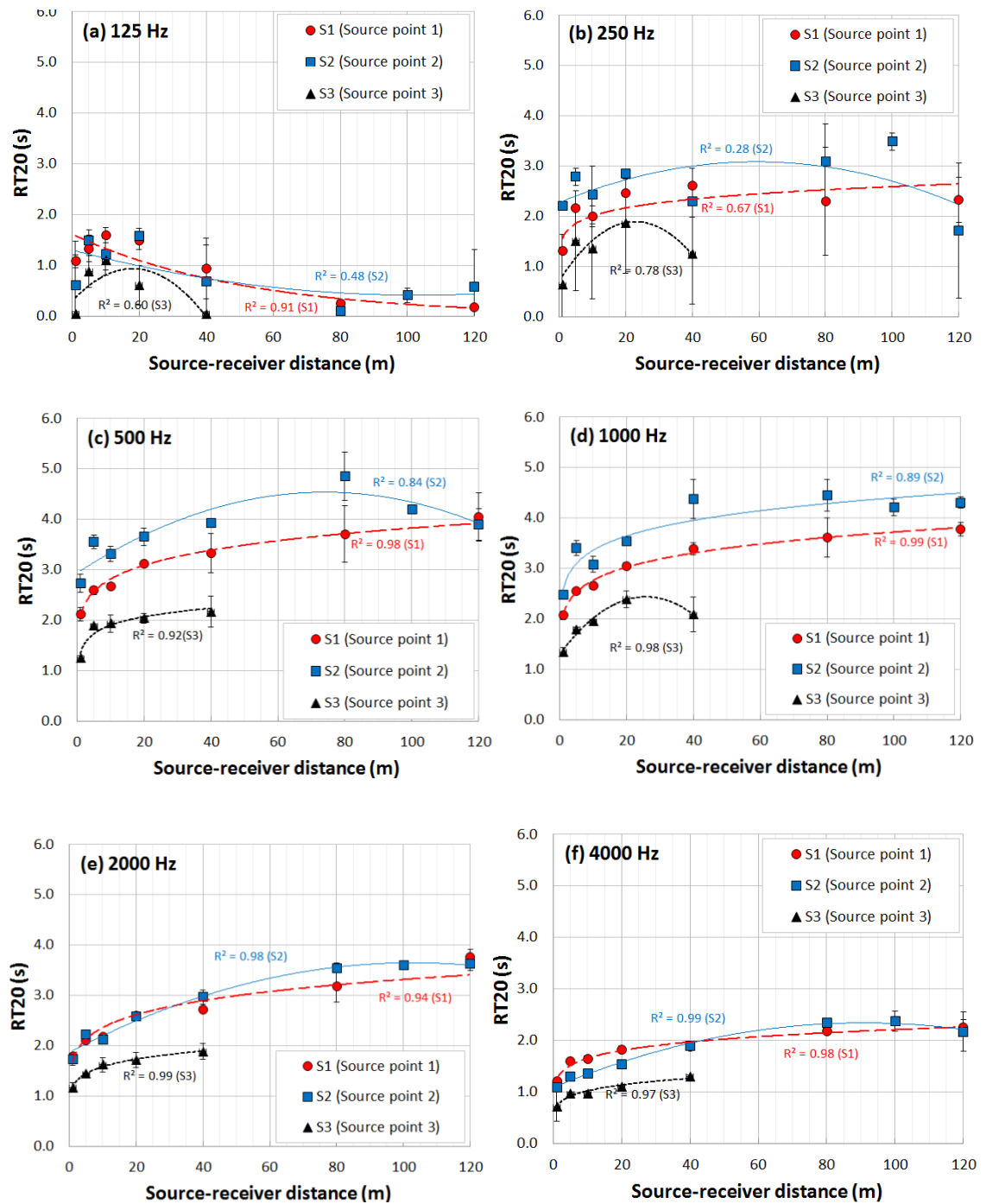


Fig. 7.7 RT20 measured at 3 source positions (S1, S2, S3) according to source-receiver distance, with regression curves (S1: ---, S2: —, S3: ----) and correlation coefficients R<sup>2</sup>: (a) 125 Hz; (b) 250 Hz; (c) 500 Hz; (d) 1000 Hz; (e) 2000 Hz; (f) 4000 Hz

similar at all frequencies. However, visible differences in RT20 are observed below 1000 Hz, by 1.2 sec at 500 Hz, showing the effects of different building dispositions relative to the source points. On the other hand, the difference in RT20 above 2000 Hz is insignificant. The RT20s measured at S3 are 1.8 sec less at 500 Hz in comparison with the RT20s measured at S1 and S2. This suggests that building façades can strongly affect the acoustic characteristics of outdoor spaces, as expected.

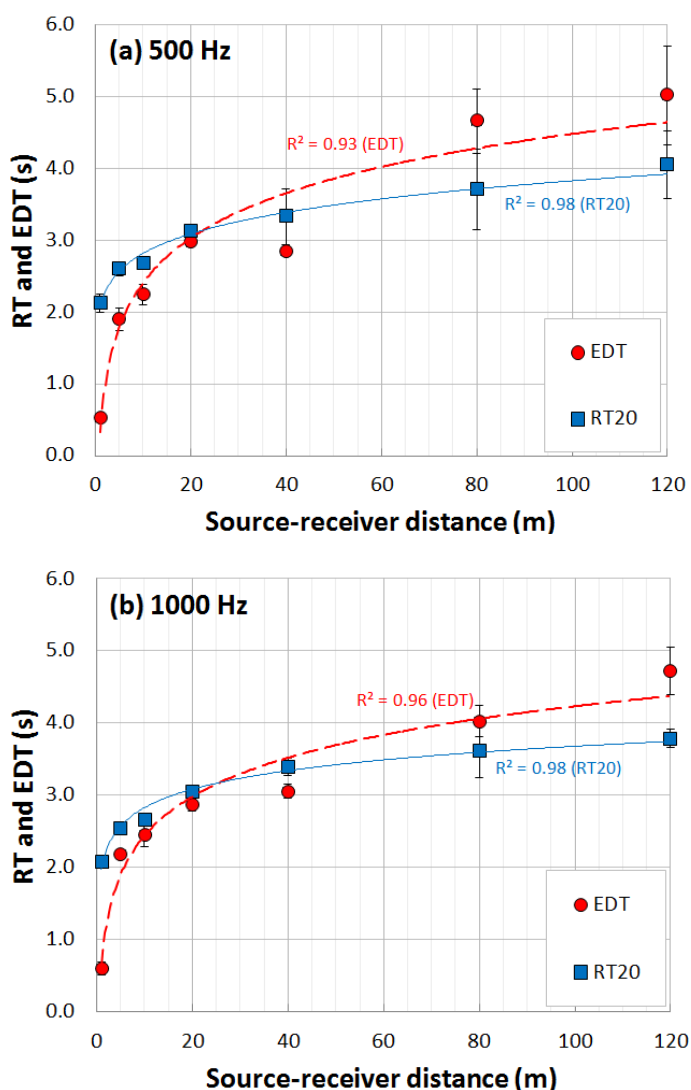


Fig. 7.8 RT20 and EDT measured at S1, with regression curves (EDT: — —, RT20: — ) and correlation coefficients  $R^2$ : (a) 500 Hz; (b) 1000 Hz

A comparison between the RT20 and EDT measured at S1 is shown in Figure 7.8 for 500 Hz and 1000 Hz. It can be seen that above a certain distance, say 40 m, EDT is longer than RT20 at both frequencies. This is perhaps because the direct sound affects the relatively short EDT in comparison with RT20 within short source-receiver distances. On the other hand, EDT is longer than RT20 beyond 40 m, perhaps due to the narrow gap with a width of 13 m at 40 m from S1, as this can reduce the effect of reflected sound from boundaries, so as the sound energy loss at the late part of decay curve.

In an apartment complex, acoustic parameters related to speech index such as RASTI can be useful in terms of the use of PA (public address) systems as well as soundscape applications (Davies *et al.*, 2009). RASTI is evaluated as 5 grades: 0 - 0.3, bad; 0.3 - 0.45, poor; 0.45 - 0.6, fair; 0.6 - 0.75, good; 0.75 - 1.0, excellent (IEC, 2003). In Figure 7.9, the RASTI measured at S1, S2 and S3 is shown according to the source-receiver distance, where the measurement results which were influenced by strong background noise are excluded. It can be seen that RASTI measured at S1 and S2 is from 0.7 to 0.4 approximately within 120 m, and the value decreases with the increase of distance. On the other hand, RASTI measured at S3 has a range between 0.8 and 0.65 within 40 m, relating to its shorter RT20, compared to S1 and S2. It is noted that while the results are presented as a function of distance from the source, with signal-to-noise ratio ignored, speech intelligibility in such outdoor spaces could often be dominated by background noise, especially at far source-receiver distances.

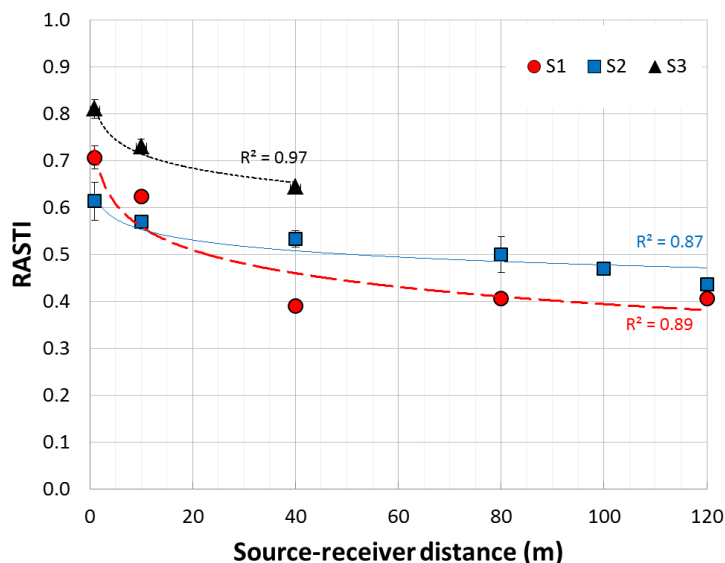


Fig. 7.9 RASTI according to source-receiver distance at S1, S2 and S3 with regression curves (S1: —, S2: —, S3: ----) and correlation coefficients  $R^2$

Figure 7.10 shows a comparison between sound attenuation calculated in semi-free field with hard ground and that measured at S1, S2 and S3. The sound levels are with reference to the SPL at 1 m. In the near field, the difference between semi-free field condition and measured sound attenuation is insignificant, which indicates the strong influence of the direct sound. The difference between measured values at S1 and semi-free field theoretical values becomes more important with the increase of source-receiver distance, up to 8 dB, which indicates the effect of multiple reflections between building façades. On the other hand, the effect of building façades on increasing sound levels at S3 is about 5 dB in maximum within 80 m, which correspond to Kang's (2007) results based on simulation.



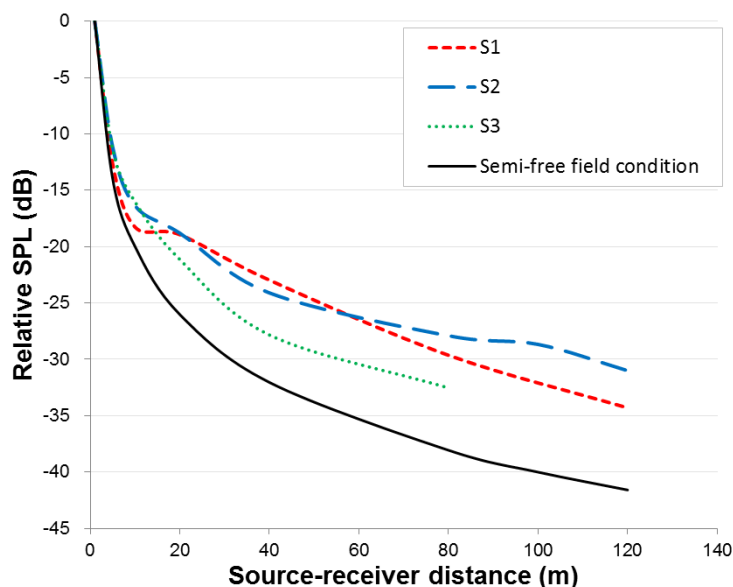


Fig. 7.10 Sound attenuation according to source-receiver distance at S1, S2 and S3

### 7.3.3 Acoustic Parameters of the Outdoor Square (S4)

The outdoor space where S4 is located can be regarded as a square with complicated building dispositions. In Figure 7.11, the RT20 and EDT for 5 receiver points are presented. The result shows that the RT20 generally increases with increasing source-receiver distance and the RT20 value is about 3.4 sec at 500 Hz. Moreover, the RT20 is relatively long compared to the EDT. With the increased source-receiver distance, the EDT also increases. In comparison with the result in the outdoor space with building façades on both sides, EDT is approximately 1 sec less at the same source-receiver distance with 20m due to different building layout. The RASTI at the 5 receiver points is shown in Figure 7.12. It can be seen that RASTI decreases from 0.8 to 0.5 with increased source-receiver distance, corresponding to increased reverberation.

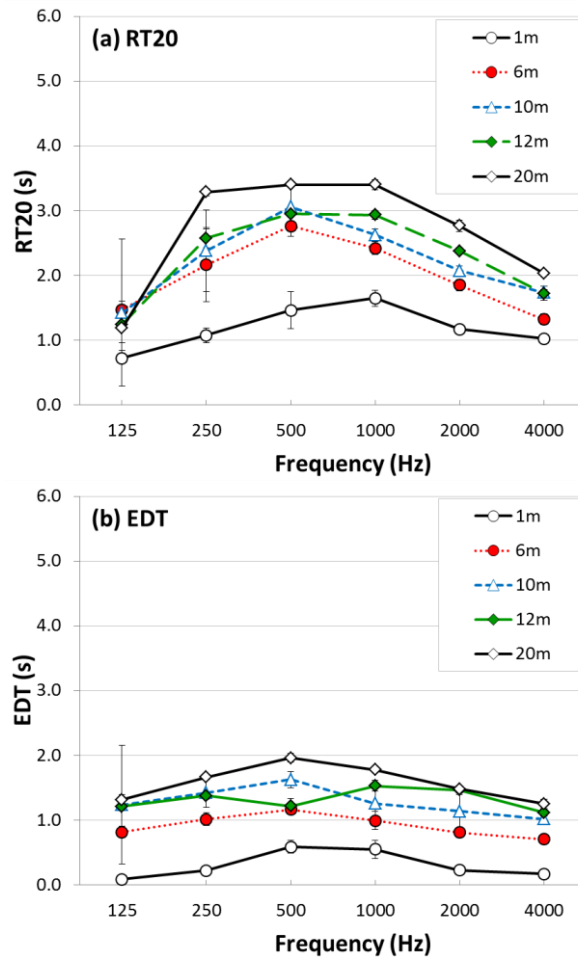


Fig. 7.11 RT20 and EDT according to source-receiver distance measured at S4: (a) RT20; (b) EDT

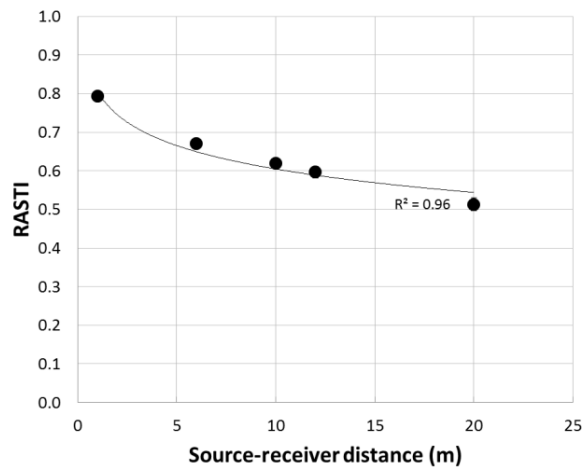


Fig. 7.12 RASTI according to source-receiver distance at S4 with a regression curve and correlation coefficient  $R^2$

### 7.3.4 Acoustic Parameters with Different Receiver Heights (S2)

With the source position of S2, the measurement of acoustic parameters including RT20, EDT and RASTI was carried out along the building height. The result in Figure 7.13 shows RT20 is insignificantly changed according to the receiver height, which suggests RT20 is dominated by the late part of impulse response with similar decay pattern according to the receiver height. The RT20 at 500 Hz is approximately 3 sec, which is similar to that in a previous study using a scale modelling test (Lee *et al.*, 2007). On the other hand, the

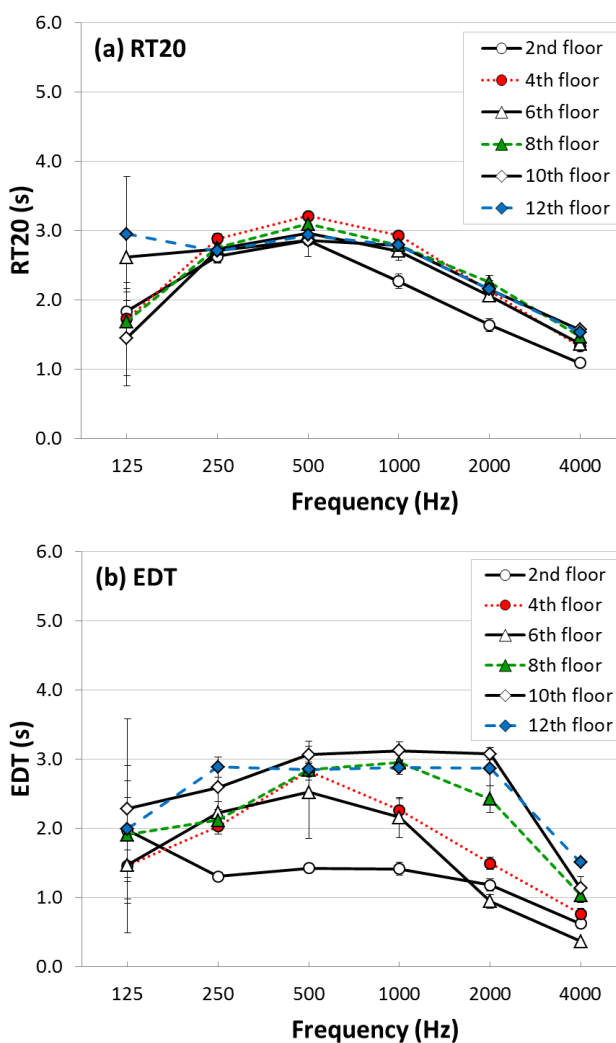


Fig. 7.13 RT20 and EDT at different floor levels: (a) RT20; (b) EDT

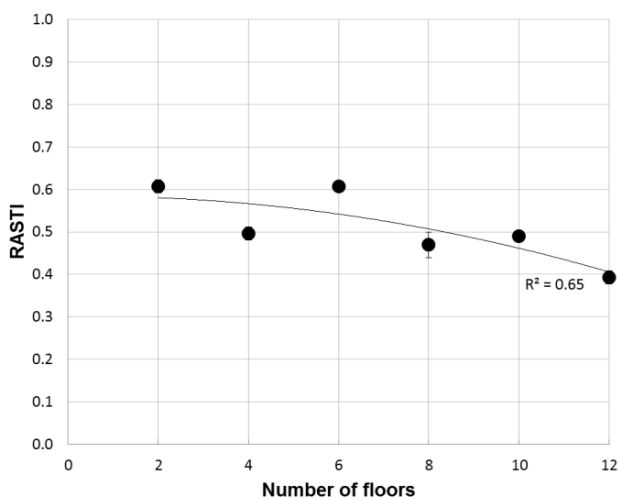


Fig. 7.14 RASTI at different receiver heights with S2, and a log regression and correlation coefficient  $R^2$

EDT is strongly influenced by the receiver height, generally increasing with increasing receiver height from 1.4 sec to 3.2 sec at 500 Hz, suggesting the importance of the direct sound energy on the early part of decay curve according to the receiver height. Correspondingly, RASTI generally decreases with increasing receiver height from 0.6 to 0.4, as shown in Figure 7.14.

## 7.4 Summary

In this chapter, in-situ measurements in three outdoor spaces in an apartment complex have been carried out to evaluate acoustic parameters, including the RT20, EDT, RASTI and SPL distribution. These acoustic parameters are selected to characterise the sound field in the outdoor spaces, which are also be used to validate the acoustic computer simulation programme, ODEON, used in Chapter 8.

The measurement methodology using a starter pistol showed good reproducibility of the RT20 above 500 Hz. It has also been confirmed that signal to noise ratio of the starter

pistol is enough to measure RT20 within the source-receiver distance of 120 m. Therefore, it can be said that the measurement methodology is applicable to large-scale parametric work in Chapter 8.

The results show that the RT20 in a long outdoor space with two-side building façades is over 4 sec at 500 Hz and 1000 Hz, which suggests the requirement for acoustic treatments using appropriate façade material and building layout. The RT20 increases with increasing source-receiver distance above 500 Hz. The EDT is longer than the RT20 beyond a certain source-receiver distance, at about 40 m. The RT20 in the long outdoor space with a single-side façade is about 1.8 sec less at 500 Hz in comparison with the long space with two-side building façades. In comparison with the situation in a semi-free field, the measured SPL is about 5 dB and 8 dB higher in the outdoor spaces surrounded by one-side and two-side building façades, respectively. In the outdoor square, the RT20 and EDT also increase with the increase of source-receiver distance. In comparison with the result in the long outdoor space surrounded by two-side building façades, the EDT is shorter at the same source-receiver distance. The RASTI also decreases with increasing source-receiver distance. The measurement results at different receiver heights from the 2nd to 12th floors show that the receiver height plays an insignificant role in the RT20. On the other hand, the EDT increases with increasing receiver height, especially at high frequencies. The RASTI also decreases with increasing source-receiver distance.

Although the experimental results derived from the in-situ measurement suggest useful data to understand sound propagation in apartment complexes, it is still necessary to study more systematically by considering various factors such as different building

## Chapter 7. A Preliminary Study on Acoustic Characteristics of Outdoor Spaces in an Apartment Complex

---

configuration, disposition and size, etc. In upcoming work, a series of field measurements and predictions will be carried out according to the various factors mentioned above to provide a more accurate description of the reverberation and sound attenuation in the outdoor spaces of apartment complexes.

## **8 A Parametric Study on Outdoor Reverberation in Apartment Complexes**

The aim of this chapter is to clarify the designable factors affecting outdoor reverberation. A series of field measurements were carried out for 15 outdoor spaces in 6 apartment complexes. The 15 outdoor spaces were categorised into 5 types of building layouts for a parametric study. Based on the field measurements, an empirical method to approximate RT using AutoCAD has also been suggested. After a review of previous studies in Section 8.1, Section 8.2 describes the methodology used for this chapter. With five types of building arrangements, measurement results are examined in Section 8.3. By using the measurement data, an empirical method to determine outdoor reverberation is proposed in Section 8.4. In Section 8.5, initial results for the vegetation effect on RT are covered. Section 8.6 summarises key findings of this chapter.

### **8.1 Introduction**

High-rise apartment buildings have been universally built for residential purposes due to increasing population density in urbanised cities. An apartment complex consists of several numbers of apartment buildings in a limited boundary of land with various types of building layouts and blocks. Outdoor spaces in an apartment complex are planned by considering many architectural, environmental and social factors such as car parking, natural lighting and outdoor activities (Baik, 2003). Recently, the importance of the outdoor spaces for leisure and rest is being paid attention too, especially with the increase of the available land for such uses due to underground car parking. Therefore, designing comfortable sound environments in the outdoor spaces can contribute to

improving the living quality of residents.

Previous studies indicate that RT is an important parameter for characterising sound fields in urban spaces because the decay rate determining RT is influenced by the complicate acoustic phenomenon such as multiple reflections, diffraction and diffusion due to surrounding buildings (Lyon, 1974). RT also plays a role in determining spatial impression of urban spaces (Jeon *et al.*, 2011).

Due to the reasons outlined above, numerous studies have been carried out to predict RT in street canyons and urban squares with different boundary conditions and sizes (Kang, 2000, 2005; Picaut *et al.*, 1999). A series of in-situ and scale modelling measurements have also been conducted to investigate sound propagation and RT in urban spaces (Aylor *et al.*, 1973; Ko *et al.*, 1978; Picaut *et al.*, 2005; Steenackers *et al.*, 1976; Wiener *et al.*, 1965; Yeow, 1976, 1977).

In comparison with street canyons and squares, RT in outdoor spaces of apartment complexes could be more important because residents require high level of comfortable sound environments for leisure and rest. Therefore, it is important for architects to understand how architectural designs can affect RT in the outdoor spaces. In this chapter, a series of field measurements were carried out for 15 outdoor spaces in 6 apartment complexes. The 15 outdoor spaces were categorised into 5 types of building layouts for a parametric study. Based on the field measurements, an empirical method to approximate RT using AutoCAD has also been suggested in this chapter. Lastly, the effect of vegetation on sound field control in an apartment complex is investigated by using acoustic computer simulation.



## 8.2 Methodology

### 8.2.1 Studied sites

In this chapter, a series of field measurements were conducted to investigate RT in 15 outdoor spaces of six apartment complexes in Korea. The apartment complexes were selected by taking the type of building layouts and blocks into account. Figure 8.1 shows the bird's-eye views for each apartment complex. In Figure 8.2, photographs for each site are shown. Table 8.1 describes the site and measurement conditions for each apartment complex.

As shown in Figure 8.1 and 8.2, it can be seen that each apartment complex has different building layouts, blocks, size and height. On the other hand, most of building façades consists of acoustically reflective surfaces with concrete walls and window balcony, which can result in relatively long RT and strong echoes.



Fig. 8.1 Bird's-eye views for each apartment complex: (a) Site 1; (b) Site 2; (c) Site 3; (d) Site 4; (e) Site 5; (f) Site 6



Fig. 8.2 Photographs for each apartment complex: (a) Site 1; (b) Site 2; (c) Site 3; (d) Site 4; (e) Site 5; (f) Site 6

Table 8.1 Site and measurement conditions for each apartment complex

	Site 1	Site 2	Site 3	Site 4	Site 5	Site 6
Name	Jeon-Nong	Shin-Jung 2 <sup>nd</sup>	Shin-Jung 5 <sup>th</sup>	Pa-Ju	Jeung- Pyung	Chon-Wang
No. of buildings	15	20	8	11	6	13
No. of flats	867	471	238	648	504	1044
No. of floors	9~15	3~7	9~15	12~25	10~15	9~18
Measurement date	13 <sup>th</sup> .Nov. 2010	24 <sup>th</sup> .May. 2011	24 <sup>th</sup> .May. 2011	23 <sup>rd</sup> .Aug. 2011	26 <sup>th</sup> .Aug. 2011	7 <sup>th</sup> .Oct. 2011
Temp. (°C)	11.1	21.5	21.5	24.3	26.4	21.2
Humidity (%)	56.5	39.5	39.5	60.1	57.5	57.5
Wind speed (m/s)	< 3.3	< 2.0	< 2.0	< 2.1	< 1.5	< 2.1

In Figure 8.3, 15 measurement zones in the apartment complexes are shown. The building layouts surrounding outdoor spaces are categorised into 5 types as linear-shaped (i.e.,  $-$ ), parallel-shaped (i.e.,  $=$ ), L-shaped, U-shaped and  $\square$ -shaped types. The building blocks also have 4 different types which can be categorised as linear, L, U and Y types. The number of source and receiver points at each measurement zone is described in Table 8.2, with a total of 209 points being used. The source-receiver distance for each measurement zone was determined by considering the size of the outdoor spaces.

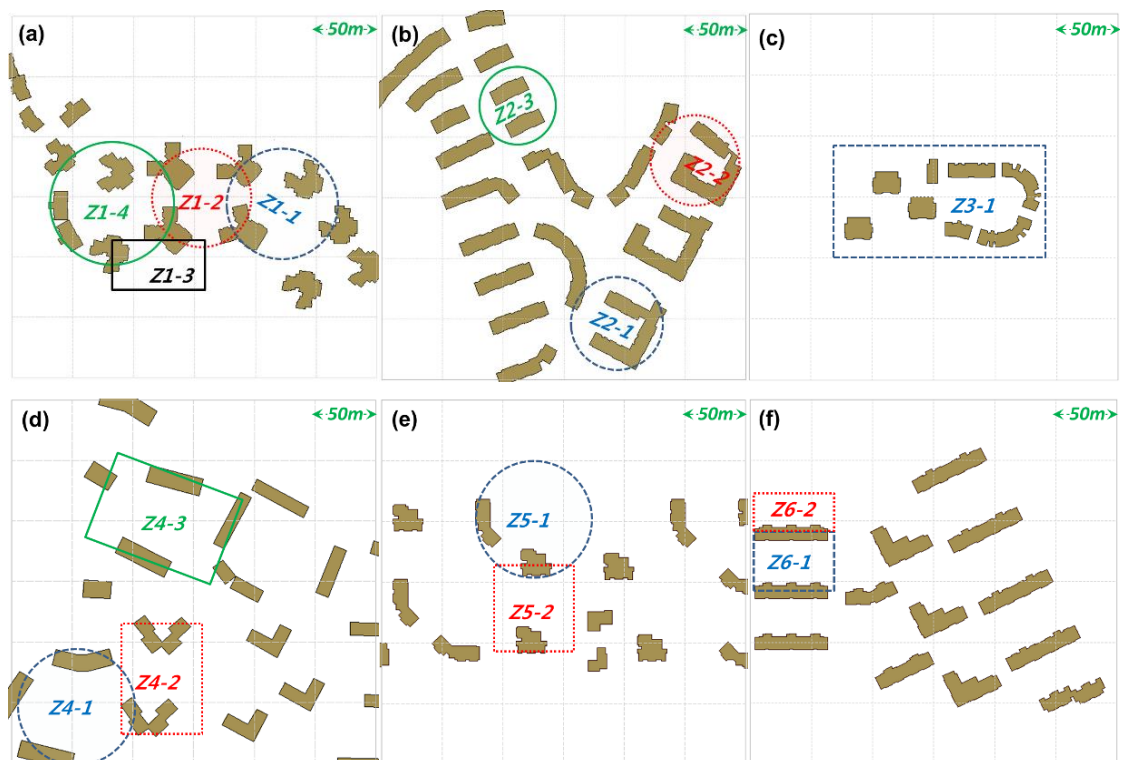


Fig. 8.3 Ground plan and measurement zones for each apartment complex: (a) Site 1; (b) Site 2; (c) Site 3; (4) Site 4; (5) Site 5; (6) Site 6

Table 8.2 Details for site and measurement conditions for each measurement zone

	Name of zone	No. of sources	No. of receiver	Total No. of measurement points	Type of building layout
Site 1	Z1-1	1	5	5	U
	Z1-2	1	5	5	□
	Z1-3	1	6	6	–
	Z1-4	1	5	5	□
Site 2	Z2-1	4	5	20	U
	Z2-2	4	5	20	U
	Z2-3	2	5	10	=
Site 3	Z3-1	3	6	18	□
Site 4	Z4-1	4	6	24	U
	Z4-2	4	5	20	L
	Z4-3	4	6	24	=
Site 5	Z5-1	3	4	12	L
	Z5-2	2	4	8	=
Site 6	Z6-1	4	5	20	=
	Z6-2	3	4	12	–

### 8.2.2 Measurement method

RT was measured with an impulsive sound source, a starter pistol, which can produce strong signal to noise ratio. The signal to noise ratio of the starter pistol was estimated from Chapter 7. The impulse response for the starter pistol was captured using the two channel Symphonie system (01dB) with ½” microphone (G.R.A.S. Type MCE 201) and preamplifiers (01dB-Stell Pre 12H). The four channel Harmonie system (01dB) was also used with ½” microphone (G.R.A.S. Type 40AF) and preamplifiers (G.R.A.S Type 26AG). Figure 8.4 illustrates the experimental condition. Gun shots for each measurement were repeated five times and averaged to calculate RT. RT for the impulse responses recorded from the field measurement was analysed using Dirac programme from B&K. In this chapter, the decay range is selected as T20 (-5 dB to -25 dB)

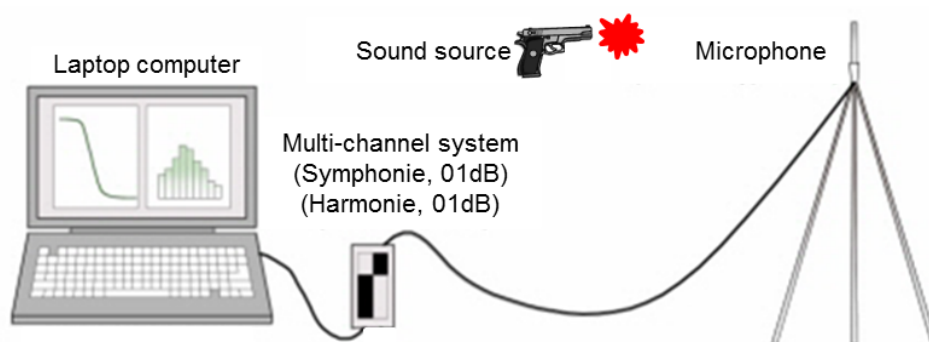


Fig. 8.4 Illustration for the experimental condition

## 8.3 Measurement results

### 8.3.1 Overall characteristics and distribution of RT

In Figure 8.5, maximum, average and minimum RT20 measured at each measurement zone are shown with different frequencies from 125 Hz to 4000 Hz in octave bands to examine the overall characteristics and distribution of it in the outdoor spaces. The result shows that differences in RT20 between maximum and minimum values for each measurement zone are important at all frequencies, which indicates the unevenly distributed RT20 in the outdoor space. It can be seen that maximum, average and minimum RT20 is different according to each measurement zone as well, which implies the importance of architectural design in terms of RT20. It is noted that RT20 is relatively long at 500 Hz and 1000 Hz in comparison with other frequencies. Maximum RT20 at 500 Hz is found at Z1-2 with about 4 sec.

Figure 8.6 shows the overall averaged RT20 for maximum, average and minimum values measured at the 15 measurement zones. The results indicate that RT20 at mid frequency (500 Hz and 1000 Hz) is relatively high in comparison with low and high frequencies. This is perhaps due to the energy sinking through gaps between buildings

by diffraction at low frequency, and atmospheric absorption and diffusion at high frequencies. For the maximum value in Figure 8.6, RT20 with about 2.7 sec at 1000 Hz indicates that sound field in the outdoor spaces is reverberant.

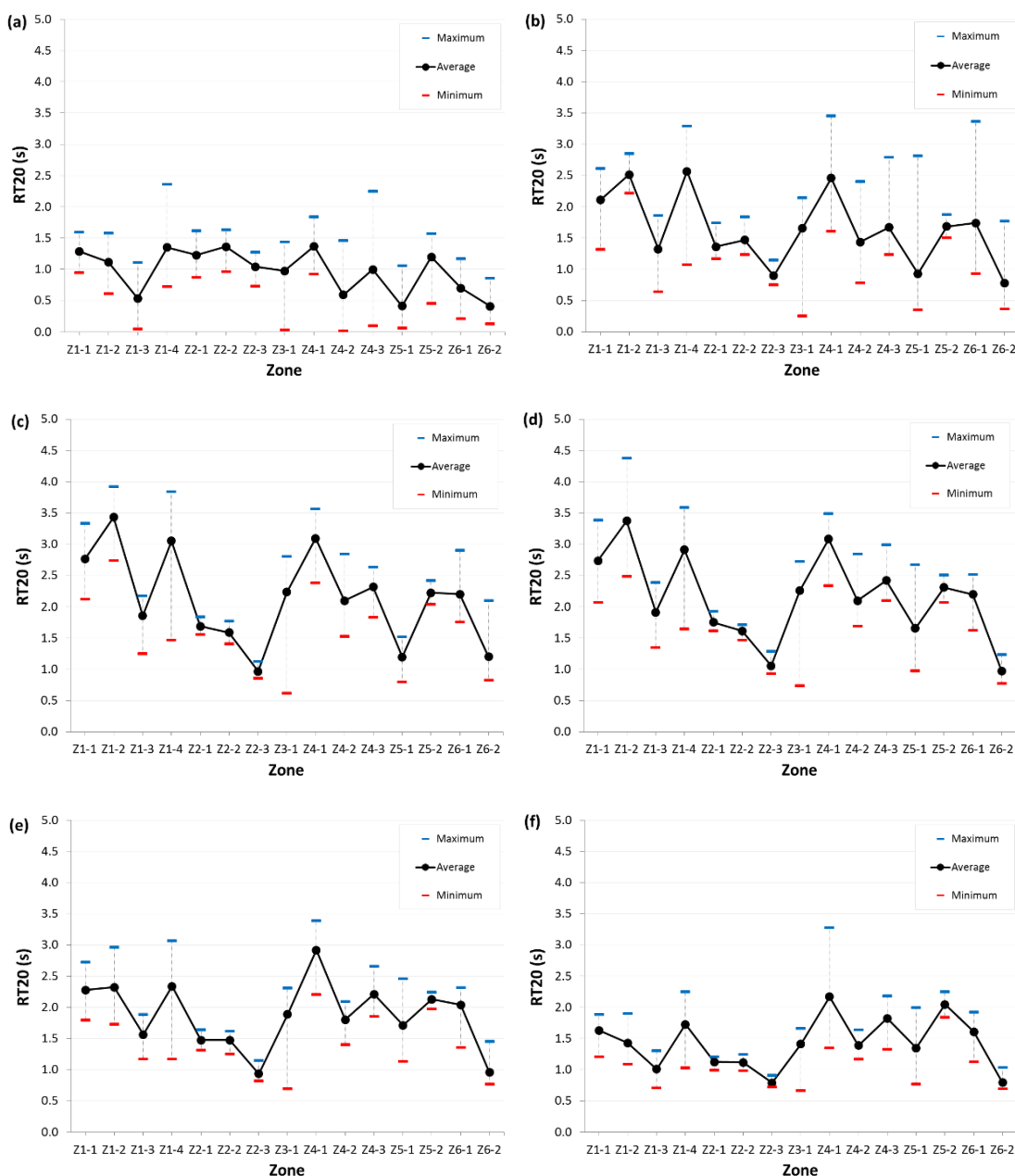


Fig. 8.5 Maximum, average and minimum RT20 with frequency at the 15 outdoor spaces: (a) 125 Hz; (b) 250 Hz; (c) 500 Hz; (d) 1000 Hz; (e) 2000 Hz; (f) 4000 Hz

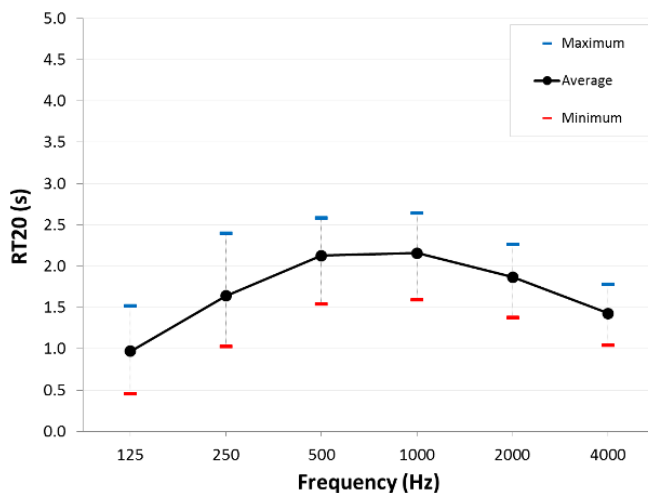


Fig. 8.6 Overall averaged RT20 for maximum, average and minimum values measured at the 15 outdoor spaces

In urban spaces, source-receiver distance is one of the important factors determining RT20. In Figure 8.7, therefore, RT20 measured at different source receiver distances in the 15 measurement zones is presented. The result suggests that RT20 is considerably different according to each measurement zone although the source-receiver distance is the same. This implies that different architectural designing can affect RT20.

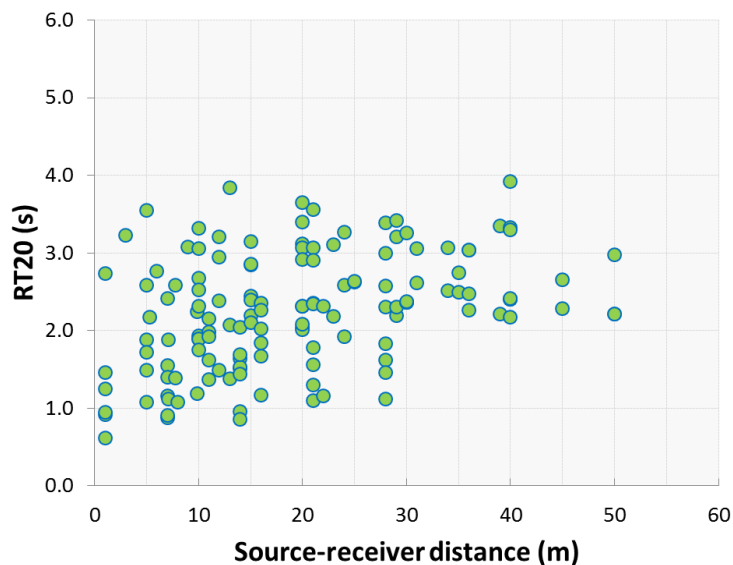


Fig. 8.7 Overall RT20 at 500 Hz with different source-receiver distances measured at the 15 measurement zones

In summary, the results for the overall characteristics and distribution of RT20 suggest that architectural design can affect RT20, and there is a possibility to control RT20 by determining suitable source-receiver distance, building layouts and building blocks.

### **8.3.2 RT for the linear-shaped building layout**

Among the 15 measurement zones studied here, there are two measurement zones with the linear building layout. Z1-3 and Z6-2 has the linear building layout with different types of building blocks. In Figure 8.8, RT20 is shown with source-receiver distance and frequency for the two measurement zones. The source and receiver points were located in a line of sight to examine the effect of source-receiver distance on RT20. The result in Figure 8.8(a) shows that RT20 is increased to about 2 sec with increasing source-receiver distance for both measurement zones. It is shown that RT20 at the receiver points near a sound source is relatively short due to the strong effect of direct sound. On the other hand, the variation in RT20 is rather insignificant above a certain distance, say about 10 m. In terms of the regression curves, it can be seen that the gradient is similar to each other.

In Figure 8.8(b), RT20 at the source-receiver distance of around 20 m is examined with frequencies from 125 Hz to 4000 Hz in octave band. The standard deviation error bar indicates the variation in the RT20 for the five repetitions of the measurement. The result shows that RT20 at 1000 Hz is relatively long in comparison with that for other frequencies for Z1-3. On the other hand, RT20 for Z6-2 has the highest value at 500 Hz. In comparison with Z6-2, RT20 for Z1-3 has rather high values at all frequencies by 1.4 sec at 1000 Hz.



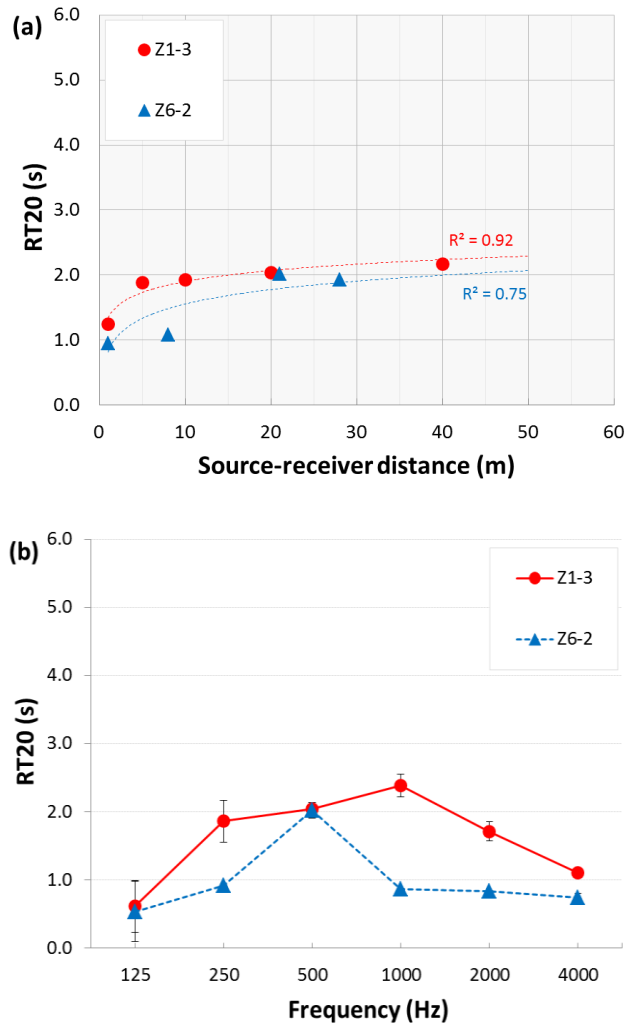


Fig. 8.8 RT20 for the linear building layout: (a) RT20 at 500 Hz with different source-receiver distances; (b) RT20 with frequency at the source-receiver distance with 20 m

### 8.3.3 RT for the parallel-shaped building layout

RT20 for the parallel building layout is dealt with in 3 measurement zones; Z2-3, Z4-3 and Z6-1. Figure 8.9(a) shows RT20 at 500 Hz with different source-receiver distances. The result shows that RT20 is increased with increasing source-receiver distance. In comparison with Z2-3, RT20 at Z4-3 and Z6-1 is relatively long, about 2 sec at the source-receiver distance of 20 m. This is thought to be mainly due to wide distance between the parallel buildings, although surrounding building topology can affect RT20.

However, it is noticeable that the gradient of the regression curves for the 3 measurement zones are similar to each other. It can also be seen that the maximum RT20 for the parallel building layout is 2.4 sec.

Figure 8.9(b) shows RT20 with frequency at the source-receiver distance of around 20 m. It can be seen that RT20 at 500 Hz is relatively long in comparison with that at other frequencies for Z4-3 and Z6-1. On the other hand, RT20 for Z2-3 is similar at all frequencies, being about 1 sec. The difference in RT20 between Z4-3 and Z2-3 is about 1.2 sec at 500 Hz.

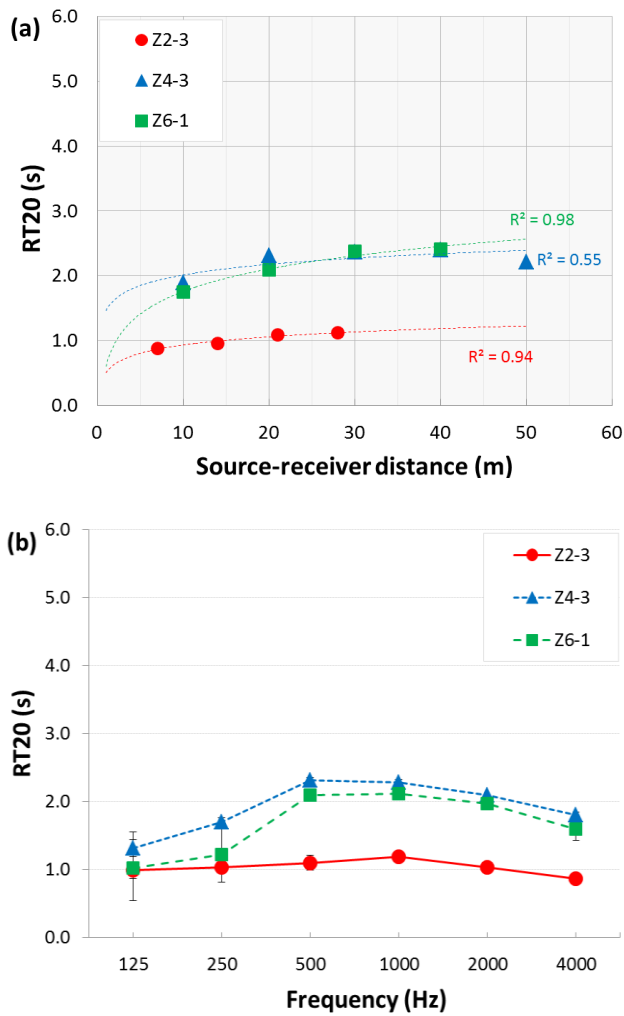


Fig. 8.9 RT20 for the parallel building layout: (a) RT20 at 500 Hz with different source-receiver distances; (b) RT20 with frequency at the source-receiver distance with 20 m

### 8.3.4 RT for the L-shaped building layout

In Figure 8.10(a), RT20 at 500 Hz is examined according to different source-receiver distances for Z4-2 and Z5-1 with the L-shaped building layout. The source and receiver was located in a line-of-sight. The result shows that RT20 is increased with increasing source-receiver distance, although there is a difference in RT20 by 1.6 sec between the two measurement zones. It is thought that the reason for the difference in RT20 is that Z4-2 is surrounded by another building reflecting sound energy back to the measurement zone. At the near field from a sound source, it can be

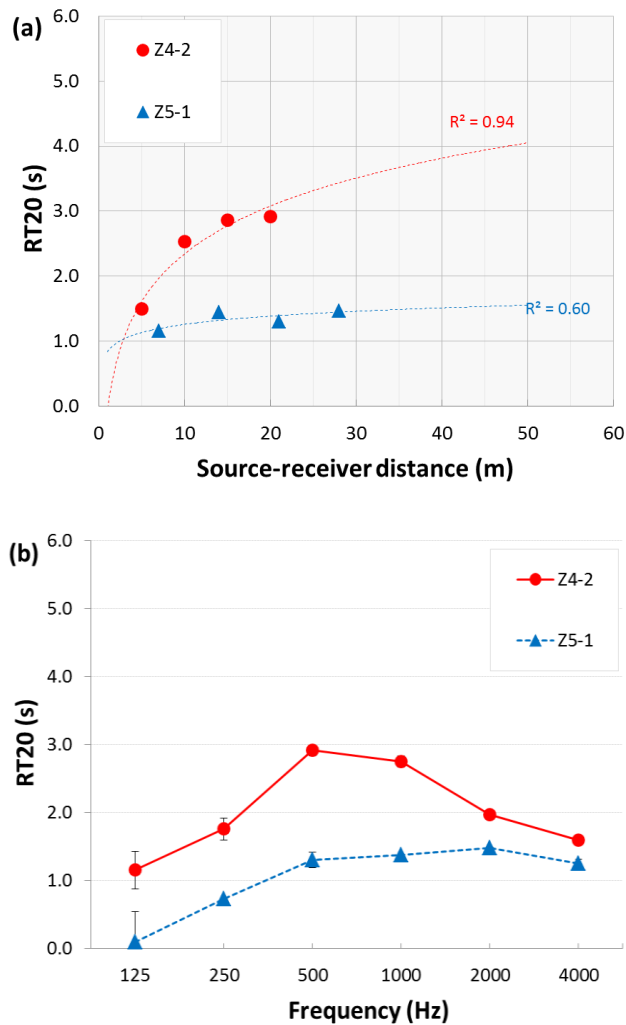


Fig. 8.10 RT20 for the L-shaped building layout: (a) RT20 at 500 Hz with different source-receiver distances; (b) RT20 with frequency at the source-receiver distance with 20 m

seen that RT20 is rapidly changed with the increasing source-receiver distance. On the other hand, there is an insignificant effect of the source-receiver distance beyond 15 m on RT20. It is noticeable that the gradient of the logarithm curves for Z4-2 is relatively rapid in comparison with that for Z5-1. The maximum RT20 for the studied L-shaped building layouts is about 3 sec indicating a reverberant sound field.

In Figure 8.10(b), RT20 for the 2 measurement zones is examined with frequency in octave bands at the source-receiver distance of 20 m. It can be seen that RT20 for Z4-2 has higher values at all frequencies than that for Z5-1. The maximum difference in RT20 between Z4-2 and Z5-1 is found at 500 Hz with 1.6 sec. It is also shown for Z4-2 that RT20 at 500 Hz is relatively long in comparison with that of other frequencies. On the other hand, RT20 at high frequency is similar to that at mid frequency for Z5-1.

### **8.3.5 RT for the U-shaped building layout**

With source-receiver distance and frequency, RT20 for the U-shaped building layouts is evaluated in Figure 8.11. The measurement zones with the U-shaped building layout are Z1-1, Z2-1, Z2-2 and Z4-1. In Figure 8.11(a) showing RT20 at 500 Hz, it can be seen that increasing source-receiver distance plays an important role in increasing RT20, especially at near field from a sound source. The regression curves show that RT20 is increased with the increasing source-receiver distance logarithmically. It is also shown that there is a difference in RT20 according to each measurement zone. In particular, RT20 for Z2-2 is relatively short by 1.4 sec at around 20 m in comparison with Z1-1 due to different sizes of the outdoor spaces. It can also be seen that RT20 can be increased to 3.2 sec. It is noted that the gradient of the 4 regression curves is similar to each other, especially from above 10 m.

In Figure 8.11(b), showing RT20 at the source-receiver distance of 20 m, RT20 for Z1-1 and Z4-1 is relatively long at most of frequencies in comparison with that for Z2-1 and Z2-2. It can be seen that RT20 at mid frequency (500 Hz and 1000 Hz) has relatively high values in comparison with low and high frequencies. This implies that RT20 at mid frequencies can play an important role in determining reverberance in the outdoor spaces with the U-shaped building layout.

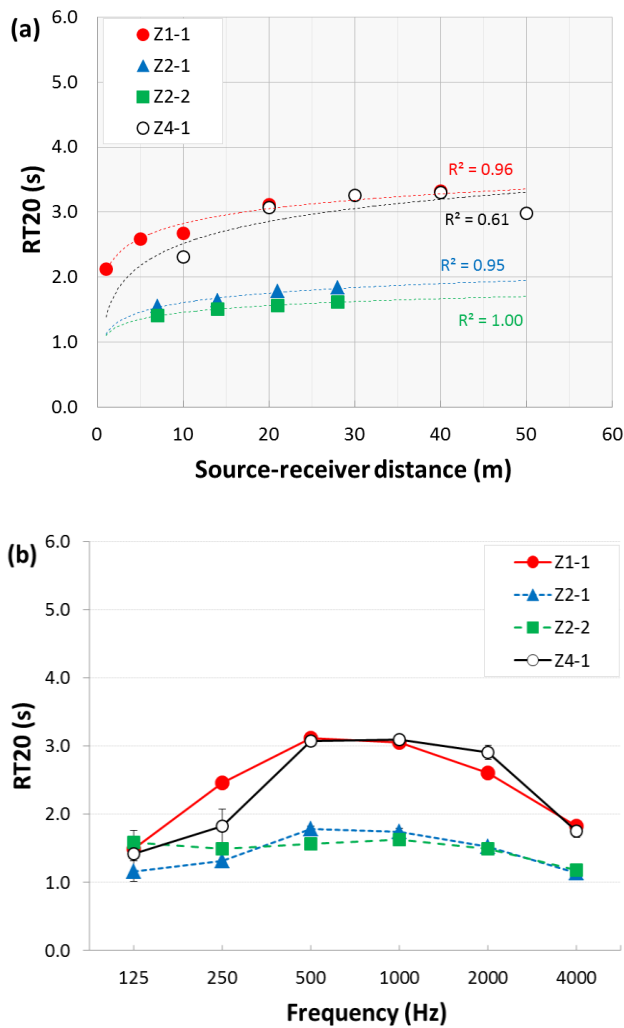


Fig. 8.11 RT20 for the U-shaped building layout: (a) RT20 at 500 Hz with different source-receiver distances; (b) RT20 with frequency at the source-receiver distance with 20 m

### 8.3.6 RT for the □-shaped building layout

RT20 for the 3 measurement zones with the □-shaped building layout is studied here with source-receiver distance and frequency. The 3 measurement zones are Z1-2, Z1-4 and Z3-1. In Figure 8.12(a), RT20 at 500 Hz is shown with different source-receiver distances. The result shows that RT20 is increased with the increasing source-receiver distance logarithmically for the 3 measurement zones. The difference in RT20 between Z1-2 and Z3-1 is found to be 2.2 sec at the source-receiver distance of 5 m. It is shown

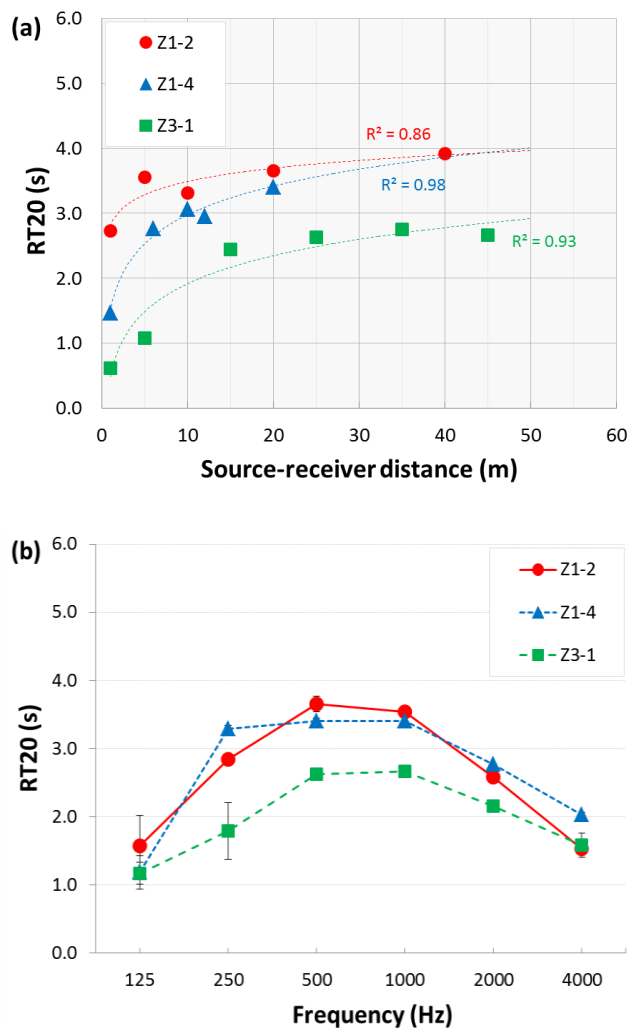


Fig. 8.12 RT20 for the □-shaped building layout: (a) RT20 at 500 Hz with different source-receiver distances; (b) RT20 with frequency at the source-receiver distance with 20 m

that the gradient of the regression curves is similar each other, especially from above 10

m. The maximum RT20 in Figure 8.12(a) is about 4 sec for Z1-2 indicating a very reverberant sound field.

Figure 8.12(b) shows that RT20 at mid frequency is relatively long in comparison with that at low and high frequencies. It can be seen that the graphs for the 3 measurement zones have a similar tendency with a shape of bell.

#### **8.4 Empirical method to estimate RT**

In the last few decades, acoustic simulation programmes have been developed to predict sound field using different numerical methods. To use acoustic simulation programmes, however, architects need to learn some special techniques and knowledge on acoustics. Therefore, it could be useful for architects to predict RT in outdoor spaces of apartment complexes as simple as possible using AutoCAD during the design process. In this section, a method of how to predict RT approximately in outdoor spaces is proposed by combining AutoCAD and empirical methods based on the experimental data.

It is well known from Sabine's equation that absorption power and volume of a space play an important role in determining RT. In comparison with enclosed spaces, outdoor spaces have different sound fields mainly due to open ceiling and gaps between buildings, which can be treated as boundaries with the absorption coefficient of 1.0. Generally, apartment buildings consist of concrete walls and windows with acoustically flat and reflective surface. Therefore, it is expected that openness of an outdoor space is an important factor determining RT. In terms of volume, the size of an outdoor space as well as the building height can have an influence on RT. To evaluate the openness and size-related parameter of an outdoor space, in this chapter, a ray-tracing technique is

applied by drawing 360 rays (1 degree between rays) emitted from a sound source, which can be easily drawn on AutoCAD. The openness of an outdoor space is calculated by the percentage of the effective rays reached on building façades for the 360 rays. Averaged ray length for the effective ray is also used to evaluate the size of outdoor spaces. Therefore, the openness and averaged ray length can be calculated by Eq. 8.1 and Eq. 8.2. Figure 8.13 shows the example of the method for drawing effective rays at Z1-1. Table 8.3 describes the openness, and averaged ray length and building height for each measurement zone.

$$\text{Openness} = \frac{n}{360} \times 100(\%) \quad \text{Eq. 8.1}$$

$$\text{Averaged ray length} = \frac{\sum_{i=1}^n L_i}{n} \text{ (m)} \quad \text{Eq. 8.2}$$

where, n: Number of the effective rays

L: Length of the effective ray (m)

In Figure 8.14, the relationship of RT20 with openness and averaged ray length is shown. RT20 in Figure 8.14 is the value measured at the source-receiver distance of around 20 m at which RT20 is insignificantly changed with increasing source-receiver distance. The regression curve in Figure 8.14(a) shows that RT20 is decreased with the increasing openness. On the other hand, it can be seen that RT20 is increased with the increasing averaged ray length. Although both regression curves show the effect of openness and averaged ray length on RT20 reasonably, the correlation coefficients are relatively low less than 0.16.



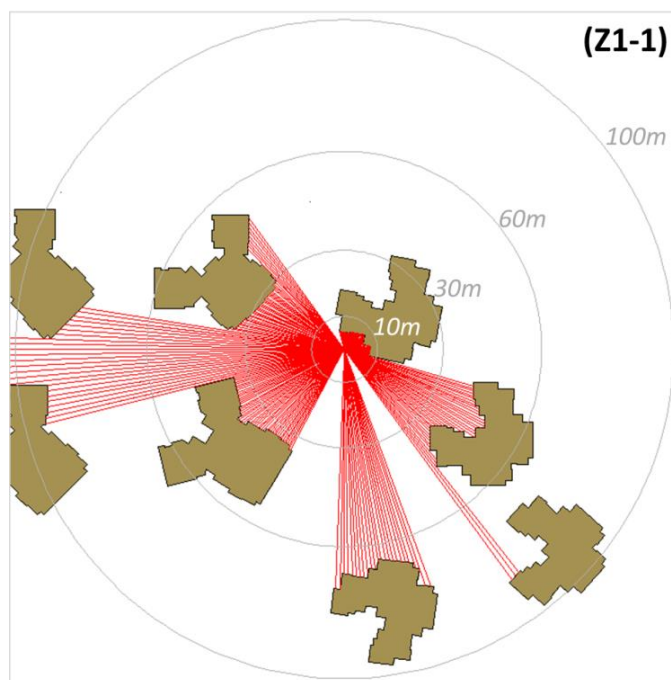


Fig. 8.13 Example of the calculation method for effective ray and openness at Z1-1

Table 8.3 Openness, averaged ray length and building height for each measurement zone

Measurement zone	Openness (%)	Averaged ray length (m)	Averaged building height (m)
Z1-1	23.1	39.2	39
Z1-2	9.7	37.4	39
Z1-3	42.2	44.8	39
Z1-4	6.9	35.2	39
Z2-1	2.2	16.1	21
Z2-2	0.0	13.8	12
Z2-3	38.3	39.7	12
Z3-1	3.1	23.6	36
Z4-1	34.2	51.6	63
Z4-2	5.6	39.4	70
Z4-3	21.1	54.8	45
Z5-1	29.7	32.0	42
Z5-2	29.7	58.7	42
Z6-1	35.0	34.3	41
Z6-2	50.6	22.8	45

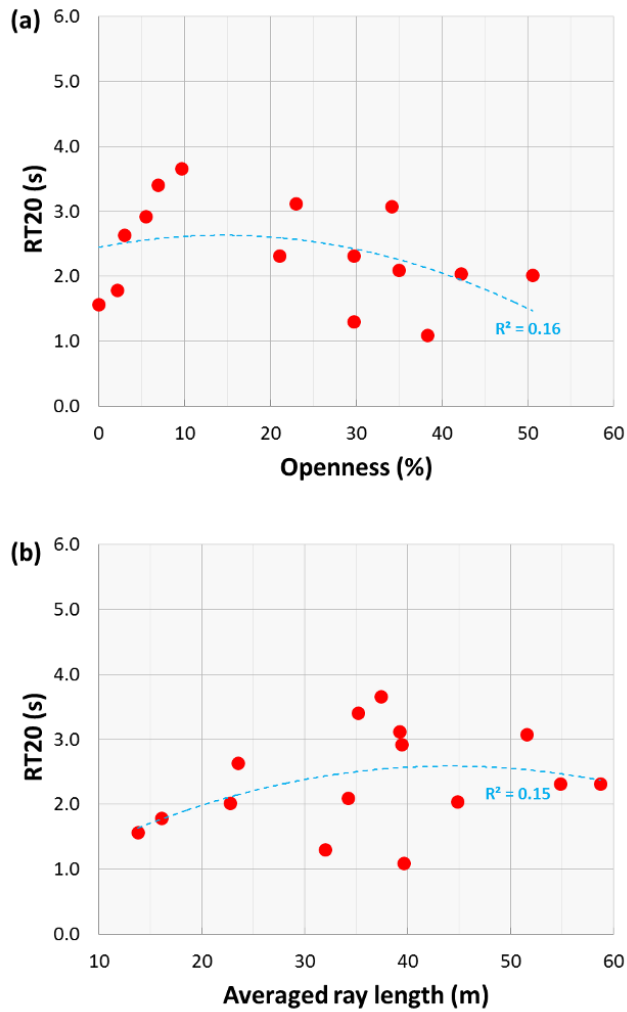


Fig. 8.14 Relationship of RT20 with openness and averaged ray length

To improve the correlation coefficient between RT20 and parameters, weighted ray length and area are introduced, which can be calculated using Eq. 8.3 and Eq. 8.4 below. The weighted ray length is the parameter considering openness and averaged ray length. On the other hand, the weighted area is the parameter considering openness, averaged ray length and averaged building height. In Figure 8.15, the relationship of RT20 with the weighted ray length and area is shown.

$$\text{Weighted ray length} = \frac{(100 - \text{Openness})}{100} \times \text{Averaged ray length (m)} \quad \text{Eq. 8.3}$$

$$\text{Weighted area} = \frac{(100 - \text{Openness})}{100} \times \text{Averaged ray length} \times \text{Averaged building height (m}^2\text{)} \quad \text{Eq. 8.4}$$

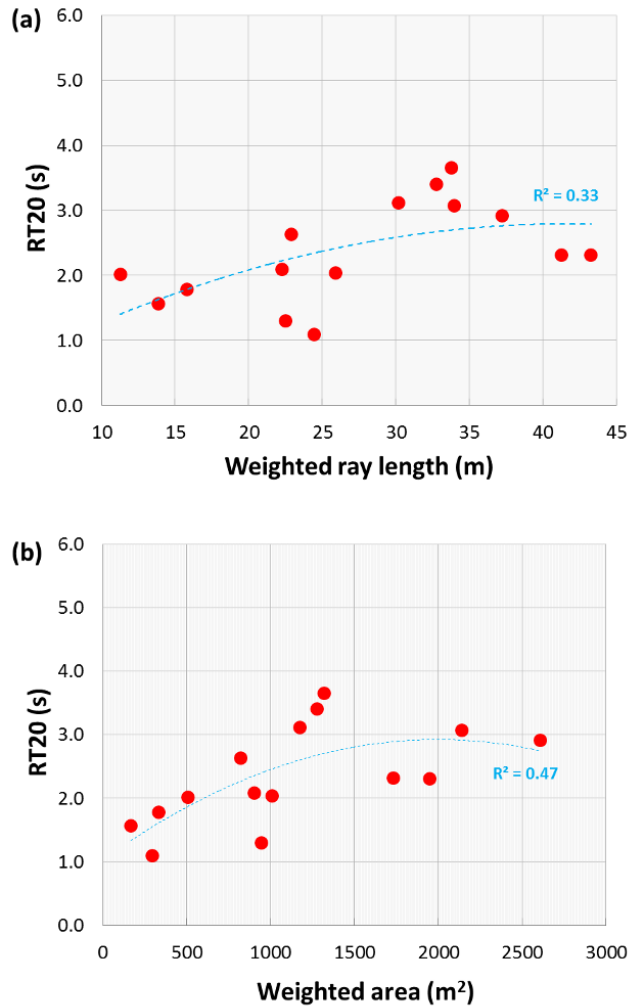


Fig. 8.15 Relationship of RT20 with the weighted ray length and area

In Figure 8.15(a), it can be seen that the correlation coefficient for the weighted ray length is improved to 0.33. The correlation coefficient for the weighted area has a relatively high value with 0.47 in comparison with other parameters. Table 8.4 describes the empirical formula of the regression curve as well as the correlation coefficient for each parameter. Therefore, RT20 at the source-receiver distance with 20 m can be predicted approximately using the empirical formula.

Table 8.4 Empirical formula and correlation coefficient for each parameter

Parameter	Empirical formula	Correlation coefficient ( $R^2$ )
Openness (%)	$y = -0.0009x^2 + 0.0259x + 2.4441$	0.16
Averaged ray length (m)	$y = -0.0010x^2 + 0.0914x + 0.5706$	0.15
Weighted ray length (m)	$y = -0.0015x^2 + 0.1242x + 0.1921$	0.33
Weighted area (m <sup>2</sup> )	$y = -0.0000x^2 + 0.0019x + 1.0315$	0.47

From the empirical formula for the weighted area in Table 8.4, RT20 at the source-receiver distance of 20 m can be approximated. As shown in Figure 8.8(a), 8.9(a), 8.10(a), 8.11(a) and 8.12(a), RT20 is generally increased with the increasing source-receiver distance logarithmically. Therefore, RT20 at different source-receiver distances can be predicted empirically if two factors (gradient of logarithmic curve and RT20 at the source-receiver distance with 20 m) are known. In Table 8.5, the formula for the regression curves in Figure 8.8(a), 8.9(a), 8.10(a), 8.11(a) and 8.12(a) are given to obtain the gradient for each measurement zone. The gradients are also averaged with the same building layouts. The averaged gradient for the 15 measurement zone is also calculated. By selecting the suitable gradient considering building layouts, RT20 can be predicted approximately according to source-receiver distance easily. For example, RT20 at the source-receiver distance of 5 m for the □-shaped building layout can be predicted approximately by the 5 steps below;

1. Calculate the weighted area using AutoCAD
2. Calculate RT20 at a source-receiver distance with 20 m using the empirical formula in Table 8.4:  $y = -0.0000x^2 + 0.0019x + 1.0315$  (x: weighted area, y: RT20)
3. Select the gradient for the courtyard building layout in Table 8.5:  
 $y=0.5189\ln(x)+a$  (x: source-receiver distance, y: RT20, a: constant)

4. Calculate constant  $a$  using RT20 calculated from Step 2
5. Calculate RT20 at the source-receiver distance at 5 m ( $x=5$  in Step 3)

Although the proposed empirical method to predict RT20 approximately in outdoor spaces of apartment complexes has a limitation in terms of accuracy, this simple calculation method could provide a useful tool for architects to presume in the design stage about how much the outdoor space is reverberant. Moreover, this method would be able to valid for similar conditions to one studied here.

Table 8.5 Empirical formula for RT20 in outdoor spaces of apartment complexes

Building layout	Measurement zone	Empirical formula	Correlation coefficient ( $R^2$ )	Averaged gradient	
				Each type	Total
-	Z1-3	$y = 0.2427\ln(x) + 1.3409$	0.92	0.2809ln(x)	0.4048ln(x)
	Z6-2	$y = 0.3191\ln(x) + 0.8197$	0.75		
=	Z2-3	$y = 0.5008\ln(x) + 0.6059$	0.98	0.3068ln(x)	
	Z4-3	$y = 0.2360\ln(x) + 1.4697$	0.55		
	Z6-1	$y = 0.1835\ln(x) + 0.5109$	0.94		
L	Z4-2	$y = 1.0608\ln(x) - 0.1002$	0.94	0.6219ln(x)	
	Z5-1	$y = 0.1829\ln(x) + 0.8381$	0.51		
U	Z1-1	$y = 0.3283\ln(x) + 2.0695$	0.96	0.2955ln(x)	
	Z2-1	$y = 0.2107\ln(x) + 1.1235$	0.95		
	Z2-2	$y = 0.1523\ln(x) + 1.1074$	1.00		
	Z4-1	$y = 0.4906\ln(x) + 1.3870$	0.61		
□	Z1-2	$y = 0.2948\ln(x) + 2.8101$	0.86	0.5189ln(x)	
	Z1-4	$y = 0.6397\ln(x) + 1.5017$	0.98		
	Z3-1	$y = 0.6221\ln(x) + 0.4834$	0.93		

### 8.5 Vegetation in the outdoor spaces

To predict the effect of vegetation in reducing RT20 in an outdoor space, the computer simulation programme, ODEON v.11.23, is used. It is assumed that green walls are placed on the whole surface of building façades, except for windows. Absorption coefficient of the green wall is the value measured in Chapter 3. The absorption and scattering coefficients of building materials such as concrete and glass were selected within the ranges given in the programme. Figure 8.16 illustrates the computer model for the apartment complex studied in Chapter 7. As shown in Figure 8.17, prediction of RT20 is carried out for the receivers within 120 m of the source, S1.



Fig. 8.16 Computer model for the apartment complex studied in Chapter 7



Fig. 8.17 Points of source and receivers

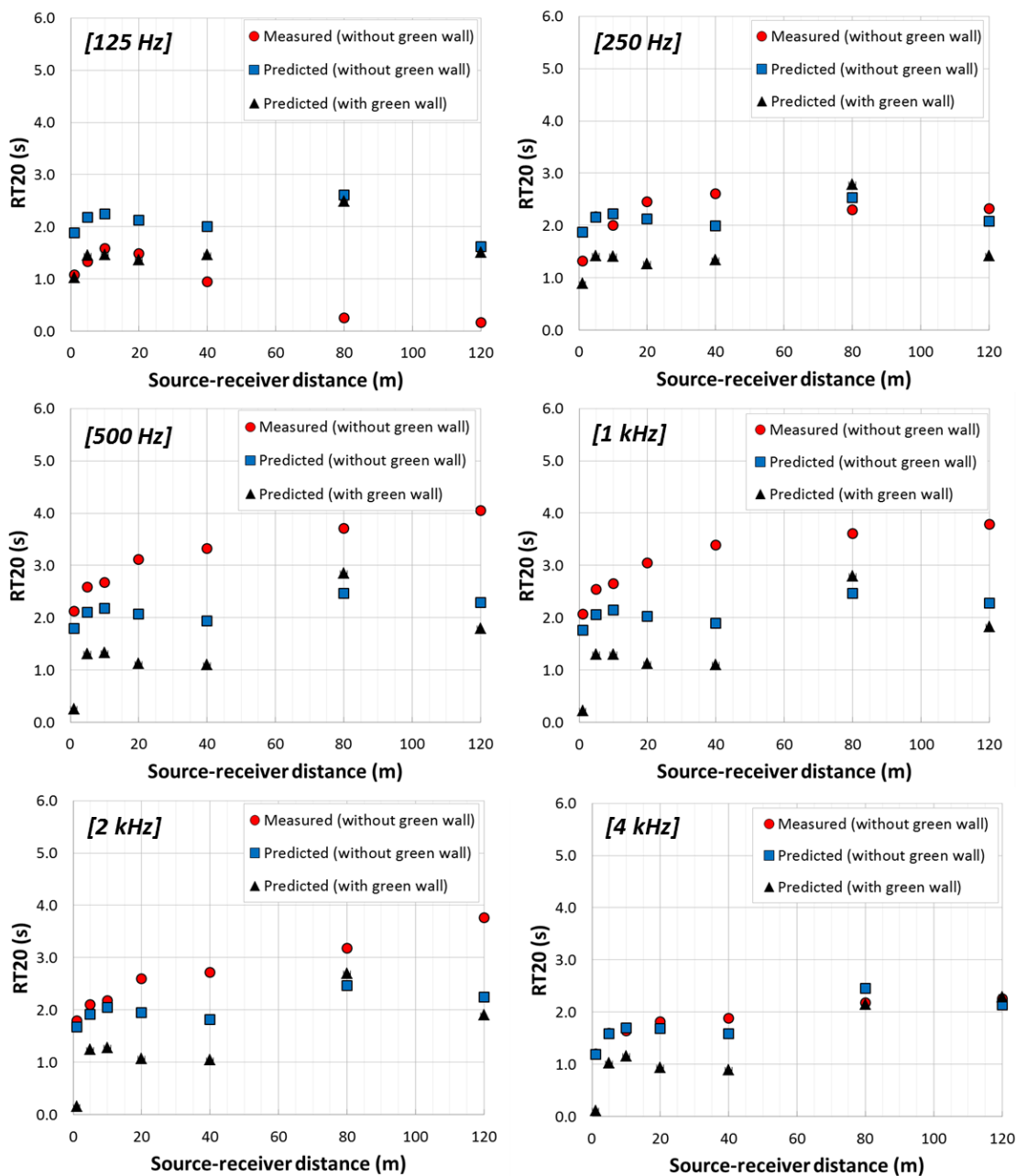


Fig. 8.18 Measured (without green wall) and predicted (with and without green wall) results at 125 Hz to 4 kHz in octave bands

Figure 8.18 shows the measured (without green wall) and predicted (with and without green wall) results at 125 Hz to 4 kHz in octave bands. It can be seen that in comparison with the measured value, the predicted value is rather inaccurate with discrepancies over 5 % (Bork, 2000), except at 4 kHz. This is due to inaccuracies in modelling of the

apartment complex, indicating further work on the modelling calibration. The predicted results show that façades with green walls are effective in reducing RT20 at relatively close distances from the source, say within 40 m. At 500 Hz, the maximum difference in RT20 between building façades with and without green wall is 0.95 sec, which is a 46 % decrease in sound energy. Although this initial work showed the effectiveness of vegetation in reducing RT20, further work will be carried out to investigate the effect of vegetation in reducing noise level and RT systematically, by considering different landscape schemes at various apartment complexes with different building layouts, openness, building heights, etc.

## **8.6 Summary**

In this chapter, a series of field measurements for RT20 were carried out for the 15 outdoor spaces in 6 apartment complexes, which were determined by considering different building layouts, blocks, sizes and height for a parametric study. The result for the overall characteristics and distribution of RT20 indicated that RT20 is influenced by source-receiver distance, building layout and sizes. It was also demonstrated that, generally, RT20 at mid frequency (500 Hz and 1000 Hz) is relatively long in comparison with that at low and high frequencies. The overall averaged RT20 for the maximum value in the outdoor spaces was 2.7 sec at 1000 Hz, which shows the outdoor spaces have a reverberant sound field. With increasing source-receiver distance, RT20 is generally increased logarithmically. It was also found that RT20 is rapidly changed at near field from a sound source due to the strong effect of direct sound. On the other hand, there is an insignificant change in RT20 above a certain source-receiver distance, say about 15 m.



For the studied cases, RT20 for the linear-shaped building layout is increased with the increasing source-receiver distance to about 2 sec at 500 Hz. In case of the parallel-shaped building layout, RT20 is strongly influenced by the width between parallel buildings, which causes the difference in RT20 of 1 sec. Maximum RT20 at 500 Hz for the parallel building layout was 2.4 sec. The result for the L-shaped building layout suggested that RT20 can be changed with different surrounding building conditions by 1.6 sec. Maximum RT20 for the studied L-shaped building layout is about 3 sec. For the U-shaped building layout, RT20 was changed by 1.4 sec with different sizes of the measurement zones. It was also shown that RT20 can be increased to 3.2 sec. It was found that RT20 at 500 Hz was about 4 sec at maximum for the □-shaped building layout.

The results suggest that an empirical method considering openness, averaged ray length and building height can be used to predict RT20 approximately in the outdoor spaces, which enables architects to presume RT20 during the design process.

As for the vegetation effect in reducing RT20, it was seen that building façades with green wall can reduce RT20 at 500 Hz by 0.95 sec (46 % decrease) compared to that without green wall.

Although RT20 is a useful index to examine the influence of surrounding geometries on sound field, it is still necessary to carry out more systematic studies on acoustic parameters for evaluating acoustic comfort in urban situations based on subjective evaluation. The importance of this future work is discussed in Chapter 9.

## **9 Conclusions and Future Work**

This thesis studied the effects of natural and sustainable materials including vegetation, green roof systems and green walls on noise reduction and sound field control in urban spaces. The concept of this study started with a hypothesis that well-planned use of natural materials can provide useful reductions in noise levels and reverberation in urban spaces.

For a better understanding of the interaction between sound waves and vegetation/trees, this study investigated the acoustic properties of low-growing vegetation and a single tree. Application of green roof systems on a low barrier was implemented to examine the effect of a vegetated low barrier on noise reduction at street level. Through a case study, a practical method for noise control by using vegetation in a courtyard was also suggested. Measurement results for outdoor sound propagation in high-rise residential buildings were presented. Use of vegetation for outdoor noise control in apartment complexes was also investigated. In the following sections, key findings of each research topic are addressed. Limitations and worthwhile future works are also discussed.

### **9.1 Contributions of the thesis**

#### **9.1.1 Examination on the acoustic properties of vegetation**

Sound absorbing and scattering properties of vegetation become more important as it is increasingly grown on building façades and the ground in urban spaces. Vegetation consists of mainly two components including the growing media (soil) and the plant (leaf, stem and root), which play different roles in absorbing and scattering sound.

Therefore, it is necessary to characterise systematically how each or combined components become effective.

In Chapter 3, a series of measurements were carried out in a reverberation chamber to examine random-incidence absorption and scattering coefficients of vegetation, by considering various factors such as soil depth, soil moisture content and the level of vegetation coverage.

The results for different soil depths (50, 100, 150, 200 mm) showed that even the thin soil layer with a depth of 50 mm provided a absorption coefficient of about 0.9 at around 1 kHz and there were only slight changes of absorption coefficient of about 0.1 with increased soil depth. A decrease in absorption coefficient by about 0.6 was observed with the increase in soil moisture content. With increasing vegetation coverage, the absorption coefficient increased by about 0.2 at low and mid frequencies, whereas over about 2 kHz the absorption coefficient was slightly decreased by about 0.1. It was shown that the stronger effect on sound absorption and scattering by aboveground vegetation components (excluding roots and soil) was found at higher frequencies with increasing vegetation coverage. The maximum absorption and scattering coefficients of aboveground vegetation studied here were 0.49 at 5 kHz and 0.43 at 2.5 kHz, respectively. It was also found that a green wall with highly porous substrate kept a relatively high absorption coefficient of about 0.6 even though it was nearly saturated.

The overall results indicate that vegetation can be used as an effective measure for absorbing/scattering sound energy propagating through urban areas. Thus, it is expected that well-planned use of vegetation will reduce noise levels and RT in urban spaces.

### **9.1.2 Quantification of scattered sound energy from a tree**

In urban spaces surrounded by buildings, trees may be effective in dispersing sound energy, and this could affect sound level distribution and street canyon reverberation. To quantify this effect of trees and to allow it to be included in numerical predictions, Chapter 4 examined sound scattered from a single tree in open field by means of RT. Five trees of different species and crown sizes were considered. The influence of ground condition, receiver height, crown size and shape, foliage condition, and source-receiver angle and distance has been assessed.

The results showed that RT is proportional to the tree size, which is the most determining factor. The maximum RT measured was 0.26 sec at 4 KHz for the studied trees when they were in leaf. The presence of leaves increased RT at high frequencies, typically by 0.08 sec at 4 kHz. It was also demonstrated that the source-receiver angle can affect the characteristics of decay curves. With increasing source-receiver distance within 40 m, RT was slightly changed. It was shown that ground condition and receiver height affect the decay curves, especially at low and mid frequencies, where scattering is of relatively limited importance.

The overall results indicate that trees can play an important role in outdoor sound propagation in urban spaces, especially at high frequencies and with large trees. Based on the measured data, it is expected that downward scattering from trees can increase sound levels at ground level in urban street canyons, especially at high frequencies.

### **9.1.3 Examination of potential use of green roof systems on a low barrier**

Green roof systems have become commonly used in urban spaces due to numerous

ecological and environmental benefits. Various kinds of green roof systems can also be used at street level, on the top of underground car parks for example. In this situation, it is important to systematically examine the acoustic effects of designable parameters, especially for diffracted sound waves.

In Chapter 5, therefore, a series of measurements were carried out in a semi-anechoic chamber using green roof systems consisting of Zinco and limestone-based substrates. They were placed on a box with a height of 1200 mm. Numerical simulations were also carried out for selected cases. Studied parameters included the area, depth, type and position of the green roof system, and the type of vegetation.

The results showed that such green roof systems can reduce SPL effectively at the receiver side of the boxes. Within the ranges of the parameters considered, the effect of the depth and type of substrates is relatively small compared to that of the overall configurations of the system. By adding pruned leaves on the green roof there is only a small noise reduction above 4 kHz but optimised absorption treatment could bring up to 4 dBA noise reduction for traffic noise. The position of the green roof system affects the pattern of SPL reduction differently at different frequency ranges.

#### **9.1.4 Verification on noise reduction effects of vegetation in a courtyard**

Courtyards surrounded by buildings often have acoustic defects such as strong flutter echoes and long RT that can increase noise annoyance. Therefore, it is important to absorb and diffuse sound energy propagating such places.

Chapter 6 investigated how applicable landscape designs can contribute to controlling sound fields in a courtyard. Through a case study, differences between courtyard sound

fields were examined by in-situ measurements before and after applying a practical landscape design using vegetation, wood decking and street furniture. In addition, computer simulations were carried out to explore the acoustic effects of applicable landscape designs using vegetation including climbing Ivy, green wall, grass and bedding plants.

The results for the in-situ measurements showed reductions in sound levels and RT at 500 Hz of 3.1 dB and 40 % (1.0 sec), respectively. The results for the computer simulation showed that the green wall on the façade can reduce speech levels and RT at 500 Hz by 9.3 dBA and 81 % (2.1 sec), respectively. The bedding plants on the ground decreased the speech level by 2.2 dBA and increased RT at 500 Hz by 12 % (0.3 sec). At different floor levels in the accommodation building, the speech level and RT at 500 Hz were decreased by the vegetation by up to 5.5 dBA and 66 % (1.1 sec), respectively.

Results highlight that landscape designs using vegetation in courtyards can provide acoustic benefits such as reductions in sound levels and RT. Thus, it is expected that overall residential environments could be improved in terms of noise reduction with the help of effective landscape designs.

#### **9.1.5 Investigation of sound propagation in high-rise apartment complexes**

Many apartment complexes in Korea feature underground car parks thus releasing more of the landscape for residents' leisure, rest, or socialising. The acoustic characteristics of these outdoor spaces can therefore make a contribution to the overall quality of the environment.

Experimental study in Chapter 7 investigated the acoustic characteristics of outdoor

spaces surrounded by multi-storey apartment buildings. In-situ measurements in three positions were carried out to evaluate the acoustic parameters, including RT, EDT, RASTI and SPL distribution.

The results showed that RT was generally rather long, over 4 sec at 500 Hz. On the other hand, RT at 125 Hz and 250 Hz was relatively short, about 0 to 3 sec. Above 500 Hz, RT increased with increasing source-receiver distance. EDT was longer than RT over a certain source-receiver distance at about 40 m. In terms of sound distribution, measured SPL was up to 8 dB higher compared to the semi-free field situation, indicating the effects of multiple reflections. The above results imply that sound fields in outdoor spaces surrounded by high-rise residential buildings need to be controlled by means of architectural treatments using sustainable acoustic absorbers and diffusers such as vegetation.

#### **9.1.6 Evaluation of parameters on reverberation in apartment complexes**

A comfortable sound environment in the outdoor spaces of apartment complexes contributes to the improvement of the overall environmental quality. It is expected that RT of outdoor spaces surrounded by multi-storey buildings depends on many designable factors such as the openness, volume and building layouts, vegetation, etc.

Chapter 8 therefore investigated the influential factors for RT in outdoor spaces surrounded by buildings with complicated topographical conditions. A series of measurements were carried out for 15 outdoor spaces in 6 apartment complexes with different building layouts. In particular, the effect of source-receiver distance on RT was also investigated for each site. The 15 outdoor spaces were categorised into 5 types as linear, parallel, L, U and courtyard building layouts.

The result showed that RT20 at 500 Hz and 1 kHz is relatively long compared to that at low and high frequencies. With increasing source-receiver distance, RT20 increases logarithmically. For the studied cases, the maximum RT20 at 500 Hz was about 4 sec. An empirical method considering the openness, averaged ray length and building height was also suggested, to predict RT20 approximately in outdoor spaces. It was also shown that vegetation in the apartment complex is effective in reducing RT20.

The overall results suggest that RT in outdoor spaces of apartment complexes is influenced by source-receiver distance, building layouts and vegetation. Based on the empirical method considering openness, averaged ray length and building height, it would be possible to predict RT approximately in the outdoor spaces, which enables architects to presume RT during the design process.

## **9.2 Future work**

### **9.2.1 Prediction of random-incidence absorption and scattering coefficients**

While a series of measurements have been carried out in Chapter 3, it is still necessary to be able to determine random-incidence absorption and scattering coefficients of vegetation using methods which are simpler and quicker than direct measurement in a reverberation chamber using relatively large specimens.

Previous studies suggested that normal-incidence absorption coefficients can be converted to a random-incidence absorption coefficient approximately using theoretical models (Makita *et al.*, 1988). Thus, prediction methods based on normal-incidence absorption coefficients of vegetation need to be modelled to characterise various factors affecting random-incidence absorption coefficients.



Recently, a method based on FDTD has been proposed for predicting the random-incidence scattering coefficient, which could also be applied for predicting the scattering coefficient of vegetation (Redondo *et al.*, 2009; Redondo *et al.*, 2007). By using the prediction method, various factors affecting the scattering coefficient of vegetation could be clarified.

### **9.2.2 Numerical modelling of scattering of sound by trees**

Although many field measurements have been carried out in Chapter 4, further work is still needed to characterise the effect of factors such as leaf size, leaf shape and thickness, but also the distribution of biomass over the crown. Numerical modelling of scattering of sound by trees, as well as scale modelling could further clarify the physical phenomena involved, and allow evaluation of potential applications.

### **9.2.3 Noise reduction by vegetated low barriers in real urban situations**

As experiments were carried out in a semi-anechoic chamber with a point source located near the barrier, it does not simulate real urban situations. It would therefore be useful, in future work, to study the effects of green roof systems on noise reduction more systematically, by taking real urban situations into account.

### **9.2.4 Practical landscape designs in a courtyard**

To further advance the research, it is necessary to consider various factors of landscape designs affecting the sound field in courtyards. Previous studies showed that sound absorption distribution and boundary conditions have an influence on sound attenuation and RT in street canyons and urban squares (Kang, 2000, 2001, 2005). With a given amount of vegetation, therefore, there is a need to suggest a method to determine cost-

effective landscape design schemes according to different boundary conditions.

Acoustic properties of vegetation are influenced by many factors such as substrate type, composition, depth and moisture content as well as the species and coverage of plants (Horoshenkov *et al.*, 2006; Horoshenkov *et al.*, 2011; Yang *et al.*, 2013). Therefore, a systematic study is necessary to clarify the effects of these factors individually on sound field control.

At different floors of adjacent buildings, noise reduction by landscape designs could be influenced by meteorological factors dependent on local statistics for wind speed, wind direction and temperature gradients (Blumrich *et al.*, 2002; Van Renterghem *et al.*, 2005). This suggests the need further studies on sound attenuation by landscape designs according to different meteorological conditions.

It is expected that vegetation is also effective in controlling the sound fields of enclosed reverberant spaces such as lobbies, atriums, underground stations and shopping malls. Therefore, vegetation may also be useful if it is installed in such indoor spaces to improve speech transmission index and speech privacy (Kang, 1996a, 1998; Rindel, 2010).

### **9.2.5 Application of vegetation in outdoor spaces of apartment complexes**

Although the initial work has been started, it is important to examine the effect of vegetation on noise reduction and reverberation in different types of apartment complexes. Based on the measured data in Chapter 7 and Chapter 8, the sound field can be predicted and calibrated through computer simulation programmes. As the size of the model is relatively large, programmes based on ray-tracing or radiosity methods are

suitable for predicting SPL distribution and RT. It is also expected that noise mapping programmes can also be used for predicting sound propagation in outdoor spaces, as well as examining the acoustic effects of vegetation.

### **9.2.6 Acoustic parameters for evaluating acoustic comfort in urban situations**

In contrast to the study on sound quality in concert halls and classrooms, little has been attempted to examine acoustic parameters for designing urban spaces where the pattern of arrival of reflected sound is different, in comparison with the enclosed spaces.

As stated in Chapter 7 and 8, sound environments in outdoor spaces of residential areas play an important role in improving overall life quality. Therefore, it is useful to examine the relationship of various acoustic parameters with noise annoyance of residents.

Although sound attenuation and RT have been used to characterise sound fields in urban spaces, it is still needed to investigate the relationship of spatial impression and noise annoyance with various acoustic parameters related to energy (i.e., G-strength, D50, C80 and  $T_s$ ), reverberation (i.e., EDT and RT) and binaural response (i.e., apparent source width ASW, listener envelopment LEV and IACC) in urban situations. Based on the subjective evaluation, it is expected that suitable acoustic parameters as well as acoustic targets can be recommended to design comfortable sound environments in outdoor spaces of urban areas.

## REFERENCES

- Albert, D. G., & Liu, L. (2010). The effect of buildings on acoustic pulse propagation in an urban environment. *Journal of the Acoustical Society of America*, 127(3), 1335-1346.
- Alexandri, E., & Jones, P. (2008). Temperature decreases in an urban canyon due to green walls and green roofs in diverse climates. *Building and Environment*, 43(4), 480-493.
- Attenborough, K. (1988). Review of ground effects on outdoor sound propagation from continuous broadband sources. *Applied Acoustics*, 24(4), 289-319.
- Attenborough, K., Li, K. M., & Horoshenkov, K. (2007). *Predicting outdoor sound*: Taylor & Francis.
- Aylor, D. (1972). Sound Transmission through Vegetation in Relation to Leaf Area Density, Leaf Width, and Breadth of Canopy. *Journal of the Acoustical Society of America*, 51(1B), 411-414.
- Aylor, D., Parlange, J. Y., & Chapman, C. (1973). Reverberation in a city street. *Journal of the Acoustical Society of America*, 54(6), 1754-1757.
- B&K. (2010). DIRAC v5. User's manual
- Baik, H. S. (2003). *Creating outdoor space for everyday life in multi-family housing estate*. Doctoral thesis Doctoral thesis, Yonsei University.
- Ball, L. M. (1942). Air Raid Siren Field Tests. *Journal of the Acoustical Society of America*, 14(1), 10-13.
- Baulac, M., Defrance, J., & Jean, P. (2005). *Optimization of low height noise protections in urban areas*. Paper presented at the Proceedings of Forum Acusticum 2005, Budapest, Hungary.
- Baulac, M., Guillou, A., Defrance, J., & Jean, P. A. (2008). *Calculations of low height noise barriers efficiency by using Boundary Element Method and optimisation algorithms*. Paper presented at the Acoustics 08, Paris, France.
- Benkreira, H., Horoshenkov, K., Khan, A., Mandon, A., & Rohr, R. (2011). *The effect of*

*drying on the acoustic absorption of novel green noise insulation*. Paper presented at the European Drying Conference - EuroDrying'2011, Spain.

Berglund, B., Lindvall, T., & Schwela, D. H. (1999). *Guidelines for Community Noise*. Geneva, Switzerland: World Health Organization.

Berglund, B., & Nilsson, M. E. (2006). On a Tool for Measuring Soundscape Quality in Urban Residential Areas. *Acta Acustica united with Acustica*, 92(6), 938-944.

Blumrich, R., & Heimann, D. (2002). A linearized Eulerian sound propagation model for studies of complex meteorological effects. *Journal of the Acoustical Society of America*, 112, 446-455.

Bork, I. (2000). A comparison of room simulation software-The 2nd round robin on room acoustical computer simulation. *Acta Acustica united with Acustica*, 86(6), 943-956.

Bradley, J. S. (1986). Predictors of speech intelligibility in rooms. *The Journal of the Acoustical Society of America*, 80(3), 837-845.

Burns, S. H. (1979). The absorption of sound by pine trees. *Journal of the Acoustical Society of America*, 65(3), 658-661.

Carles, J. L., Barrio, I. L., & de Lucio, J. V. (1999). Sound influence on landscape values. *Landscape and Urban Planning*, 43(4), 191-200.

Cheal, C., Yang, H., & Kang, J. (2011). *Experimental study on the effects of vegetation coverage and soil depth and water content on sound absorption*. Paper presented at the Proceedings of 6th European Acoustics Association - Forum Acusticum, Aalborg, Denmark.

Connelly, M. R. (2011). *Acoustical characteristics of vegetated roofs-contributions to the ecological performance of buildings and the urban soundscape*. University of British Columbia.

Cox, T. (2009). *Acoustic absorbers and diffusers: theory, design and application*: Taylor & Francis.

Davies, H. G. (1978). Multiple-reflection diffuse-scattering model for noise propagation in streets. *Journal of the Acoustical Society of America*, 64, 517-521

## References

---

Davies, W., Mahnken, P. Z., Gamble, P., & Plack, C. (2009). *Measuring and mapping soundscape speech intelligibility*. Paper presented at the Proceedings of Euronoise 2009, Edinburgh, U.K.

Delany, M., Rennie, A., & Collins, K. (1972). Scale model investigation of traffic noise propagation (Vol. Acoustics Report Ac 58). Teddington (UK): National Physical Laboratory.

Ding, L., Van Renterghem, T., & Botteldooren, D. (2010). *Measurement methodology for the acoustic scattering of a single tree*. Paper presented at the Proceedings of the 20th international congress on acoustics - ICA 2010, Sydney, Australia.

Dunnett, N., & Kingsbury, N. (2004). *Planting green roofs and living walls*: Timber Press Portland, OR, USA.

Embleton, T. F. W. (1963). Sound propagation in homogeneous deciduous and evergreen woods. *Journal of the Acoustical Society of America*, 35(8), 1119-1125.

Ettouney, S. M., & Fricke, F. R. (1973). Courtyard acoustics. *Applied Acoustics*, 6(2), 119-132.

Eyring, C. F. (1946). Jungle Acoustics. *Journal of the Acoustical Society of America*, 18(2), 257-270.

Fan, Y., Zhiyi, B., Zhujun, Z., & Jiani, L. (2010). The investigation of noise attenuation by plants and the corresponding noise-reducing spectrum. *Journal of Environmental Health*, 72(8), 8-15.

Fang, C.-F., & Ling, D.-L. (2003). Investigation of the noise reduction provided by tree belts. *Landscape and Urban Planning*, 63(4), 187-195.

Fioretti, R., Palla, A., Lanza, L., & Principi, P. (2010). Green roof energy and water related performance in the Mediterranean climate. *Building and Environment*, 45(8), 1890-1904.

Fricke, F. (1984). Sound attenuation in forests. *Journal of Sound and Vibration*, 92(1), 149-158.

Fritschi, L., Brown, L., Kim, R., Schwela, D., & Kephapopolous, S. (2011). Burden of Disease from Environmental Noise: Quantification of Healthy Life Years Lost in

Europe. Copenhagen, Denmark: WHO European Centre for Environment and Health.

Getter, K. L., & Rowe, D. B. (2006). The role of extensive green roofs in sustainable development. *HortScience*, *41*(5), 1276-1285.

Gidlöf-Gunnarsson, A., & Öhrström, E. (2007). Noise and well-being in urban residential environments: The potential role of perceived availability to nearby green areas. *Landscape and Urban Planning*, *83*(2-3), 115-126.

Gidlöf-Gunnarsson, A., & Öhrström, E. (2010). Attractive "quiet" courtyards: A potential modifier of urban residents' responses to road traffic noise? *International Journal of Environmental Research and Public Health*, *7*(9), 3359-3375.

Gregoire, B. G., & Clausen, J. C. (2011). Effect of a modular extensive green roof on stormwater runoff and water quality. *Ecological Engineering*, *37*(6), 963-969.

Haron, Z., Yahya, K., Zakaria, R., & Oldham, D. (2009). Modeling of sound propagation in urban streets containing trees using Markovian technique. *Malaysian Journal of Civil Engineering*, *21*(1), 55-68.

Heimann, D. (2003). Numerical Simulations of Wind and Sound Propagation Through an Idealised Stand of Trees. *Acta Acustica united with Acustica*, *89*(5), 779-788.

Hornikx, M., Botteldooren, D., Van Renterghem, T., & Forssén, J. (2011). *Modelling of scattering of sound from trees by the PSTD method*. Paper presented at the Proceedings of Forum Acusticum 2011, Aalborg, Denmark.

Hornikx, M., & Forssén, J. (2007). The 2.5-dimensional equivalent sources method for directly exposed and shielded urban canyons. *Journal of the Acoustical Society of America*, *122*, 2532-2541.

Hornikx, M., & Forssén, J. (2009). Noise abatement schemes for shielded canyons. *Applied Acoustics*, *70*(2), 267-283.

Horoshenkov, K. V., & Mohamed, M. H. A. (2006). Experimental investigation of the effects of water saturation on the acoustic admittance of sandy soils. *Journal of the Acoustical Society of America*, *120*, 1910-1921

Horoshenkov, V., Hothersall, C., & Mercy, E. (1999). Scale modelling of sound propagation in a city street canyon. *Journal of Sound and Vibration*, *223*(5), 795-819.

## References

---

- Horoshenkov, V. K., Khan, A., Benkreira, H., Mandon, A., & Rohr, R. (2011). Acoustic properties of green walls with and without vegetation. *Journal of the Acoustical Society of America*, *130*(4), 2317-2317.
- Huisman, W. H. T., & Attenborough, K. (1991). Reverberation and attenuation in a pine forest. *Journal of the Acoustical Society of America*, *90*, 2664-2677.
- IEC. (2003). IEC 60268-16: Sound system equipment-Part 16: Objective rating of speech intelligibility by speech transmission index: International Electrotechnical Commission.
- Ismail, M. R., & Oldham, D. J. (2005). A scale model investigation of sound reflection from building façades. *Applied Acoustics*, *66*(2), 123-147.
- ISO. (1993). ISO 9613-1: Acoustics-Attenuation of sound during propagation outdoors (Part 1: Calculation of the absorption of sound by the atmosphere). Genève, Switzerland: International Organization for Standardization.
- ISO. (1996). ISO 9613-2: Acoustics - Attenuation of sound during propagation outdoors (Part 2: General method of calculation). Genève, Switzerland: International Organization for Standardization.
- ISO. (2003). ISO 354: Acoustics-Measurement of sound absorption in a reverberation room. Genève, Switzerland: International Organization for Standardization.
- ISO. (2004). ISO 17497-1: Acoustics-Measurement of random-incidence scattering coefficient in a reverberation room.
- ISO. (2008). ISO 3382-2: Acoustics - Measurement of room acoustic parameters - Part 2: Reverberation time in ordinary rooms. Genève, Switzerland: International Organization for Standardization.
- Iu, K. K., & Li, K. M. (2002). The propagation of sound in narrow street canyons. *Journal of the Acoustical Society of America*, *112*(2), 537-550.
- Jeon, J., Lee, P., Hong, J., & Cabrera, D. (2011). Non-auditory factors affecting urban soundscape evaluation. *Journal of the Acoustical Society of America*, *130*(6), 3761-3770.
- Jim, C. Y. (2004). Green-space preservation and allocation for sustainable greening of



compact cities. *Cities*, 21(4), 311-320.

Jim, C. Y., & Chen, W. Y. (2006). Impacts of urban environmental elements on residential housing prices in Guangzhou (China). *Landscape and Urban Planning*, 78(4), 422-434.

Jones, R. C. (1946). A Fifty Horsepower Siren. *Journal of the Acoustical Society of America*, 18(2), 371-387.

Kang, J. (1988). Experiments on the subjective assessment of noise reduction by absorption treatments. *Chinese Noise and Vibration Control*, 5, 20-28.

Kang, J. (1996a). Improvement of the STI of multiple loudspeakers in long enclosures by architectural treatments. *Applied Acoustics*, 47(2), 129-148.

Kang, J. (1996b). Modelling of train noise in underground stations. *Journal of Sound and Vibration*, 195(2), 241-255.

Kang, J. (1996c). Sound attenuation in long enclosures. *Building and Environment*, 31(3), 245-253.

Kang, J. (1998). Scale modelling for improving the speech intelligibility from multiple loudspeakers in long enclosures by architectural acoustic treatments. *Acta Acustica united with Acustica*, 84(4), 689-700.

Kang, J. (2000). Sound propagation in street canyons: Comparison between diffusely and geometrically reflecting boundaries. *Journal of the Acoustical Society of America*, 107, 1394-1404

Kang, J. (2001). Sound propagation in interconnected urban streets: a parametric study. *Environment and Planning B*, 28(2), 281-294.

Kang, J. (2002a). *Acoustics of Long Spaces: theory and design guidance*: Thomas Telford.

Kang, J. (2002b). Numerical modelling of the sound fields in urban streets with diffusely reflecting boundaries. *Journal of Sound and Vibration*, 258(5), 793-813.

Kang, J. (2002c). Numerical modelling of the speech intelligibility in dining spaces. *Applied Acoustics*, 63(12), 1315-1333.

- Kang, J. (2002d). Reverberation in rectangular long enclosures with diffusely reflecting boundaries. *Acta Acustica united with Acustica*, 88(1), 77-87.
- Kang, J. (2005). Numerical modeling of the sound fields in urban squares. *Journal of the Acoustical Society of America*, 117, 3695-3706.
- Kang, J. (2007). *Urban sound environment*. London: Taylor and Fransis.
- Kang, J., Huang, H., & Sorrill, J. (2009). *Experimental study of the sound insulation of extensive green roofs*. Paper presented at the Proceedings of the 38th International Congress on Noise Control Engineering - Internoise 2009, Ottawa, Canada.
- Kang, J., & Zhang, M. (2010). Semantic differential analysis of the soundscape in urban open public spaces. *Building and Environment*, 45(1), 150-157.
- Kaye, G., & Evans, E. (1940). *The sound-absorbing properties of some common outdoor materials*. Paper presented at the Proceedings of the Physical Society.
- Kerber, G., & Makarewicz, R. (1981). An optical scale model of traffic noise propagation in an urban environment. *Applied Acoustics*, 14(5), 331-345.
- Ko, N. W. M., & Tang, C. P. (1978). Reverberation time in a high-rise city. *Journal of Sound and Vibration*, 56, 459-461.
- Kragh, J. (1981). Road traffic noise attenuation by belts of trees. *Journal of Sound and Vibration*, 74(2), 235-241.
- Kragh, J., Plovsing, B., Storeheier, S., Taraldsen, G., & Jonasson, H. (2002). Nordic Environmental Noise Prediction Methods, Nord2000 Summary Report. General Nordic Sound Propagation Model and Applications in Source-Related Prediction Methods. *Delta report, June*.
- Ksiazek, K., Fant, J., & Skogen, K. (2012). An assessment of pollen limitation on Chicago green roofs. *Landscape and Urban Planning*, 107(4), 401-408.
- Langdon, F. (1976). Noise nuisance caused by road traffic in residential areas: Part I. *Journal of Sound and Vibration*, 47(2), 243-263.
- Lee, K. P., & Davies, H. G. (1975). Nomogram for estimating noise propagation in urban areas. *Journal of the Acoustical Society of America*, 57(6), 1477-1480.

## References

---

- Lee, P. J., Kim, Y. H., Jeon, J. Y., & Song, K. D. (2007). Effects of apartment building façade and balcony design on the reduction of exterior noise. *Building and Environment*, 42(10), 3517-3528.
- Luttik, J. (2000). The value of trees, water and open space as reflected by house prices in the Netherlands. *Landscape and Urban Planning*, 48(3-4), 161-167.
- Lyon, R. H. (1974). Role of multiple reflections and reverberation in urban noise propagation. *Journal of the Acoustical Society of America*, 55, 493-503
- Lyon, R. H., Blair, C. N., & DeJong, R. G. (1977). *Evaluating effects of vegetation on the acoustical environment by physical scale-modeling*. Paper presented at the Proceedings of the conference on metropolitan physical environment.
- Makita, Y., & Hidaka, T. (1988). Comparison between Reverberant and Random Incident Sound Absorption Coefficients of a Homogeneous and Isotropic Sound Absorbing Porous Material Experimental Examination of the Validity of the Revised cos Law. *Acta Acustica united with Acustica*, 66(4), 214-220.
- Martínez-Sala, R., Rubio, C., García-Raffi, L. M., Sánchez-Pérez, J. V., Sánchez-Pérez, E. A., & Llinares, J. (2006). Control of noise by trees arranged like sonic crystals. *Journal of Sound and Vibration*, 291(1-2), 100-106.
- Martens, M. J. M. (1980). Foliage as a low-pass filter: Experiments with model forests in an anechoic chamber. *Journal of the Acoustical Society of America*, 67, 66-72.
- Martens, M. J. M., & Michelsen, A. (1981). Absorption of acoustic energy by plant leaves. *Journal of the Acoustical Society of America*, 69(1), 303-306.
- Martens, M. J. M., Severens, P. P. J., Van Wissen, H. A. W. M., & Van Der Heijden, L. A. M. (1985). Acoustic reflection characteristics of deciduous plant leaves. *Environmental and Experimental Botany*, 25(3), 285-292.
- Mentens, J., Raes, D., & Hermy, M. (2006). Green roofs as a tool for solving the rainwater runoff problem in the urbanized 21st century? *Landscape and Urban Planning*, 77(3), 217-226.
- Mijic, M., & Pavlovic, D. S. (2012). Measurement of reverberation gain in an urban environment. *Journal of the Acoustical Society of America*, 132(3), 1417-1426.

## References

---

- Mulholland, K. (1979). The prediction of traffic noise using a scale model. *Applied Acoustics*, 12(6), 459-478.
- Navrud, S. (2002). The state-of-the-art on economic valuation of noise: Final Report to the European Commission Directorate-General (DG) Environment.
- Nota, R., Barelds, R., & van Maercke, D. (2005). Harmonoise WP3 engineering method for road traffic and railway noise after validation and fine-tuning. *Deliverable of WP3 of the HARMONOISE project. Document ID HAR32TR-040922-DGMR20*.
- Öhrström, E., Skånberg, A., Svensson, H., & Gidlöf-Gunnarsson, A. (2006). Effects of road traffic noise and the benefit of access to quietness. *Journal of Sound and Vibration*, 295(1-2), 40-59.
- Oldham, D., & Mohsen, E. (1979). A model investigation of the acoustical performance of courtyard houses with respect to noise from road traffic. *Applied Acoustics*, 12(3), 215-230.
- Oldham, D. J., Egan, C. A., & Cookson, R. D. (2011). Sustainable acoustic absorbers from the biomass. *Applied Acoustics*, 72(6), 350-363.
- Onaga, H., & Rindel, J. H. (2007). Acoustic characteristics of urban streets in relation to scattering caused by building facades. *Applied Acoustics*, 68(3), 310-325.
- Padgham, M. (2004). Reverberation and frequency attenuation in forests—implications for acoustic communication in animals. *Journal of the Acoustical Society of America*, 115, 402-410.
- Pal, A. K., Kumar, V., & Saxena, N. C. (2000). Noise attenuation by green belts. *Journal of Sound and Vibration*, 234(1), 149-165.
- Picaut, J., Le Pollès, T., L'Hermite, P., & Gary, V. (2005). Experimental study of sound propagation in a street. *Applied Acoustics*, 66(2), 149-173.
- Picaut, J., & Simon, L. (2001). A scale model experiment for the study of sound propagation in urban areas. *Applied Acoustics*, 62(3), 327-340.
- Picaut, J., Simon, L., & Hardy, J. (1999). Sound field modeling in streets with a diffusion equation. *Journal of the Acoustical Society of America*, 106, 2638-2645

## References

---

Price, M. A., Attenborough, K., & Heap, N. W. (1988). Sound attenuation through trees: measurements and models. *Journal of the Acoustical Society of America*, 84, 1836-1844

Redondo, J., Pic, R., Avis, M. R., & Cox, T. J. (2009). Prediction of the Random-Incidence Scattering Coefficient Using a FDTD Scheme. *Acta Acustica united with Acustica*, 95(6), 1040-1047.

Redondo, J., Picó, R., Roig, B., & Avis, M. (2007). Time domain simulation of sound diffusers using finite-difference schemes. *Acta Acustica united with Acustica*, 93(4), 611-622.

Reethof, G. (1973). Effect of plantings on radiation of highway noise. *Journal of the Air Pollution Control Association*, 23(3), 185-189.

Reethof, G., McDaniel, O., & Heisler, G. (1977). *Sound absorption characteristics of tree bark and forest floor*. Paper presented at the Proceedings of the Conference on Metropolitan Physical Environment.

Richards, D. G., & Wiley, R. H. (1980). Reverberations and amplitude fluctuations in the propagation of sound in a forest: implications for animal communication. *American Naturalist*, 381-399.

Rindel, J. H. (2010). Verbal communication and noise in eating establishments. *Applied Acoustics*, 71(12), 1156-1161.

Schlatter, W. R. (1971). *Sound power measurement in a semi-confined space*. Massachusetts Institute of Technology.

Smyrnova, Y., Kang, J., Cheal, C., Tijjs, E., & de Bree, H. E. (2010). *Laboratory test of sound absorption of vegetation*. Paper presented at the Proceedings of EAA EuroRegio congress on sound and vibration, Ljubljana, Slovenia.

Steenackers, P., Myncke, H., & Cops, A. (1976). Reverberation in town streets.

Swearingen, M. E., & White, M. J. (2007). Influence of scattering, atmospheric refraction, and ground effect on sound propagation through a pine forest. *Journal of the Acoustical Society of America*, 122, 113-119.

Takebayashi, H., & Moriyama, M. (2007). Surface heat budget on green roof and high reflection roof for mitigation of urban heat island. *Building and Environment*, 42(8),

2971-2979.

Tang, S. H., & Ong, P. P. (1988). A Monte Carlo technique to determine the effectiveness of roadside trees for containing traffic noise. *Applied Acoustics*, 23(4), 263-271.

Tang, S. H., Ong, P. P., & Woon, H. S. (1986). Monte Carlo simulation of sound propagation through leafy foliage using experimentally obtained leaf resonance parameters. *Journal of the Acoustical Society of America*, 80(6), 1740-1744.

Tarrero, A. I., Martín, M. A., González, J., Machimbarrena, M., & Jacobsen, F. (2008). Sound propagation in forests: A comparison of experimental results and values predicted by the Nord 2000 model. *Applied Acoustics*, 69(7), 662-671.

Thomas, P., Renterghem, T. V., Boeck, E. D., Dragonetti, L., & Botteldooren, D. (2013). Reverberation-based urban street sound level prediction. *The Journal of the Acoustical Society of America*, 133(6), 3929-3939.

Tucker, M. R., Messik, J. K., & Stokes, C. (1995). Topsoil: North Carolina Department of Agriculture.

Tunick, A. (2003). Calculating the micrometeorological influences on the speed of sound through the atmosphere in forests. *Journal of the Acoustical Society of America*, 114(4), 1796-1806.

Tyagi, V., Kumar, K., & Jain, V. K. (2006). A study of the spectral characteristics of traffic noise attenuation by vegetation belts in Delhi. *Applied Acoustics*, 67(9), 926-935.

Umnova, O., Attenborough, K., & Linton, C. M. (2006). Effects of porous covering on sound attenuation by periodic arrays of cylinders. *Journal of the Acoustical Society of America*, 119(1), 278-284.

Van Renterghem, T., & Botteldooren, D. (2002). Effect of a Row of Trees Behind Noise Barriers in Wind. *Acta Acustica united with Acustica*, 88(6), 869-878.

Van Renterghem, T., & Botteldooren, D. (2008a). Numerical evaluation of sound propagating over green roofs. *Journal of Sound and Vibration*, 317(3-5), 781-799.

Van Renterghem, T., & Botteldooren, D. (2008b). Numerical evaluation of tree canopy shape near noise barriers to improve downwind shielding. *Journal of the Acoustical*

*Society of America*, 123, 648-657.

Van Renterghem, T., & Botteldooren, D. (2009). Reducing the acoustical façade load from road traffic with green roofs. *Building and Environment*, 44(5), 1081-1087.

Van Renterghem, T., & Botteldooren, D. (2010). The importance of roof shape for road traffic noise shielding in the urban environment. *Journal of Sound and Vibration*, 329(9), 1422-1434.

Van Renterghem, T., & Botteldooren, D. (2011). In-situ measurements of sound propagating over extensive green roofs. *Building and Environment*, 46(3), 729-738.

Van Renterghem, T., Botteldooren, D., & Verheyen, K. (2012). Road traffic noise shielding by vegetation belts of limited depth. *Journal of Sound and Vibration*, 331(10), 2404-2425.

Van Renterghem, T., Hornikx, M., Forssen, J., & Botteldooren, D. (2013). The potential of building envelope greening to achieve quietness. *Building and Environment*, 61(0), 34-44.

Van Renterghem, T., Salomons, E., & Botteldooren, D. (2006). Parameter study of sound propagation between city canyons with a coupled FDTD-PE model. *Applied Acoustics*, 67(6), 487-510.

Van Renterghem, T., Salomons, E. M., & Botteldooren, D. (2005). Efficient FDTD-PE model for sound propagation in situations with complex obstacles and wind profiles. *Acta Acustica united with Acustica*, 91(4), 671-679.

Veisten, K., Smyrnova, Y., Klæboe, R., Hornikx, M., Mosslemi, M., & Kang, J. (2012). Valuation of Green Walls and Green Roofs as Soundscape Measures: Including Monetised Amenity Values Together with Noise-attenuation Values in a Cost-benefit Analysis of a Green Wall Affecting Courtyards. *International Journal of Environmental Research and Public Health*, 9(11), 3770-3788.

Volkman, J. E., & Graham, M. L. (1942). A Survey on Air Raid Alarm Signals. *Journal of the Acoustical Society of America*, 14(1), 1-9.

Wardman, M., & Bristow, A. L. (2004). Traffic related noise and air quality valuations: evidence from stated preference residential choice models. *Transportation Research*

## References

---

*Part D: Transport and Environment*, 9(1), 1-27.

Watanabe, T., & Yamada, S. (1996). Sound attenuation through absorption by vegetation. *Journal of the Acoustical Society of Japan (E)*, 17(4), 175-182.

Wiener, F. M., Malme, C. I., & Gogos, C. M. (1965). Sound propagation in urban areas. *Journal of the Acoustical Society of America*, 37, 738-747.

Wilhelmsson, M. (2000). The impact of traffic noise on the values of single-family houses. *Journal of Environmental Planning and Management*, 43(6), 799-815.

Wong, N. H., Kwang Tan, A. Y., Tan, P. Y., Chiang, K., & Wong, N. C. (2010). Acoustics evaluation of vertical greenery systems for building walls. *Building and Environment*, 45(2), 411-420.

Wunderli, J., & Salomons, E. (2009). A model to predict the sound reflection from forests. *Acta Acustica united with Acustica*, 95(1), 76-85.

Wunderli, J. M. (2012). An extended model to predict reflections from forests. *Acta Acustica united with Acustica*, 98(2), 263-278.

Yang, H., Kang, J., & Cheal, C. (2013). Random-incidence absorption and scattering coefficients of vegetation. *Acta Acustica united with Acustica*, in press.

Yang, H. S., Kang, J., & Choi, M. S. (2012). Acoustic effects of green roof systems on a low-profiled structure at street level. *Building and Environment*, 50(0), 44-55.

Yang, W., & Kang, J. (2005). Acoustic comfort evaluation in urban open public spaces. *Applied Acoustics*, 66(2), 211-229.

Yeow, K. W. (1976). External reverberation times observed in built-up areas. *Journal of Sound and Vibration*, 48(3), 438-440.

Yeow, K. W. (1977). Decay of sound levels with distance from a steady source observed in a built-up area. *Journal of Sound and Vibration*, 52, 151-154.

Yu, C. J., & Kang, J. (2009). Environmental impact of acoustic materials in residential buildings. *Building and Environment*, 44(10), 2166-2175.

Yu, L., & Kang, J. (2010). Factors influencing the sound preference in urban open



## References

---

spaces. *Applied Acoustics*, 71(7), 622-633.

Zeng, X., Christensen, C. L., & Rindel, J. H. (2006). Practical methods to define scattering coefficients in a room acoustics computer model. *Applied Acoustics*, 67(8), 771-786.

---

## PUBLICATIONS

The thesis is based on the work contained in the following papers:

### Refereed Journal Papers

- H. Yang, J. Kang and M. Choi, “Acoustic effects of green roof systems on a low-profiled structure at street level”, *Building and Environment*, 50, 44-55, 2012, DOI: <http://dx.doi.org/10.1016/j.buildenv.2011.10.004>
- H. Yang, M. Kim and J. Kang, “Acoustic characteristics of outdoor spaces in an apartment complex”, *Noise Control Engineering Journal*, 61(1), 1-10, 2013, DOI: <http://dx.doi.org/10.3397/1.3702001>
- H. Yang, J. Kang and C. Cheal, “Random-incidence absorption and scattering coefficients of vegetation”, *Acta Acustica united with Acustica*, 99(3), 379-388, 2013, DOI: <http://dx.doi.org/10.3813/AAA.918619>
- H. Yang, J. Kang, C. Cheal, T. Van Renterghem and D. Botteldooren, “Quantifying scattered sound energy from a single tree by means of reverberation time”, *Journal of the Acoustical Society of America*, 134(1), 264-274, 2013, DOI: <http://dx.doi.org/10.1121/1.4808175>
- M. Kim, H. Yang, J. Kang, “A case study on controlling sound fields in a courtyard by landscape designs”, *Landscape and Urban Planning*, 2013 (in revision)

### Refereed Conference Papers

- H. Yang, M. Choi and J. Kang, “Laboratory study of the effects of green roof systems on noise reduction at street levels for diffracted sound”, Inter-Noise 2010,

---

Lisbon, Portugal, (2010)

- H. Yang, M. Choi and J. Kang “Acoustic effects of designable factors for the application of green roof systems on street-level low-profiled structures”, EAA Euroregio 2010, Ljubljana, Slovenia, (2010)
- C. Cheal, H. Yang, J. Kang and Y. Smyrnova, “Experimental study on the effects of vegetation coverage and soil depth and water content on sound absorption”, Forum Acusticum 2011, Aalborg, Denmark, (2011)
- H. Yang, M. Kim and J. Kang, “Acoustic characteristics of outdoor spaces in an apartment complex”, Inter-Noise 2011, Osaka, Japan, (2011)
- H. Yang, J. Kang, C. Cheal, T. Renterghem and D. Botteldooren, “Sound dispersion and reverberation by a single tree”, Inter-Noise 2011, Osaka, Japan, (2011)
- H. Yang, C. Cheal and J. Kang, “Random-incidence absorption and scattering coefficients of low-growing plants”, Euronoise 2012, Prague, Czech, (2012)
- H. Yang, M. Kim, J. Kang and S. Jung, “Parametric study on sound field of outdoor spaces in apartment complexes”, Inter-Noise 2012, New York, America, (2012)
- H. Yang, M. Kim and J. Kang, “Case study on acoustic improvement by refurbishment with natural elements in a courtyard”, Inter-Noise 2012, New York, America, (2012)
- H. Yang, M. Kim, J. Kang and H. Cho, “Noise reduction by natural elements in a courtyard”, Meeting of the Institute of Acoustics, Watford, United Kingdom, (2012)
- J. Kang, H. Yang and C. Cheal, “Absorption and scattering characteristics of soil and foliage”, Proceedings of the Institute of Acoustics, Vol. 35, Pt.1, Nottingham, United Kingdom, (2013)